Molecular level cytocompatibility evaluation of a thermoresponsive substrate for bioengineering of corneal construct towards ocular surface regeneration

THESIS SUBMITTED

BY

VIJI MARY VARGHESE

IN PARTIAL FULFILLMENT OF THE REQUIREMENTS

FOR THE DEGREE OF

DOCTOR OF PHILOSOPHY

SREE CHITRA TIRUNAL INSTITUTE FOR
MEDICAL SCIENCES AND TECHNOLOGY
THIRUVANANTHAPURAM – 695 012

MARCH 2009

DECLARATION

I, Viji Mary Varghese, hereby declare that I had personally carried out the work depicted in the thesis entitled "**Molecular level cytocompatibility evaluation of a thermoresponsive substrate for bioengineering of corneal construct towards ocular surface regeneration**" under the direct supervision of Dr. TV Kumary, Scientist-F, Division of Implant Biology, Biomedical Technology Wing, Sree Chitra Tirunal Institute for Medical Sciences and Technology, Thiruvananthapuram, Kerala, India. External help sought are acknowledged.

Viji Mary Varghese

Dr. TV Kumary,
Scientist F

Tissue Culture Laboratory,
Division of Implant Biology,
Biomedical Technology Wing,
Sree Chitra Tirunal Institute for Medical Sciences and Technology,
Thiruvananthapuram – 695012

CERTIFICATE

This is to certify that Ms. Viji Mary Varghese, Division of Implant Biology of this Institute, has fulfilled the requirements of the regulations relating to the nature and prescribed period of research for the PhD degree of the Sree Chitra Tirunal Institute for Medical Sciences and Technology, Thiruvananthapuram. The work entitled "**Molecular level cytocompatibility evaluation of a thermoresponsive substrate for bioengineering of corneal construct towards ocular surface regeneration"** was carried out under my direct supervision.

Dr. TV Kumary

The Thesis

Entitled

Molecular level cytocompatibility evaluation of a thermoresponsive substrate for bioengineering of corneal construct towards ocular surface regeneration

Submitted by

Viji Mary Varghese

For

Doctor of Philosophy

Sree Chitra Tirunal Institute
for Medical Sciences and Technology
Thiruvananthapuram

Evaluated and Approved

by

Dr. T V Kumary
Scientist G
Implant Biology
(Supervisor)

Prof. H N Madhavan
Director of Research
Vision Research Foundation
Sankara Nethralaya, Chennai

To the One who made everything possible.....
(Mark:10:27)

CONTENTS

ACKNOWLEDGEMENTS

Without a note of gratitude to all who helped me in these five years of academic life, this thesis will be incomplete.

I sincerely thank my research supervisor, Dr. TV Kumary, for her excellent support, advices and guidance throughout these years. I also wish to thank her for all her efforts in correction of this thesis by staying back after office hours. I thank members of my doctoral advisory committee, Dr. Mira Mohanty, Dr. Sreenivasan K and Dr. PV Mohanan for their timely suggestions, ideas and comments in each stage of the work.

I am grateful to Dr. K Mohandas, Director of our Institute and Dr. G. S. Bhuvaneshwar, Head of BMT Wing for all the facilities provided during the course of my work. I am thankful to The Registrar and Deputy Registrar for their academic assistance.

I am grateful to Council of Scientific and Industrial Research, India for the research fellowship. Financial assistance from Department of Biotechnology is also acknowledged. I am greatly indebted to Commonwealth Scholarship Commission for giving me a wonderful opportunity to do part of my work in United Kingdom using split site doctoral fellowship. I express my sincere thanks to Prof. H. S. Dua, University of Nottingham, for giving me an opportunity to work under his expertise for one year. I am greatly indebted to Dr. Andy Hopkinson, University of Nottingham, who introduced me to the world of proteomics and provided me with information whenever I approached. I am thankful to the staff of Core proteomics facility, University of Nottingham for their help in identification and characterisation of proteins using mass spectrometry. I also acknowledge all my colleagues in Larry A Bonso laboratory, University of Nottingham for their support and friendship.

I have received a lot of help from many people during my research in the Institute. Sincere thanks are due to Ms. Vidya Raj for help in preparation and characterisation of copolymer used in this study. I also wish to acknowledge all the other staff of Lab for Polymer Analysis for their help in characterisation techniques. I am grateful to Dr. T. V. Anilkumar for giving me training in confocal microscopy and letting me use the equipment. I thank all the staff of Division of Toxicology especially Sumithra for the help in procurement of rabbit eye tissues. Thanks are due to Mr. Sumesh for the help in contact anagle measurement and Ms. Leena Joseph for the support in profilometric studies. I leave a grateful note to Dr. Lissy K

Krishnan, Dr. Divya, Dr. Krishna Prasad, Dr. Anughya Bhatt and Mr. Renjith for their help in tritiated thymidine uptake assay and flow cytometry. I gratefully acknowledge Dr. H. K. Varma and Mr. Sreekumar for their help in environmental scanning electron microscopy.

I am thankful to all staff of implant biology for their support and encouragement. Special thanks are due to my labmates, Dr. Anilkumar P. R., Ms. Usha Vasudev, Ms. Deepa, Mr. Tilak, Mr. Anwar, Mr. Rojan and Ms. Nithya for all their support and help. A special note of gratitude to Dr. Anilkumar P. R. who helped me learn the preliminary lessons of cell sheet retrieval. Help in polymer preparation and characterisation by Nithya is also acknowledged. I thank Tilak for his support in various in vitro studies.

All my friends, both in and out of the campus, were a constant source of relief. I thank Ms. Susan, Ms. Josna, Ms. Bindu, Ms. Chithra, Dr. Asha, Dr. Divya, Ms. Nithya and Ms. Viola for their friendship and support. Sincere thanks are due to Ms. Manitha, Ms. Aparna, Ms. Anitha, Ms. Roshni, and Ms. Parvathy for their caring companionship and prayer support whenever I needed it.

It is difficult to express my gratitude to my family, who were my strength and all time support. Without the prayer support, patience, encouragement, love and caring from my husband, I could not have finished my research. He was always there for me, especially when I was frustrated and tensed. I can never repay the love and support showered by my parents and my brother throughout my life. I am really thankful to God for my in-laws, who supported me very well with their prayers and encouragement.

How will I express my gratitude to my Lord, my God....This life is not enough to thank Him for all the divine mercy, love and providence that He showers on me. He is always with me to fill me with new hope, to hold me with His victorious right hand and to strengthen me whenever I am weak. I exclaim your glory and love, O Lord.

Viji Mary Varghese

LIST OF FIGURES

LIST OF TABLES

ABBREVIATIONS

[3H]	-	Tritiated
1-D	-	First dimensional
2DE	-	Two dimensional gel electrophoresis
AIBN	-	Azobisisobutyronitrile
AM	-	Amniotic membrane
AMT	-	Amniotic membrane transplantation
APS	-	Ammonium persulphate
ATR	-	Attenuated total reflectance
BCIP	-	5-Bromo-4-chloro-3'-indolyphosphate p-toluidine salt
BM	-	Basement membrane
BSA	-	Bovine serum albumin
CECL	-	Corneal epithelial cell line
CEM	-	Corneal epithelial medium
CK3	-	Cytokeratin 3
DMSO	-	Dimethyl sulphoxide
dNp63	-	Delta Np63
DSC	-	Differential scanning calorimetry
DTT	-	Dithiothreitol
ECM	-	Extra cellular matrix
EDTA	-	Ethylene diamine tetra acetic acid
EGF	-	Epidermal growth factor
ESC	-	Embryonic stem cells
ESEM	-	Environmental scanning electron microscope
FBS	-	Foetal bovine serum
FDA	-	Fluorescein Diacetate
FITC	-	Fluorescein isothiocyanate
FN	-	Fibronectin
FTIR	-	Fourier transform infrared spectroscopy
h	-	Hours
HBSS	-	Hank's buffered salt solution
HEMA	-	2-Hydroxy ethyl methacrylate
HGF	-	Hepatocyte growth factor

HLA	-	Human leukocyte antigen
HyQ	-	HyQ SFM MegaVir medium
IGF	-	Insulin growth factors
IGFBP	-	Insulin growth factor binding protein
IMDM	-	Iscove's modified dulbecco's medium
kDa	-	Kilo Dalton
KGF	-	Keratinocyte growth factor
LCST	-	Lower critical solution temperature
LEC	-	Limbal epithelial crypt
LiEC	-	Limbal epithelial cells
LSC	-	Limbal stem cells
LSCD	-	Limbal stem cell deficiency
MEM	-	Minimal essential medium
MMA	-	Methyl methacrylate
MMP	-	Matrix metalloproteinase
MSC	-	Mesenchymal stem cells
MTT	-	3-(4, 5-Dimethylthiazol-2-yl)-2, 5-diphenyltetrazolium bromide
NBT	-	Nitro-blue tetrazolium chloride
NGAL	-	Neutrophil gelatinase associated lipocalin
NIPAAm	-	N-isopropylacrylamide
PBS	-	Phosphate buffered saline
PCNA	-	Proliferating cell nuclear antigen
PET	-	Poly ethylene terephthalate
PFA	-	Paraformaldehyde
PI	-	Propidium iodide
PIPAAm	-	Poly (N-isopropylacrylamide)
PMF	-	Peptide mass fingerprints
PVDF	-	Poly vinylidene flouride
SC	-	Stem cells
SDS	-	Sodium dodecyl sulphate
SFCEM	-	Serum free corneal epithelial medium
SFM	-	Serum free medium
SPARC	-	Secreted protein acidic and rich in cysteine
TAC	-	Transient amplifying cells

TBST	-	Tris buffered saline with 0.1% triton X-100
TCPS	-	Tissue culture polystyrene
TE	-	Tissue engineering
TEMED	-	N,N,N',N'-Tetramethyl ethylenediamine
TGFβ	-	Transforming growth factor β
TGS	-	Tris glycine SDS
TIMP	-	Tissue inhibitor of metalloproteinase
TPVG	-	Trypsin (0.25%)-EDTA (0.02%)
TRITC	-	Tetramethyl rhodamine isothiocyanate
UV	-	Ultraviolet

SYNOPSIS

Blindness is one of the most feared disabilities which can happen due to a variety of reasons. Around 6.8 million people in India are affected by corneal blindness (Sinha et al., 2005). Limbal stem cell deficiency (LSCD) could be a factor that contributes to the persistence of corneal blindness even after transplantation. Due to the disadvantages of the current treatment methods, here we employed a cytocompatible thermoresponsive substrate to generate limbal epithelial tissue structures towards ocular surface regeneration for treatment of LSCD

The thesis is divided into five chapters**: Introduction & Review of Literature, Materials & Methods, Results & Discussion, Summary & Conclusion and Future directions**

Chapter I Introduction and review of literature

Chapter I gives an introduction to the topic addressed in the thesis and reviews the literature related to the study.

Cornea is the anterior transparent window of the eye. The major function of cornea is to transmit and partially refract light into eye globe. It also acts as the barrier between optical and external environment. Cornea is made up of five layers, namely epithelium, bowman's membrane, stroma, descemet's membrane and endothelium. All these layers play important role in maintaining corneal transparency for vision. Corneal epithelium is made of 4-6 layers of non keratinized, stratified cells. Each of these layers has unique structural features enabling their respective functions. The superficial cells are the post mitotic, terminally differentiated cells with strong junctional complexes between lateral adjacent cells to give a barrier with high electrical resistance and low permeability, which is essential for maintenance of corneal homeostasis.

The regeneration and repair of corneal epithelium is carried out by adult stem cells that reside in limbus, a junctional region between cornea and sclera. These adult stem cells leave their niche after proliferation and undergo a centripetal migration to reach the superficial layer of cornea (Thoft and Friend, 1983). The stem cells retain the capacity for both self renewal and cell division to generate a fast dividing group of cells called Transient Amplifying Cells. These cells, after a few cell divisions turn into post mitotic cells and then to terminally differentiated cells by the time which it reach superficial

corneal layer. Loss of these stem cells, due to either inherited or acquired reasons, lead to a condition called limbal stem cell deficiency (LSCD) (Ang and Tan, 2004). LSCD result in different manifestations like conjunctivalisation, inflammation and persistent epithelial defect of cornea, leading to gradual opacity and blindness. Conventional corneal transplantation is not an effective treatment method as it would not replenish the stem cell source. Current treatment methods like autograft, allograft and amniotic membrane transplantation have their own disadvantages.

Ex vivo expansion of limbal cells from small biopsies on different substrates using tissue engineering approach, followed by transplantation, provided a new treatment method for LSCD. Already reported cell sources for the expansion are limbal stem cells, oral mucosal cells, mesenchymal stem cells, conjunctival cells and embryonic stem cells. Amniotic membrane had been used widely as scaffold for this *ex vivo* expansion (Koizumi et al., 2001). Amniotic membrane, being a biological substrate, always carries the risk of disease transmission (Dua and Azuara-Blanco, 1999b). Scaffolds like polymers can not be used for transplantation as these will hinder vision. Therefore, scaffold free tissue constructs are ideal for LSCD treatment in order to ensure vision.

Thermoresponsive polymers could be used in generating scaffold free tissue constructs due to their property of phase transition around lower critical solution temperature (LCST). These polymers act as hydrophobic above LCST favoring cell growth and hydrophilic below LCST favoring detachment of cells with intact cell-cell and cell-extra cellular matrix interactions. PIPAAm is such a polymer used for cell manipulation (Okano et al., 1993). Addition of hydrophobic monomers in to this modulate the LCST and increase cell adhesion and growth (Allen et al., 2003).

Any material that comes in contact with human body, tissues *in vivo* or cells *in vitro* should be cytocompatible. A few reports are available about cytocompatibility studies of PIPAAm copolymer intended for drug delivery systems (Cao et al., 2007). Extensive cytocompatibility studies were not carried out for PIPAAm or its copolymers intended for tissue reconstruction.

Use of 3T3 feeder layer from murine source was a prerequisite for the *ex vivo* expansion of limbal cells. Food and Drug Administration (FDA), USA has categorized tissues regenerated using 3T3 layers as xenogeneic. There is an ever increasing demand

for development of **scaffold and feeder free culture systems** for *ex vivo* expansion of limbal cells.

In order to achieve these two major requirements, our study was aimed at

1) Development of feeder free rabbit limbal cell culture system
2) Synthesis, characterization and cytocompatibility analysis of a thermoresponsive substrate
3) Molecular level cytocompatibility assessment using secretome analysis
4) Generation and characterization of limbal epithelial cell sheet towards ocular surface regeneration

Chapter II Materials and Methods

Chapter II describes the experimental approach adopted and has been divided into four sections

Culture and characterization of limbal cells from different sources:

Explant cultures from three different limbal sources, goat, rabbit and human, were done.

The limbal cells freshly isolated from goat limbus were analysed by flow cytometry for the presence of stem cell associated markers like p63 and ABCG2 using flow cytometry. After *ex vivo* expansion, the cells were characterized for different markers like p63, ABCG2, cytokeratin 3 (CK3) and PCNA using immunofluorescent staining.

Rabbit explant culture was optimized in terms of 1) Effect of dispase treatment, 2) Effect of medium and 3) Maintenance of stem cell like characteristics in different culture conditions, in order to establish a xeno-feeder free culture system. To study the effect of dispase, explants were cultured with and without initial dispase treatment. To analyse whether dispase treatment has any effect on culture maintenance, explants were treated with dispase for different time periods. To study effect of medium, explants were cultured in different mediums alone (Completed Panserin 801, IMDM with 10% serum) or in combination. Distance migrated by the cells from explants on different days were studied using phase contrast microscopy and image analysis in QWin software. For studying maintenance of stem cell characteristics, intensity of p63 expression in cells cultured in different medium was analysed using quantitative confocal microscopy.

Two different methodologies were adopted for human limbal explant culture. One method consisted of culturing full thickness limbal explants trimmed out of excess scleral and corneal tissue, in culture system 4. In a slightly different methodology, stromal region was peeled away from epithelial surface of trimmed limbus and then small limbal tissue pieces were cultured as explants. Human limbal cells were characterized using immunofluorescent staining of p63.

Preparation, characterization and cytocompatibility assessment of copolymer:

Copolymer of N-isopropylacrylamide (NIPAAm) and Methyl Methacrylate (MMA) was synthesized by free radical polymerization. The copolymer was characterized by fourier transform infrared spectroscopy (FTIR) and differential scanning calorimetry (DSC). The copolymer solution in isopropanol was coated on tissue culture polystyrene (TCPS) surfaces and the surfaces were characterized using attenuated total reflectance (ATR) spectra, contact angle measurement and profilometric studies.

L-929, mouse fibroblast cell line was used to analyze cytotoxicity and compatibility of the copolymer. Cytotoxicity studies were carried out according to ISO-10993-5 using direct contact test. As the copolymer was intended for corneal epithelial regeneration, SIRC, a corneal cell line was cultured to understand how it favours the cell adhesion and viability of the specific cell type. Cytocompatibility was analysed in terms of 1) cell viability by neutral red staining, 2) cell attachment and doubling time by tritiated thymidine uptake assay, 3) cell metabolism by MTT assay, 4) cell cycle analysis by propidium iodide staining, followed by flow cytometry analysis 5) cytoskeletal organization by Phalloidin FITC staining and 6) expression of different markers like deltaNp63, ABCG2, CK3 and Connexin 43 in human limbal cells cultured on NIPAAm-MMA at mRNA level by reverse transcriptase PCR. Thermoresponsive efficacy ie; the ability of the copolymer to detach cells when incubated under LCST was studied by transferring confluent L929 cells to polyvinylidene fluoride (PVDF) membrane.

Secretome analysis as a tool to study specific molecular level cytocompatibility:

Primary human limbal cells and an SV-40 immortalised human corneal epithelial cell line were used to study molecular level cytocompatibility of NIPAAm-MMA. TCPS and NIPAAm-MMA were used as substrates for cell line culture. Along with these, amniotic membrane (AM) was also used as substrate for primary limbal culture. The culture medium from each cell type and substrate was collected separately. The collected

medium was concentrated, quantified and cleaned up for two dimensional gel electrophoresis. After the 2D run, the gel images were compared against the respective cellular proteins using delta2D software to find out unique spots that could be potential secretory proteins. Gel images of different collected mediums were compared against each other to identify differences. The selected potential spots were identified using MALDI-TOF. Confirmation of some interesting proteins was done using MS/MS analysis and western blotting.

Generation and characterization of limbal cell sheet:

Goat and rabbit limbal cells were cultured on NIPAAm-MMA plates till confluency. The cell sheet was retrieved by incubating under LCST of copolymer.

The retrieved rabbit cell sheet was assessed for its viability by fluorescein diacetate staining, intactness by environmental scanning electron microscopy (ESEM), transparency by the visibility of alphabets beneath cell sheet and expression of different markers by immunofluorescent staining for actin organization, ZO-1, occludin, p63 and Connexin 43.

The goat cell sheet was assessed for its intactness (ESEM) and expression of different markers by immunofluorescent staining for p63, CK3 and actin organization.

Chapter III Results and Discussion

Chapter III includes results of the various experiments and discussion of the data under respective headings.

Culture and characterization of limbal cells from different sources:

69% of the limbal cells freshly isolated from goat limbus was found to be positive for p63, a stem cell associated marker while 3.2% were positive for ABCG2, a putative stem cell marker. P63, CK3 and ABCG2 expression was found in cultured goat limbal cells. PCNA expression was not found when stained after 7 days of culture while it increased by 21st day.

The results from rabbit limbal explant culture with or without dispase treatment indicated that initial enzyme treatment is not mandatory for long term explant culture. The duration of enzyme treatment was also important as it had a definite impact in the integrity of migrated cells. Optimization of medium resulted in formulation of a modified microenvironment (Culture system 4 – Panserin 801 and IMDM in 1:1 ratio with 5%

serum) which supported formation of autofeeder layers, thus enabling avoidance of xeno feeders like 3T3 fibroblast cells. Intensity of p63 expression can be considered as degree of stemness. Quantitative confocal microscopy revealed that the modified culture system supports maintenance of stem cell like characteristics. Significant decrease in intensity of p63 expression was observed in the cells when the medium was IMDM with 10% serum. In human limbal culture, p63 expression was observed.

Preparation, characterization and cytocompatibility analysis of copolymer:

Polymeric form of MMA, Polymethyl methacrylate (PMMA) is one of the widely used biocompatible polymers in ocular applications such as intra ocular lens and contact lens. In this study, largely considering the favourable features of PMMA a copolymer of N-isopropylacrylamide and Methyl Methacrylate was synthesised and characterised. NIPAAm was incorporated to provide thermoresponsiveness whereby cells can be detached as intact cell sheets, avoiding the use of proteolytic enzymes. Moreover, this can assist in formation of scaffold free tissue constructs. MMA, being widely used as a biomaterial in its polymeric form, was incorporated to modulate LCST. FTIR spectra showed characteristic peaks of both NIPAAm and MMA to be present in the copolymer. DSC scan revealed LCST of the copolymer to be around 30°C. ATR spectra showed the characteristic peak of amide carbonyl group at 1650 cm^{-1}, indicating coating of the copolymer on TCPS surface. The difference in contact angle measurement in the bare (TCPS) (83.7 ± 1.63) and coated surfaces (63.3 ± 0.75) gave evidence for coating. Decrease in the surface roughness on coated surface (Ra=3.37 ± 0.188 nm, where Ra is the arithemetic average of absolute values) compared to the TCPS (Ra=6.06 ± 0.679 nm) gave further evidence of coating.

The L929 cells exhibited normal morphology after 24 hours of direct contact with NIPAAm-MMA indicating its non-cytotoxicity. Morphology of the L929 and SIRC cells were similar on both TCPS and NIPAAm-MMA. Both the cell lines cultured on the copolymer were viable and healthy. Cell attachment rate and doubling time of L929 cells on TCPS and NIPAAm-MMA were similar. Results of MTT assay suggested metabolically active cells on NIPAAm-MMA even after 96 hours of culture. Results of cell cycle analysis showed that none of the stages in the cell cycle was affected after 24 hours of culture on NIPAAm-MMA. Good cell spreading was indicated by actin staining. Presence of progenitor and differentiated population on NIPAAm-MMA dishes was

evidenced by PCR studies. The thermoresponsive nature was proved by the transfer of cultured cells to PVDF membrane.

Secretome analysis as a tool to study specific molecular level cytocompatibility:

When the images of gels from collected medium of cell line cultured on TCPS and NIPAAm-MMA were compared against each other using delta 2D software, a similar protein profile was observed. This indicated that no additional potential spots for secretory proteins were there in either of the gels. 25 potential spots were identified by MALDI-TOF and it was found that 64% of the analysed spots were secretory proteins. No unique spots were found in the gels of primary secretome collected from TCPS and NIPAAm-MMA. Additional spots were found in the gels of collected medium from primary cells grown on AM. 36 potential spots were identified using MALDI-TOF and 89.2% were secretory proteins. Many of these proteins were already reported as having important functions in cornea. Based on their role in different processes like corneal wound healing, epithelial adhesion, migration, and extracellular defense, proteins like SPARC, βig-h3, Cystatin-C, Neutrophil gelatinase associated lipocalin (NGAL) and metalloproteinase inhhibitor-1 were confirmed using MS/MS analysis.

Based on the difference in expression on different substrates & secretomes and role in corneal processes like transparency, extracellular defense, epithelial migration and corneal wound healing, western blotting was done for proteins (NGAL, Interleukin-6, Mimecan and βig-h3). The results correlated with the gel image analysis and mass spectrometry findings. NGAL was found to be expressed more in primary secretomes compared to cell line secretome. Interleukin-6 was expressed more in cell line secretome compared to primary secretome. In both these cases, there was no difference in the expression of these proteins on TCPS and NIPAAm-MMA. Mimecan and βig-h3 was expressed more in secretome of primary cells cultured on AM, which could be due to matrix remodeling of amniotic membrane.

Culturing of human corneal epithelial cell line and primary human limbal cells on the copolymer revealed its suitability in corneal tissue engineering applications.

Generation and characterization of limbal cell sheet:

Contiguous cell sheet with intact cell-cell contacts was obtained by peeling off with forceps after incubating under LCST of copolymer. The cell sheet was successfully mounted on to a doughnut shaped PVDF membrane, in order to facilitate transplantation

studies. The cell sheet was found to be intact except where explants were kept. The cells in the rabbit cell sheet were found to be viable and healthy as evidenced by FDA staining. Both the cell sheets exhibited cortical staining pattern for actin cytoskeletal organization. The rabbit cell sheet was clearly transparent on macroscopic view. Different cell junctional markers were found to be expressed in the rabbit cell sheet. Positive staining for p63 was also observed.

Chapter IV Summary and Conclusions

Chapter IV summarises the whole work and provide the drawn out conclusions.

Limbal cells from different sources were cultured and characterised. An optimised microenvironment for rabbit limbal culture resulted in formation of an autofeeder layer. Copolymerisation and coating of a thermoresponsive copolymer of NIPAAm-MMA on TCPS were confirmed using different characterisation techniques. The synthesised copolymer was found to be non cytotoxic and cytocompatible. Molecular level cytocompatibility was proved by analysing cell line and primary secretome by mass spectrometry and western blotting. Culturing of primary limbal cells from different sources on the copolymer proved its suitability for corneal tissue engineering. Thermoresponsive nature of the copolymer resulted in easy retrieval of limbal cell sheets. The cell sheet was found to be viable, transparent and intact. Expression of different markers in the cell sheet proved maintenance of cell-cell interactions. Presence of progenitor population in the cell sheet ensured its success after transplantation.

A cost effective and easy method to prepare thermoresponsive surfaces was employed in this study. Formation of autofeeder layer in modified microenvironment was an interesting finding. Molecular level cytocompatibility analysis of thermoresponsive copolymer had not been reported earlier. Use of secretome analysis in determining molecular level cytocompatibility of different substrates was suggested in this study. Suitability of the copolymer for generation of limbal epithelial cell sheet was shown.

Chapter V Future directions

- Development of xenobiotic free epithelial equivalents can be achieved by using autologous serum and defined constituents instead of foetal bovine serum and bovine pituitary extract.

- Preclinical studies for long follow up periods will give further evidence for the suitability of cell sheet in restoring vision.
- Use of cell sheet for other applications like '*in vitro* toxicity studies' can also be studied.
- Application of the thermoresponsive copolymer in generation of the stroma and endothelium of cornea will be another interesting future prospective.
- Since AM stroma is abundant in proteins like Mimecan and βig-h3, incorporation of these in to the thermoresponsive surface will be an added advantage.

References

Allen LT, Fox EJ, Blute I, Kelly ZD, Rochev Y, Keenan AK, Dawson KA, Gallagher WM. 2003. Interaction of soft condensed materials with living cells: phenotype/transcriptome correlations for the hydrophobic effect. Proc Natl Acad Sci USA 100(11):6331-6336.

Ang LP, Tan DT. 2004. Ocular surface stem cells and disease: current concepts and clinical applications. Ann Acad Med Singapore 33(5):576-580.

Cao Y, Zhang C, Shen W, Cheng Z, Yu LL, Ping Q. 2007. Poly(N-isopropylacrylamide)-chitosan as thermosensitive in situ gel-forming system for ocular drug delivery. J Control Release 120(3):186-194.

Dua HS, Azuara-Blanco A. 1999b. Amniotic membrane transplantation. Br J Ophthalmol 83(6):748-752

Koizumi N, Inatomi T, Suzuki T, Sotozono C, Kinoshita S. 2001. Cultivated corneal epithelial stem cell transplantation in ocular surface disorders. Ophthalmology 108(9):1569-1574.

Okano T, Yamada N, Sakai H, Sakurai Y. 1993. A novel recovery system for cultured cells using plasma-treated polystyrene dishes grafted with poly (N-isopropylacrylamide). J Biomed Mater Res 27(10):1243-1251.

Sinha R, Sharma N, Vajpayee RB. 2005. Corneal blindness-Present status. Cataract & Refractive Surgery today (Oct):59-61.

Thoft RA, Friend J. 1983. The X, Y, Z hypothesis of corneal epithelial maintenance. Invest Ophthalmol Vis Sci 24(10):1442-1443.

CHAPTER 1

INTRODUCTION & REVIEW OF LITERATURE

1.1 Vision loss

Vision loss is one of the most feared disabilities which can happen in acute or chronic conditions. Acute visual loss can be caused by conditions like media opacities (eg: corneal edema), retinal diseases and functional disorders. Vision can be lost chronically by age related conditions like cataract, corneal opacities and diabetic retinopathy. In 2002, according to World Health Organisation, around 161 million people were visually impaired world wide, out of which 37 million were totally blind. Out of the total blind population, 5.1% is affected by corneal opacities. 23.5% of world's bind population resides in India (Thomas et al., 2005). According to a report in 2005, approximately 6.8 million people are affected by corneal blindness in India (Sinha et al., 2005). It may increase up to 8.4 million in 2010.

1.2 Eye – the organ for vision

Eye is the organ that gives us the sense of vision and helps us to learn about the surrounding world more than other sense organs.

The eyeball is situated in a bony orbit in the skull and there are soft fatty layers of tissue in the orbit that protects the eye ball. Eyeball can be divided into 1) anterior segment, bounded by cornea and lens, filled with aqueous humor and 2) posterior segment, region posterior to lens, filled with vitreous humor. Wall of the eye ball is composed of three tunics, an outer layer of fibrous sclera and cornea, a middle vascular layer comprising choroid, iris and ciliary body and an inner neural layer of retina.

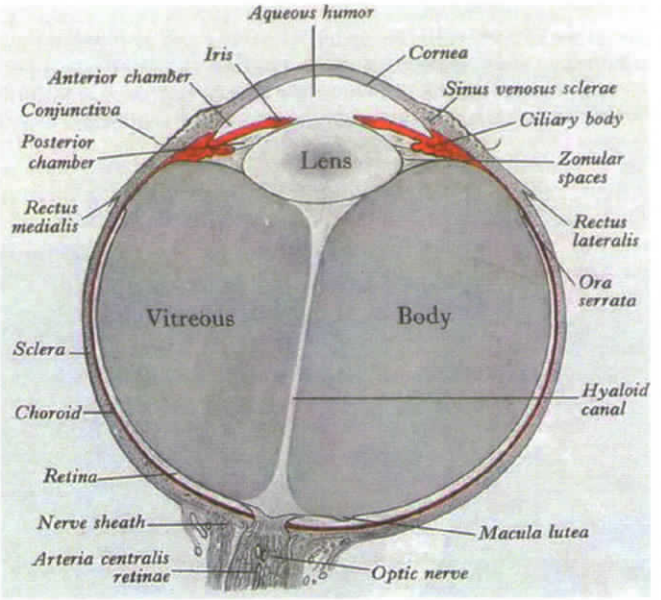

Figure 1-1: Different parts of eye (Courtesy: Gray's Anatomy)

1.2.1 Path of light

The anterior transparent portion of outer tunic namely cornea helps in refraction of light. Behind the cornea, the anterior chamber is filled with aqueous humor. Cornea along with aqueous humor directs light to the lens. Iris in the middle layer controls the amount of light reaching lens using pupil. The crystalline lens behind the iris and pupil focuses the light on to retina. Rods and cones in retina convert the light signal to impulses that are sent to brain where it gets interpreted.

1.2.2 Cornea

Cornea is the transparent, avascular portion of the outer fibrous tunic. It serves as a mechanically tough, chemically impermeable barrier between inner chamber of eye and surrounding environment. The cornea should be transparent, refract light and provide protective interface with environment. Cornea comprises of one sixth of the outer tunic. The central cornea which is also called optical zone is thinner than peripheral region. Cornea is made up of five different layers: epithelium, bowman's layer, stroma, descemet's membrane and the endothelium (Figure 1-2).

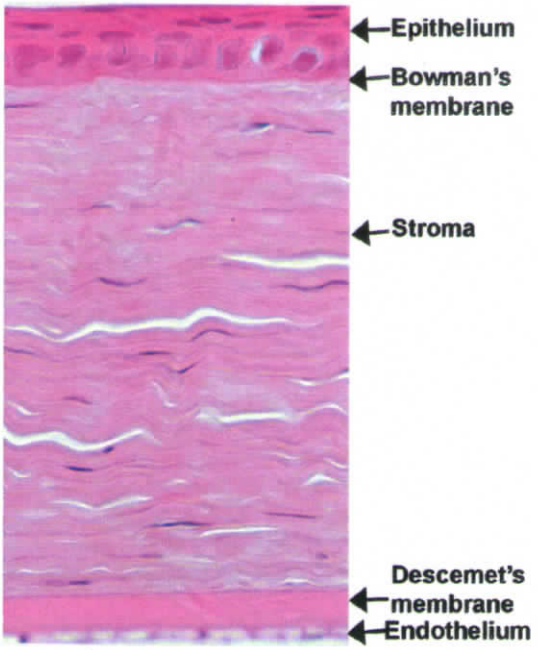

Figure 1-2: Transverse section of cornea showing different layers.

The main function of cornea is the refraction of light that falls on it. It accounts for 70% of total refractive power of eye. Collagens in the corneal stroma provide its toughness and help in maintaining ocular pressure. The homogenous arrangement of collagen fibrils in stroma accounts for corneal transparency. Swelling of cornea is prevented by its endothelial layer that actively pumps out the water.

1.2.3 Corneal epithelium

Corneal epithelium is made of 4-6 layers of non keratinized, stratified cells. It constitutes ten percent of corneal thickness. The surface of cornea is always kept wet by tear film so as to prevent damage to the epithelium. Epithelium can be divided into a superficial squamous layer, middle wing cell layer and a basal cell layer. Each of these layers has unique structural features enabling their respective functions. The superficial cells are the post mitotic, terminally differentiated cells with strong junctional complexes between lateral adjacent cells to give a barrier with high electrical resistance and low permeability, which is essential for maintenance of corneal homeostasis (Boulton and Albon, 2004). Usually there are two layers of superficial cells with microscopic projections like microvilli, reticulations and microplicae. The epithelium turns over approximately every seven days. The superficial cells have few organelles. There is a fibrillar glycocalyx, also called buffy coat, on the surface of superficial cells that help in the adherence of tear film to cornea.

The second epithelial layer (wing cells) consists of polyhedral cells and they represent the transitional stage of basal cells to superficial cells. A major structural component of the wing cells are tonofilaments that help to maintain its shape.

The basal columnar cells are more like progenitors for the superficial epithelial cells. They contain more cellular organelles compared to the anterior layers. They are attached to basal lamina by hemidesmosomes and anchoring fibrils.

1.2.4 Limbus

Limbus is of 1.5 mm width, located at the corneoscleral junction between conjunctiva and cornea, its inner edge being called corneal limbus and its outer edge the scleral limbus. It is a specialized tissue with high vascularisation and innervation. Unlike in cornea and sclera, melanin pigmentation is abundant in limbus to protect the cells from harmful effects of ultraviolet (UV) light.

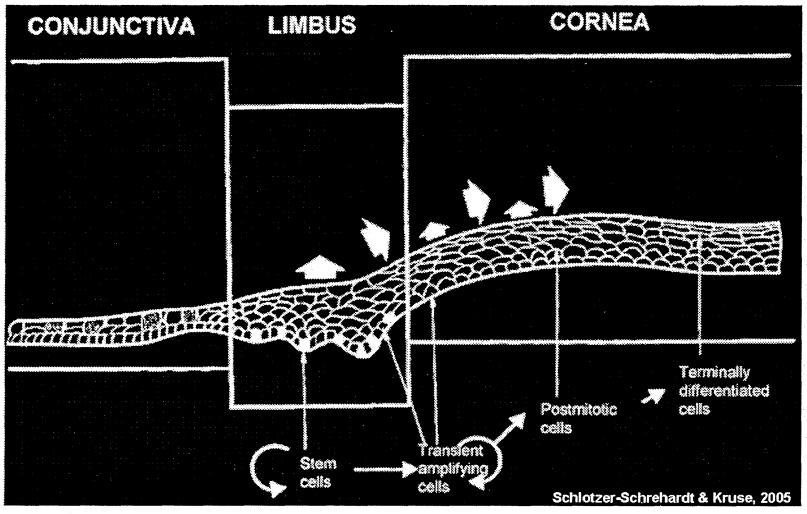

Figure 1-3: Schematic representation of concept of LSC and their role in corneal epithelial maintenance.

Basal cells of limbal epithelium contain a population of unipotent stem cells (SC), known as limbal stem cells (LSC) which is responsible for the repair and regeneration of corneal epithelium (Figure 1-3). Limbal epithelium is 10 to 15 layers thick, being broadest in upper and lower regions (Cardoen and Foets, 1999).

1.3 Corneal epithelial stem cells

The X Y Z hypothesis of corneal epithelial regeneration (Figure 1-4) stated that corneal epithelial loss should be balanced by cell replacement (Thoft and Friend, 1983).

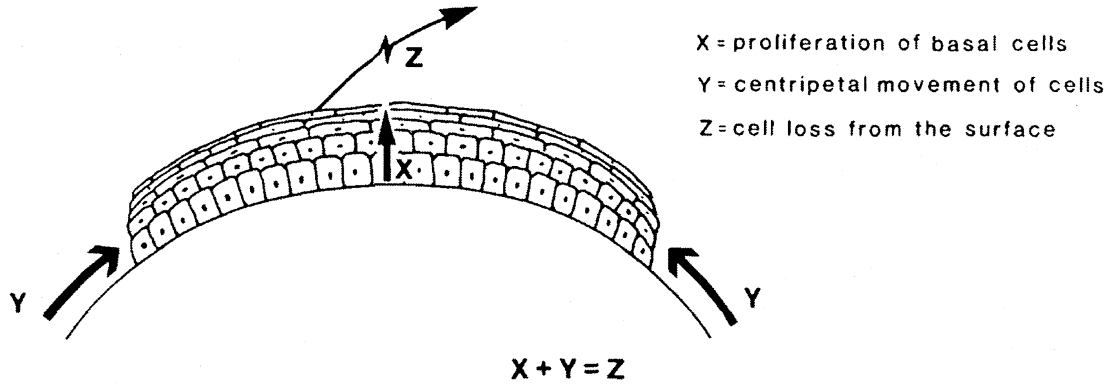

Figure 1-4: X, Y, Z hypothesis of corneal epithelial maintenance

As cornea maintains its cell mass by a process of cell loss, renewal, and regeneration, it must have a reservoir of 'stem cells' (Dua, 1995). Corneal epithelial stem cells/LSC, after proliferation, undergo a centripetal migration in restoring the superficial corneal epithelial cells. LSC retain the capacity for both self renewal and cell division to generate a fast dividing group of cells called Transient Amplifying Cells (TAC) (Lehrer et al., 1998). TAC can undergo a limited number of cell divisions before they become terminally differentiated cells.

1.3.1 Location of LSC

The spatial arrangement of LSC is not well known (Schlotzer-Schrehardt and Kruse, 2005). It was believed that SC are found as small clusters in the basal layer. Vogt in 1921 described a structure called Palisades of Vogt in the limbus. This is the undulating basal membrane with papillae or pegs of limbal stroma extending upward (Gipson, 1989). They are more prominent in lower limbus. It was reported that anatomy of these structures are unique for each individual (Goldberg and Bron, 1982). Palisades of Vogt are thus considered as a unique structure that provides the SC niche for LSC. The structure of the palisades are analogous to repositories of SC in monkey palm epidermis (Dua et al., 2003). Highly pigmented melanocytes, antigen presenting Langerhan's and suppressor T lymphocytes are present in palisades of Vogt.

A more specialized anatomical structure called limbal epithelial crypt (LEC) that extends from the peripheral aspect of the undersurface of an interpalisade rete ridge and located deep into substantia propria was described as possible niche (Dua et al., 2005). In this study, they have shown that all the cells in the crypt are epithelial in nature and staining for ABCG2, a stem cell marker was densest in the crypt.

1.3.2 Limbal stem cell niche

Niche is the special microenvironment around SC that consists of cellular and extracellular components (Li et al., 2007). Niche regulates the self renewal and fate of SC. Niche provides protection against external stimuli that leads into differentiation and apoptosis. In limbus the anatomic structure of palisades of Vogt indicate that it could be the SC niche. The undulating structure of the palisades results in close contact of the basal cells with limbal stroma. Limbal stroma is highly vascularised and innervated compared to cornea. The cells in stroma are poorly defined. However, presence of mesenchymal cells has been indicated in limbal stroma (Polisetty et al., 2008).

As aforementioned, LEC are now being studied for the possibility of being SC niche. Eventhough corneal SC niche is not fully characterized or defined, several studies pointed to the unique features of limbus and its basement membrane (BM) that could contribute to its 'niche' nature.

The BM of limbus is different from cornea in its composition. Laminin α2-β2 chains and collagen α1, 2 chains are present only in limbus. Alpha-3 chain of collagen is present in cornea (Tuori et al., 1996) while it is not there in limbus. The BM may have a role in determining the SC distribution (Li et al., 2007). The BM of the limbal epithelium shared many similarities with that of the conjunctival epithelium (Schlotzer-Schrehardt et al., 2007), including positive labelling for type IV collagen α1 and α2 chains, laminin α5, β2, and γ1 chains, nidogen-1 and -2, and thrombospondin-4. However, type IV collagen α3, type V collagen, fibrillin-1 and 2, thrombospondin-1, and endostatin were present in the corneal BM, which were lacking or more weakly expressed in the limbal and conjunctival BMs. As compared to both the corneal and conjunctival BMs, the limbal BM showed a markedly increased immunoreactivity for laminin α1, α2, β1 chains, agrin, laminin γ3 chain, BM40/SPARC and tenascin-C.

Melanocytes in the limbal basal region could be possibly niche cells as they help in protection of limbal cells from UV damage by transferring melanin pigment to the epithelial cells (Higa et al., 2005). Melanin pigments were found at the apex of cytokeratin 19 positive cells, forming a pigmented cap towards ocular surface. Melanocytes were reported to possess dendritic processes that extend to the neighbouring epithelial cells. Limbal stromal microenvironment has an important role in maintaining the SC niche (Espana et al., 2003). When corneal epithelium is recombined with live

limbal stroma, the basal cells lose their cytokeratin 3 (CK3) and connexin 43 expression indicating de-differentiation. On the other hand, limbal basal cells acquired CK3 expression when recombined with corneal stroma.

Niche could be characterized by slow cycling cells or the unique protein expression pattern. Slow cycling detection technique has not been extensively used to identify cellular components of limbus. Eventhough, expression of some proteins vary in limbus compared to cornea or conjunctiva, nothing could be kept as bona fide marker. A set of markers are analysed for their expression in limbus and such a pattern may be used to predict niche.

Connexin 43, a gap junction protein is absent in basal layers of limbus while it is present in all other layers of cornea (Dong et al., 1994; Matic et al., 1997; Wolosin et al., 2000). It was proposed that light staining of Connexin 43 indicated TAC and complete absence indicated SC. Absence of gap junction segregates SC from surroundings, thus protecting them from adverse influences.

Cytokines are likely to play a role in LSC regulation. In the ocular surface, they can be divided into four groups out of which three constitute the network of potential epithelial-mesenchymal cytokine dialogue (Li and Tseng, 1995). Those which are important for epithelial-mesenchymal interaction are: type I: cytokines released from epithelial cells to modulate fibroblasts, type II: regulators of both epithelial and fibroblast cells and type III: produced by corneal epithelial cells. Some of these cytokines are likely to be important for SC maintenance. Transforming Growth Factor β (TGFβ) 1, 2, and 3 receptors are located in the limbal epithelium. Since TGFβ is known to inhibit LSC proliferation, it may play a role in SC maintenance in the limbus (Boulton and Albon, 2004). Indeed many cytokines and growth factors have been suggested to affect SC regulation, cell proliferation and migration (Daniels et al., 2001; Imanishi et al., 2000).

1.3.3 Evidence of SC in limbus

1.3.3.1 Laboratory evidence

A comparison between cultures of central cornea, peripheral cornea and limbus showed that limbal cells grow better than those in peripheral cornea which in turn was more than those in central cornea (Ebato et al., 1987; 1988). It was shown that doubling time of limbal cells were 80 ± 14 hours (h) while that of peripheral corneal cells were 131

± 25 h. The limbal cells were uniformly small and polygonal cells, but peripheral corneal cells reached a variety of sizes.

It was demonstrated that limbal basal cells gave rise to holoclones in cultures while corneal basal cells gave rise to meroclone and paraclone colonies (Pellegrini et al., 1999). Cells that form holoclones in culture are primitive SC. Cells forming smaller 'meroclones' and abortive 'paraclones' represent different stages of TAC (Barrandon and Green, 1987). Eventhough on stimulation, limbal basal cells can exhibit high proliferative capacity, normally they are established to be slow cycling cells using tritiated thymidine assay (Cotsarelis et al., 1989).

A 64 kilo dalton (kDa) cytokeratin protein, CK3, was found in central cornea and suprabasal layers of limbus but not in limbal basal cells. It was hypothesised that cells acquire this protein as they go through differentiation pathway and hence limbal basal cells are less differentiated (Schermer et al., 1986). p63, a transcription factor essential for regenerative proliferation, was suggested as a marker of LSC (Pellegrini et al., 2001). p63 was detected in the basal layers of limbal epithelium and in holoclones formed by limbal cells in culture. Yeung et al, reported regional variations in expression of desmoglein, a cell membrane protein and tenascin C, extra cellular matrix (ECM) protein in limbus (Yeung et al., 2008). Desmoglein was lowest in LEC while suprabasal layers of limbus had the greatest expression. Tenascin C was expressed highest in LEC while it was lower in upper layers of limbus. Alpha-9 integrin and N-cadherin are expressed by LSC. Limbal basal cells uniquely stain for some other markers like ABCG2 (de Paiva et al., 2005; Watanabe et al., 2004) and Keratin 19 compared to corneal epithelium and suprabasal layers of limbus. ABCG2 is a member of ATP binding cassette transporters and is found in many other SC. De Paiva et al reported that 2.5%-3.0% of the limbal cells were positive for ABCG2 and could be sorted by flow cytometry. ABCG2 positive cells had high colony forming efficiency in culture.

Small cell size with high nuclear cytoplasmic ratio (Arpitha et al., 2005) of certain cells in the basal layer of limbus is considered as another indication of their SC properties. Confocal microscopy (Romano et al., 2003) and flow cytometry (De Paiva et al., 2006) had demonstrated that small cells are present in limbal basal layer compared to corneal basal layer. According to electron microscopy observations, the basal cells of the limbal epithelium demonstrates features of immature cells such as small cell size with a

cytoplasm rich in tonofilaments, euchromatin- rich nuclei and barely detectable nucleoli (Chen et al., 2004).

Transmission electron microscopy studies (Schlotzer-Schrehardt and Kruse, 2005) revealed two types of cells in the epithelial papillae of limbal Palisades of Vogt. According to their studies, few small putative SC were found surrounded by larger melanin containing early putative TAC. The putative SC did not form any cytoplasmic processes to connect to underlying matrix. They were found resting on a delicate BM with heterochromatin rich nuclei, without distinct nucleoli, a sparse cytoplasm containing minute melanin granules, few mitochondria, ribosomes and few intermediate filaments. Hemidesmosomes and intercellular junctions were largely absent. On the other hand, putative TAC contained nuclei with increased euchromatin and distinct nucleoli, prominent melanin granules and tonofilament bundles and cell processes interdigitating with the underlying matrix. Synchrotron infrared microspectroscopy studies coupled with multivariate analysis suggested that there are significant differences in the conformation of nucleic acids between SC and TAC (German et al., 2006).

1.3.3.2 Clinical evidence

Several studies showed that cells migrate from limbus to the centre of cornea in a centripetal manner in normal epithelial turnover eventhough it is slow compared to wound healing. In experimental animals, it was observed that limbal pigment migrate onto clear cornea after inducing trauma (Mann, 1944). Donor cornea of opposite sex from that of host was used in rabbits to study the replacement of donor tissue in eye (Kinoshita et al., 1981). When sex chromatin analysis was performed after different time intervals, they observed a time dependent decrease of donor corneal epithelium. More evidence was provided by the observation of movement of epithelial microcysts from the suture line to donor cornea (Kaye, 1980). Cells from the donor tissue of limbal allograft were found to survive for a long time compared to that from penetrating keratoplasty (Shimazaki et al., 1999). By using India ink, centripetal migration of limbal cells to corneal epithelium was demonstrated in mouse (Buck, 1979; 1985). Full thickness of corneal epithelium was removed in rabbits and it was observed that wound was repaired completely within 12 to 16 h. Role of cells from peripheral cornea was understood by the movement of Indian ink markers placed in them. Buck et al (Buck, 1979) had also studied the distance migrated to the central region by superficial and wing cells from peripheral cornea using same

technique. Migration of pigment onto central cornea has been described in humans also (Goldberg and Bron, 1982).

Removal of limbal epithelium led to an abnormal corneal epithelial wound healing which was characterised by conjunctival epithelial ingrowth, vascularisation and delayed healing with recurrent erosion, which gives further evidence to the role of these cells in proper corneal epithelial regeneration (Chen and Tseng, 1990; 1991). Use of limbal cells for reconstruction of corneal surface in ocular injuries is a clinical evidence for limbal location of SC. Further evidence come from the fact that limbus is the predominant site for corneal tumour formation (Waring et al., 1984).

1.3.4 Characteristics of LSC

Stem cell has been defined as 'a cell that can continuously produce unaltered daughters and also has the ability to produce daughter cells that have different, more restricted properties' (Smith, 2006). From the above cited evidences, characteristics of LSC (Schlotzer-Schrehardt and Kruse, 2005) can be summarised as:

- Low differentiation with a primitive phenotype
- Slow cell cycle with presence of label retaining cells
- High proliferative capacity after activation through wounding or in *in vitro* culture conditions
- Potential to form holoclones in culture
- Ability for unlimited self renewal
- High nuclear cytoplasmic ratio with a small size

1.3.5 Role in corneal epithelial maintenance

Limbal stem cells have the capability of asymmetric cell division giving rise to self renewal and TAC. The TAC will undergo further cell divisions and migrate both horizontally and vertically to the central cornea where they differentiate terminally and desquamate. The number of cell divisions that TAC can undergo depends upon the environmental signals.

It was reported that physical wounding of corneal epithelium led to replication of slow cycling cells (Lavker et al., 2004). The undisturbed TAC has 72 h cell cycle time while induced TAC cycle time is 24 h and they can undergo additional cell divisions than

normal. The extent of involvement of limbal or peripheral corneal cells in wound healing depends also on the size of epithelial defect (Sandvig et al., 1994).

But whether this process has any role during homeostasis is still controversial. Kinoshita suggested that LSC may not be producing TAC constantly to renew central corneal epithelium (Kinoshita, 2008). According to his opinion, TAC may be having more proliferative capacity than the researchers think of. According to a group that did theoretical kinetic analysis of centripetal movement velocity (Sharma and Coles, 1989), the velocity was 100 to 200μm per week which indicated that cells from limbus will take 6 months to reach central cornea.

1.4 Limbal Stem Cell Deficiency (LSCD)

When limbal basal epithelium or limbal stroma is damaged, then a condition termed limbal stem cell deficiency arises. Deficiency in SC automatically leads to limited renewal of epithelium and abnormal epithelial regeneration. Thus LSCD results in poor epithelial regeneration, chronic stromal inflammation, corneal vascularisation and conjunctival epithelial ingrowth. Other symptoms include reduced vision, photophobia, recurrent pain, melting and perforation of cornea (Dua et al., 2000). Out of this, conjunctivalisation serves as the sine qua non criterion of LSCD as most of the other symptoms are common for other corneal diseases. The conjunctivalised corneal surface always shows a stippled late staining pattern with fluorescein. It is thinner than adjacent normal corneal epithelium, irregular, prone to recurrent erosions and attracts new blood vessels (Dua et al., 2000). Conjunctivalisation can be suggested by loss of palisades of Vogt under slit lamp microscope and late fluorescein staining (Dua et al., 1994). The definitive diagnosis is given by impression cytology of corneal surface followed by staining for goblet cells (Puangsricharern and Tseng, 1995). Impression cytology refers to the application of a cellulose acetate filter to the ocular surface to remove the superficial layers of the ocular surface epithelium (Singh et al., 2005). Correct diagnosis is needed in corneal diseases with LSCD as penetrating keratoplasty may fail in these cases. Grafted corneas will not be a permanent cure as those corneal epithelial cells have only a limited life span.

Limbal stem cell deficiency can be classified into different types based on different factors like etiology and extension of affected area. It can be either hereditary in which stem cells are congenitally absent/dysfunctional or acquired. Aniridia and

epidermal dysplasia are examples for hereditary LSCD while chemical burns and Steven Johnson Syndrome are examples for acquired. Based on etiology factors, LSCD can be divided into two categories (Puangsricharern and Tseng, 1995). Category I (secondary LSCD) comprises of diseases with a known etiology like chemical/thermal burns, multiple surgeries and contact lens wear. Category II (primary) do not have a clear history and results in gradual loss of SC functions over time, probably due to malfunctioning of limbal stroma. Some of the examples are aniridia, congenital erythrokerato-dermia and keratitis associated with multiple endocrine deficiencies. When patients show signs of LSCD with no disease conditions, it is termed as idiopathic LSCD (Espana et al., 2002). If the LSCD is developed as a result of ocular surgeries or chronic medical treatment, it is considered as iatrogenic LSCD (Holland and Schwartz, 1997; Schwartz and Holland, 1998). LSCD can also be categorized as localized/partial or diffuse/complete (Ang and Tan, 2004; Dua and Azuara-Blanco, 2000b). In localized LSCD, there will be some sectors of healthy limbal tissue. Based on the eyes affected, they can be unilateral or bilateral.

1.4.1 Treatment for partial LSCD

1.4.1.1 Sequential sector conjunctival epitheliectomy

Partial LSCD is treated based upon the extension of conjunctivalisation on corneal surface. If the patient is asymptomatic and visual axis is clear, then surgical intervention is unnecessary. If visual axis is covered, sequential sector conjunctival epitheliectomy could be performed (Diaz-Valle et al., 2007; Dua et al., 2000). In this procedure, the conjunctival epithelium is debrided by scraping under slit lamp microscope after applying topical anesthesia. This improves vision by enhancing corneal epithelialisation of visual axis and can be done even when only two clock hour of intact limbal tissue remains. Yet, two clock hour limbal tissue is not sufficient to form a normal corneal epithelium all over corneal surface as it induces overexhaustion of the limbal epithelium. In order to enhance re-epithelialisation of cornea in such cases, amniotic membrane (AM) could be transplanted along with surgical removal of conjunctivalisation (Diaz-Valle et al., 2007).

1.4.1.2 Ipsilateral limbal translocation

Ipsilateral limbal translocation is another treatment method for partial LSCD (Nishiwaki-Dantas et al., 2001). The healthy region of limbus was translocated to the deficient area without intervening in the contralateral eye. Complete re-epithelialisation

and regression in edema and stromal inflammation was observed. The group suggested that the procedure redistributed limbal population in eye and thereby enhanced normal healing.

1.4.1.3 Amniotic membrane transplantation (AMT)

Amniotic membrane transplantation was done in cases of partial LSCD after superficial keratectomy to remove conjunctivalised surface (Anderson et al., 2001a). A follow up period of 25.8 months revealed no recurrent epithelial erosion or epithelial defect. Another group also suggested AMT as an effective means of visual rehabilitation in partial LSCD (Sangwan et al., 2004). For reconstruction of corneal surface, AMT with fibrin glue (Kheirkhah et al., 2008) was also reported, making it suture less.

1.4.2 Treatment for total LSCD

Based upon whether single or both eyes are involved, treatment may differ. If it is unilateral, autograft could be performed and if it is bilateral, allograft would be an option. Amniotic membrane transplantation and *ex vivo* expansion of cells are also other treatment methods for total LSCD.

1.4.2.1 Autograft

Autografts are limited to unilateral LSCD or diffused bilateral ones. For this procedure, sufficient amount of healthy limbal tissue for harvesting should be available (Ang and Tan, 2004). Usually the procedure involves transfer of two grafts of limbal tissue from unaffected or less affected eye to the severely injured eye (Kenyon and Tseng, 1989). This technique had been reported as a treatment method for different types of LSCD such as acute and chronic chemical burns, thermal burns, contact lens induced keratopathy and LSCD developed due to multiple surgeries. According to the surgical results by Kenyon, autografts helped in rapid surface healing, increased visual acuity and regression of all symptoms of LSCD (Kenyon, 1989). Autografts were also used for treatment of recurrent and advanced pterygia with no further recurrence (Shimazaki et al., 1996). It was reported that epithelialisation was completed within 12 days after doing autografts (Frucht-Pery et al., 1998). As fairly large limbal pieces are needed for this procedure, there is a chance of surgically induced LSCD formation in healthy eye, which is one of the major disadvantages of the procedure (Ang and Tan, 2004).

Limbal grafts always include a carrier tissue along with LSC. The carrier tissue can be either conjunctiva (conjunctival limbal graft) or peripheral cornea (keratolimbal graft). Dua and Azuro-blanco used 2 mm of peripheral cornea and 3 mm of bulbar conjunctiva as carriers for limbal autograft in order to provide sufficient microenvironment for the SC (Dua and Azuara-Blanco, 2000a). They also closely monitored growth of conjunctival epithelium over cornea postoperatively to ensure proper corneal epithelialisation.

Amniotic membrane transplantation was also reported along with autografts for the treatment of unilateral LSCD. Use of AM was reported in both recipient and donor eyes to facilitate healing and relief after autograft (Meallet et al., 2003).

1.4.2.2 Allograft

This can be either from cadaveric eye or from Human leukocyte antigen (HLA) matched living relative donor. From cadaveric eye, the whole 360 degree limbus can be transplanted into the recipient. Fresh eyes were usually collected to obtain healthy limbal cells (Dua and Azuara-Blanco, 1999a). Dua and Azuara-Blanco described a modified technique for allo-limbal transplantation from cadaveric eyes. They dissected the peripheral cornea, limbus and 1-2 mm conjunctiva by superficial lamellar dissection after trephining the central cornea out. The graft tissue contained an open ring of peripheral, limbal & conjunctival epithelium (wherever available) and superficial corneal, limbal & scleral stroma. Postoperative immunosuppression was given with FK-506 for 18 months after surgery.

Tsai and Tseng had also reported use of cadaveric limbus as allograft after removing the fibrovascular pannus from the recipient eyes using superficial lamellar keratectomy (Tsai and Tseng, 1994). Oral cyclosporine was given for immunosuppression.

HLA matched living relatives can be used as donors as this may reduce risk of immunorejection. Similar to autograft procedure, two '2 clock hour' limbus from donor would be transferred to the recipient eye after removing fibrovascular pannus (Daya and Ilari, 2001). Allograft was reported to be better when combined with penetrating keratoplasty (Ozdemir et al., 2004). Use of AM along with allografts were also reported (Gomes et al., 2003; Tseng et al., 1998).

The main disadvantages of allografts are the risk of rejection and the administration of immunosuppressants for a long time after surgery. Systemic immunosuppression is needed even if the donor is an HLA matched relative. Compared to autografts, failure rate of allografts is high. Eventhough early successes were reported with allografts, subsequent follow ups showed that fifty percent of these fail within three to five years (Ang and Tan, 2004; Ilari and Daya, 2002; Solomon et al., 2002).

1.4.2.3 Tissue engineered constructs

Tissue engineered constructs with *ex vivo* expansion of limbal or alternative cell source on different substrates are now being employed for corneal surface reconstruction especially in cases of LSCD, due to the disadvantages of the current treatment methods. This technique enables formation of epithelial structures from small biopsies, size ranging from 1-2 mm^2. The expanded cell sheet with or without substrate is then transplanted to the stromal bed after clearing the conjunctival epithelium from corneal surface. The most commonly used substrate is AM. Due to many disadvantages of AM like risk of disease transmission, carrier free constructs using polymeric substrates became an interesting research area in corneal tissue engineering (TE).

A brief introduction to TE and its applications in the treatment of LSCD are detailed below.

1.5 Tissue engineering

According to Langer and Vacanti, 'Tissue engineering is an interdisciplinary field that applies the principles of engineering and life sciences toward the development of biological substitutes that restore, maintain, or improve tissue function' (Langer and Vacanti, 1993). This field is being broadened by scientists all over the world with the scope of overcoming donor organ shortages eventually. Injecting cells, enhancing tissue formation *in vivo* by providing growth factors and reconstructing a tissue substitute by seeding cells on artificial/biological scaffolds are different modes of TE. Tissue reconstruction now includes the addition of growth factors or necessary cues in the scaffold for the formation of three dimensional structures with vascularisation and even nerve regeneration.

1.5.1 Cell sources

Limbus is the main source of cells for reconstruction of corneal epithelium. Epithelial cells can be cultured from either cell suspension or explants of limbal tissue. For treatment of partial and diffused total LSCD, a small biopsy from the contra-lateral eye of patient could be taken which would be then expanded *ex vivo*. The limbal tissue could be treated with dispase II and other enzymes like trypsin to make cell suspension which can then be seeded directly onto the substrates or after a passage on polystyrene dishes (Du et al., 2003). Limbal expansion from explants was reported by different groups. Initial treatment of explants with dispase II was also reported (Hernandez Galindo et al., 2003; Meller et al., 2002).

If the LSCD is bilateral and complete, scientists have to depend on allogeneic cell sources and this may lead to rejection or prolonged immunosuppressive therapy. In order to avoid that, researches are being carried out to look into alternative sources for autologous cells. There are reports available about looking into the feasibility of oral mucosal cells as an alternative (Kinoshita et al., 2004; Kinoshita and Nakamura, 2004; Nakamura and Kinoshita, 2003). Oral mucosal biopsy specimen of 3-4 mm^2 would be taken from oral cavity under anaesthesia. It could be used as explants or single cell suspension for the expansion of the cells. The cytokeratin profiling of these cultured cells showed that they are similar to limbal epithelial cells (LiEC) (Madhira et al., 2008). Some of the SC markers like Np63 and p75 are also expressed in both cell types. Long term follow ups are necessary to understand how these cell sheet constructs behave on corneal surface. In a midterm follow up, it was reported that all the eyes after oral mucosal sheet transplantation manifested some extent of peripheral corneal vascularisation (Inatomi et al., 2006). After 2 years of follow up, the central corneal surface was found to be covered with oral mucosal cells (Satake et al., 2008), which means these cells had not acquired the properties of corneal cells completely. They have also observed that in some cases, conjunctival cells gradually invaded to the central cornea.

Eventhough conjunctivalisation of corneal surface is a bonafide marker of LSCD, conjunctival epithelium was also reported as an alternative source of autologous cells (Tanioka et al., 2006). The culture conditions used in the experiment rendered the conjunctival epithelial cells to act phenotypically as corneal epithelium. As in the case of oral mucosal cells, long term study is necessary to determine whether the conjunctival

cells will differentiate to goblet cells *in vivo* on the corneal surface even though they resembled corneal cells *in vitro*.

Mesenchymal stem cells (MSC) from bone marrow was also reported to be used for reconstruction of corneal surface in rats (Ma et al., 2006). Vision in rat eyes was improved after transplantation of MSC on AM compared to the controls. Interestingly, these cells did not differentiate into corneal epithelial cells. It was suggested the effect of MSC could be due to inhibition of inflammation and angiogenesis. Effect of systemic application of MSC in cases of partial LSCD due to alkali burn was also reported (Ye et al., 2006). Presence of pre-labelled MSC in cornea and limbus after its systemic application was observed. They suggested that these MSC enhanced wound healing and cell proliferation, resulting in a clearer cornea and thus could be used as a treatment method for alkali burns.

As embryonic stem cells (ESC) are pluripotent, attempts were done to differentiate these cells to corneal epithelial cells. Human ESC had been differentiated into corneal epithelial like cells by providing limbal microenvironment which included collagen IV coated substrate and limbal fibroblast conditioned medium (Ahmad et al., 2007). Mouse ESC were induced to form epithelial progenitor cells by culturing on collagen IV and transferred to damaged corneas (Homma et al., 2004) where a complete re-epithelialization was observed.

1.5.2 Feeder layer

Use of feeder layers had acted as a pre requisite for limbal cell culture (Koizumi et al., 2001; Nakamura et al., 2003; Nishida et al., 2004a). The most commonly used one is 3T3 mouse fibroblast feeder layer. The cells, either single suspension or explants, can be directly cultured on the mitomycin treated feeder layers. Otherwise, 3T3 cells are cultured in wells and the limbal cells are cultured on culture inserts kept in these wells, enabling availability of secretory factors from feeder layers indirectly. Koizumi et al cultured limbal explants on AM with indirect 3T3 coculturing and airlifting (Koizumi et al., 2001). Airlifting involves reducing the amount of media and thereby exposing the upper surface of cells to air. J2-3T3 (Pellegrini et al., 1999) and NIH/3T3 (Nishida et al., 2004a) were reported to be used as feeder layer in limbal cell culture. Nishida et al discussed that J2-3T3 promotes better colonisation. Therefore, the property of the limbal cells might change based on the feeder layers used. Human ESC grown on 3T3 feeders incorporated

non human sialic acid, N-glycolylneuraminic acid (Neu5GC), to which there are antibodies in human system (Martin et al., 2005). Food and Drugs administration, USA has classified products generated using 3T3 feeder layers as xenogeneic (Murakami et al., 2006). Attempts to develop human amniotic epithelial cells as feeder layer for limbal cell culture after treatment with mitomycin-C had been reported (Chen et al., 2007). Another report suggested use of human adipose derived MSC as novel feeder layer (Sugiyama et al., 2008). MRC-5, a human fibroblast cell line was also used as feeder layer for limbal cell culture in serum free conditions in order to attain xenobiotic-free culture system (Notara et al., 2007).

1.5.3 Substrates

Eventhough substrates for corneal epithelial reconstruction should comply with several criteria of scaffolds for TE; it should be different in certain aspects due to the special functions of cornea. As the general criteria, substrates should favour adhesion and growth of cells and should not be toxic to cells or produce inflammatory response *in vivo*. But at the same time, if transplanted, they should not hinder vision and should be as close as to the refractile and transmissible properties of cornea. Some of the major substrates for corneal epithelial reconstruction are detailed below.

1.5.3.1 Fibrin gel

Fibrin, a product from fibrinogen, during clot formation is widely used in medical applications. It is usually generated *in vitro* by mixing fibrinogen and thrombin solution in presence of sodium chloride, calcium chloride or some cross linking factors. Fibrin is used in the form of fibrin glue in the field of vascular TE. Some of the other applications reported for fibrin were as delivery system for growth factors (Bhang et al., 2007) and as bone substitute in bone TE (Kneser et al., 2005).

There are reports available about their use in ocular surface construction also. Limbal cells were cultured on fibrin gel in presence of 3T3 feeder layers, which was then transplanted to total LSCD patients after airlifting (Rama et al., 2001). According to their observation, clonogenicity, morphology and growth rate of limbal cells on fibrin gels were similar to that on plastic. One year follow up of the experiment proved that corneal surface was covered with CK3 positive cells. However, visual acuity was not significantly improved even after one year, maybe due to stromal scarring.

Another group from Canada has also reported the use of fibrin gels in the expansion of limbal cells and subsequent transplantation in rabbits (Talbot et al., 2006). They had done the follow up at short time periods after surgery and had reported degradation of fibrin gel within seven days of transplantation. The suitability of cross-linked fibrin gel for potential transplant was analysed by studying the growth kinetics and phenotype of human epithelial SC after suspending in fibrin gel (Han et al., 2002).

1.5.3.2 Amniotic membrane

It is the inner layer of the fluid filled foetal sac with a single layer of epithelial cells, a thick basement membrane and an avascular stromal matrix (Endo et al., 2004). It appears one week following conception. The apical surface of epithelial cells has many microvilli and the intercellular junctions between epithelial cells are formed by desmosomes. The ultrastructural details of amniotic epithelium give indication of the specialised functions. These epithelial cells are specifically adapted for being a protecting layer, secretory layer and intercellular & transcellular transport (Dua and Azuara-Blanco, 1999b). The prominent BM has similarities to conjunctival and corneal BM. It has been reported that α5 chain of collagen IV is present both in AM and corneal BM (Endo et al., 2004).

The use of AM in surgical treatment was first reported by Davis in 1910 (Dua and Azuara-Blanco, 1999b). Amniotic membrane is used as a biological dressing in skin burns and chronic ulcers. It could also be used as an adjunctive in vaginal reconstruction and to prevent tissue adhesion in different surgical procedures. Its use in ophthalmology is reported from 1940s eventhough its use has been tremendously increased since last two decades. Several properties of AM favoured its use in treating ocular surface disorders. Amniotic membrane can be used either as a bandage/support (Anderson et al., 2001a) or as an epithelial construct after *ex vivo* expansion of corneal cells for transplantation (Koizumi et al., 2001). Therapeutic use of AM was already reported for treating various corneal disorders like LSCD, band keratopathy (Anderson et al., 2001b), neurotrophic corneal ulcers (Khokhar et al., 2005), conjunctival disorders like vernal conjunctivitis (Sridhar et al., 2001), conjunctival melanoma (Paridaens et al., 2001), in glaucoma and oculoplastic surgery.

1.5.3.2.1 Properties of AM

Many reports suggested that AM promotes epithelialisation. It could be acting as a temporary BM on which the remaining limbal cells can grow in cases of partial LSCD. Basement membrane helps adhesion and migration of epithelial cells. Various growth factors in the AM also may be helping epithelial growth. There are reports (Deolinda de Oliveira Pena et al., 2007; Koizumi et al., 2000b) of presence of TGFβ, Epidermal Growth Factor (EGF), Fibroblast Growth Factor, Keratinocyte Growth Factor (KGF), Interleukin-10, Hepatocyte Growth Factor (HGF) and various other growth factors in AM. EGF, KGF and HGF are strong mitogens of corneal epithelial cells (Kinoshita et al., 2001), but these growth factor levels are reduced in preserved AM as the epithelial cells are no more viable.

Amniotic membrane has also been shown to prevent cellular apoptosis. Reduction of apoptosis was reported in corneal keratocytes after applying AM to eyes which underwent excimer laser photoablation in rabbits (Wang et al., 2001). Human limbal cells cultured on intact AM demonstrated fewer apoptotic cells as compared with those on plastic dishes (Sun et al., 2006). cDNA microarray analysis and other confirmation tests revealed that interleukin receptor antagonist is expressed in large amounts in cultures on intact AM. While AM was reported to reduce apoptosis in these cells, it had also been reported as inducing apoptosis on activated macrophages.

It was suggested that AM can serve as a SC niche for limbal basal cells (Grueterich et al., 2003). Nerve growth factor (NGF) signaling was reported to favour LSC survival (Touhami et al., 2002). Nerve growth factor is found in high and therapeutic levels in AM and blocking of NGF significantly reduced expansion of limbal cells. Intact AM has maintained limbal epithelial phenotype, as shown by staining for connexin 43 and BrdU assay for cultures (Grueterich et al., 2002).

Amniotic membrane is reported to be antifibrotic. While in contact with corneal fibroblasts, it downregulates TGFβ1 signaling in these cells, thereby reducing fibroblast activation. Production of TGFβ1, Interleukin-8 and granulocyte-macrophage stimulating factor was reduced in conjunctival fibroblast cultures on AM compared to that on plastic dishes, indicating anti-inflammatory property of AM (Solomon et al., 2005). During AMT, AM is usually sutured with the basement membrane up. The stroma of AM that is

in contact with ocular surface is avascular and thus believed to inhibit formation of new vessels.

1.5.3.2.2 Disadvantages of AM

Eventhough AM has several properties that could help its use as a treatment option for ocular surface disorders, failures of AMT were also reported by different groups. Joseph et al reported that AMT did not help to restore the ocular surface in case of severe acute burns (Joseph et al., 2001). Maharajan et al suggested that use of AMT can be associated with a number of failures (Maharajan et al., 2007). They observed that only 62.5% AMT were successful even in presence of functioning stem cells. The failures of AMT could be mainly attributed to inter and intra variations in different AM. Variations in the levels of TGFβ1 was reported even within different regions of AM (Hopkinson et al., 2006b). Different factors like the health of mother and foetus and habits of mother (eg: smoking) can affect the quality of AM. Handling and preservation techniques of AM can also affect the success of AMT.

Amniotic membrane, being a biological substrate can be a carrier for many transmissible diseases. The donor has to be checked for certain infections during procurement of AM and after 6 months which makes the use of AM possible only after this period (Dua and Azuara-Blanco, 1999b). This is to allow a window period for some conditions like HIV infections. Even then, the donors are not tested for diseases like Creutzfeldt–Jakob disease (CJD).

1.5.3.3 Stimuli responsive polymers

These are materials that can undergo conformational or phase changes in response to various environmental stimuli (de Las Heras Alarcon et al., 2005). They are also called 'smart', 'intelligent' or 'environmentally sensitive' polymers. These polymers find a wide variety of applications including microfluidic systems (Barker et al., 2000), drug delivery (Kikuchi and Okano, 2002), nanoscale technologies, and cell sheet engineering. Most of the research work had been done in this field using light, electric signals, pH and temperature as stimuli. The polymer response is usually due to many co-operative interactions like progressive ionization or loss of hydrogen bonding, which eventhough individually small, will lead to a final large structural change (de Las Heras Alarcon et al., 2005).

Photoresponsive polymers are those that have photochromic molecules in their macromolecular structure (Casolaro, 1998). On irradiation, these moieties undergo reversible stereochemical arrangements which results in structural changes. Photoresponse effects include light induced variations in viscosity and solubility and regulation of binding and releasing of drugs. pH responsive hydrogels find its biggest application in drug delivery systems due to the existence of different pH in different parts of the body. For example, gastric pH is low compared to that in intestine region. Thus, a pH responsive material can deliver drug in one of these regions avoiding the other. These hydrogels are prepared with ionizable groups, mainly carboxyl, sulfonic and amino groups.

Thermoresponsive polymers act on the stimulus of temperature.

1.5.3.3.1 Thermoresponsive polymers

The temperature around which phase transition occurs in these types of polymers is called lower critical solution temperature (LCST) or cloud point. Below this temperature, the polymers will be hydrophilic by forming hydrogen bonds with water molecules in the surrounding. As the temperature shifts above LCST, the polymer becomes hydrophobic by loosing the hydrogen bonds. When the temperature increases, the entropic state gains over the enthalpic state of hydrogen bonding.

Different polymers with hydrogen bonding sites show this property of change in behaviour due to shift in temperature. Some of them are poly (N-vinyl caprolactam) (PVCL), copolymers of poly (propylene oxide) and poly (ethylene oxide) (PPO-PEO) and poly (N-isopropylacrylamide) (PIPAAm). PVCL becomes hydrophobic in the range of 25-35^{o}C. Copolymers of PPO-PEO become semi solid gels above LCST and find application in pharmaceutical industry.

N-isopropylacrylamide (NIPAAm), chemical formula of $C_6H_{11}NO$, is classified as a hazardous and toxic chemical in the form of monomer. But PIPAAm is a non toxic temperature responsive polymer that was initially used in immunoassays, chromatographies and drug permeation studies. Poly (N-isopropylacrylamide) became an interesting candidate in biomedical field as its LCST (32^{o}C) lies close to body temperature/optimum culture temperature. Along with the optimum LCST, presence of hydrophobic isopropyl groups made it a promising material in drug delivery systems. The hydrophobic group will interact with cells and proteins inside the body above LCST.

Micelles, shells or hydrogels of PIPAAm and its copolymers had been widely used for delivering drugs (Chung et al., 1999; Kim et al., 2000; Zhang et al., 2002). This polymer had found its application in different chromatography techniques also (Kanazawa et al., 1997; Lakhiari et al., 1998; Yamanaka et al., 2003). The polymer allows attachment and growth of cells above LCST while it favours detachment of the cells due to its hydrophilic nature below its LCST. Thus cells could be obtained as a contiguous sheet with cell-cell and cell-ECM interactions. As the temperature shift enabled phase transition property, the polymer was utilised for two or three dimensional manipulation of cultured cells.

1.5.3.3.2 Poly (N-isopropylacrylamide) as cell culture substrate

Use of PIPAAm in culturing and detaching cells was first reported by Takezawa et al. They cultured human dermal fibroblasts on PIPAAm surfaces conjugated with collagen (Takezawa et al., 1990). Monolayered fibroblasts were detached by incubating under LCST of the polymer. Thus, they suggested that the polymer provides a potential technology in cell culture. Around same time, Yamada et al reported hepatocyte culture on tissue culture polystyrene (TCPS) dishes grafted with PIPAAm (Yamada et al., 1990). After some years, another group from Canada reported similar work using a copolymer of PIPAAm (Rollason et al., 1993). In their work, they cultured a cell line on a copolymer of NIPAAm and N-t-butyl acrylamide with an LCST of 8^{o}C. They also demonstrated retrieval of cells by incubating at 4 ^{o}C for 1 h.

The extensive study and use of this polymer in TE field was carried out by a Japanese group led by Teruo Okano. Their first report of the polymer was about its use in retrieving bovine endothelial cells and rat hepatocytes (Okano et al., 1993). The cell detachment from the polymer surface is not only due to the hydration of polymer below its LCST, but also by active cell metabolism (Okano et al., 1995). Sodium azide, an inhibitor of ATP synthesis was used to demonstrate the role of cellular metabolism in the process. Role of intracellular signalling and cytoskeletal organisation in cell detachment process was also demonstrated by the same group. Genistein, a tyrosine kinase inhibitor, cycloheximide, a protein synthesis inhibitor and phalloidin, actin stabiliser was used in addition to sodium azide to study the cell metabolic processes during cell detachment (Yamato et al., 1999).

The conventional method to harvest cells from a substrate is to use enzymes like trypsin or dispase. Trypsin treatment results in single cell suspension where cell-ECM and cell-cell junctions/interactions are not preserved. Similarly dispase also degrades deposited ECM to detach cells from substrate. The use of the polymer in maintaining cell-ECM interactions was showed by Kushida et al. Using immunoblotting and immunofluorescence, they showed that fibronectin (FN) deposited by the cells during their growth was also recovered from the polymer surfaces during detachment (Kushida et al., 1999). When hepatocytes cultured on FN precoated polymer surfaces was retrieved, it was found that FN remained intact on places where there was no direct cell attachment (Yamato et al., 2000). This showed that cellular activity might be needed for release of FN during detachment.

Molecules like insulin were entrapped in the grafted polymer to make it available for the basal side of cells cultured on the polymer surface so that growth rates would be enhanced (von Recum et al., 1998). The grafting density influenced availability of the entrapped molecules to the cells.

Various types of cells were cultured on the thermoresponsive polymer and shown to maintain their functions after retrieval of cell sheet. These include corneal endothelial cells, renal epithelial cells, vascular endothelial cells and cardiomyocytes. For instance, retrieved corneal endothelial cell sheets maintained Na+, K+ ATPase activity and tight junctions by which it preserve proper hydration of corneal stroma (Sumide et al., 2006). The polymer was also exploited for developing three dimensional tissue structures by layering individual cell sheets harvested separately. Cardiac patch like structures were generated by layering cardiomyocyte cell sheets (Shimizu et al., 2002). Similar attempts to create three dimensional tissue structures using PIPAAm was reported from our laboratory (Anil Kumar et al., 2007b).

Cell sheet engineering, a term coined by the group of Okano for tissue reconstruction using temperature stimuli polymers, had found applications in reconstruction of corneal epithelium also. Limbal explants were cultured on temperature responsive surface in the presence of 3T3 feeder layer which would be then transferred to the ocular surface with the help of a membrane support (Nishida et al., 2004a). Oral mucosal cells were cultured on PIPAAm as an alternative source in obtaining cell sheet for corneal reconstruction (Nishida et al., 2004b). In all these works, the main disadvantage was the use of 3T3 feeder layer.

1.5.3.3.3 Copolymers of NIPAAm

Many copolymers of NIPAAm were also formulated to suit various needs. To accelerate cell sheet recovery, various hydrophilic monomers like poly ethylene glycol (Hyeong Kwon et al., 2003) and 2-carboxyisopropylacrylamide (CIPAAm) (Ebara et al., 2003) were copolymerised with NIPAAm. In the case of copolymer with CIPAAm, it was postulated that the carboxyl group in both monomers accelerated cell sheet recovery. To further accelerate cell sheet recovery, these copolymers were grafted to porous cell culture membranes (Hyeong Kwon et al., 2003). This was to increase the water accessibility to the grafted surface for rapid hydration when incubated under LCST.

Copolymers with hydrophobic monomers like n-butyl Methacrylate (BMA) were synthesised to modulate LCST and control of cell detachment (Tsuda et al., 2004). Cell sheet detachment from copolymers with small amounts of BMA was similar to pure PIPAAm surfaces. Copolymers with BMA were also used to create patterned surfaces for coculturing heterotypic cells (Tsuda et al., 2005). Recovered co-cultured cell sheets were suggested to be more tissue mimicking.

1.6 Cytocompatibility studies of polymeric materials

Any material intended for medical application should be safe for the human body. Therefore, all polymeric materials that come in contact with body fluids, tissues *in vivo* or cells *in vitro* should be proven cytocompatible before use. Different international standards have speculated *in vitro* and *in vivo* biocompatibility tests. A material is said to be cytocompatible when it induces no toxic response, support cell adhesion, spreading, migration, proliferation and preserve cell functionality. *In vitro* cytotoxicity tests like direct contact, test on extract and indirect contact tests are usually performed for the preliminary screening of materials as a first level testing. Moreover, this is a mandatory test for all biomaterials/devices irrespective of their nature or duration of contact as per ISO 10993-1(2003). The materials that are non cytotoxic would undergo further cytocompatibility tests as a second level testing. The materials that are going to be used as part of body implants are screened by different *in vivo* tests also.

Mammalian cell lines are commonly used for testing cytotoxicity and cytocompatibility. The mostly used cell lines for cytotoxicity assays are HeLa human cells and L929 mouse fibroblast cells. Different tests are being employed worldwide to study various aspects of cytocompatibility. For instance, morphology of the cultured cells

can be examined by phase contrast or electron microscopy. To analyse cell viability, neutral red staining, trypan blue exclusion assay, fluorescent techniques like acridine orange-ethidium bromide (Nair et al., 2008) and Fluorescein Diacetate (FDA) staining (Bachle et al., 2006) could be employed. Cell growth on materials can be studied by techniques like direct cell counting, protein/DNA measurement, tritiated thymidine uptake assay (Prasad et al., 2007) and Proliferating Cell Nuclear Antigen (PCNA) staining (Nair et al., 2008).

Based upon the end use of the material and the cell type with which it comes in contact, specific cytocompatibility tests using respective cell types could also be done to assess the effect on biofunctions. For instance, the important application of ceramic materials is their use as bone TE scaffolds. Hence, to analyse cytocompatibility of those materials osteoblast cells, primary (Torricelli et al., 2001) and cell line (Kim et al., 2004b), are being used. Specific tests like alkaline phosphatase assay are being employed to study the osteoblast cell functions. Like wise, cytocompatibility of materials intended for vascular TE scaffolds or those that come in contact with blood could be analysed using human umbilical vein endothelial cells (HUVEC) (Bordenave et al., 1992). Analysis of nitric oxide synthesis by HUVEC after culturing on materials had been reported (Prasad et al., 2007). To study specific functions of cells after being in contact with polymeric materials, primary cells are preferred as many of these functions might be lost in cell lines. Primary cells could simulate *in vivo* conditions more closely than cell lines eventhough repeatability and reproducibility might be a problem.

Cell-material interaction studies using corneal cells were also reported earlier. Different ocular cell lines were used to study the biocompatibility of biodegradable polymers with the potential end use as viscoelastic agents or surgical implants (Huhtala et al., 2008). Cytotoxicity of ocular permeation enhancers had been tested using rabbit and human corneal epithelial cells (Burgalassi et al., 2001). Human corneal epithelial cells was used for assessing cell adhesion on modified poly dimethyl siloxane intended for developing keratoprostheses (Aucoin et al., 2002). Similarly, corneal epithelial cell adhesion studies was reported on modified poly (Hydroxy Ethyl Methacrylate) (Merrett et al., 2001). Some of the ocular materials like those for intraocular lens and contact lens need the property of non adhesiveness, as cell adhesion could be detrimental for their function. While corneal epithelial cells are used to test the non adhesiveness of contact lens materials, endothelial cells are used for intraocular lens materials. Draize eye

irritancy test involves testing cosmetics or other chemicals in restrained animal's, especially rabbit's eyes to check their irritancy level. Due to strong criticisms from ethics groups, now-a-days, cytotoxicity tests using corneal cell lines along with many other tests were being investigated as alternatives for Draize eye test (Earl et al., 1995; Tani et al., 1999).

Similar to all newly developed biomaterials that have to undergo different tests to prove suitability, PIPAAm based materials should also be proven cytocompatible for its end use. Along with the role in cell sheet engineering, another major application of PIPAAm based materials is their use in drug delivery systems and gene transfection vectors. There are a few reports available for the cytocompatible studies of PIPAAm copolymers intended for drug delivery. 3-(4, 5-Dimethylthiazol-2-yl)-2, 5-diphenyltetrazolium bromide (MTT) assay was utilised to study cytotoxicity of PIPAAm-chitosan hydrogel synthesised for ocular drug delivery (Cao et al., 2007). Quan et al studied the potential use of a series of stimuli sensitive PIPAAm-co- propyl acrylic acid nanogels for drug delivery. The group reported that the copolymer showed a better cytocompatibility than PIPAAm nanogel (Quan et al., 2008).

1.7 Current scenario

- *Ex vivo* expansion of limbal cells was always carried out on xenogeneic feeder layers which have the risk of xenotoxicity, contamination and disease transmission to human system. A xeno-feeder free limbal cell culture system is in ever increasing demand.
- The most commonly used substrate for *ex vivo* expansion of limbal cells is AM which carries risk of disease transmission (Dua and Azuara-Blanco, 1999b). Most of the biomaterials are not suitable as they can hinder the vision by affecting the transparency. Due to the special functional requirements of cornea, scaffold free tissue constructs will be ideal for the treatment of LSCD.
- Eventhough the use of PIPAAm in tissue engineering has been reported as described earlier, few reports are available from India. A group from Sankar Nethralaya had studied a copolymer of NIPAAm which is commercially known as Mebiol gel (Sudha et al., 2006) marketed by Mebiol Inc., Japan. In their experiments they were applying the cells as

well as polymer to the ocular surface after culturing cells *in vitro,* so that it would form a gel coating (Sitalakshmi et al., 2008). The role of PIPAAm in creating carrier free tissue structures is not being utilised and there is a chance of traces of polymer gels to be entrapped in ocular surface after transplantation.

- Different methods had been reported for the fabrication of thermoresponsive polymers and surfaces. For preparing surfaces suitable for tissue reconstruction, the main reported methods are electron beam irradiation (Nandkumar et al., 2002; Yamato et al., 2001), plasma polymerisation (Canavan et al., 2005), UV light irradiation (Chen et al., 1998) and gamma ray irradiation (Anil Kumar et al., 2007a). Other techniques like free radical and atom transfer radical (Siegwart et al., 2008) polymerisation and thermal initiated polymerisation (Reddy et al., 2008) were also reported to be employed for synthesis of thermoresponsive polymers. Most of these methods utilise expensive equipments that may not be available in all laboratories.
- Extensive cytocompatibility studies were not carried out for PIPAAm or any of its copolymers intended for tissue reconstruction. Molecular level cytocompatibility studies using PIPAAm has not been attempted earlier.
- Different aspects of the substrate like hydrophobicity, surface energy and chemical composition influence cell adhesion and growth (Ito, 1999). Reports suggested that incorporation of hydrophobic monomers along with NIPAAm increased cell adhesion and growth (Allen et al., 2003). Thus, probably low amount of a hydrophobic monomer could maintain the thermoresponsiveness while helping the growth of various types of cells. Introduction of hydrophobic monomers could modulate the LCST also.
- As poly (methyl methacrylate) is widely used for ocular applications, MMA was used as the hydrophobic monomer to modulate LCST and surface wettability.
- To treat LSCD world over, a scaffold free tissue construct generated in a xeno-feeder free culture system is need of the hour.

1.8 Hypothesis

It is hypothesised that utilising TE, a xeno-feeder free culture system with cytocompatible stimuli responsive substrate can generate intact corneal construct, having the native architecture, as an ideal solution towards ocular surface regeneration.

1.9 Objectives of the study

- To optimise culture conditions for *ex vivo* expansion of limbal epithelial cells which would help in
    1. Avoiding the use of feeder layers
    2. Enabling formation of multilayered and contiguous cell sheet
    3. Maintenance of stem cell characteristics
- To prepare thermoresponsive surface using a simple and cost effective method.
- To analyse the biocompatibility of the thermoresponsive surface at cellular and molecular level using different cell lines and primary human limbal cells.
- To generate epithelial sheet structures that mimic the natural tissue architecture.
- To characterise the cell sheet for assessing its suitability towards ocular surface reconstruction.

CHAPTER 2

MATERIALS AND METHODS

2.1 Culture and characterisation of limbal cells from different sources

2.1.1 Materials

Iscove's modified Dulbecco's medium (IMDM), Foetal bovine serum (FBS) (Gibco BRL, India), Insulin (Gibco BRL, UK), Dispase II (Roche, USA), Anti-p63, Anti-CK3 antibodies (Chemicon International, USA), Bovine serum albumin (BSA), Fluorescein isothiocyanate (FITC) conjugated anti-mouse secondary antibody, Tetramethyl rhodamine isothiocyanate (TRITC) conjugated anti-mouse secondary antibody, Penicillin, Streptomycin, Triton X-100, Paraformaldehyde (PFA), EGF, Dimethyl sulphoxide (DMSO), Amphotericin, Trypsin (Sigma, USA), Anti-PCNA, Fluorescent mounting medium (Dako, Denmark), Panserin 801 with supplements (Pan, GmBH, Germany), Cholera toxin (Quadratech,UK), Ethylenediaminetetraacetic acid (EDTA) (Himedia, India) and Anti-Human ABCG2 antibody (BD pharmingen, India) were used.

2.1.2 Goat limbal culture

2.1.2.1 Presence of progenitor population in goat limbus

To calculate the percentage of limbal epithelial population showing progenitor characteristics, cells were freshly isolated from limbus and analysed for progenitor markers using flow cytometry.

Goat heads were collected from slaughterhouse within 2-4 h of death. The cornea with excess sclera was dissected out of the eye and put in sterile Hank's buffered salt solution (HBSS) (Appendix I) with antibiotics. The limbus was then excised out from the remaining tissue and was treated with dispase II (1.2 IU/ml) for 1 h at 37°C. To obtain a single cell suspension, the loosened epithelial sheet was treated with Trypsin (0.25%)-

EDTA (0.02%) (TPVG) (Appendix I) for 15 minutes at 37°C. It was pipetted several times to ensure single cell suspension. The cells were pelleted and dispensed in 4% PFA at a concentration of 10^6 cells/ml for 30 minutes. After centrifugation and 2 subsequent washes with phosphate buffered saline (PBS) (Appendix I) containing 0.1% triton X-100, the primary antibodies (anti-p63, anti-ABCG2) were added and incubated for 1 h. After washing, the cell pellet was incubated with secondary anti-mouse antibody conjugated with FITC for 30 minutes.

Single cell suspension of labelled cells in PBS were analysed using a flow cytometer (FACS, Aria, BD, USA) for fluorescent emissions and side & forward light scattering.

2.1.2.2 Explant culture

The limbus after removal of excess surrounding tissue was treated with dispase II for 30 minutes and cut into small pieces under aseptic conditions. Two or three pieces were kept as explants in each culture dish. IMDM (Appendix I) with 10% FBS or completed Panserin 801 with 5% FBS was used to culture these explants. The explants were incubated at 37°C in a humidified CO_2 incubator.

2.1.2.3 Characterisation of cells by immunofluorescent staining

The limbal cells grown *in vitro* were analysed for p63, CK3, PCNA and ABCG2. Briefly, the cells cultured on cover slips were fixed in 4% PFA at room temperature for 30 minutes followed by washing and permeabilisation with PBS containing 0.1% triton X-100. The cells were preincubated with 1% BSA in PBS containing 0.1% triton X-100 for 15 minutes to minimize non specific binding of antibodies. Cells were incubated with primary antibody for 1 h in a humidified chamber. After the samples were washed with PBS containing 0.1% triton X-100, they were incubated with FITC/TRITC conjugated antimouse IgG for 1 h in dark. Double immunofluorescent staining was performed for p63 and PCNA. In this, the cells were stained for p63 according to the above protocol. Secondary antibody used was anti-mouse IgG conjugated with FITC. Then it was incubated with anti-PCNA antibody followed by secondary antibody conjugated with TRITC with in between washes. After thorough washing with PBS, the coverslips were mounted on glass slides with fluorescent mounting medium. The slides were observed under 40x oil immersion objective of Laser Scanning Confocal Microscope (LSM510

META, Carl Zeiss, Germany) using Argon 488 laser for excitation of FITC and He-Ne 543 laser for TRITC.

2.1.3 Optimisation of culture conditions for rabbit limbal explant culture

2.1.3.1 Limbal explant culture

Anterior portion of eye including cornea, limbus and a little of sclera was dissected out from New Zealand white rabbits after autopsy for other experimental purposes with permission from Institute Animal Ethics Committee. The tissue was collected in HBSS with 200 μg/ml streptomycin and 200 IU/ml penicillin.

Excess sclera and cornea were trimmed out carefully to get the intact limbal region. 1-2 mm^2 pieces were cut and kept as explants in 35 mm culture dish with epithelial side up. The explants were incubated at 37°C in a humidified CO_2 incubator, after feeding with sufficient medium.

2.1.3.2 Effect of dispase

To investigate whether the duration of dispase treatment have any effect on cell migration and culture maintenance, limbal explants were treated with dispase II (1.2 IU/ml) for different time periods like 10, 30 and 60 minutes.

Explant cultures were established with and without dispase treatment to assess the necessity of enzyme. The distance migrated by cells from explants in both conditions was analysed. Photographs of migrated cells were taken on different days using DC150 camera attached to Leica DMIL inverted phase contrast microscope (Leitz, Germany). Microphotographs of fifteen randomly selected explants in each medium were used for analysing migration distance. The migration distance of cells from explants was calculated using the feature 'Interactive measurements' in Qwin software (Leica). Lines were drawn from the explant boundary to the point of migration of cells at different regions in each image. The average distance was calculated by the software.

2.1.3.3 Effect of medium

In this study, four different culture systems were used, as given in Table 2-1.

Culture system	Constituents
1	Completed panserin 801 with 5% FBS
2	IMDM with 10% FBS
3	IMDM and completed panserin 801 in 1:1 ratio with 5% FBS
4	Culture system 2 for initial days, which would be replaced by culture system 3 afterwards.

Table 2-1: Constituents of different culture systems used for limbal cell culture

Panserin 801, (keratinocyte basal medium) was provided with bovine pituitary extract, EGF, hydrocortisone, insulin, phosphoethanolamine and ethanolamine as supplements from the manufacturer. These supplements were added to the basal medium under sterile condition according to manufacturer's protocol. All these culture systems were supplemented with 100 µg/ml streptomycin and 100 IU/ml penicillin.

To assess the effect of medium on migration of limbal cells in explant culture, all culture systems except 4 was used. The distance migrated by the cells on 2^{nd} and 4^{th} day from explants in different culture systems was calculated as given in section 2.1.3.2

2.1.3.4 Maintenance of stem cell characteristics in different culture conditions

The maintenance of stemness was assessed by immunofluorescent staining of p63 in the cultured cells after one week. The protocol followed was as given in section 2.1.2.3. In each culture system, five different fields were photographed for p63 expression, keeping the fluorescent detection settings constant for all photographs. Four cells from each field were randomly selected for assessing the intensity. The intensity of expression of the marker in each medium was assessed using the 'Profile' feature in LSM510 software from Carl Zeiss. A line was drawn across the length of nucleus and the intensity corresponding to points at an interval of around 0.5 µm was calculated by the software. This was averaged and taken as the mean intensity of p63 expression of each cell.

2.1.3.5 Statistical analysis

The results in graph are given as average ± standard deviation. The results were statistically analysed using Analysis of Variance (ANOVA). $p<0.001$ was considered significant.

2.1.4 Human limbal cell culture

Human corneoscleral rim was obtained after penetrating keratoplasty. After removing excess sclera, the limbal region was cut into small pieces which were used for explant cultures in culture system 4. The cells were stained for p63, as given in section 2.1.2.3.

For part of work, slightly different methodology was adopted for human limbal explant culture. The corneoscleral rim obtained after surgery was processed under a dissection microscope. The rim was initially cut into two halves from which excess sclera would be trimmed off. The stroma and endothelium was then split and peeled away from the epithelial surface by creating an incision through the thickness of the rim and using forceps to split the tissue. The epithelium was cut into 8-12 small explants which were then seeded individually onto gridded TCPS plates with epithelial side up. Around 750 µl corneal epithelial medium (CEM) (Appendix I) was added through the edges of the culture dishes and spread in the whole plate using pastuer pipette. Next day, more medium was added to the cultures. The confluency was checked routinely on the TCPS by counting the square grids covered by cells on the plate surface. The cultures were fed with fresh medium once in two days.

2.2 Preparation, characterisation and cytocompatibility assessment of copolymer as a cell culture substrate

2.2.1 Materials

NIPAAm, MMA, (Aldrich, Germany), Azobisisobutyronitrile (AIBN), Isopropanol, Sodium hydroxide (NaOH), (Merck Chemicals, India) Benzene, Acetone (SD fine chemicals, India), 35 mm & 60 mm tissue culture dishes (Nunclon, USA & Greiner Bioone, Germany), Neutral red, Minimal essential medium (MEM), Penicillin, Streptomycin, L-glutamine, Trichloro acetic acid, Trypsin, MTT, PFA, Phalloidin-FITC, Propidium iodide (PI), Sodium dodecyl sulphate (SDS) (Sigma, USA), FBS, RNAse free water (Gibco BRL, UK), Sodium bicarbonate, EDTA (Himedia, India), Tritiated ([3H])

thymidine (American Radiolabelled Chemicals), Poly vinylidene fluoride (PVDF) membrane (Millipore,India), RLT buffer, quantitect reverse transcription kit, RNeasy mini kit (Qiagen,UK), PCR primers (Eurofins MWG operon, UK) and Amplitaq gold enzyme (Applied biosystems, USA) were used.

2.2.2 Preparation of NIPAAm-MMA

NIPAAm and MMA were taken in 9:1 ratios and dissolved in benzene. Temperature was raised to 60°C. AIBN was added as initiator and nitrogen was bubbled through the whole reaction mixture for 10 minutes. It was kept stirring at 60°C until the polymerisation was completed (Figure 2-1). The copolymer was then dissolved in acetone and again precipitated in water. The process was repeated thrice to remove unreacted monomers. The final cleaned copolymer was dissolved in isopropanol.

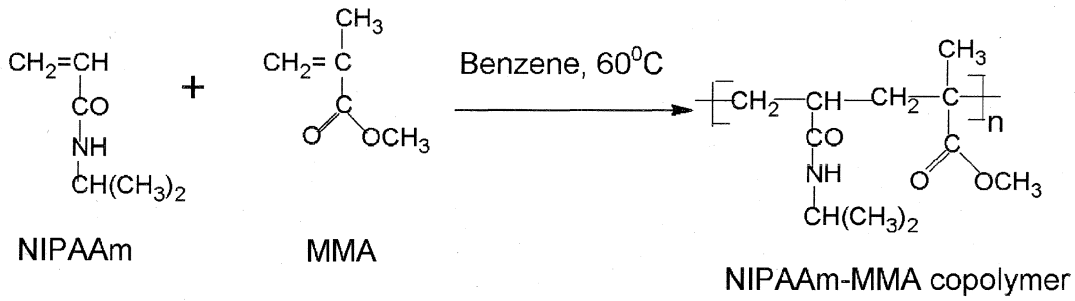

Figure 2-1: Scheme representing copolymerisation of NIPAAm and MMA

Differential Scanning Calorimetry (DSC) and Fourier Transform Infrared Spectroscopy (FTIR) were used to study physicochemical properties of the prepared copolymer.

2.2.3 Characterisation

2.2.3.1 Sample preparation

A viscous solution of NIPAAm-MMA copolymer in isopropanol was poured onto glass slides and kept in hot air oven overnight. The formed coating was then powdered and given for DSC (~10 mg) and FTIR.

2.2.3.2 FTIR

FTIR deals with infrared spectra and can be used to identify compounds or sample compositions.

Powdered copolymer was mixed with optical grade Potassium Bromide (KBr) mixture. Spectra were measured for the mixture as well as pure KBr which was kept as

blank in the range of 400-4000 cm^{-1} on a Nicolet 5700 spectrometer. Spectra were recorded at a resolution of 4 cm^{-1} and number of scans were 32.

2.2.3.3 DSC

DSC is a thermoanalytical technique used to study phase transitions. Lower critical solution temperature of the copolymer was determined using DSC (DSC 2920 TA Instruments, Delaware, USA) with TA 4000 controller as reported earlier (Zhang et al., 2004). Prior to measurements, the sample was immersed in deionised water at room temperature and allowed to swell to equilibrium. About 10 mg of equilibrium swollen sample was sealed hermetically and thermal analysis was performed from 25°C to 55°C at a heating rate of 3°C in nitrogen atmosphere. The samples were cooled to 25°C and reheated up to 55°C and the change in the heat flow in the second run was taken as LCST.

2.2.4 Preparation of thermoresponsive surfaces

The copolymer solution in isopropanol was coated on TCPS by adding the solution to the surface for a few seconds and removing the excess. The coated plates (NIPAAm-MMA plates) were then kept in hot air oven at 65°C overnight. The excess unbound polymer was washed several times with cold deionized water and left in oven for drying. Before cell culture experiments, the plates were sterilised by ethylene oxide.

2.2.5 Characterisation of thermoresponsive surface

2.2.5.1 Attenuated total reflectance (ATR) spectra

Attenuated Total Reflectance spectra was used to assess the surface chemistry of the copolymer coated surface. A Thermo Nicolet 5700 model FTIR fitted with a horizontal ATR accessory with diamond crystal was used to obtain spectrum. Spectra were taken in the wavelength region 400 cm^{-1} to 2000 cm^{-1} from 32 scans.

2.2.5.2 Profilometry

For analysing surface roughness, 1mm x 1 mm of coated and bare dishes were assessed using Talysurf CLI 1000 (Taylor Hobson UK) with the software Talymap Gold (version 4.1), high resolution non contact confocal point gauge (CLA) with a range of 300 μm. At least 10 profile lines were extracted from the levelled surface measurement, from which surface roughness was calculated by the software.

2.2.5.3 Contact angle

Static water contact angle was measured using sessile drop technique (NRL contact Angle Goniometer). Distilled water (3 µl) was gently placed on the samples using a dispenser. The contact angles were measured using a video based measuring device (Data Physics OCA 15 plus, Germany) and software (SCA 20 software). All samples were measured thrice and averaged.

2.2.6 General cytocompatibility

2.2.6.1 Cell line

A mouse fibroblast cell line, L929 (American type culture collection (ATCC)) and a rabbit corneal cell line, SIRC (National centre for cell science, Pune) were used for cytocompatibility studies. The cells were maintained in completed MEM (Appendix I) with 5% FBS.

On confluency, the cells were passaged using TPVG. One ml of TPVG was added to the cells after removal of medium and incubated at 37°C for few minutes. The solution was removed when the cells started rounding up. The cells were again incubated at 37°C to enable complete detachment of cells. The cells were then counted using a haemocytometer. According to the experimental need, optimum number of cells was seeded to culture dishes.

2.2.6.2 Cytotoxicity assay

Cytotoxicity of the copolymer was assessed by direct contact test according to ISO 10993-5. Copolymer coated surfaces (0.4 mm^2 pieces) were placed directly on sub confluent L929 cells, cultured in 12 well plates. After 24 h, the cells were observed for any toxic effects including cell death, morphology changes and vacuolisation. The cells were also stained with neutral red after 24 h to check toxicity of the material.

2.2.6.3 Cell morphology and viability

The cells were trypsinised and seeded onto polystyrene dishes as well as NIPAAm-MMA plates at a concentration of 2 x 10^4 cells/cm^2. Cell viability on the copolymer was tested using neutral red. Neutral red solution (0.5 mg/ml) in normal saline was added to cells after 24 h of culture on NIPAAm-MMA dishes and incubated for 10 minutes. Photographs were taken using Leica DMIL inverted phase contrast microscope (Leitz, Germany).

2.2.6.4 Cytoskeletal staining

The cells were fixed with 4% PFA for 30 minutes and permeabilised with PBS containing 0.1% triton X-100 for 10 minutes. The cells were then stained with phalloidin conjugated FITC for 30 minutes. After thorough washing with PBS, the cells were observed under inverted fluorescent microscope (I3 filter, Leica DMI 6000, Leitz, Germany).

2.2.6.5 Cell attachment and doubling time

The experiment was performed based on a protocol reported earlier (Prasad et al., 2007) with minor modifications. In brief, L929 cells in log phase were labelled with [3H] thymidine by maintaining in medium containing 5 μCi/ml of [3H] thymidine until they reached confluency. Then the cells were trypsinised and seeded to 35 mm culture dishes at a concentration of 2 x 10^4 cells/cm^2. To assess initial attachment of cells, the medium from culture dishes were removed and unattached cells were pelleted after 4 h of cell seeding. DNA was extracted for [3H] thymidine counting according to an already reported protocol (Shivakumar et al., 1992). Briefly, 0.5 ml of 0.1 N NaOH containing 0.1% SDS was added to cell pellet. After mixing thoroughly, the solution was kept at room temperature for 15 minutes. To this, 0.5 ml of trichloro acetic acid was added and kept for 1 h at 4°C. It was then spun down at 10,000 g for 15 minutes at 4°C. After the supernatant was removed, 1 ml of ethanol was added and incubated in icebath for 30 minutes. After centrifugation, the pellet was airdried and dissolved in 250 μl of 0.1M NaOH. Scintillation fluid (0.5 ml) from Triathler was added to this before taking reading. Aliquots of cells equal to the initial seeding density were used to determine the radioactive count of known number of cells. [3H] thymidine was measured in a liquid scintillation counter (TRIATHLER Multilabel-tester, Hidex, Finland). The attached cells were calculated based on the count of unattached cells and count of known number of cells.

For the quantification of cell doubling time, the cells were maintained in fresh medium containing 2.5 μCi/ml of [3H] thymidine for 72 h. The cells were harvested afterwards and [3H] thymidine was measured as described above. Doubling time was calculated from the count obtained at 4 h and 72 h using the formula:

Doubling time = log (2)/K where K = (2.3 x log(N1/N0))/ T1-T0

Where T0 = initial time point

T1 = final time point

N0 = number of cells at T0

N1 = number of cells at T1

2.2.6.6 MTT assay

After growing the cells on TCPS and NIPAAm–MMA plates for 48 and 96 h, MTT (0.5mg/ml in serum free MEM) was added and incubated for 4 h at 37°C. The cells were then lysed and converted dye was solubilised using isopropanol for 20 minutes with mild shaking. Optical density of the released purple formazan was measured at 570 nm (Biotek Reader, USA). Medium alone was considered as reagent blank.

2.2.6.7 Cell cycle analysis

L929 cells were cultured on NIPAAm-MMA dishes and TCPS for 24 h. The cells were trypsinised and pelleted at 300 g for 10 minutes. The pellet was then fixed in ice cold 70% ethanol for 1 h. The cells were treated with RNAse (200 µg/ml) for 45 minutes at 37°C. PI (50 µg/ml) was added and incubated for 5 minutes before analysing in flow cytometer (FACS Aria, BD USA).

2.2.6.8 Statistical analysis

The results are represented as average ± standard deviation, wherever applicable. Error bars in graphs represent standard deviation. Significance was calculated using one way ANOVA. $p < 0.001$ was considered significant.

2.2.7 Specific cytocompatibility

2.2.7.1 Human limbal culture

Explant culture was established as given in section 2.1.4. The explants were cultured in CEM until the growth reached 5-10%. It was then transferred to serum free CEM (SFCEM) till it reached confluency.

2.2.7.2 Detection of markers using reverse transcriptase PCR

Primary human LiEC were treated with RLT buffer for lysing cells after 2 weeks of culture. RNA was extracted using Qiashredders and RNeasy Mini Kit according to manufacturer's protocol. The isolated RNA was eluted in 15 µl of RNAse free water. The concentration of RNA was determined using Nanodrop Spectrophotometer (NanoDrop® ND-1000 UV-Vis Spectrophotometer).

Human Gene	Forward primer	Reverse primer	Amplicon size
HPRT	5'-TGA TAG ATC CAT TCC TAT GAC TGT AGA-3'	5'-AAG ACA TTC TTT CCA GTT AAA GTT GAG-3'	126 bp
dNp63	5'-CAG ACT CAA TTT AGT GAG-3'	5'- AGC TCA TGG TTG GGG CAC-3'	440 bp
CK3	5'-GGC AGA GAT CGA GGG TCT C-3'	5'- GTC ATC CTT CGC CTG CTG TAG- 3'	145 bp
Connexin 43	5'-CCT TCT TGC TGA TCC AGT GGT AC-3'	5'- ACC AAG GAC ACC ACC AGC AT-3'	154 bp
ABCG2	5'-CAC AGT CTT CAA GGA GAT CAG CTA-3'	5'- CCC AGT ACG ACT GTG ACA ATG-3'	135 bp

Table 2-2: Primer sequences for PCR

The first strand cDNAs were synthesised from 1.5 μg of RNA using Quantitect reverse transcription kit according to manufacturer's instructions. Expression of deltaNp63 (dNp63), CK3, Connexin 43 and ABCG2 in cells cultured on different substrates was checked by PCR amplification for 37 cycles using respective primers (Table 2-2). Semiquantitative PCR was performed for ABCG2 by terminating reactions at 22, 27, 32 and 37 cycles. The amplicons were run through 1% agarose gels, visualised using an UV transilluminator and photographed using a Nikon digital camera with the help of Nikon capture control software.

2.2.8 Thermoresponsiveness

The L929 cells were cultured on NIPAAm-MMA plates until confluency. The medium was removed and a PVDF membrane was kept on top of the cells carefully. Few drops of medium were added to keep the membrane wet. A coverslip was kept on top of membrane to ensure contact of membrane with cells. The plate was incubated below LCST of copolymer, ie; at 20°C for 30 minutes and the PVDF membrane was removed. The plate was observed under phase contrast microscope to check transfer of cells from plate to PVDF membrane.

2.3 Secretome analysis as a tool to analyse specific molecular compatibility of copolymer and to study cellular function on different substrates

2.3.1 Materials

Epilife basal medium, Human keratinocyte growth supplement, gentamicin/amphotericin B solution (Cascade biologics, USA), PBS, 3-[(3-Cholamidopropyl)dimethylammonio]-1-propanesulfonate (CHAPS), Dithiothreitol (DTT), Bromophenol Blue, Trizma Base, Nitro-Blue Tetrazolium Chloride (NBT)/ 5-Bromo-4-Chloro-3'-Indolyphosphate p-Toluidine Salt (BCIP), Glycerol, Sodium acetate, Sodium thiosulfate, Tris Buffered Saline (TBS), Thermolysin, Tween 20, Corning Transwell culture inserts (Sigma,UK), DMEM/F12, FBS, Tryple express (Gibco BRL,UK), HyQ SFM Megavir medium (HyQ) (Thermo fisher scientific, Germany), Tissue culture flasks, 35 mm culture dishes, 60 mm culture dishes, 6 well plates (Nunclon, USA), Urea, Thiourea (Zoom reagents, Invitrogen), IPG buffer, Destreak (HED), SDS (Plus one grade), Iodoacetamide (IAA) (Plus one grade), APS (Plus one grade), TEMED (Plus one grade), BSA, 2D quantitation assay kit, 2D clean up kit, ETTAN daltsix gel caster, Immobiline 3-11 NL 18 cm strips, full range rainbow marker (GE healthcare,UK), Protogel (30%(w/v) acrylamide: 0.8%(w/v) Bis-acrylamide, 37.5:1 stock) (National Diagnostics, Hull, UK), Methanol, 20x 2(N-morpholino)ethanesulfonic acid (MES) buffer Nupage, 20x Transfer buffer Nupage, NuPAGE 12 well gels, LDS buffer (Invitrogen,UK), Mineral oil, Acetic acid, Silver nitrate (Fisher Scientific,UK), EDTA, Sodium carbonate (BDH laboratory supplies,UK), 0.2 μm filter (Sartorius,UK), 3000 Da cut off column (Vivascience, Sartorius Vivascience GmbH, UK), Anti-mimecan, Anti-neutrophil gelatinase associated lipocalin (NGAL), Anti-interleukin 6 (IL-6) (R&D systems, UK), Anti-βig-h3 (Santa Cruz biotechnology Inc., USA), Secondary anti-rat IgG conjugated with alkaline phosphatase, Secondary anti-mouse IgG conjugated with alkaline phosphatase (Thermo Fisher Scientific, UK), PVDF membrane (Millipore, UK) and Tris Glycine SDS (TGS) buffer (Biorad, UK) were used.

2.3.2 Optimisation of culture medium

Human corneal epithelial cell line (CECL) and primary limbal cells were used for secretome analysis. Culture medium was optimised for both cell types to obtain serum free conditions. The different mediums used were CEM, SFCEM, Epilife and HyQ.

Epilife completed was prepared by adding human keratinocyte growth supplement and gentamicin/amphotericin B solution, according to manufacturer's instructions.

For both cell line and primary cells, indirect and direct mode of culture was attempted in order to optimise the culture conditions. Direct mode was the culturing of cell line or explants directly in different medium. For cell line, indirect mode included culturing of cells in Epilife completed for 24 h after passaging and then transferring into different media in 1:1 ratio for 24 h followed by complete transfer. In primary cell culture, indirect mode included culturing of explants in CEM till the cells reached 5-10% confluency followed by transfer into other media in 1:1 ratio for 24 h followed by complete transfer. The final optimised technique was as follows.

The cells were transferred to serum free medium (SFM) before collecting supernatant as serum can contaminate and hinder the secretome analysis. In primary limbal culture, the cells were washed to remove the maximum possible extent of serum contamination before culturing them in SFCEM. SFCEM was added to the cells at a confluency of around 10%, after removing CEM and the cells were left on rocker with minimum shaking for 15 minutes. The medium was replaced with new SFCEM and left in incubator for 30 minutes. The whole process was repeated and then required amount of SFCEM was added to the cells before leaving them in incubator for collection of medium. In cell lines, the cells were passaged into SFCEM for collection of medium.

2.3.3 Preparation of AM

Placentas were obtained from patients undergoing elective caesarean after taking their consent. All procedures were carried out under a class II laminar flow hood following an established protocol (Hopkinson et al., 2006b). This involved separating the amniotic sac from the remaining placenta using scissors. Chorion and amnion were separated manually and the amnion was washed in 0.9% saline thrice for 30 minutes each to remove blood contamination. Spongy layer was removed from the stromal side of the amnion (Hopkinson et al., 2006b). After another brief wash, 4 cm^2 pieces of amnion were cut and stored in PBS at -80°C for six months prior to use.

Membrane segments were thawed and washed in 20 ml PBS twice for 10 minutes each. These membranes were then considered transplant ready membranes. For tissue culture, amniotic epithelial cells were removed enzymatically using established methodology (Hopkinson et al., 2008). A solution of 125 µg/ml thermolysin was prepared

in PBS. Each membrane segment was spread with epithelial side up in a Petri dish and then treated with 6-10 ml thermolysin solution for 9 minutes at room temperature. This was followed by sequential washing in 10 ml PBS thrice to remove cells and neutralise the enzyme by dilution. A final wash was performed in SFCEM to remove the PBS. The denuded AM could be used immediately or stored in SFCEM at -20°C until use.

2.3.4 Human limbal explant culture on AM, TCPS and NIPAAm-MMA

To avoid folding of AM and to increase surface area during culturing, the following method was adopted. The membranes of Transwell culture inserts were removed. The transwell insert was kept upside down and the denuded AM was spread with BM side down so that when returned to the correct orientation the BM would be facing up. The AM was secured in place using O-rings made in house from polypropylene tubes. Limbal explants were placed on to the AM and cultured in CEM in both lower and upper chambers. The cultures were fed with fresh medium once in two days.

Limbal explant culture was done in TCPS and NIPAAm-MMA plates as given in section 2.1.4. In all the substrates, the cells were transferred to SFCEM when it reached 5-10% confluency.

2.3.5 Cell line culture on TCPS and NIPAAm-MMA

An SV40 immortalised human CECL was used for the experiments. For revival, the cells were brought to 37°C in a water bath immediately after taking from the cell rack kept in liquid nitrogen. The cells were then added drop by drop into 10 ml medium taken in a culture flask and incubated at 37°C in a 5% CO_2 incubator. The culture was maintained in Epilife medium with added supplements. To passage the cells, the flask was washed with PBS after discarding the medium and the cells were incubated with 1 ml of Tryple for 10 minutes at 37°C. Epilife medium was added to dilute out the enzyme and the released cells were centrifuged at 2000 rpm for 8 minutes. The cell pellet was resuspended in SFCEM and seeded to TCPS and NIPAAm-MMA. The medium was changed and fresh medium added once in two days.

2.3.6 Secretome analysis

Secretome is the term used to denote the total proteins secreted out of cell. Therefore, secretome analysis essentially included proteomic techniques. The protocol

adopted for secretome analysis is represented in the flow chart (Figure 2-2), each of which is described below.

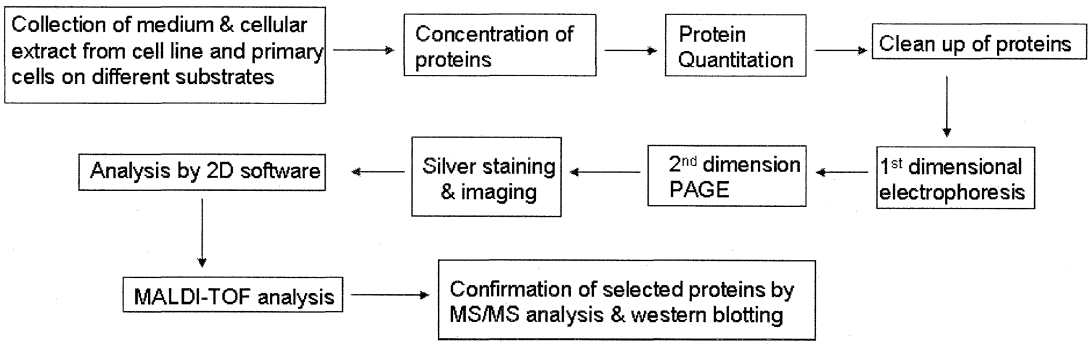

Figure 2-2: Flow chart for secretome analysis

2.3.6.1 Collection of culture supernatant for secretome analysis

The culture period for collecting medium was optimised. The different time points checked for collecting media ranged from 16-72 h. Three sets of time point were used for collections; i) 72/48h – 72 h after passaging followed by 48 (120^{th}) h ii) 48/24h - 48 h after passaging followed by 24 (72^{nd}) h and, iii) 24/16h - 24 h after passaging followed by 16 (40^{th}) h.

The different substrates used in the study of secretome were; (i) TCPS, (ii) NIPAAm-MMA dishes and (iii) AM. Cell line was cultured on TCPS and NIPAAm-MMA while primary cells were cultured on all three substrates. Medium from both cell types were collected and was immediately filtered twice through 0.2 μm filter and stored in -20°C till use.

The cells were lysed with either RLT buffer for RNA analysis or TBS with 0.1% triton X-100 (TBST)/1x LDS buffer for whole cell protein analysis. These samples were stored in -80°C till use.

2.3.6.2 Protein concentration and quantitation

The amount of protein secreted by cells is low, therefore the supernatant from many cultures of similar samples were pooled to obtain sufficient protein amounts for two-dimensional gel electrophoresis (2DE). Protein was concentrated 40-150 fold using a 3000 Da cut off column and the protein was quantified using 2D quantitation assay kit, according to manufacturer's recommendation. Standards were prepared from BSA provided with the kit. The optical density was measured at 490 nm in Thermo max plate reader (Molecular devices, UK).

2.3.6.3 Protein purification

For preparative gels, 80-100 µg proteins and for analytical gels, 150-200 µg proteins were used. These were purified using 2D clean up kit according to manufacturer's instructions. Briefly, the protein was mixed well with precipitant and incubated on ice for 15 minutes. This was followed by addition of co-precipitant and subsequent centrifugation. After the supernatant was aspirated out, a wash with co-precipitant was given. The pellet was then dispersed in 25 µl of deionised water. Acetone and a wash additive were added to this and further dispersion of the pellet was accomplished. This was stored in -20°C overnight with occasional vortexing. The protein was pelleted and after airdry, resolubilised in 75 µl of 1x IEF buffer (Appendix I) for 45 minutes at room temperature, followed by 30 minutes sonication. Before loading, the samples were centrifuged at 15,000 rpm for 15 minutes to remove any insoluble material.

2.3.6.4 First dimensional (1-D) electrophoresis

In this stage, the proteins are separated based on their isoelectric point.

The 1-D electrophoresis was carried out in 18 cm, pH 3-11 nonlinear, immobiline drystrips. Each strip was rehydrated in 340 µl of 1x rehydration buffer (Appendix I) which was uniformly spread in the wells of rehydration tray on to which the strip was placed with gel side down. To prevent evaporation of the buffer, 2 ml mineral oil was poured into the wells. Rehydration was done overnight at room temperature.

Rehydrated strips were placed with gel side up into the IPGphor 3 manifold (GE health sciences, UK) and then covered with 108 ml mineral oil. Cups for loading sample were placed at the anode end of the gel around 2 cm into the strip and paper wicks pre-wetted with 150 µl of deionised water were placed on both ends of each strip. The samples were loaded and electrodes were kept in place with appropriate fitting. The necessary settings were chosen in the software (Table 2-3) and the electrophoresis was carried out for 5:41 h with 75 µA/strip at 20°C. After the 1-D electrophoresis, the strips were kept in -20°C till use.

Step	*Ramping type*	*Voltage*	*Volt hours*
1	Step	500	500
2	Gradual	1000	800
3	Gradual	10000	16500
4	Step	10000	6200

Table 2-3: Parameters for 1-D electrophoresis

2.3.6.5 Second dimensional electrophoresis

The second dimension of electrophoresis involves separation of proteins that is already at their isoelectric points according to their mass.

The gels were cast using Ettan DALTsix gel caster. Glass plate and spacers were cleaned thoroughly with ethanol and deionised water. The casting apparatus was set up with alternating gel plates and spacers according to manufacturer's instructions. Six gels could be casted each time by a total volume of 450 ml of casting solution. Casting solution was prepared as detailed in Appendix I, without the addition of APS and TEMED and pre-chilled to 4°C for 2 h. APS and TEMED were added to the solution to initiate polymerisation and the solution was mixed well before immediately pouring into the caster through the top inlet until it reached about 5 mm below the top of the small plates. Water saturated butanol (1.5 ml) was added using a needle on to the gel front to make an even gel surface. It was left undisturbed for 1-2 h to allow full polymerisation. The casting apparatus was dismantled and the gels were stored in 1x TGS buffer at 4°C.

Electrophoresis was carried out using Ettan DALTsix electrophoresis system (GE healthcare, UK). The immobiline strips were thawed and allowed to reach room temperature. Each strip was then equilibrated in 10 ml SDS equilibration buffer (Appendix I) containing 100 mg DTT for 10 minutes, followed by an equilibration in the same buffer with 250 mg of IAA for 10 minutes. Equilibration maximises protein solubility in the strip to facilitate transfer to the 2nd dimension during electrophoresis. The strips were located onto the top of gels with large plate down, gel side up and anode side of strip on left hand side. 3-5 µl of marker (12-225 kDa) on a small paper strip was also kept on to the gels, adjacent to the immobiline strips. 2 ml of pre-warmed agarose

solution (0.8%) was layered on top of the strips. The running buffer used in the lower tank was 1X TGS and that in the upper chamber of tank was 2x TGS. The gels were placed in the tank and run initially for 1 hour at 10 mA/gel. This is to organise the proteins for entering the SDS gel. The second phase run was for 4.5- 5 h at 25 W/gel.

2.3.6.6 Staining of gels

After the run, gels were removed from the tank and the gel plates were opened carefully so that the gels were not torn. The gels were immediately transferred to fixation solution (Appendix I) carefully without breaking the gels. After fixation, the gels were stored in deionised water overnight. Silver staining technique was carried out to visualise the proteins. The procedure is described below (Table 2-4) and the details of solutions are given in Appendix I. The stained gels were photographed using a Nikon digital camera with the help of Nikon capture control software that provided optimum settings.

Process	*Time (minutes)*
Fixation	2 x 15
Sensitisation	30
Wash (ultra pure water)	3 x 5
Impregnation (2.5 g/l silver nitrate)	20
Wash (ultra pure water)	2 x 1
Development	According to protein load (up to 7 minutes)
Termination (14.6 g/l EDTA)	30
Wash (ultra pure water)	2 x 5

Table 2-4: Different steps in silver staining

2.3.6.7 Analysis of gels

The gel images were analysed using Delta 2D v3.4 software. Different pseudo colours were given to the spots on different gels. Analysis was carried out by matching

similar spots using warping strategies. The analysis was performed to achieve 2 main goals.

1. To identify potential spots in the secretome of primary epithelial cells and the cell line.
2. To identify differences in the secretory proteins on different substrates.

The different gel images analysed using the software to identify potential secretome and/or differences were those representing:

- Pooled culture supernatant of primary LiEC on TCPS
- Pooled culture supernatant of LiEC on AM
- Pooled culture supernatant of LiEC on NIPAAm-MMA
- Pooled culture supernatant of CECL on TCPS
- Pooled culture supernatant of CECL on NIPAAm-MMA
- Cellular TBST extract of LiEC on TCPS
- Cellular TBST extract of LiEC on AM
- Cellular TBST extract of LiEC on NIPAAm-MMA
- Cellular TBST extract of CECL on TCPS
- Cellular TBST extract of CECL on NIPAAm-MMA

To achieve the goals, each conditioned medium was compared to the respective cellular extract and after identifying potential secretome, these conditioned media were compared against each other to identify differences. The digital software made composites of compared gels and matched spots were given a pseudo colour different from other spots. The spots of interest were then characterised by Mass spectrometry.

2.3.6.8 Mass spectrometry

For mass spectrometric analysis, the spots of interest were excised out including the gel pieces and destained using 15 mM potassium ferricyanate/50 mM sodium thiosulphate. The proteins were reduced and permanently modified by alkylation so that disulphide bridges will not be reformed. The gel pieces were dehydrated and then soaked with trypsin to allow digestion of proteins. The peptide fragments were eluted and Matrix-assisted laser desorption/ionization Time Of Flight Mass Spectrometry (MALDI-

TOF-MS) (Waters/Micromass, Elstree, UK) was performed. For generating potential peptide mass fingerprints (PMF) for each protein, peaks corresponding to ions from gel alone, trypsin autolysis fragments and a mixture of keratin fragments were avoided from the raw data. The PMF were searched in relevant sites (http://www.matrixscience.com/ using MASCOT) and databases (http://www.expasy.ch/sprot/) to identify the proteins. The PMF searches were performed using a peptide tolerance of ± 0.2 Da and identifications based on atleast 3 peptide matches were accepted. Searches for each spot were done against 'all entries' in swissprot database and spots with a score more than 68 was accepted. The spots that did not get significant score in 'all entries' was again searched only against 'homosapiens' in swissprot database and spots with score of 56 or more was accepted.

For the confirmation of some of the proteins of interest, MS/MS analysis was done using nano - Electrospray Ionisation – Quadrupole - Time of Flight - Mass spectrometry/Mass spectrometry (ESI-Q-TOF-MS/MS) (Waters/Micromass, Elstree, UK).

2.3.6.9 Western blotting

The required amount of protein was mixed with 1x LDS buffer to get a final maximum volume of 20 µl. Each sample was then heat-denatured at 98°C for 4 minutes. Two Nupage gels were kept in electrophoretic tank with the smaller plate facing each other, after removing combs. MES buffer was added to the electrophoretic tank so that the wells were covered. 500 µl of NuPage antioxidant was added into the buffer. The samples were then loaded to wells. One well was loaded with 5 µl marker (12-225 kDa). The run was carried out for 45 minutes at 200 V. During the run, components of blotting apparatus were prepared. Blotting paper and sponges were immersed in 1x transfer buffer (Appendix I). The PVDF membrane (sequence grade) was pre-wet in methanol for 1 minute and transferred quickly to transfer buffer, taking care that it did not get dried. After the run, the gel plates were opened carefully and the blotting module was assembled as given below.

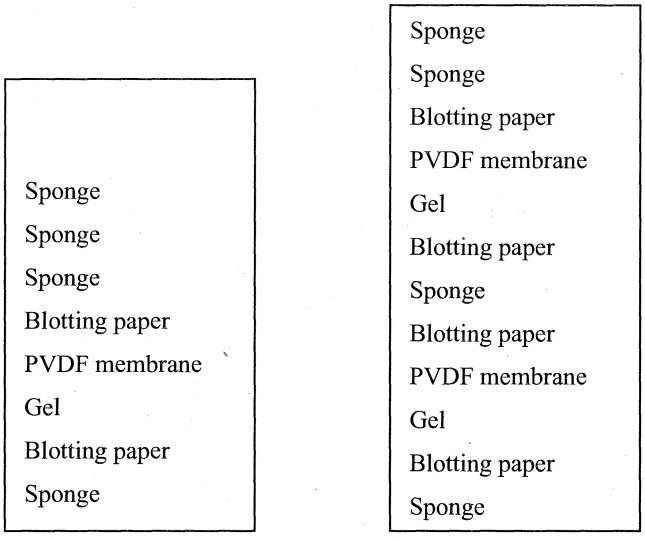

Figure 2-3: Schematic representation of western blot set up in case of one and two gels respectively

The blotting was carried out at 30 V, 168 mA for 1 h in novex minicell and western blot system (Invitrogen, UK). After blotting, the PVDF membrane was transferred quickly to TBST. Then it was transferred to blocking buffer (5% milk powder in TBST) for 1 h on a rocker. This was followed by three quick washes and three 5 minute washes of the blot with TBST. The blot was left overnight at 4°C in primary antibodies (anti-Mimecan, anti-NGAL, anti-IL6, anti-βig-h3) properly diluted with antibody buffer (2% BSA in TBST). The washing procedure was repeated next day and the blot was incubated with secondary antibody conjugated with alkaline phosphatase for 1 h. After washing, 8 ml NBT/BCIP was added and left until bands developed.

2.4 Generation and characterisation of limbal epithelial cell sheet

2.4.1 Materials

Anti-ZO-1 antibody, Anti- Occludin antibody (Zymed laboratories, USA), Anti-p63, Anti-CK3, Anti-connexin 43 antibodies (Chemicon International, USA), Phalloidin-FITC, PI, FDA, Anti-mouse antibody conjugated with FITC, Anti-rabbit antibody conjugated with FITC, PFA (Sigma, USA), Fluorescent mounting medium (Dako, Denmark) and PVDF membrane (Millipore, India) were used.

2.4.2 Goat limbal cell sheet retrieval

Goat limbal cells were cultured on thermoresponsive copolymer until it reached confluency. The goat limbal cell sheet was incubated below 10°C for 15 minutes and

peeled off using forceps. The cell sheet was assessed for its intactness and expression of different markers.

2.4.3 Analysis of cell sheet

2.4.3.1 Environmental scanning electron microscopy (ESEM)

The cell sheet was fixed in neutral buffered formalin for 1 h soon after retrieval. It was then observed directly under ESEM (FEI QUANTA 200, Japan) using high vaccum secondary electron detector.

2.4.3.2 Cytoskeletal staining

The staining procedure was performed as given in section 2.2.6.4 for cell sheet. For counterstaining, the cell sheet was incubated with PI for 1 minute. After washing, it was mounted and observed under confocal microscope with Argon 488 laser for excitation of FITC and He-Ne 543 laser for PI.

2.4.3.3 Characterisation of cell sheet

The cell sheet was fixed in either 4% PFA or neutral buffered formalin for a minimum of 1 h. The staining procedure was carried out for p63 and CK3 as given in section 2.1.2.3. The mounted sheets were observed under confocal microscope (LSM510 META, Carl Zeiss, Germany). Depth code analysis of p63 was done with z stack images using LSM510 software.

2.4.4 Rabbit limbal cell sheet retrieval

Rabbit limbal explants were cultured for 2 weeks on thermoresponsive surface. For rabbit cell sheet retrieval, the plates were incubated at 20°C for half an hour. The sheet was peeled off using a forceps or sterile poly ethylene terephthalate (PET) strip under a dissection microscope. The cell sheet was assessed for its viability, intactness, transparency, barrier function and expression of different markers.

2.4.5 Analysis of cell sheet

2.4.5.1 Environmental scanning electron microscopy (ESEM)

The procedure was carried out as given in section 2.4.3.1.

2.4.5.2 Cell sheet viability

The cell sheet was incubated with FDA (10 μg/ml in medium) for 5 minutes, soon after retrieval. The sheet was washed in PBS and observed under inverted fluorescent microscope (I3 filter, Leica DMI 6000, Leitz, Germany).

2.4.5.3 Assessment of transparency

Transparency was assessed by the visibility of letters behind the cell sheet.

2.4.5.4 Cytoskeletal staining

The staining procedure was performed as given in section 2.4.3.2.

2.4.5.5 Assessment of barrier function

Barrier function was assessed by staining for ZO-1 and occludin in cell sheet. The cell sheet was fixed in either 4% PFA or neutral buffered formalin for a minimum of 1 h. The staining procedure was carried out as given in section 2.1.2.3. Cell sheet was counterstained with PI. The sheets were mounted and observed under confocal microscope (LSM510 META, Carl Zeiss, Germany).

2.4.5.6 Characterisation of cell sheet

The cell sheet was fixed and stained for p63 and connexin 43 as given in section 2.1.2.3. Counterstaining with PI was given in case of connexin 43. The mounted sheets were observed under confocal microscope (LSM510 META, Carl Zeiss, Germany).

CHAPTER 3

RESULTS AND DISCUSSION

3.1 Culture and characterisation of limbal cells from different sources

3.1.1 Goat limbal cell culture

Due to easy availability of goat eyes, cell culture was standardised using goat limbal cells.

3.1.1.1 Presence of progenitor population in goat limbus

To confirm presence of the progenitor population in limbal cells, the freshly isolated cells were stained against p63 and ABCG2 and characterised by flow cytometry. It has been shown from the results that 69% of the total analysed cells were p63 positive and 3.2% were ABCG2 positive (Figure 3-1).

p63, a homologue of transcription factor p53, is found in the nuclei of different cells with proliferative potential. It was reported that p63 was expressed strongly in LSC while weak expression was demonstrated in young TAC with proliferative potential and no expression in differentiated phenotypes (Pellegrini et al., 2001). Similarly, Chee et al suggested that p63 is expressed in both LSC and young TAC, and it is only the intensity of expression that varies between these cells (Chee et al., 2006). As the analysis by flow cytometry was not intensity dependent, this study might have showed up LSC as well as young TAC, resulting in a high percentage of positive cells. It is evident from the side scatter-forward scatter plot that cells with small size and low side scatter properties were the p63 positive cells (Figure 3-1a). These features had been attributed to SC like cells.

ABCG2 had been proposed as a universal SC marker and could be considered as marker for putative limbal SC. De Paiva et al reported that this protein is mainly located

in limbal basal layer (de Paiva et al., 2005). Findings of this study correlated well with their flow cytometry result of 2.5% - 3% ABCG2 positive cells.

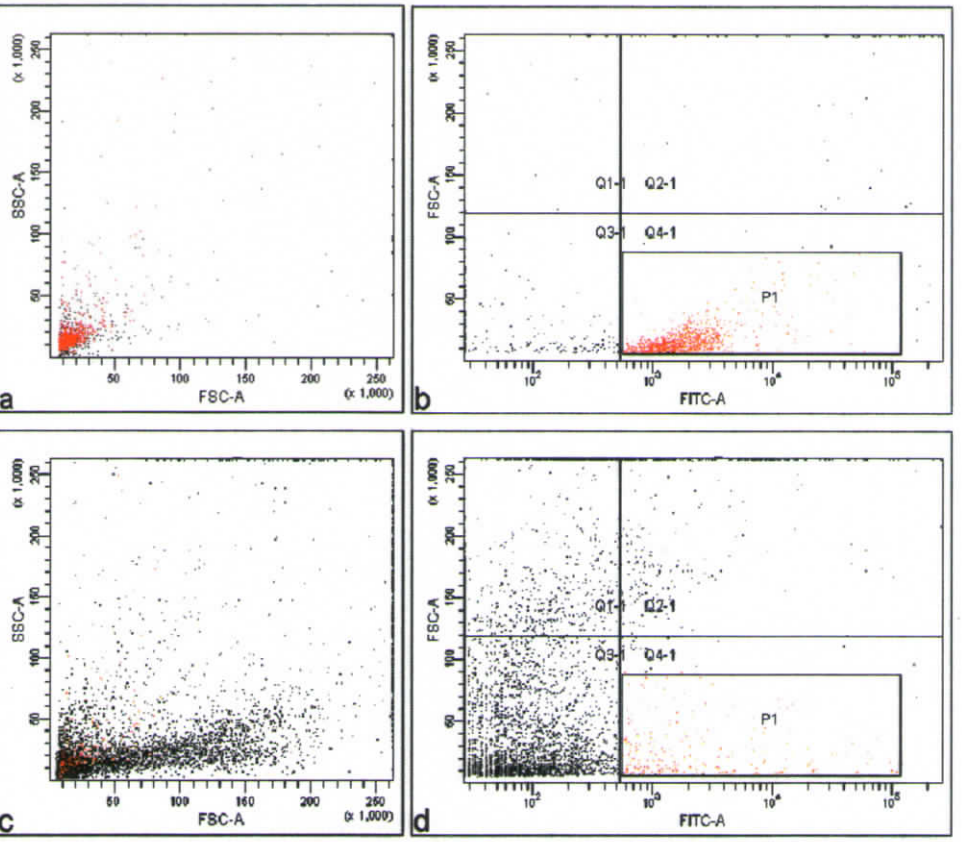

Figure 3-1: Flow cytometry analysis of different markers. a & b represent analysis of p63, 69% of analysed cells were found to be p63 positive. c & d represent ABCG2 analysis, 3.2% cells were positive. Forward and side scatter (a&c) in both cases showed that the positive cells were of small size with low side scattering properties.

3.1.1.2 Limbal explant culture

The limbus was treated with dispase for around 30 minutes and cultured in either IMDM with 10% FBS or Panserin 801 with 5% FBS. In both culture conditions, cells with melanin were found to be migrating from explant (Figure 3-2). In the transverse sections of limbus, melanin pigmented cells in the basal layer was quite evident (Figure 3-3). Thus, the pigmented cells *in vitro* gave evidence for migration of limbal basal cells in culture. Presence of melanin pigmentation in limbus was thought to give protection to limbal cells from harmful UV radiation (Schlotzer-Schrehardt and Kruse, 2005). Melanin is produced and transported by melanocytes which are distributed in the basal layer with their cellular projections extending to surrounding epithelial cells (Higa et al., 2005).

As seen in Figure 3-2 (c), colony like appearances were observed repeatedly when cultured in IMDM with 10% FBS. The cells that initially migrated from the explant acted

as autofeeder layer on which another epithelial layer started to spread and proliferate. Probably, it could be the stromal cells that migrated initially in IMDM with 10% FBS, which acted as feeder layer for the limbal epithelial progenitor cells to migrate out.

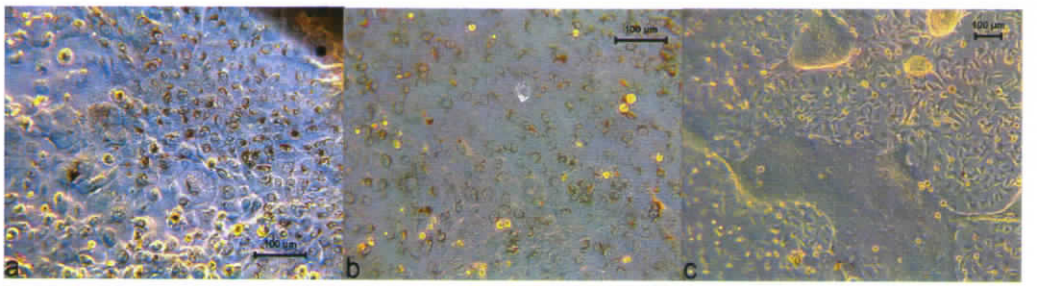

Figure 3-2: Goat limbal cells in culture a) Panserin 801 with 5% FBS, b) IMDM with 10 % FBS, c) Formation of multilayer in IMDM with 10% FBS

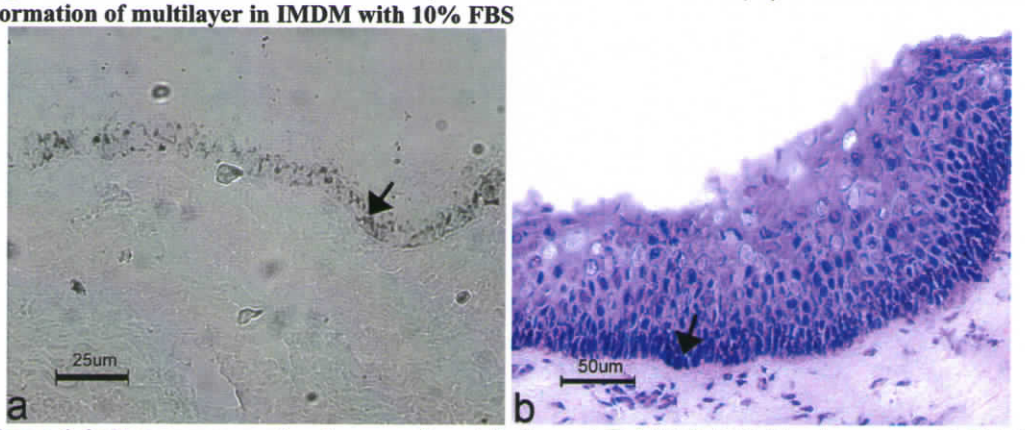

Figure 3-3: Transverse section images of goat limbus. a) Bright field light microscopy, b) Toluidine blue staining. Melanin deposition can be seen in basal cells of limbus in both images (arrow).

3.1.1.3 Characterisation of cells

The cultured cells were stained for p63, CK3 after culturing for one week and ABCG2 after culturing for 2 weeks (Figure 3-4). The cells that migrated out from the explant might be in different proliferative stages, which resulted in positive staining for differentiated cells also.

The cells after culturing for 7 and 21 days were stained for p63 and PCNA simultaneously. PCNA is a specific marker for proliferating cells. PCNA expression was not found on the 7th day staining while it increased on 21st day (Figure 3-5). p63 intensity decreased from 7th day to 21st day. This finding correlated with already reported results. Pellegrini et al reported that cells expressing high levels of p63 frequently did not express PCNA (Pellegrini et al., 2001). Thus, high levels of p63 indicate cells with proliferative potential rather than cells which are actively proliferating (Chee et al., 2006).

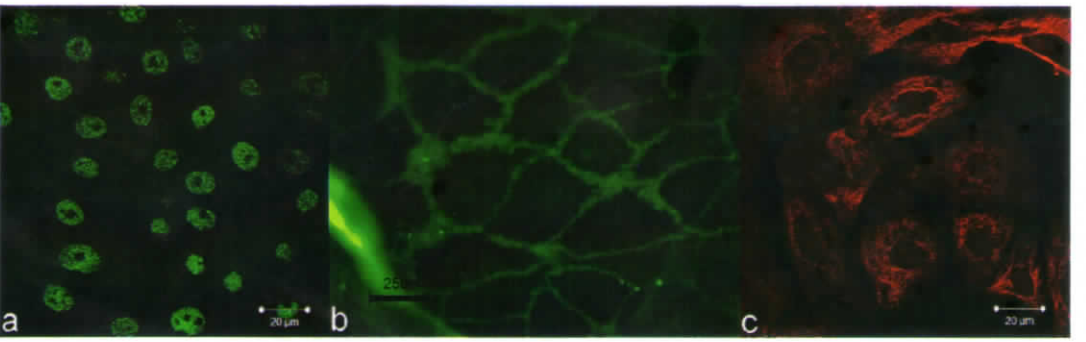

Figure 3-4: Immunofluorescent images of goat limbal cells a) p63, b) ABCG2, c) CK3

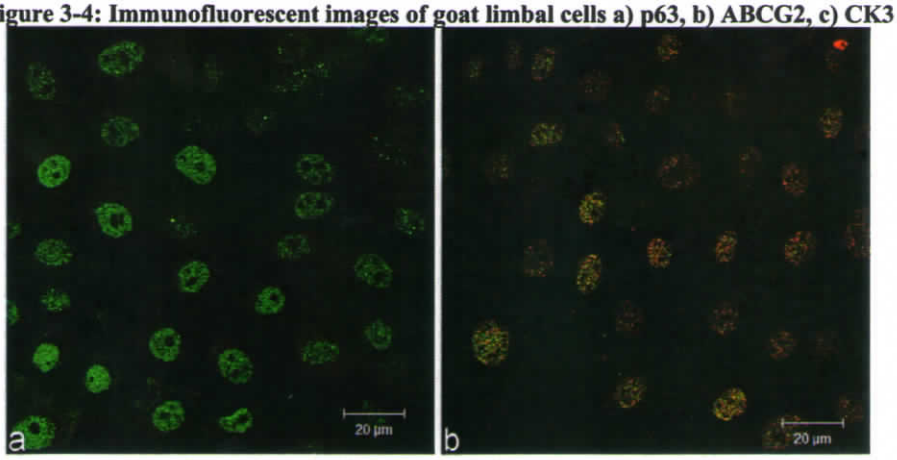

Figure 3-5: Double immunofluorescent images of goat limbal cells stained for p63 (green) and PCNA (red). a) 7 days, b) 21 days. By 21 days, PCNA expression increased compared to 7th day while p63 expression decreased.

3.1.2 Optimisation of culture conditions for rabbit limbal cells

3.1.2.1 Effect of dispase

The explants were treated with dispase for different time periods like 10, 30 and 60 minutes. The duration of enzyme treatment had a definite impact in the integrity of migrated cells over the culture period (Figure 3-6). As the time period of dispase treatment increased, the heterogeneity of migrated cells increased. The cells also tend to be more deteriorated as the dispase treatment increased.

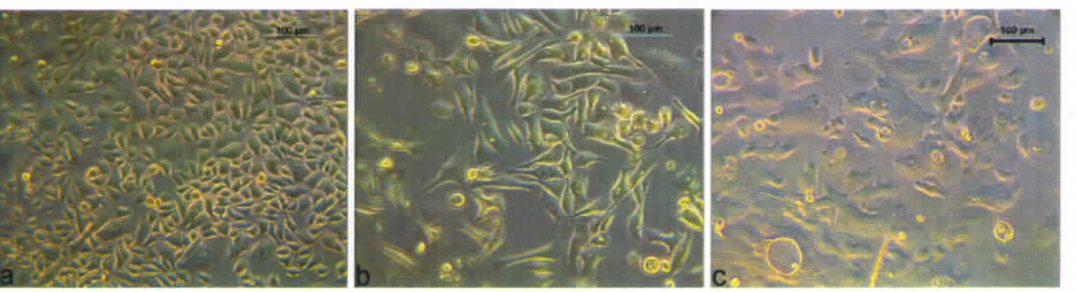

Figure 3-6: Rabbit limbal cells migrated from explants treated with dispase for different duration [a) 10 minutes, b) 30 minutes, c) 60 minutes], after 7 days

Dispase is a neutral metalloprotease used to loosen or release epithelial cells from substratum. It cleaves the BM zone region. Initial treatment with dispase for explant as well as cell suspension culture was widely reported in limbal cell culture (Meller et al., 2002; Zhang et al., 2005). Eventhough dispase is considered to be a mild enzyme compared to trypsin, this experiment showed that treatment duration is also important. Extensive blebbing of corneal basal cells by increased incubation with dispase was reported earlier (Spurr and Gipson, 1985). Limbal stem/progenitor cells are situated in basal layer. Thus, dispase treatment could be damaging to limbal epithelial progenitor cells. Hence the necessity of dispase was evaluated by culturing explants with or without enzyme treatment.

The experiment had been carried out in different medium conditions. There was significant decrease in the migratory distance in culture system 1 & 2 on 2^{nd} day when explants were not treated with dispase ($p<0.001$) (Figure 3-7 a). However, no significant difference was observed in any of the culture systems by 4^{th} day in the presence or absence of dispase treatment (Figure 3-7 b). The significant difference on 2^{nd} day implied that dispase treatment might have enabled a sudden initial migration of cells from explants. There was no influence of dispase treatment on the migratory distance as the culture period increased. As *ex vivo* expansion of cells for transplantation requires more than 4 days, the initial difference in migratory distance could be neglected. Therefore, this experiment suggested that dispase treatment is not a prerequisite for explant culture. The number of explants from which cells migrated in each culture condition also confirmed these results (Table 3-1).

Dispase treatment definitely helps to loosen or release epithelial cells from large tissue pieces. It could be the small size of the explants in the present study that helped the cells to migrate out even in the absence of any enzyme treatment. For transplantation studies, culturing without enzyme treatment will be ideal.

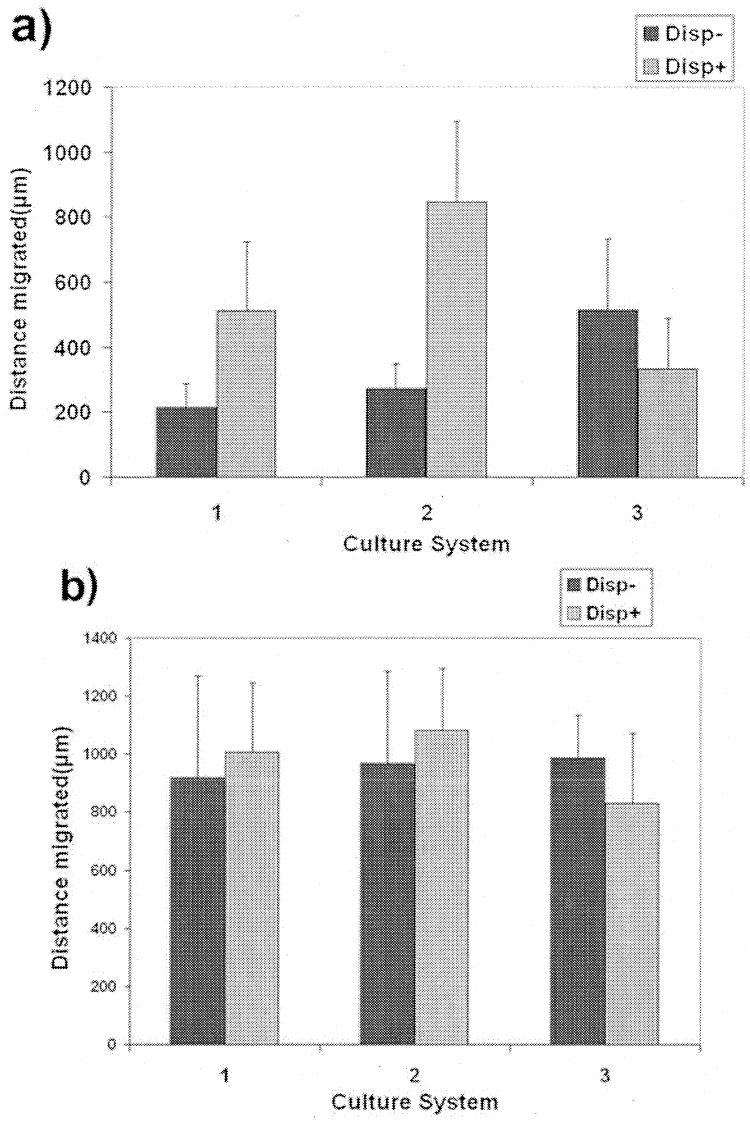

Figure 3-7: Graph showing the distance migrated by limbal cells from explants with and without dispase treatment, in different culture conditions a) 2nd day, b) 4th day (n=15). 'Disp-' is without dispase treatment and 'Disp+' is with dispase treatment.

Culture system	Dispase treated (%)	Untreated (%)
1	80	75
2	95	90
3	75	75

Table 3-1: Percentage of explants from which cells migrated in both dispase treated and untreated conditions in different culture systems on day 4. The total number of analysed explants in all conditions was 20.

3.1.2.2 Effect of medium

Different mediums alone or in combinations were used to identify the optimum one for rabbit limbal cell culture intended for cell sheet retrieval. As dispase treatment had no significant effect on cell migration from explants by 4th day, untreated explants were used for this experiment. Migration of cells in culture system 4 could not be assessed as the system involved use of two different mediums at different stages of culture. Since only the initial stage is considered for cell migration, culture system 4 was excluded.

When compared to culture system 2, there was significant increase ($p<0.001$) in the migratory distance in culture system 3 on 2nd day. However, there was no significant difference in the distance migrated by the cells in all the culture conditions by 4th day (Figure 3-8).

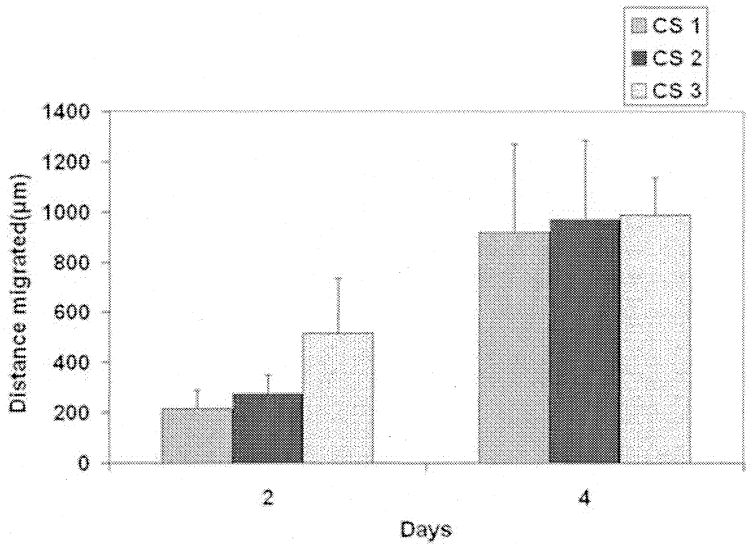

Figure 3-8: Graph showing the distance migrated by limbal cells from explants cultured in different culture systems (n=15). CS- culture system

The morphology of the migrated cells was different in each culture conditions (Figure 3-9). The cells in culture system 1 showed few cell-cell contacts and existed as single entities. In most of the cases, the cells did not form confluent cultures. But the migration in the initial days was good and similar to those in the other culture conditions. The cells in both culture system 2 and 3 had good cell-cell contacts and formed a continuous monolayer. The cells in culture system 3 were comparatively smaller in size while that in culture system 2 were more of a fibroblastic morphology.

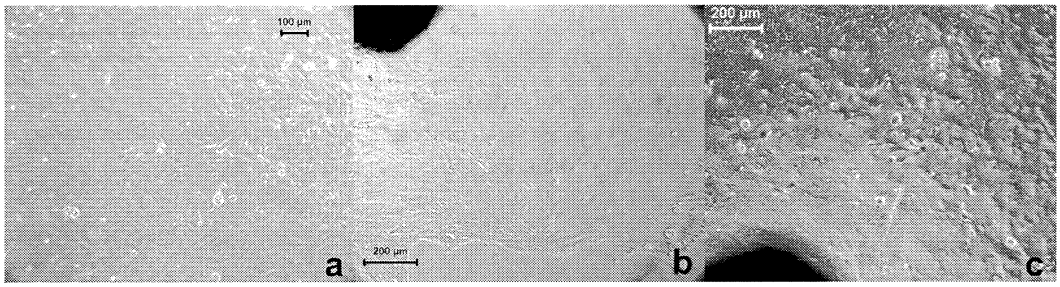

Figure 3-9: Morphology of rabbit limbal cells cultured in different culture systems for one week. a) Culture system 1, b) Culture system 2 and c) Culture system 3

Panserin 801 in culture system 1 is a keratinocyte specific medium that prevents overgrowth of fibroblasts. The supplements added in this medium selectively enhance epithelial cell growth. It was reported that fibroblast proliferation can be arrested by culturing in media containing 0.15mM Ca^{++} and same supplements (Varani et al., 1990) as provided with Panserin 801. They reported that this level of calcium is lower than that needed for fibroblast growth. Thus, the low Ca^{++} concentration in MCDB153 (0.03mM) which is the basal medium in Panserin 801, maybe the reason for prevention of fibroblast overgrowth in culture system 1. Formation of strong cell-cell contacts with thick monolayer was negligible in culture system 1. This might be due to absence of feeder layer. In the *in vivo* situation, interaction between the epithelium and stromal cells is necessary for maintaining stemness as well as proliferative capacity, as and when needed. The low cell-cell contact during monolayer formation in culture system 1 may be due to the absence of such an interaction. Murakami et al reported similar results. The cell sheet developed by them in the absence of 3T3 feeder layer and serum was fragile (Murakami et al., 2006). As serum can stimulate limbal progenitor cells into clonal proliferation (Kruse and Tseng, 1993), 5% FBS was also added to ensure proper growth of LSC. Use of autologous serum would be more preferable as it had been proved effective in proliferation and development of xenobiotic free ocular surface equivalents (Nakamura et al., 2006).

Iscove's Modified Dulbecco's Medium is a highly enriched media for rapidly proliferating cells. Lack of specific growth factors for limbal epithelial progenitor cells in culture system 2 might have led to the preferential growth of fibroblast like cells, which had probably migrated out from limbal stroma. The results obtained encouraged to check whether the fibroblast like cells could act as feeder for limbal epithelial SC. Therefore, culture system 4 was formulated.

Formation of a second epithelial cell layer on top of already migrated cells was observed in culture system 4 (Figure 3-10) on repeated experiments. Initially fibroblast like cells migrated when the medium was culture system 2. Changing in to culture system 3 might have prompted the epithelial progenitor cells to migrate out on to the preceding cell layer. Thick continuous cell layer was formed with good cell-cell contacts.

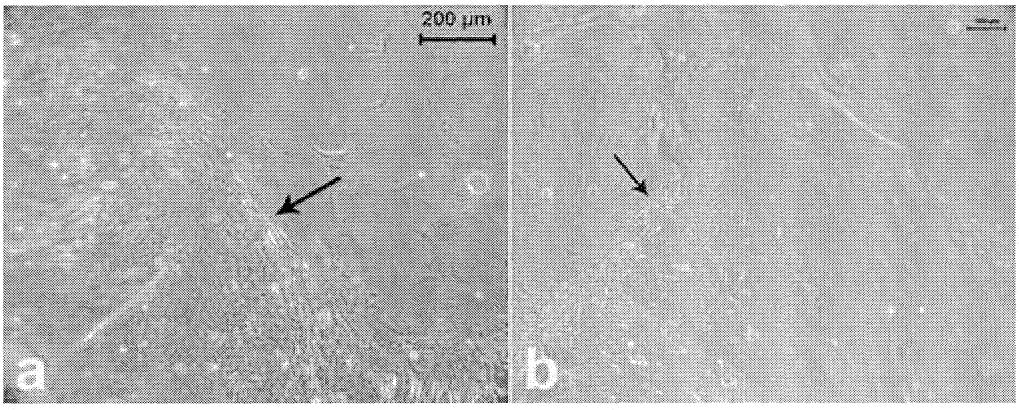

Figure 3-10: Formation of a second layer of cells on top of another in culture system 4. Arrow marks the top layer.

It was presumed that both culture system 3&4 provided a microenvironment which support maintenance of a population of already laid fibroblasts while inhibiting further proliferation. Culture system 3 might have enabled migration of both stromal cells and epithelial progenitor cells together while culture system 4 promoted migration of stromal cells only in the initial culture period.

Use of 3T3 feeder layer was widely reported for limbal cell culture (Lindberg et al., 1993; Liu et al., 2006). To avoid xenotoxicity, need for a substitute or elimination of use of feeder layer is increasingly demanding. In this study, formation of a top layer with the initial layer behaving as autofeeder helped in avoidance of the use of other feeder layers. This microenvironment provided the epithelial progenitor cells a surrogate niche where interaction with autofeeder cells and its secretome could be achieved. Clonal expansion of LSC may require additional support from TAC (Li et al., 2007) which is absent in 3T3 feeder layer. In the present technique, the migrating population might contain TAC also which would give an added advantage over the use of 3T3 cells.

In order to avoid contamination from xeno-feeder layers, different human feeder layers had also been developed and analysed (Chen et al., 2007; Sugiyama et al., 2008). Culturing on human cells from other sources certainly carries risk of pathogen transmission. Besides, it was demonstrated that interpretation of experimental data might

be limited as the culture system contain heterogenic cell types and their products (Bentz et al., 2007). As feeder layer supports the growth of epithelial cells through a vast variety of factors, attempts to achieve feeder free systems included addition of complex supplements or feeder conditioned medium. Cells had also been cultured on feeder layer during proliferative phase and further separated using robotic technology (Schneider et al., 2008). The culture system established in this study overcomes drawbacks of all these techniques. The autofeeder layer provides the SC niche for the limbal cells to proliferate and maintain, avoiding use of xeno/allogeneic feeders or addition of complex supplements.

3.1.2.3 Maintenance of stem cell characteristics

The migrated and proliferated cells from explant culture were stained for p63 after 8 days and observed under confocal microscope. Figure 3-11 (a-d) represents cells in different culture system expressing p63 marker. Figure 3-12 shows the intensity of expression in different culture system. It was observed that the intensity of p63 expression varied in different medium even though cells were found to be stained. On comparison with cells in culture system 1 using ANOVA single factor, there was a significant decrease in intensity of p63 expression in cells grown in culture system 2 ($p<0.001$).

There has been no proved 'bonafide' marker for identifying LSC till now (Chee et al., 2006; Pajoohesh-Ganji and Stepp, 2005). p63, a nuclear marker, is expressed preferentially by keratinocytes and LSC (Pellegrini et al., 2001; Radu et al., 2002) and is commonly used for characterization of limbal progenitor cells (Epstein et al., 2005; Harkin et al., 2004). To find out the ideal system that supports maintenance of stemness along with good proliferation and cell contacts, cells were stained for p63. Intensity of p63 expression was found to be varied in different medium. A gradient signal intensity of p63 was observed with the highest in limbus followed by peripheral cornea (Chee et al., 2006). Kim et al reported that smaller cells with a similar phenotype to stem cells had more p63 staining intensity compared to larger cells which might be of more differentiated phenotype (Kim et al., 2004a). Thus, p63 intensity can be considered as a marker of degree of stemness.

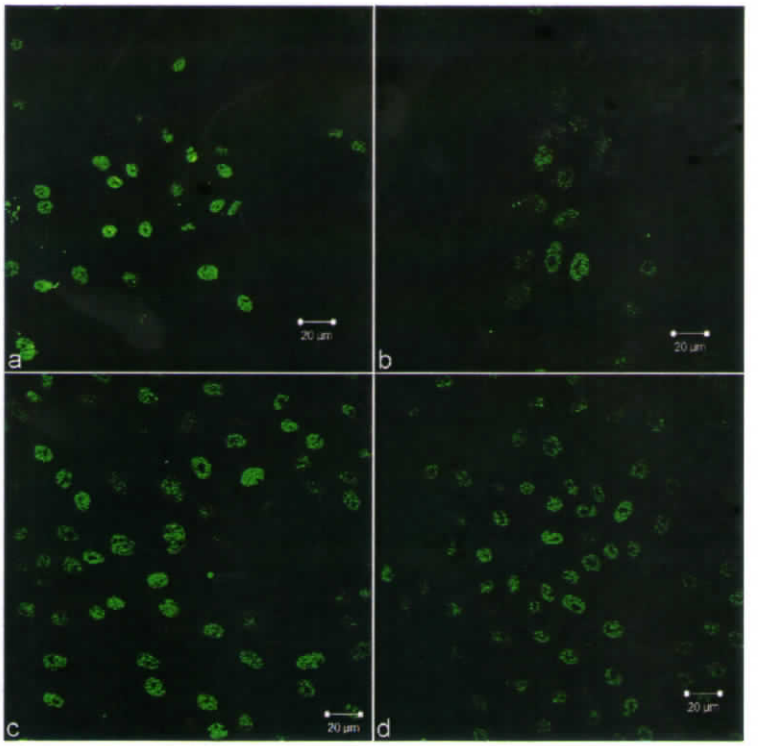

Figure 3-11: p63 expression in rabbit limbal cells in different medium. a) Culture system 1, b) Culture system 2, c) Culture system 3, d) Culture system 4

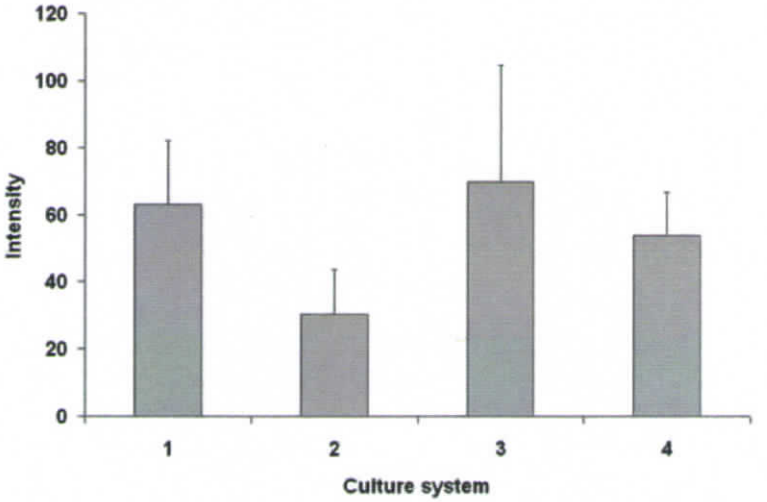

Figure 3-12: Graph showing the intensity of p63 expression in different culture system (n=20)

Although IMDM is meant for highly proliferating cells, it does not include any specific growth factors to support the selective growth of epithelial progenitor cells. It may be due to this fact that intensity of p63 expression in culture system 2 was significantly decreased from those in culture system 1. The results from this study showed that although IMDM with 10% FBS facilitated migration and growth of limbal cells from explants, it did not ensure a significant population of limbal epithelial progenitor cells in culture. Besides, the ability of migrated cells in culture system 2 to act as autofeeder and

their morphology suggested that they might be limbal stromal cells. On the other hand, all the other mediums containing Panserin 801 seem to be supporting the growth of limbal progenitor cells. This can be attributed to the presence of specific growth factors in Panserin 801.

3.1.3 Human limbal cell culture

Palisades of Vogt are very evident structures in human limbus that could also be the SC niche. Figure 3-13 a shows these structures under stereo dissection microscope. The morphology of human limbal cells *in vitro* is given in Figure 3-13 b. It was found that the cells migrated in culture system 4 expressed p63 (Figure 3-14).

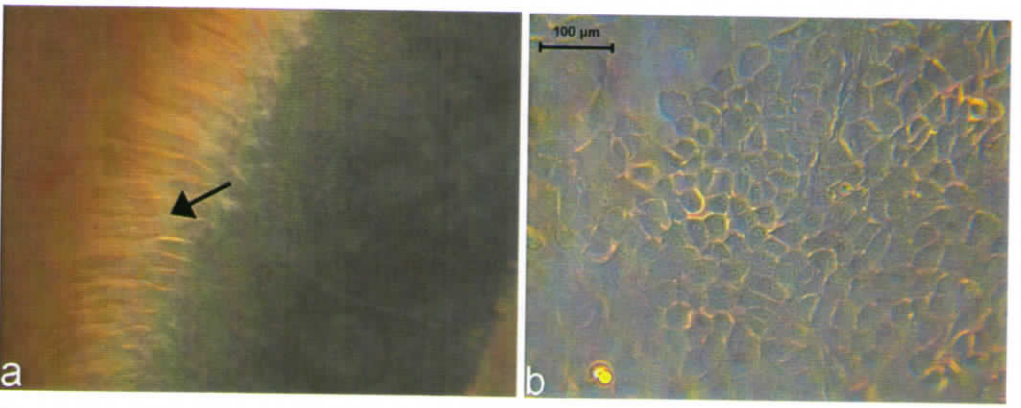

Figure 3-13: a) Palisades of Vogt (arrow) under stereo microscope, b) human limbal cells migrated from explants

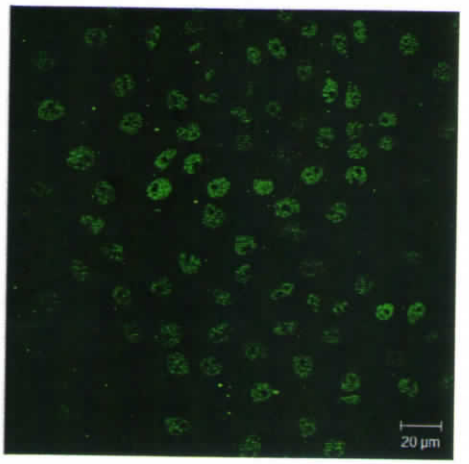

Figure 3-14: p63 expression in human limbal cells cultured in culture system 4

3.2 Preparation, characterisation and cytocompatibility assessment of thermoresponsive copolymer as a cell culture substrate

3.2.1 Preparation of NIPAAm - MMA copolymer

Polymeric form of MMA, Polymethyl methacrylate (PMMA) is one of the widely used biocompatible polymers in ocular applications such as intra ocular lens and contact lens. MMA was incorporated to modulate LCST. NIPAAm was incorporated to provide thermoresponsiveness whereby cells can be detached as intact cell sheets, avoiding the use of proteolytic enzymes. Moreover, this can assist in formation of scaffold free tissue constructs.

NIPAAm and MMA were taken in 9:1 ratio as a high percentage of MMA would lead to a low LCST, maybe even below room temperature. Crosslinker was not added during copolymerisation so that a copolymer solution could be obtained instead of a solid polymer.

Already reported common methods for preparation of thermoresponsive surfaces were electron beam irradiation and plasma polymerisation. Both of these techniques require sophisticated, expensive equipments which may not be available for all researchers. In this study, a new simple and cost effective technique was employed and utilised for creation of thermoresponsive tissue culture surfaces.

3.2.2 Characterisation

3.2.2.1 FTIR

The FTIR spectrum of the copolymer is given in Figure 3-15. The major peaks at 1627 cm^{-1} and 1538 cm^{-1}, characteristic of –NH-CO stretching and bending modes of NIPAAm, confirmed the presence of NIPAAm in the copolymer. The carbon-oxygen single bond (-CO-O-CH_3) stretching of unconjugated ester around 1130 cm^{-1} confirmed the presence of MMA in copolymer. The carbon-oxygen stretch of methyl ester around 979 cm^{-1} further substantiated the result. The carbon-oxygen stretching vibration of ester group around 1170 cm^{-1} could also be seen in the spectra which was a further evidence for the presence of MMA in the copolymer.

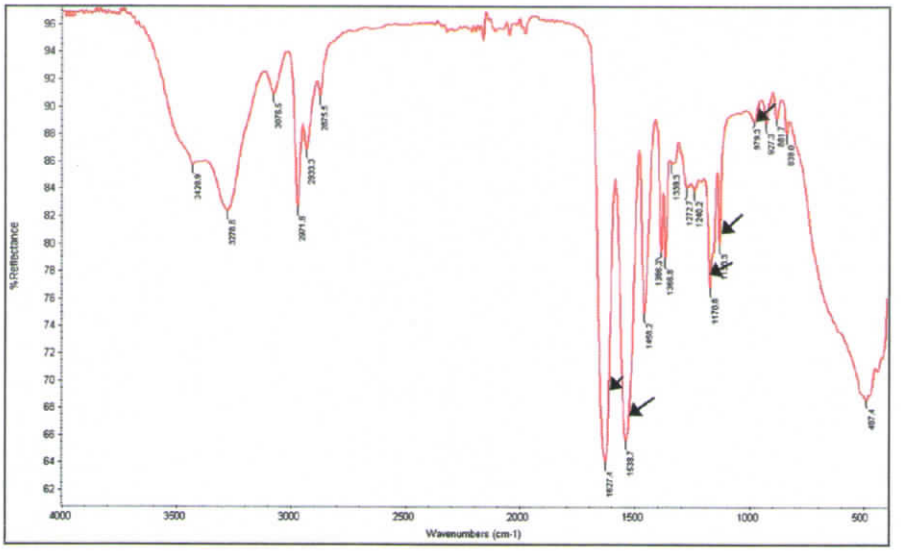

Figure 3-15: FTIR spectrum of NIPAAm-MMA copolymer. Arrows indicate characteristic peaks and confirms the presence of NIPAAm and MMA.

3.2.2.2 DSC

Thermoresponsive smart polymer undergoes phase transition from hydrophilic to hydrophobic state when temperature is raised. LCST is the point where the hydrophobic interaction of isopropyl group of NIPAAm outweighs the hydrophilic nature of the amide group on the pendant groups, forcing water out of the polymer. Figure 3-16 shows the DSC scan of the copolymer.

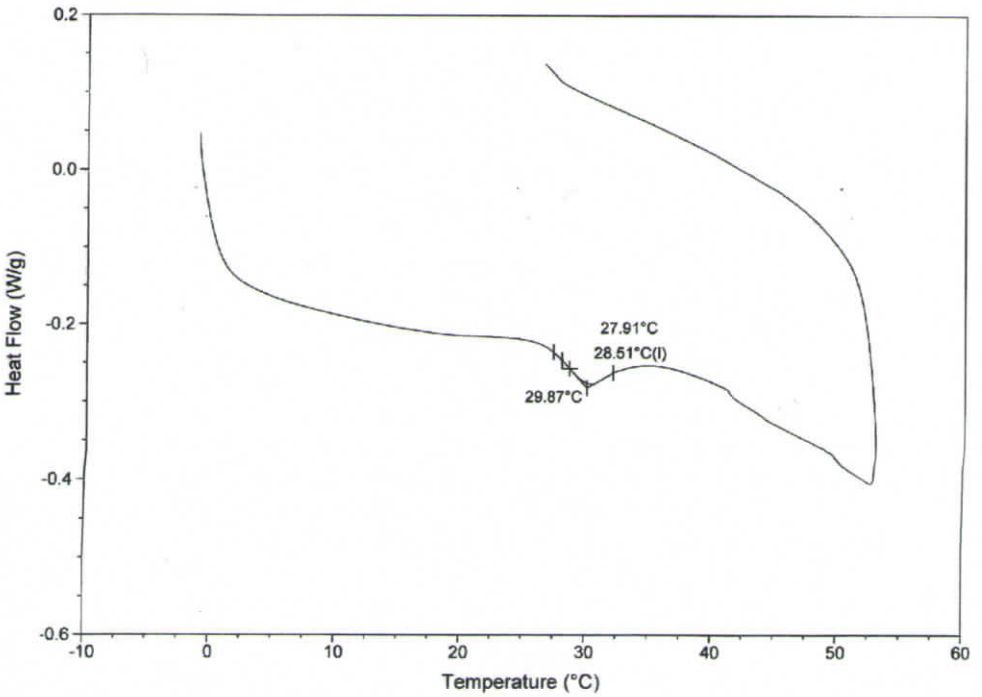

Figure 3-16: DSC scan of NIPAAm-MMA copolymer showing the LCST around 30°C

The LCST of the copolymer was centered around 30°C while that of PIPAAm is centered around 32°C (Takezawa et al., 1990). PIPAAm has a particular hydrophobic-hydrophilic ratio above and below LCST. Introduction of hydrophobic MMA disturbed this balance and changed the LCST. However, the LCST of the copolymer did not deviate much probably due to the low amount of MMA incorporated. It had been already reported that introduction of hydrophobic monomers like MMA decreases the transition temperature of the copolymer (Gao and Frisken, 2005; Tsuda et al., 2004). MMA addition did not change the LCST dramatically, which was desirable for further studies.

3.2.3 Characterisation of thermoresponsive surface

3.2.3.1 ATR

ATR spectrum of both coated and uncoated surfaces are given in Figure 3-17. The spectrum of the coated surface showed the characteristic peak of amide carbonyl group of NIPAAm at 1647 cm^{-1} while it was completely absent in bare TCPS dishes. Meanwhile, the strong peak due to monosubstituted aromatic ring was present in TCPS at 1600 cm^{-1}.

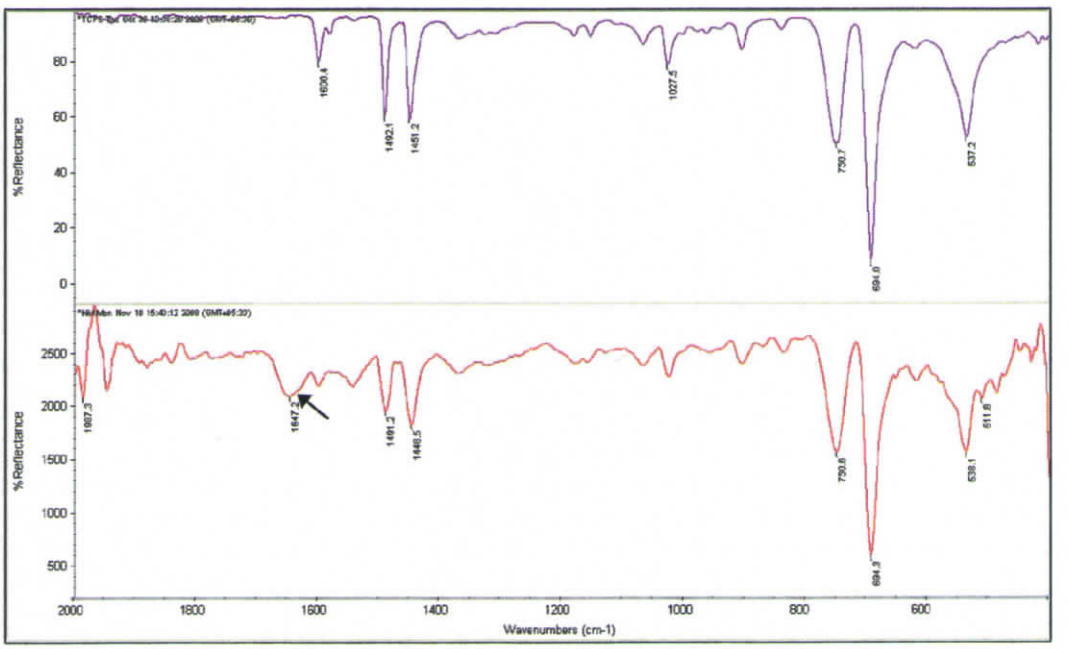

Figure 3-17: Comparison of ATR spectra of TCPS and NIPAAm-MMA. Arrow shows the peak around 1647 cm^{-1} on copolymer surface which is characteristic of NIPAAm.

3.2.3.2 Profilometry

A 1 x 1 mm coated and uncoated surfaces were scanned for surface topography. Three dimensional images showed that the uncoated surface had rougher topography compared to coated surfaces (Figure 3-18). Roughness calculation using software

confirmed this observation. The roughness parameters of both coated and uncoated surfaces are given in Table 3-2. This indicated that coating with NIPAAm-MMA covered and smoothened the TCPS surfaces.

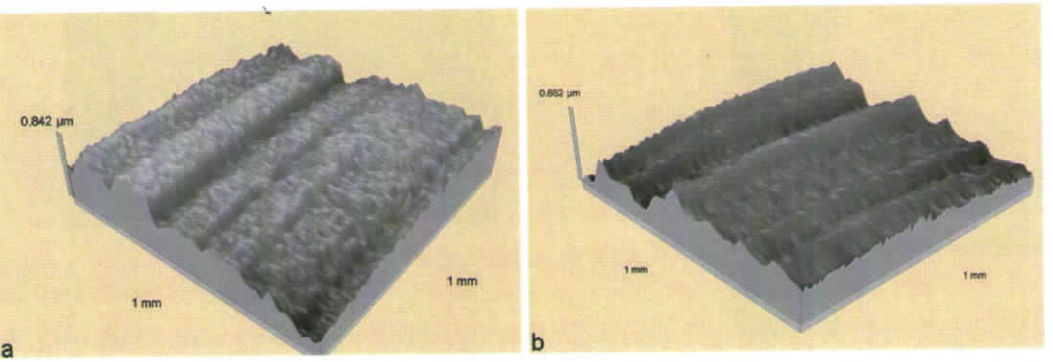

Figure 3-18: Surface topography of 1mm x 1mm surfaces. a) TCPS, b) NIPAAm-MMA

Roughness parameters	Uncoated	Coated with NIPAAm-MMA
Ra	6.06 ± 0.679 nm	3.37 ± 0.188 nm
Rq	7.39 ± 0.876 nm	4.04 ± 0.262 nm
Rp	12.1 ± 1.62 nm	5.54 ± 0.325 nm

Table 3-2: Roughness parameters of uncoated and coated surfaces. Ra – arithmetic average of absolute values, Rq – root mean squared, Rp – maximum peak height

The decrease in roughness, due to the smoothening of TCPS surfaces during the coating, gave indirect evidence for the presence of copolymer on the surface. Surface roughness play an important role in determining the cell-material interactions (Huang et al., 2004; Marinucci et al., 2006). Cell culture studies on NIPAAm-MMA suggested that a surface roughness of Ra 3.37 ± 0.188 nm was enough for the fibroblast cell line to attach and grow.

3.2.3.3 Contact angle

Wettability varies with respect to the surface chemistry of the substrate. A high contact angle indicates low degree of wetting and vice versa. The contact angle of the TCPS was found to be 83.7 ± 1.63 while that of NIPAAm-MMA plates was 63.3 ± 0.75. This change in wettability indicated coating of the surface with copolymer. The measurement was taken at 26°C, below the LCST of copolymer, which could be a reason for the comparatively high wettability of NIPAAm-MMA surface.

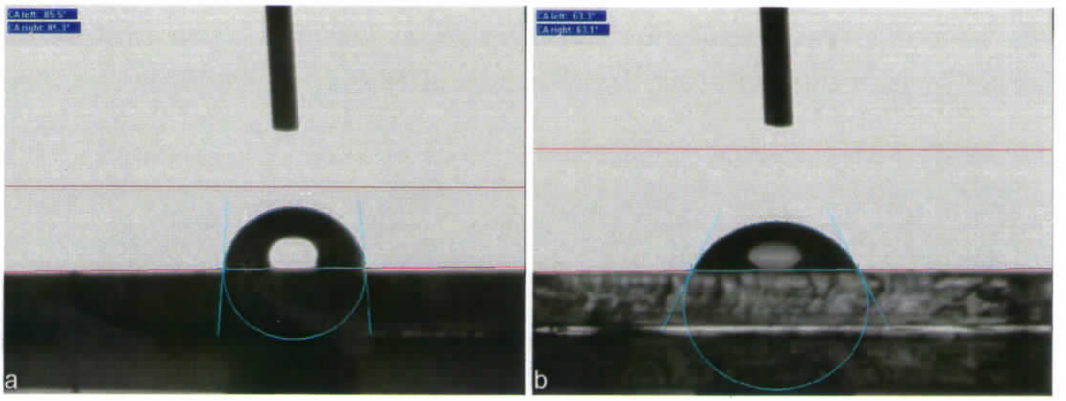

Figure 3-19: Images of contact angle measurement of a) TCPS, b) NIPAAm-MMA. NIPAAm-MMA surface had an increased wettability.

3.2.4 General cytocompatibility

3.2.4.1 Cell culture studies

L929 cells and SIRC cells were cultured on NIPAAm-MMA. L929 cell line was selected for this work because of its wide use in cytocompatibility studies and easy maintenance. Moreover, this is recommended by International standard ISO 10993-5 for *in vitro* cytotoxicity testing in biological evaluation of medical devices. As the copolymer was intended to be used in corneal surface regeneration, SIRC, a corneal cell line was cultured to understand how it favours the cell adhesion and viability of the specific cell type.

3.2.4.2 Cytotoxicity assay

The cells that came in direct contact with NIPAAm-MMA did not show any toxic effects. The cells exhibited normal morphology after 24 h (Figure 3-20 b) and stained with neutral red (Figure 3-20 c), confirming the non-cytotoxicity of NIPAAm-MMA.

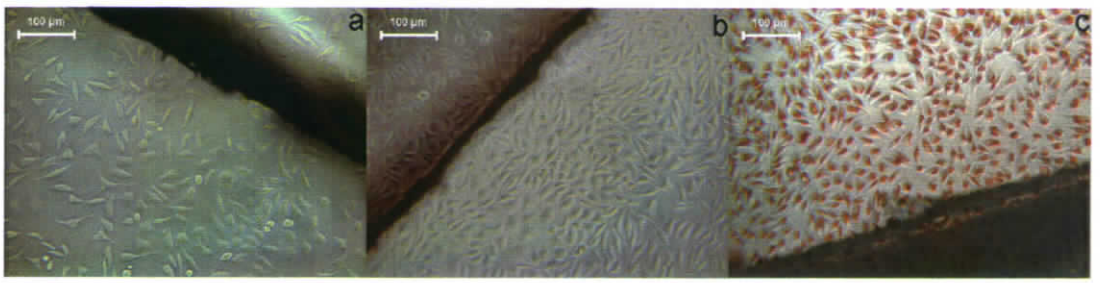

Figure 3-20: L929 cells in direct contact with the copolymer. a) 0 h, b) 24 h, c) stained with neutral red after 24 h

3.2.4.3 Cell morphology

The morphology of the L929 cells on NIPAAm-MMA, as observed under phase contrast microscope, was similar to cells on TCPS throughout the culture period. After 24

h, cells on both TCPS and NIPAAm-MMA were spread fully with small spindle processes confirming to the normal morphology of fibroblasts. The cells maintained the same status at 72 h (Figure 3-21).

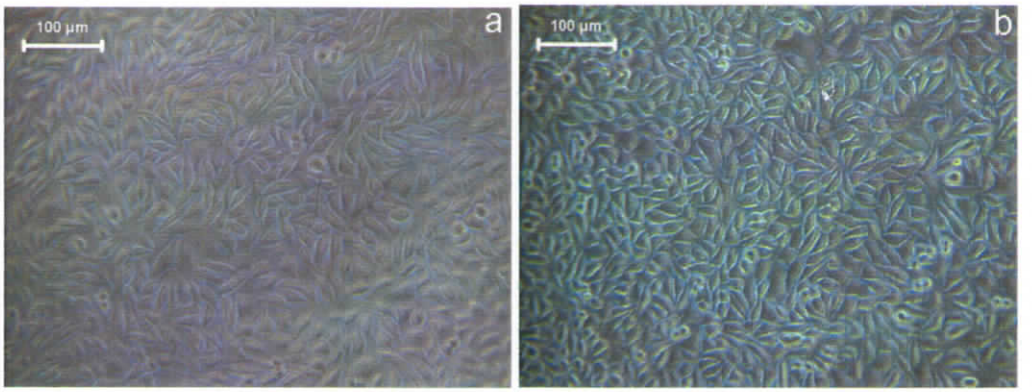

Figure 3-21: Phase contrast images of L929 cells at 72 h. a) TCPS, b) NIPAAm-MMA

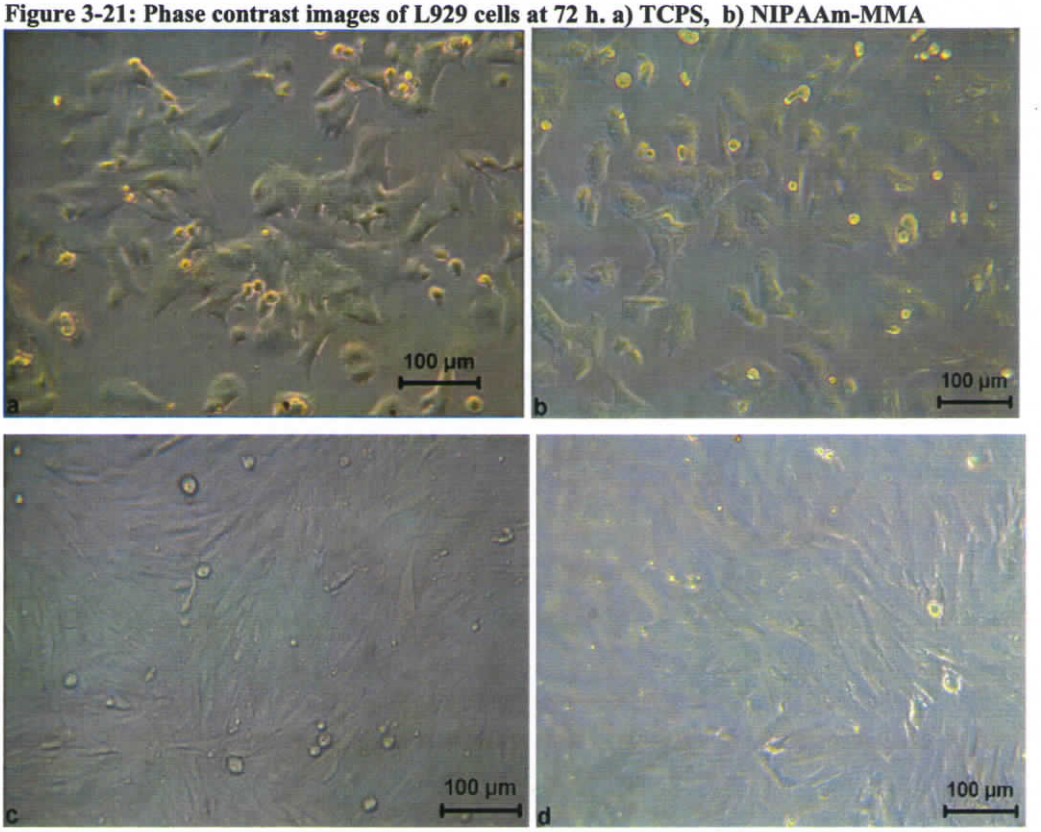

Figure 3-22: Phase contrast images of SIRC cells after 24 h [a) TCPS, b) NIPAAm-MMA] and 72 h [c) TCPS, d) NIPAAm-MMA]

After 24 h, SIRC cells started spreading on both substrates as viewed by the morphological change from round towards slight spindle shape (Figure 3-22 a&b). Monolayer of the cell line had same morphology on both TCPS and NIPAAm-MMA at 72 h (Figure 3-22 c&d).

3.2.4.4 Cell viability

Neutral red assay is one of the most common methods to study acute toxicity of materials in cell culture (Lonnroth and Dahl, 2001; Repetto et al., 2008; Werner et al., 1999). This method is based on the ability of cells to incorporate and retain the weakly cationic supravital dye within lysosomes of live cells. Thus the retention of the dye within cells indicates the cytocompatibility of cell culture substrate.

Neutral red staining revealed that both cell types were viable after culturing on NIPAAm-MMA (Figure 3-23). This result in turn indicated the cytocompatibility of culture surface.

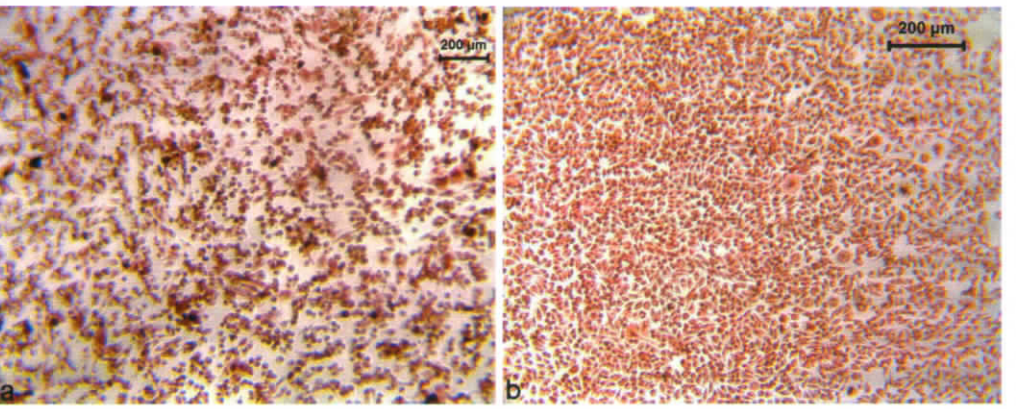

Figure 3-23: Neutral red staining of cells cultured on NIPAAm-MMA copolymer. a) SIRC cells, b) L929 cells

3.2.4.5 Cytoskeletal organization

Attachment and spreading of cells on a new substrate includes rearrangement of cytoskeleton resulting in different patterns and organization of actin, to give morphological and mechanical integrity to cells. Cytoskeletal organization could be an indicator of properties and cytocompatibility of the substrate (Kumari et al., 2002).

To check whether the spreading of cells would differ on the NIPAAm-MMA copolymer from that on TCPS, phalloidin-FITC staining was done. Cell spreading was similar on both substrates (Figure 3-24). Evenly distributed actin filaments suggested good cell spreading. Also, it was evident from the fluorescent images that the surface was not inducing any stress on the cells.

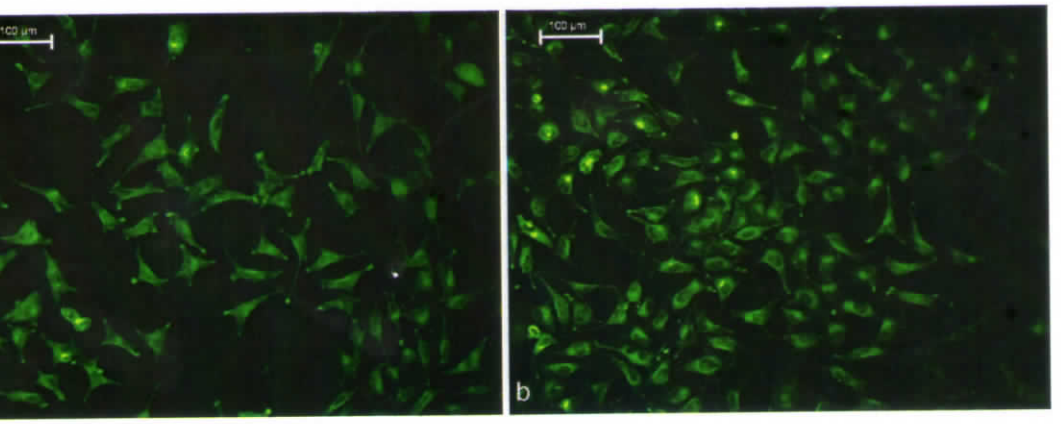

ure 3-24: Cytoskeletal organisation showing spread morphology of L929 cells. a) TCPS, b) PAAm-MMA

.4.6 Cell attachment and doubling time

Tritiated thymidine uptake assay was performed to assess the proliferative pacity of L929 cells after culturing on the NIPAAm-MMA, in comparison to TCPS. dioactively labelled thymidine, when supplied in the medium, was taken up by cells in phase. It would be incorporated into DNA during S phase which enables the antitative measurement of proliferating cells. The same method was used to analyse the tial cell attachment rate by counting the unattached cells at 4 h and subtracting that m the number of cells seeded. Radioactive labelled, known number of cells (amount eded) was taken as control to achieve this target.

Upon analysing the count of unattached cells, it was found that the number of lls attached initially on both TCPS and copolymer was similar (Figure 3-25 a). Initial ll attachment on substrate is an important event in cell material interaction as it ecedes all other functions like spreading, migration, proliferation and differentiation. is results suggested normal cell adhesion rate on copolymer.

In cell culture, doubling time is the time period required for the cells to double in eir number. Therefore, it depends on the proliferative status of cells. Doubling time of a rticular cell type on substrates that support proliferation will be less compared to bstrates that do not support proliferation. No significant increase was observed in the ubling time of cells when cultured on NIPAAm-MMA (Figure 3-25 b) which indicated at the substrate supported similar proliferation.

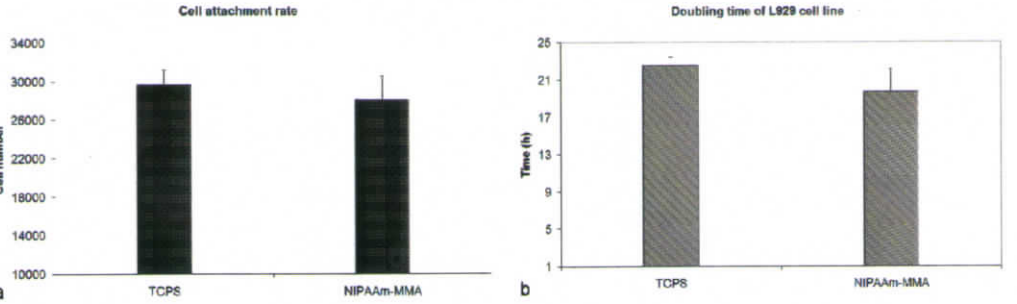

Figure 3-25: Graphs showing results of tritiated thymidine uptake assay. There was no significant difference in the attachment rate (a) and doubling time (b) of cells on both substrates. (n=3)

The results suggested that the copolymer did not have any negative influence on the adhesion and proliferation of cells.

3.2.4.7 MTT assay

This method was first described by Mosmann to detect cell survival and proliferation (Mosmann, 1983). According to published reports, MTT assay was employed for measuring cell viability (Green et al., 1984), cytotoxicity and *in vitro* evaluation of biomaterials (Uludag and Sefton, 1990). MTT assay is simple and avoids use of radio active materials in cytocompatibility testing. This assay was based on the conversion of a yellow tetrazolium salt ([3-4,5-dimethylthiazol-2-yl]-2,5-diphenyl tetrazolium bromide) by mitochondrial succinic dehydrogenases in the cell to purple formazan crystals (Figure 3-26 a).

The experiment was done for 2 different time points to check the effect of the NIPAAm-MMA on cellular metabolic activity, function and in turn viability.

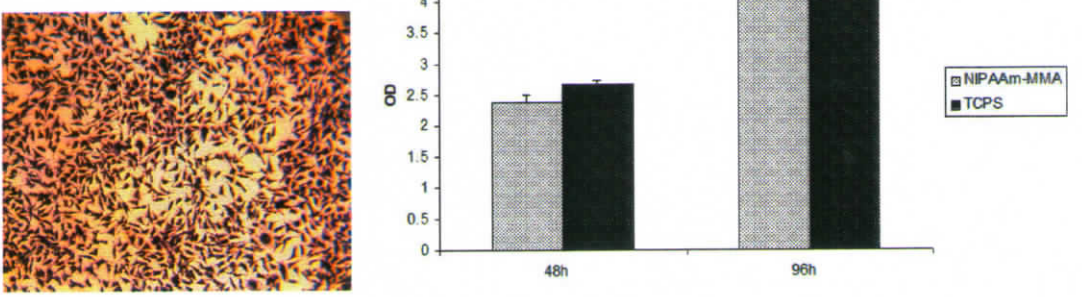

(a) (b)

Figure 3-26: a) Formazan crystals in L929 cells after incubation with MTT. b) Graph depicting results of MTT assay. At both 48 and 96 h, the cell metabolism was similar in TCPS and NIPAAm-MMA (n=3).

As seen from the graphs, the cellular activity and mitochondrial function were similar in both substrates at 48 and 96 h (Figure 3-26 b). Eventhough there was a little difference at 48 h; it was not statistically significant.

3.2.4.8 Cell cycle analysis

Cell cycle of L929 cells cultured on NIPAAm-MMA was studied using flow cytometric analysis after PI staining and compared with that on TCPS. A similar percentage of cells on both substrates in different stages of cell cycle indicated that none of the cell cycle stages was affected after 24 h of culture on NIPAAm-MMA (Figure 3-27). Percentage of dead cells (gated as 'A') on both substrates was comparable.

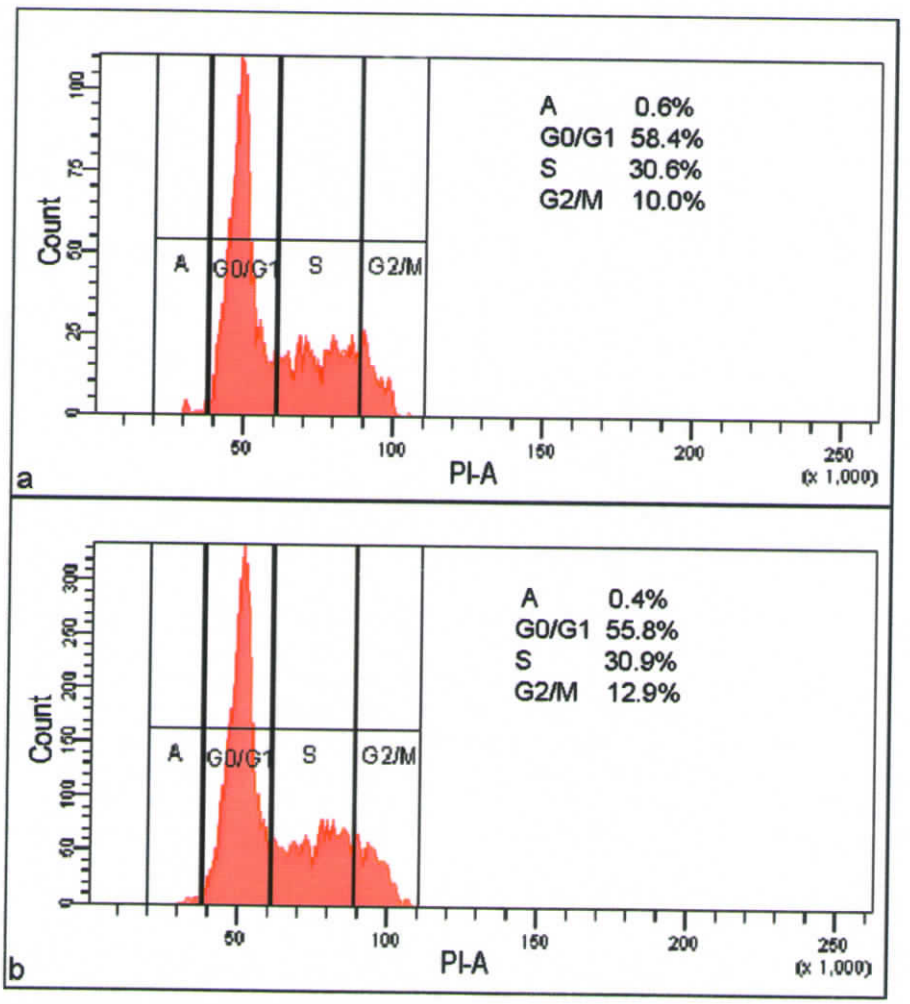

Figure 3-27: Flow cytometric data showing percentages of cells in different stages of cell cycle after 24 h. a) TCPS, b) NIPAAm-MMA

3.2.5 Specific cytocompatibility analysis using mRNA expression of progenitor and differentiated markers in human limbal cells

Expression of ΔNp63, ABCG2, CK3 and Connexin 43 at mRNA level was analysed to understand the limbal cell population on copolymer. Hypoxanthine-guanine phosphoribosyl transferase (HPRT) was used as the house keeping gene.

Semi quantitative PCR was done for ABCG2 and detectable products in gel were found at 32nd cycle of amplification in all the samples (Figure 3-28). Results of this study suggested comparable limbal stem cell population existed on different substrates.

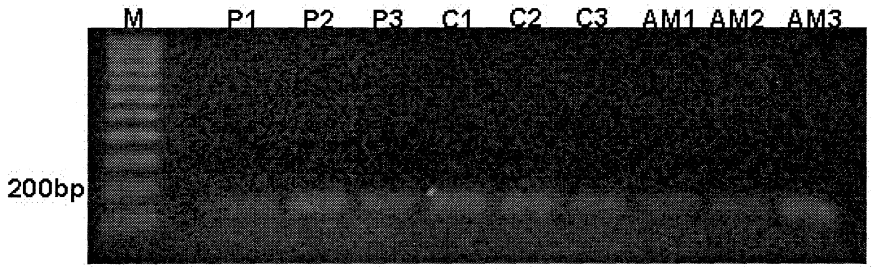

Figure 3-28: Expression of ABCG2 at 32nd cycle of amplification. M-Marker, P1, P2, P3- replicates from NIPAAm-MMA, C1, C2, C3- replicates from TCPS and AM1, AM2, AM3- replicates from amniotic membrane.

For successful transplantation and restoration of vision, presence of progenitor/stem cells is necessary in the cell sheet. A 100% differentiated population could not maintain corneal epithelial regeneration, thus leading to failure of transplantation. Surface properties along with the provided microenvironment can lead to a rapid differentiation of cells. Reverse transcription PCR helped to check whether primary limbal cell culture on NIPAAm-MMA sustained progenitor cells. The results showed that the primary culture contained population of both differentiated and progenitor cells (Figure 3-29). Based up on the proliferative status of the cells migrated from the explant, different cells would be in different stages like SC, TAC or post mitotic cells in a defined culture period. Thus, a mixture of cell population could be expected.

NIPAAm-MMA did not enhance differentiation compared to culture on TCPS. As TCPS is only a bare substrate, its ability to preserve progenitor properties of the cells is questionable. Thus, amniotic membrane, a well known limbal cell culture substrate, was also used as control to analyse expression of dNp63, connexin 43 and ABCG2 markers. AM had also been suggested as SC niche for limbal cells.

The intensity of bands suggested that the expression of these markers in both NIPAAm-MMA and AM were similar. This study showed that limbal population on AM also contained both differentiated as well as progenitor cells (Figure 3-29).

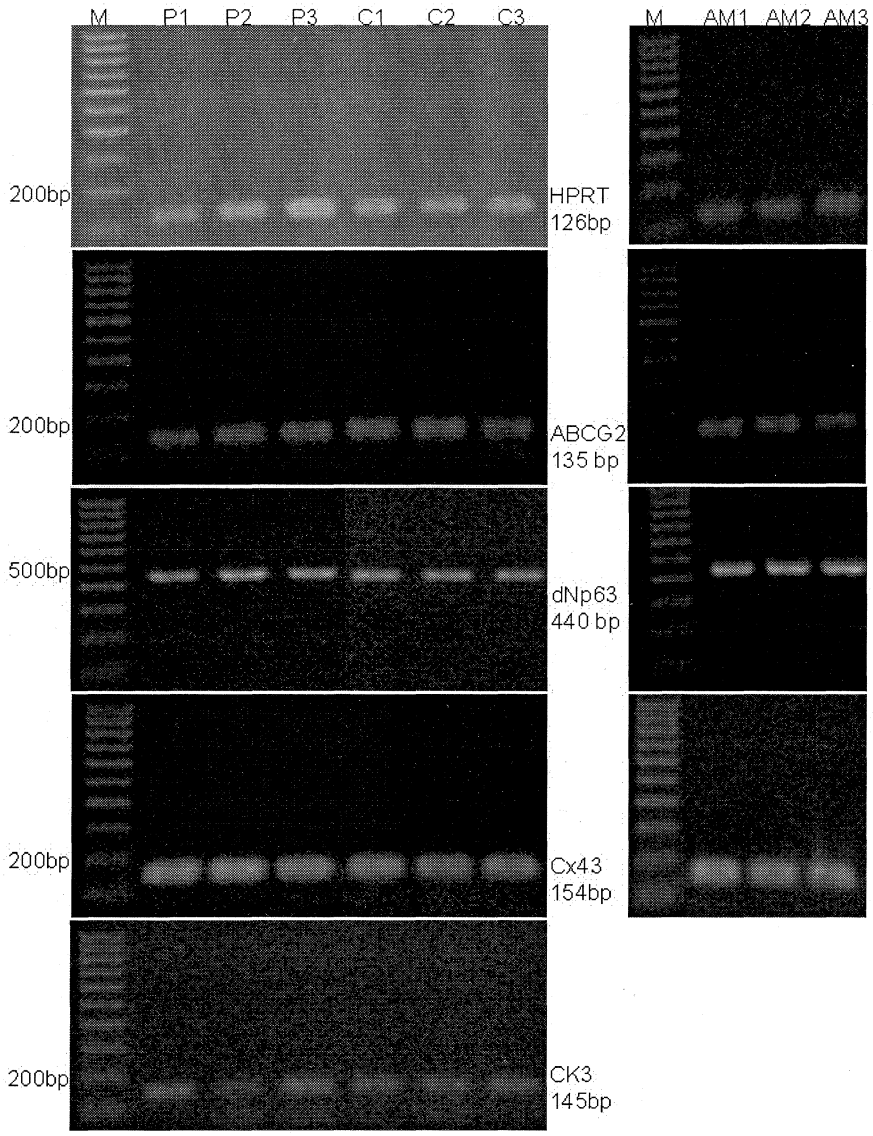

Figure 3-29: Expression of different markers in human limbal epithelial cells grown on different substrates (amplification- 37 cycles). M- Marker, P1, P2, P3- replicates from NIPAAm-MMA, C1, C2, C3- replicates from TCPS, AM1, AM2, AM3- replicates from amniotic membrane and Cx43- connexin 43.

3.2.6 Thermoresponsiveness

Incubation of cells below LCST of copolymer showed no cell remnants on the surface where PVDF membrane was kept (Figure 3-30). All the cells were transferred from the copolymer surface to the PVDF membrane at this temperature. This was achieved by the phase transition of copolymer around its LCST leaving the culture

surface hydrophilic at low temperatures. The hydrophilic nature of the copolymer below its LCST results in weakened interaction between the surface and cells with ECM compared to that between the PVDF membrane and cells, enabling the transfer (Kushida et al., 2001). This proved thermoresponsive nature of the culture surface.

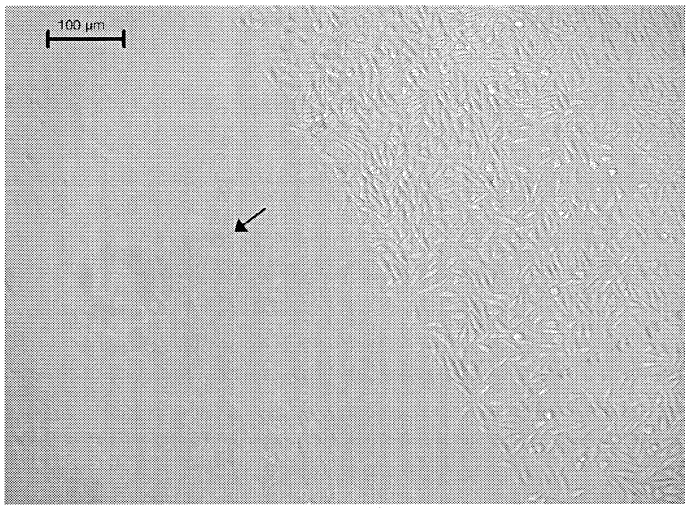

Figure 3-30: NIPAAm-MMA surface after the cells were transferred to PVDF membrane below LCST. Arrow indicates surface devoid of cells.

3.3 Secretome analysis as a tool to analyse specific molecular compatibility of copolymer and to study cellular function on different substrates

3.3.1 Optimisation of culture medium for cell line and LiEC

Serum is the most commonly used supplement in cell culture medium as it is considered essential to promote cell adhesion and proliferation. It is a complex mixture of proteins, which include albumin, immunoglobulins, growth factors, hormones, adhesion factors and many other proteins that have not been identified so far. Serum free conditions are preferred for 2DE analysis of proteins because of the abundance of serum proteins. Presence of serum proteins in gel would mask the detection of secretory proteins which are low in abundance. Furthermore serum proteins could be misidentified as secretory proteins.

The normal practise of obtaining SFM for 2D analysis is to transfer 60-70% confluent cells in to SFM following extensive washing (Volmer et al., 2005). Previous experiments showed that this procedure resulted in increased cell death and also restricted the time for which the SFM could be collected to around 24 h. Therefore, cell culture

conditions and media were optimised to eliminate use of serum to the maximum extent, and to increase the time for media collection whilst minimising cell death. This was performed for both primary LiEC and cell line

3.3.1.1 Cell line

Eventhough completed Epilife is a SFM, one of its supplements is bovine pituitary extract. Just as serum, this also contains lot of unidentified factors and albumin which can mask some of the secretory proteins, produced by cells. Hence optimisation for cell line culture was needed. To optimise the culture conditions and media for the SV40 immortalised cell line, growth was compared following indirect or direct culture in different medium based on their morphology and days for reaching confluency (Table 3-3).

Medium	Direct	Indirect
Epilife completed	+++	N A
Epilife basal (without supplements)	+	+++
CEM	++	++
SFCEM	++	+++
HyQ(no added supplements)	++	+++

Table 3-3: Different mediums and respective cell growth of cell line. +++ very good growth, ++ good growth and + average growth

The growth rate was very low in direct culture with Epilife basal medium. This was expected as it contained no growth promoting supplements. With CEM the growth rate was very high, but the cells were vacuolised and appeared unhealthy. SFCEM and HyQ gave moderate growth rate with a slight different morphology compared to those in Epilife completed (Figure 3-31). In Epilife completed, it was a mixture of polygonal and spindle shaped cells. In SFCEM, most of the cells were of polygonal shape and in HyQ & Epilife basal, most of the cells were found to be of spindle shape. However, the growth rate and morphology of cells in indirect culture with different mediums were similar. As Epilife basal did not promote cell growth, this was not used in optimisation of culture medium for primary cells.

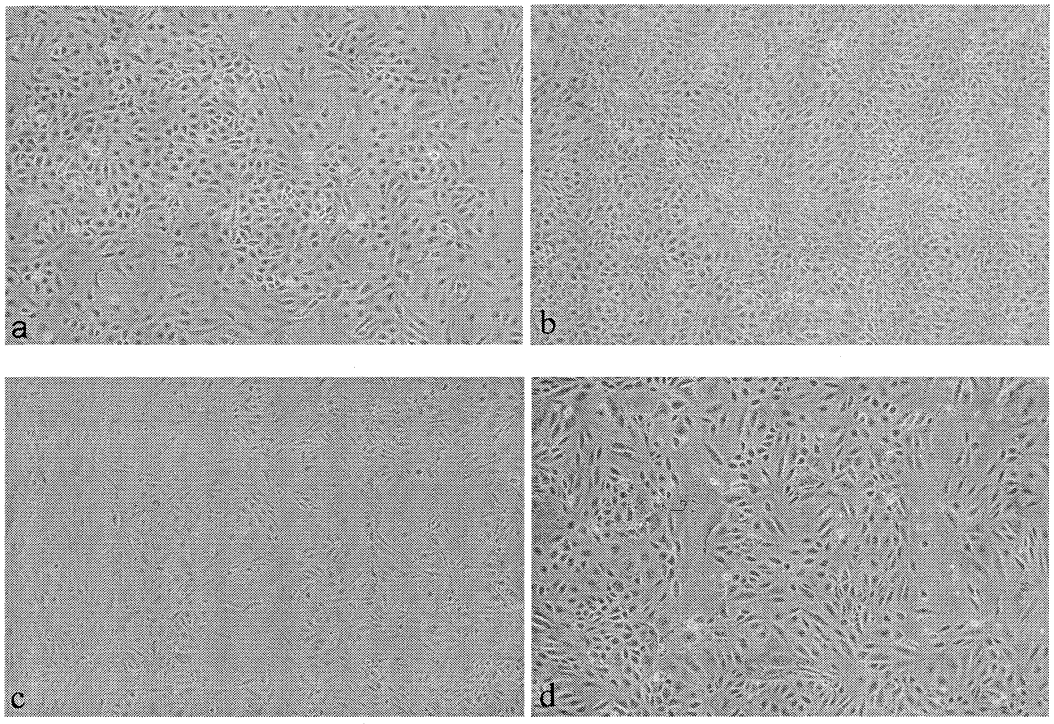

Figure 3-31: Morphology of cell line in different medium after direct mode of culture. a) Epilife completed, b) SFCEM, c) Epilife Basal, d) HyQ. All pictures were taken at 100 x magnification

3.3.1.2 Primary limbal epithelial cells

The data of both direct and indirect culture of primary cells in different media is summarised in Table 3-4.

Medium	Direct	Indirect
Epilife completed	-	++
CEM	++	N/A
SFCEM	-	+++
HyQ	-	+

Table 3-4: Optimisation of medium for LiEC culture. +++ very good growth, ++ good growth, + average growth and – poor growth

When the explants were cultured directly in Epilife completed, the cells migrated in initial stages (Figure 3-32 a), but the explants were then floated off after 3-4 days and no further migration was seen in later stages. In the indirect mode, cells in Epilife completed grew well with a mixture of polygonal shaped large, flattened and small cells (Figure 3-32 b). Direct culture of explants in SFCEM produced a little growth (Figure 3-32 d) and completely stopped within 4-5 days while no growth was observed in HyQ. In indirect culture, HyQ did not promote cell growth (Figure 3-32 f) while SFCEM promoted cell growth (Figure 3-32 e).

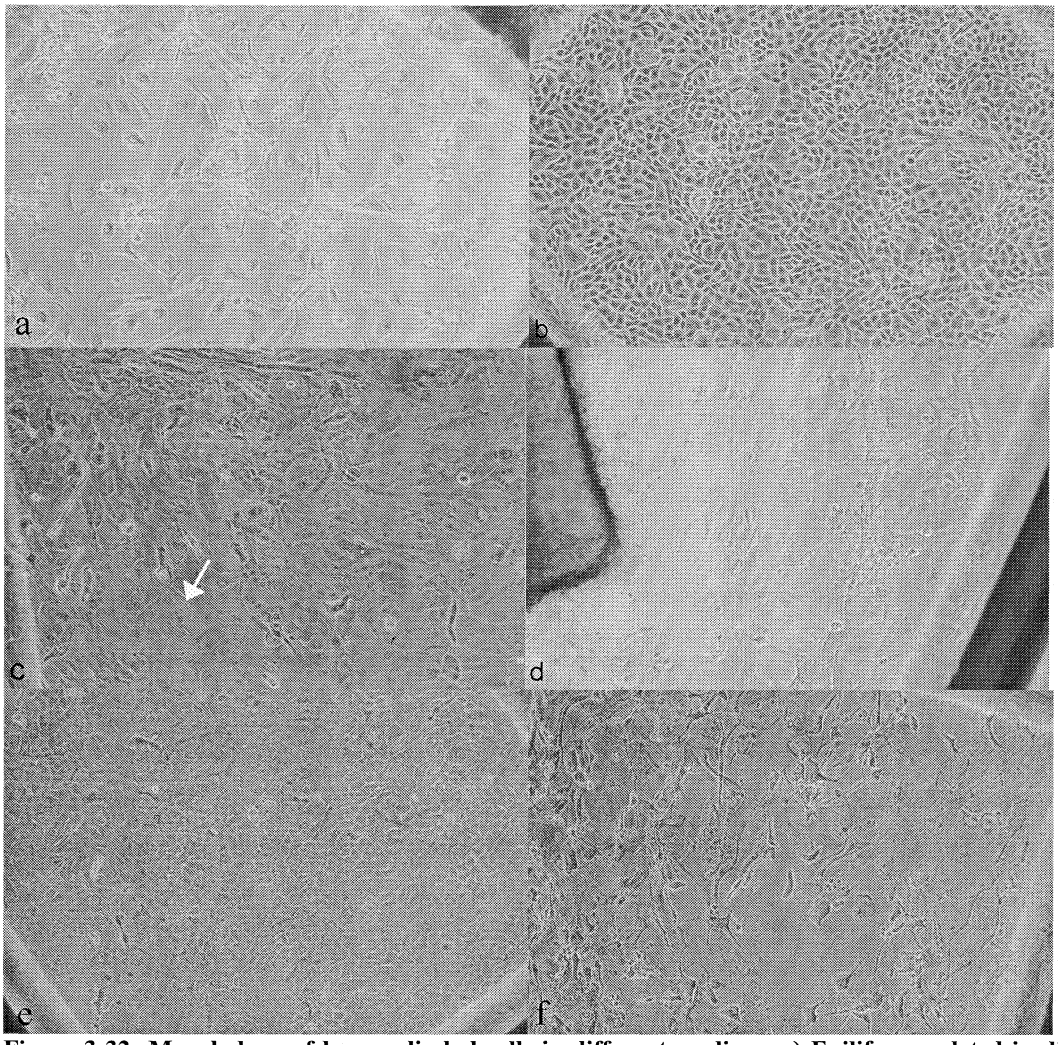

Figure 3-32: Morphology of human limbal cells in different medium. a) Epilife completed in direct mode, b) Epilife completed in indirect mode, c) CEM in direct mode, d) SFCEM in direct mode, e) SFCEM in indirect mode, f) HyQ in indirect mode. All pictures were taken at 100 x magnification

The morphology of the cells in indirect culture of SFCEM was different from those cultured in CEM alone. The cells in CEM were a mixture of large, polygonal (indicated by 'arrow' in Figure 3-32 c) and small cells with a tendency to attain flattened morphology within 2 weeks similar to superficial cells of corneal epithelium. Meanwhile, the cells that were transferred to SFCEM were all relatively small. Another interesting finding was the tendency of the cells to migrate out as multilayers in indirect culture of SFCEM (Figure 3-33 c) which was never observed in CEM. The observation was similar to the rabbit limbal cell culture in which culture system 4 promoted multilayer formation. Probably the indirect culture mode (CEM followed by SFCEM) in human limbal cell culture might have enabled a similar microenvironment in which an initial layer acted as autofeeder cells.

As comparison of the secretome from cell line and primary cells was also intended, similar culture conditions was required. SFCEM was used for the collection of secreted proteins as it supported growth of both cell line (direct mode) and primary cells (indirect mode).

The results suggested SFCEM could maintain growth of primary cells better than CEM once cell growth from the explants had been established in CEM. It is reported that serum contains proteins that can induce squamous differentiation (Masui et al., 1986). It was also reported that continuous culturing in serum supplemented medium markedly increased differentiation of mesenchymal cells (Yokoyama et al., 2008). In CEM, LiEC might be having a decreased proliferative capacity and increased differentiation capacity. SFCEM might be maintaining the proliferative potential of cells. Thus, the optimised medium conditions for primary cells not only support 2DE analysis of secretome but also maintain the proliferative and probably the progenitor potential.

3.3.2 Limbal explant culture on AM, TCPS and NIPAAm-MMA

In all substrates, explants cultured in CEM till 5-10 % outgrowth were transferred to SFCEM. This was preceded by gentle washing on rocker. Morphology of the cells and days taken for reaching confluency was similar on both TCPS and NIPAAm-MMA plates.

Denuded AM was used as substrate for limbal explant culture. It was difficult to visualise cells on AM under phase contrast microscope (Figure 3-33 a), which was due to the thickness of the AM matrix. Therefore, the out-growth was observed by holding the plates directly under light, above the eyes or using dissection microscope (Figure 3-33 b). Thus the formation of multilayer could not be confirmed.

Cryopreservation of AM for six months is essential in order to screen out certain infections like HIV, Hepatitis B & C and Syphilis. This also devitalises the amniotic epithelial cells, but the cells generally remain firmly associated with the AM basement membrane. Both intact and denuded AM have been reported to be used as substrates for corneal cell culture (Grueterich et al., 2002; Sudha et al., 2008). Intact AM contains the devitalised cells, which would be replaced by the expanding cells. Denuded AM are the ones in which BM is exposed by enzymatic/mechanical removal of epithelial cells. Comparison of intact and denuded AM for limbal culture (Koizumi et al., 2000a) revealed that denuded AM supported formation of a consistent stratified layer while the leading

edges of the outgrowths on intact AM were much less uniform. Eventhough it was suggested that intact AM supported SC properties (Sudha et al., 2008), a recent study showed that there was steady decline in these properties with distance on intact AM (Kolli et al., 2008).

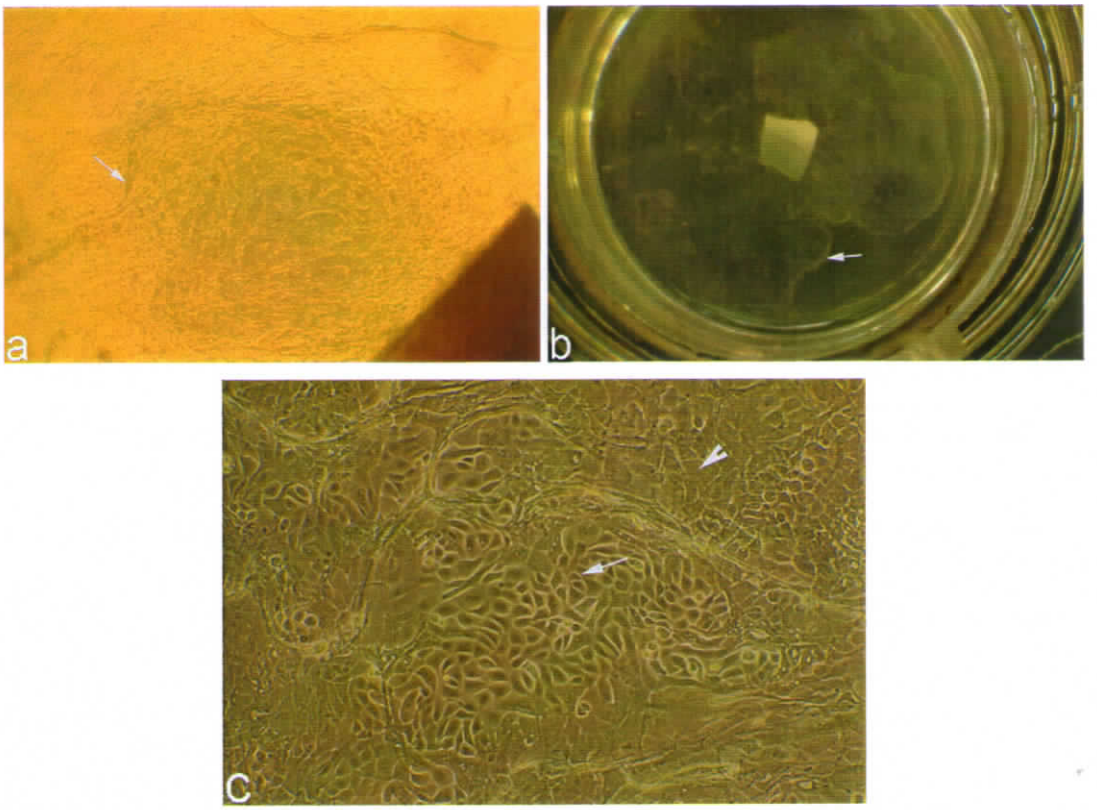

Figure 3-33: Limbal cell outgrowth. a) Cells on AM under phase contrast microscope, arrrow demarcates the outgrowth.b) Cell growth on AM under dissection microscope, arrow clearly shows the outline of growth. c) Multilayer formation of limbal cells on NIPAAm-MMA copolymer. Arrow and arrowhead show different layers.

The most reported methods for denudation are EDTA treatment (Grueterich et al., 2002; Sun et al., 2005) and dispase treatment (Wang et al., 2003). Both these techniques use mechanical scraping after respective chemical or enzyme treatment. This is reported to be destructive to the BM components (Hopkinson et al., 2008), which could in turn affect the adhesion and growth of limbal cells. Hence a new denudation technique using thermolysin enzyme was employed with subsequent vigorous shaking (Hopkinson et al., 2008). Thermolysin, a metalloendoproteinase produced by *Bacilum Thermolyticum* was first used for keratinocyte isolation in 1977. It has been reported that thermolysin produce an efficient dermal-epidermal separation (Gragnani et al., 2007). According to Gragnani et al, the histological evaluation of thermolysin treated skin samples showed separation at basal membrane zone.

3.3.3 Proteomic analysis of secretory proteins by 2DE

Two dimensional electrophoresis enables better separation of proteins compared to single dimensional electrophoresis as the technique utilises two parameters, isoelectric point and molecular weight of proteins (Tannu and Hemby, 2006). It only represents the proteins that are present within a specific mass range (10 kDa-100 kDa) and above the detectable levels of the staining method used. Silver staining was used in the experiments. Silver staining is more sensitive than coomassie blue staining, but on the other hand, it can reduce the protein recovery from the gel and thereby the efficiency of Mass spectrometry.

3.3.3.1 2D optimisation by reduction of DTT

Initial set of gels revealed that the quantity of DTT in the IEF loading buffer influences the protein profile on gel. The proteins in the basic region of the gel were distorted when the concentration of DTT was 50mM. A reduction in DTT to 25 mM rectified this issue (Figure 3-34).

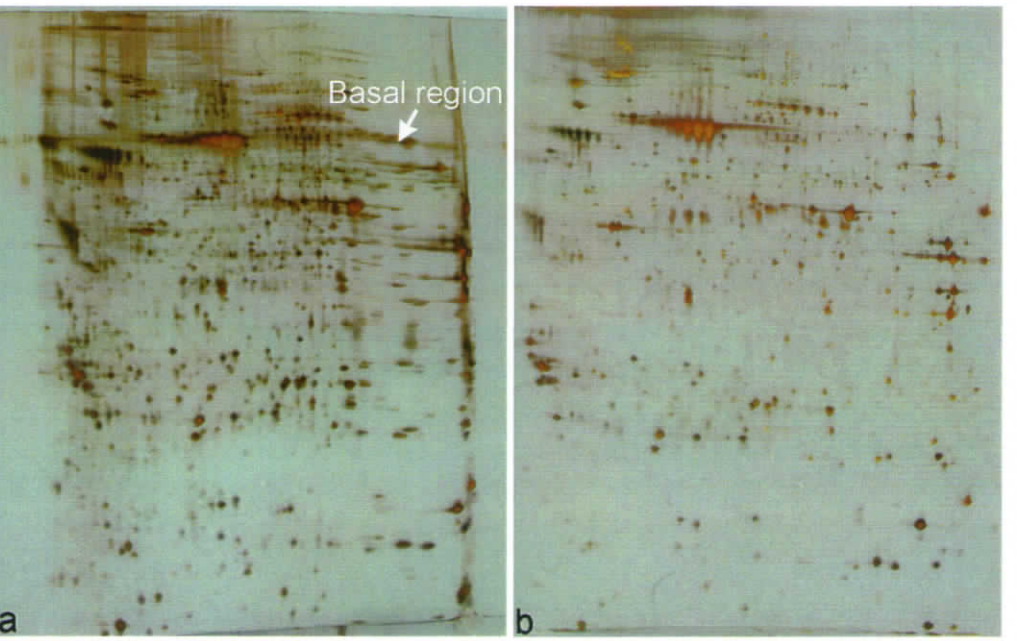

Figure 3-34: a) Gel with 50 mM DTT in IEF buffer, b) Gel with 25 mM DTT in IEF buffer

3.3.3.2 Collection of medium

Eventhough cellular extract of cultured cells had high concentration of proteins, the protein concentration in secreted fraction was very low. Therefore, pooling and concentrating of many cultures of similar conditions was essential (Volmer et al., 2005). Pooling of the samples helped to minimise inter-sample variation, thereby representing

nly the consistent proteins in the gel. Producing pooled stocks of each sample type also naintained reproducibility of gels across several batches. Preliminary 2DE analysis of ollected medium from cell line culture at 72 h showed that there were a lot of cellular roteins in the samples. Serum albumin was also present in the gel (Figure 3-35 a) which vas confirmed by mass spectrometry; even though serum was not used in the medium. The source of serum albumin was hypothesised to be the serum used for neutralising rypsin during cell passaging. The residual serum from neutralisation step could remain ound to cells, which was then carried over. This emphasises the sensitivity of the xperiments to contaminating proteins. Secreted proteins being present in low abundance equire considerable concentration. This hypothesis was proved correct when traditional rypsin was replaced with Tryple, an enzyme from Invitrogen, which does not require erum for neutralisation. Instead the enzyme was diluted using SFM. This modification ramatically reduced the appearance of serum albumin in gel (Figure 3-35 b). However, he residual BSA in the gel could be from a minimal amount of Epilife completed nedium carried over during passaging. Thus the source of residual albumin could be ovine pituitary extract.

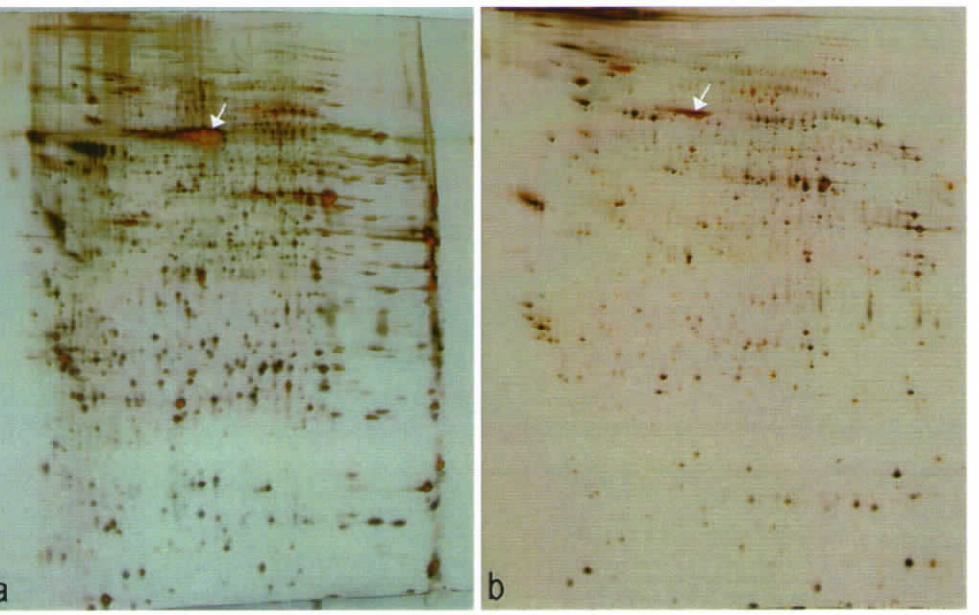

igure 3-35: Gel images of cell line secretome. BSA is indicated by arrow in both images. a) Before sing Tryple, b) After using Tryple

In primary epithelial cultures, transferring the cells on different substrates to FCEM around 5-10% confluency itself enabled continuous collection of medium for ecretome analysis.

3.3.3.3 Optimisation of culture period

As told earlier in section 3.3.3.2, a lot of cellular proteins were found in gels of cell line secretome collected at 72 h. This suggested that the cellular proteins were released from cells possibly as a result of cell lysis during cell turn over. Even though filtering of conditioned media before storage removed cell debris and floating live cells, it did not eliminate the already released soluble proteins from dead cells. Therefore, in order to minimise contamination from cellular proteins by attempting to reduce cell death, different time points were tried in collecting medium from cell line culture and the protein profile was analysed by running 2DE gels.

The amount of cellular protein contamination decreased as the interval for collecting medium decreased. Consequently, the whole protein concentration in the collected medium also decreased. Thus, in order to get a reasonable protein concentration per microlitre, concentrating down to small volumes became essential. If the medium collected at 72/48 h were concentrated 42 fold, the same collected at 24/16 h required concentration upto ~150 fold to obtain around 0.5 µg/µl of protein concentration. In effect, even though the cellular proteins decreased when the collection time was reduced, its presence in the gel could not be eliminated. This was demonstrated in the gels from different time points, as the protein profile did not change considerably (Figure 3-36). For all further analysis, the intermediate time point of 48/24 h was used for medium collection from cell line.

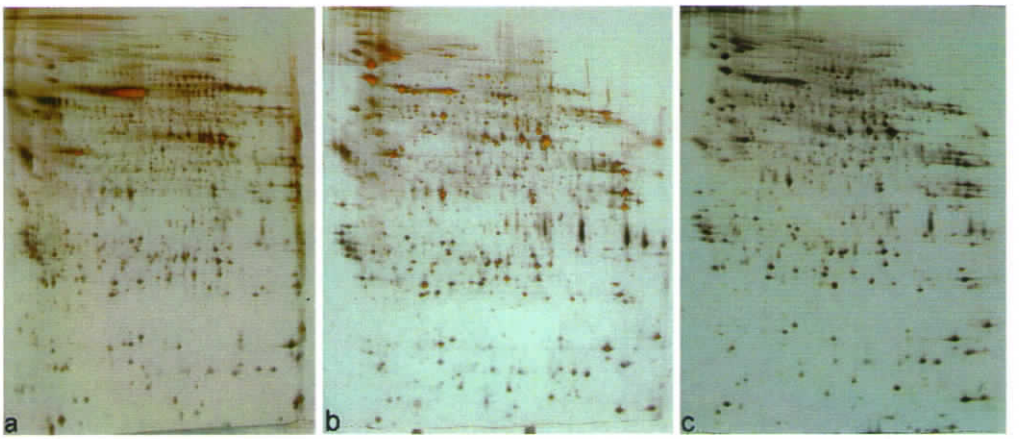

Figure 3-36: Gel images representing medium collected at different time points a) 72/48 h, b) 48/24 h, c) 24/16 h.

3.3.4 Identification of potential secretory proteins

Delta 2D software was used to compare gel images of different samples in order to identify potentially secreted proteins and the differences in their expression on different substrates. Comparison between cellular extract and collected medium in each substrate enabled to eliminate the cellular contamination in the secretome to a maximum extent as these proteins would be common to both protein profiles. TBST extracts were used for representing cellular proteins as TBST was good in extracting soluble intercellular proteins which would be there in collected medium also, if cell lysis occurred. If stronger cellular protein extraction reagents were used, the protein profile would not properly represent the soluble fraction as there would be lots of structural proteins also. And this might lead to misinterpretation of some spots in gels of collected medium as secretory even though they were originally soluble cytoplasmic proteins. The disadvantage of this may be that some proteins which are both secreted and located intercellulalry would be eliminated as the spots match in both gels.

3.3.4.1 Cell line

Images of gels of collected medium and cellular extract from cell line cultured on different substrates are given in Figure 3-37. The gel images of collected medium from cell line cultured on TCPS and NIPAAm-MMA were compared against respective cellular extracts (Figure 3-38 & Figure 3-39). Delta 2D software analysis of gels revealed three categories of spots on gels. 1) The spots that were solely seen in cell extract were intracellular or cell structural proteins and were of no interest at all (eg: green spots in Figure 3-38). 2) The matched spots between gels could be cellular protein contamination from lysed cells or the cytoplasmic presence of secreted proteins (eg: white spots in Figure 3-38). 3) The spots that were present only in collected medium gels could be potentially secreted proteins and were of interest for further studies (eg: red spots in Figure 3-38). Around 50 spots could be identified as potentially secreted after comparing the gel images of collected medium and cellular extract of the cell line cultured on both substrates. Characterisation of proteins by mass spectrometry was needed for confirming the secretory nature.

Software analysis of the gel images corresponding to cell line secretome on TCPS and copolymer did not reveal any significant detectable differences (Figure 3-40). Absence of unique spots in either gel image suggests that the secretome of cell line was

similar despite the substrate differences. NIPAAm-MMA did not have any detectable negative influence on the synthesis and secretion of proteins. As secretome is comprised of many proteins involved in a wide range of cellular functions like cell adhesion, proliferation, apoptosis and matrix remodelling, similar secretome could suggest similar cell behaviour on both substrates.

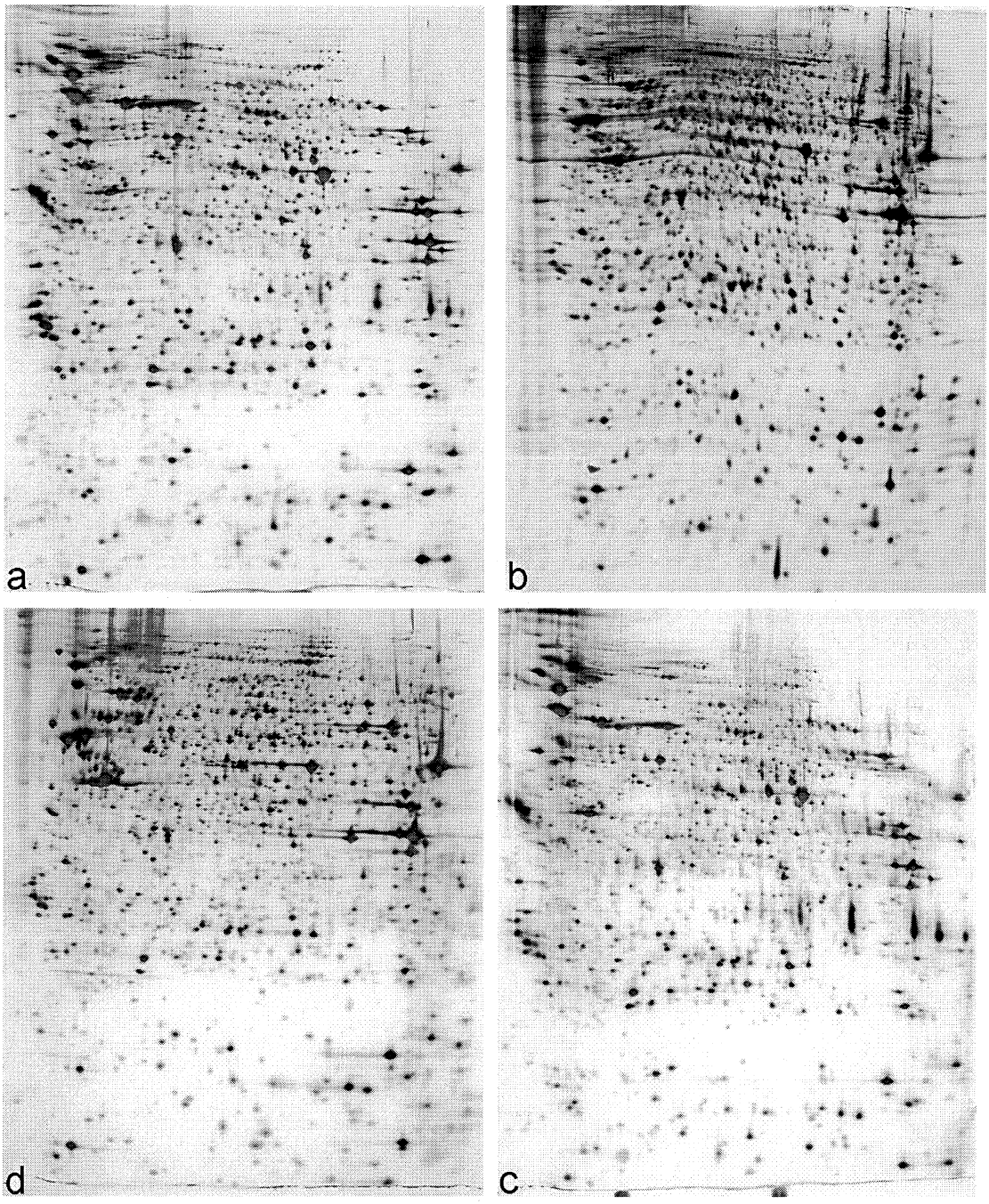

Figure 3-37: 2D gel images of cell line a) collected medium from TCPS, b) cellular extract from TCPS, c) collected medium from NIPAAm-MMA, d) cellular extract from NIPAAm-MMA

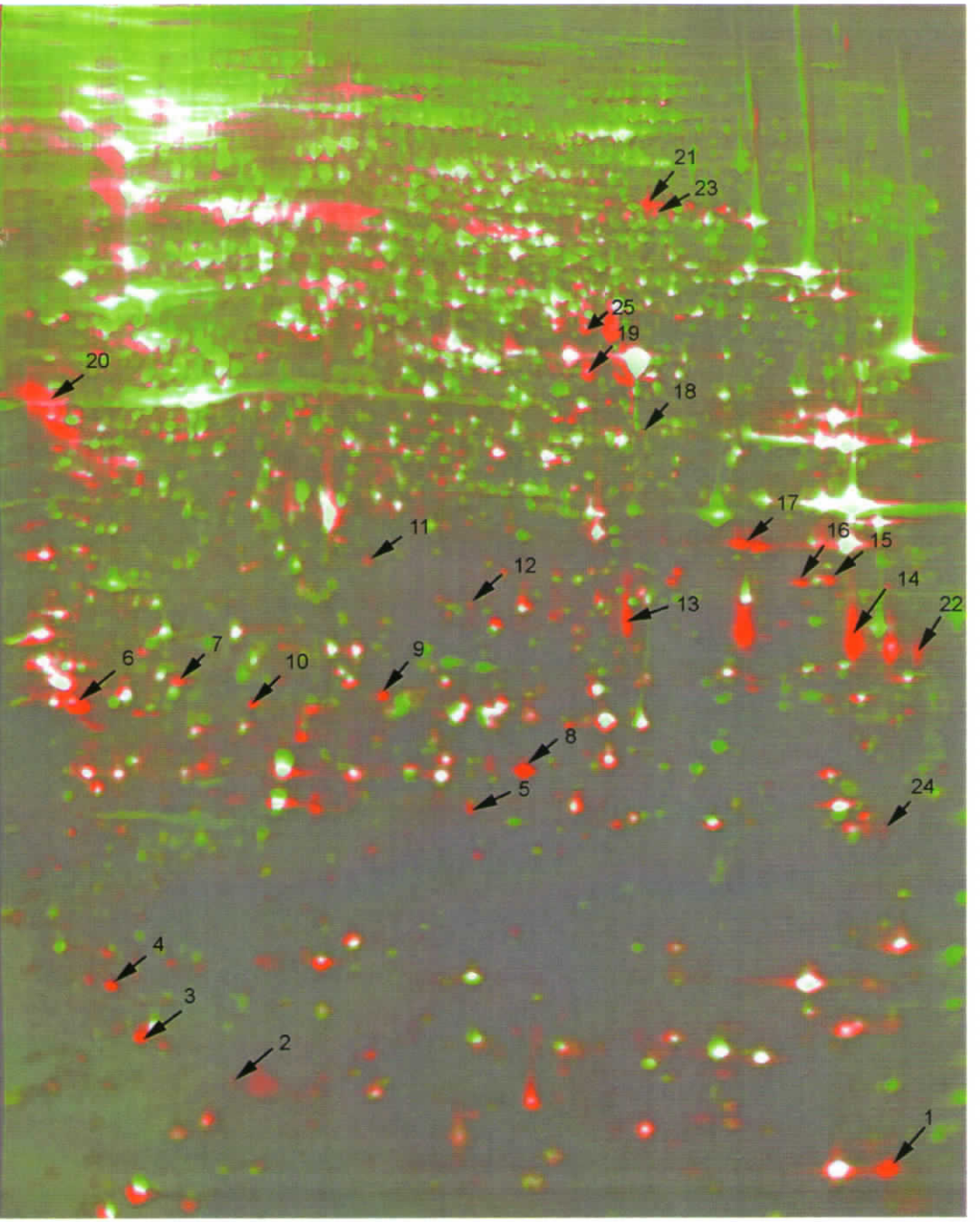

Figure 3-38: 2D gel composite image of collected medium and cellular extract of cell line from TCPS. Red indicates spots in collected medium and green indicates spots from cell extract. White spots are the matched ones from both gel images. The labelled spots from cell line were identified by mass spectrometry and prefixed by VLP in the text.

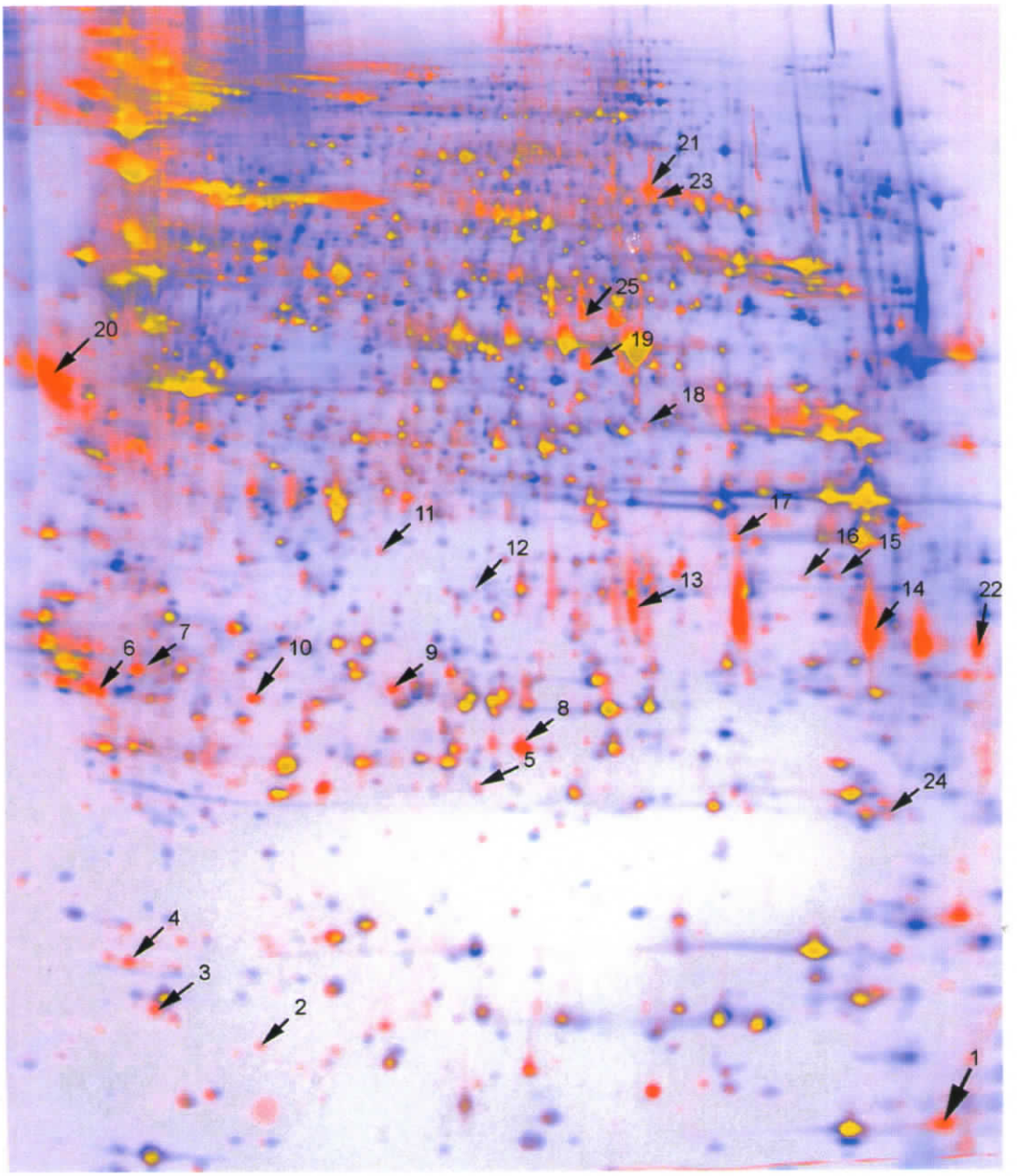

Figure 3-39: 2D gel composite image of collected medium and cellular extract of cell line from NIPAAm-MMA. Red indicates spots from collected medium and blue indicates spots from cell extract. Dark yellow spots are the matched spots from both gel images.

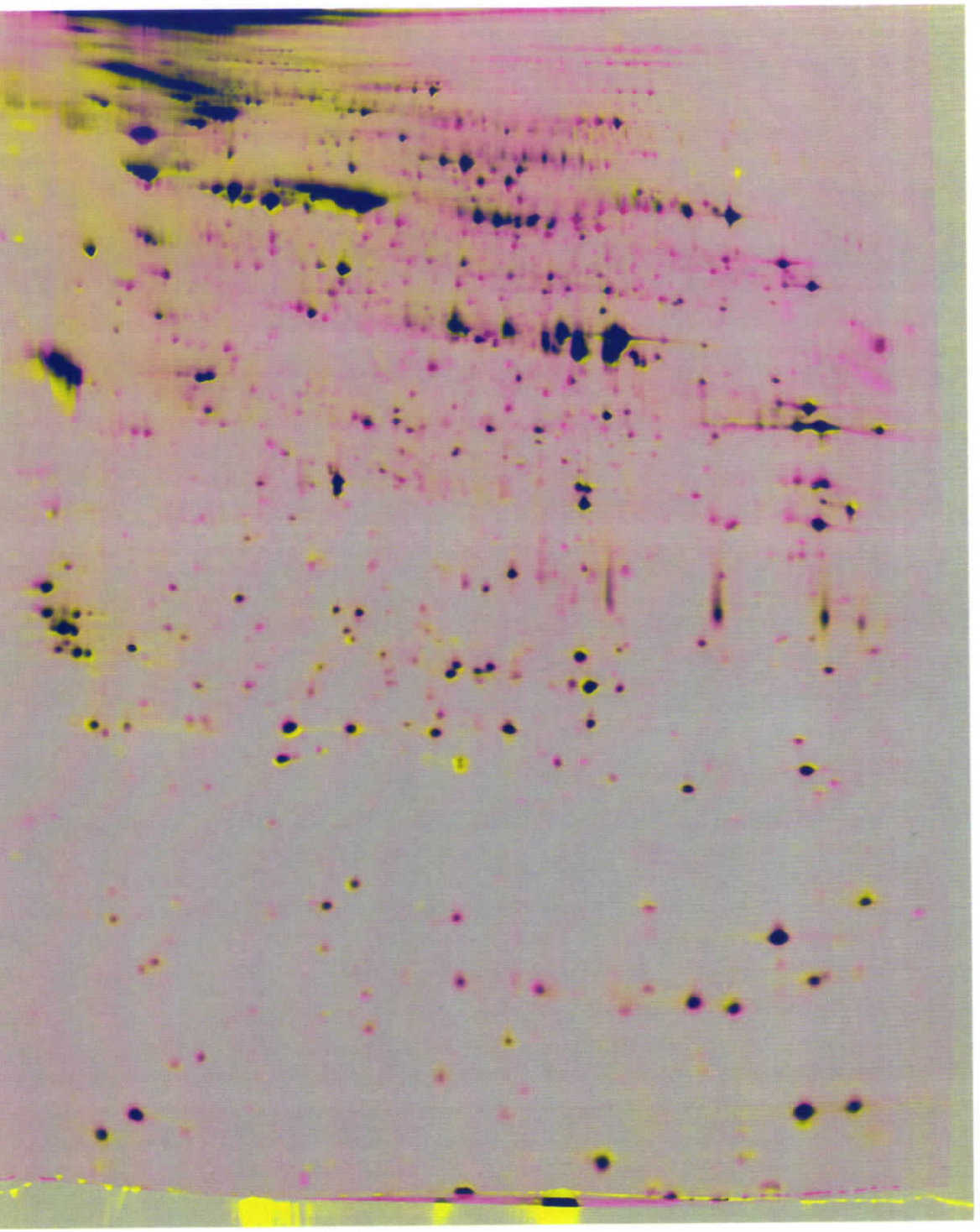

Figure 3-40: 2D gel composite image of collected medium of cell line from TCPS and NIPAAm-MMA. All the secreted proteins were matched spots eventhough amount of cellular protein contamination varied in the gels

3.3.4.2 Primary LiEC

Images of gels of collected medium and cellular extract from primary cells cultured on different substrates are given in Figure 3-41. The gel images of collected medium from three different substrates namely TCPS, NIPAAm-MMA and AM were compared with respective cellular extract using delta 2D software (Figure 3-42, Figure 3-43, Figure 3-45). The potential secretory proteins were identified by the same procedure followed in cell line secretome analysis. The results showed similar profile in both TCPS and NIPAAm-MMA (Figure 3-44), confirming the results obtained from cell line. Primary cells were used for assessing compatibility of the NIPAAm-MMA because they depict a clearer picture of specific cell response to external stimuli compared to cell line. But no unique protein spots were found in either TCPS or NIPAAm-MMA (Figure 3-44). This clearly suggests that the copolymer has similar cytocompatibility to that of TCPS and it is a suitable substrate for culturing primary and continuous cell lines.

On comparison, additional spots were found in the gel image of collected medium from AM, which was absent or faint in both TCPS and copolymer (Figure 3-45). AM is a biological substrate, which contains many types of proteins and is likely to have additional biological influence on cell behaviour. Matrix remodelling of AM during epithelial growth by different types of matrix metalloproteinases (MMP) was reported earlier (Li et al., 2006), which may result in release of proteins from AM. Therefore, the additional spots could be those released from AM by matrix remodelling or secreted by epithelial cells under influence of AM.

Some of the major proteoglycans in corneal stroma are mimecan, lumican, βig-h3 and decorin. It is the presence of the same proteins in AM stroma (Hopkinson et al., 2006a) that potentially makes it one of the most used substrate for *ex vivo* expansion of corneal epithelial cells and corneal reconstruction. Proteins like these, if released from AM during remodelling, were also of interest as they were reported to influence cell adhesion and growth (Vij et al., 2004).

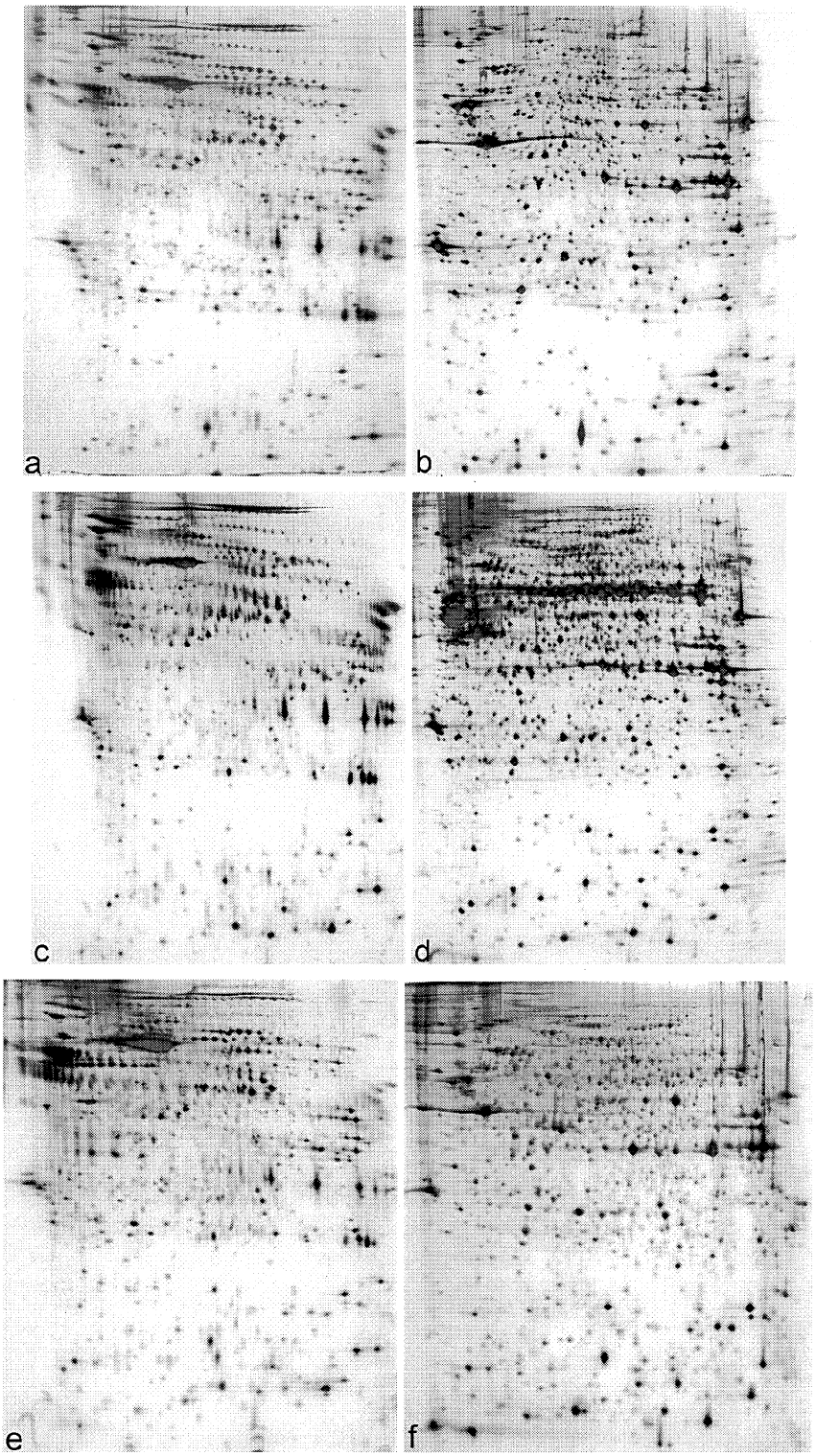

Figure 3-41: 2D gel images of primary cell culture a) collected medium from TCPS, b) cellular extract from TCPS, c) collected medium from NIPAAm-MMA, d) cellular extract from NIPAAm-MMA, e) collected medium from AM, f) cellular extract from AM

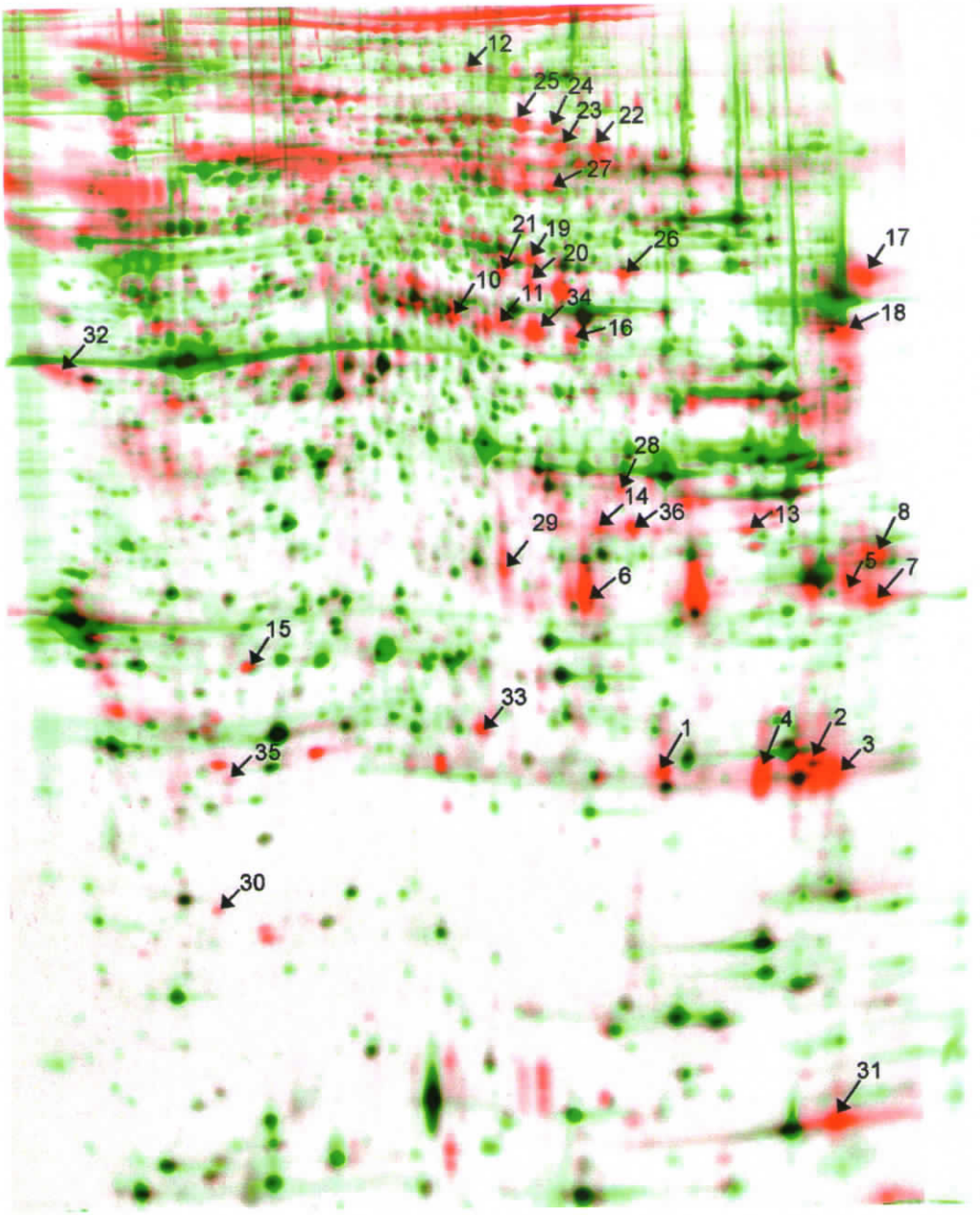

Figure 3-42: 2D gel composite image of collected medium and cellular extract of primary cells from TCPS. Green indicates spots from cellular extract and red indicates spots from secretome. The labelled spots were identified by mass spectrometry and prefixed by VPP in the text.

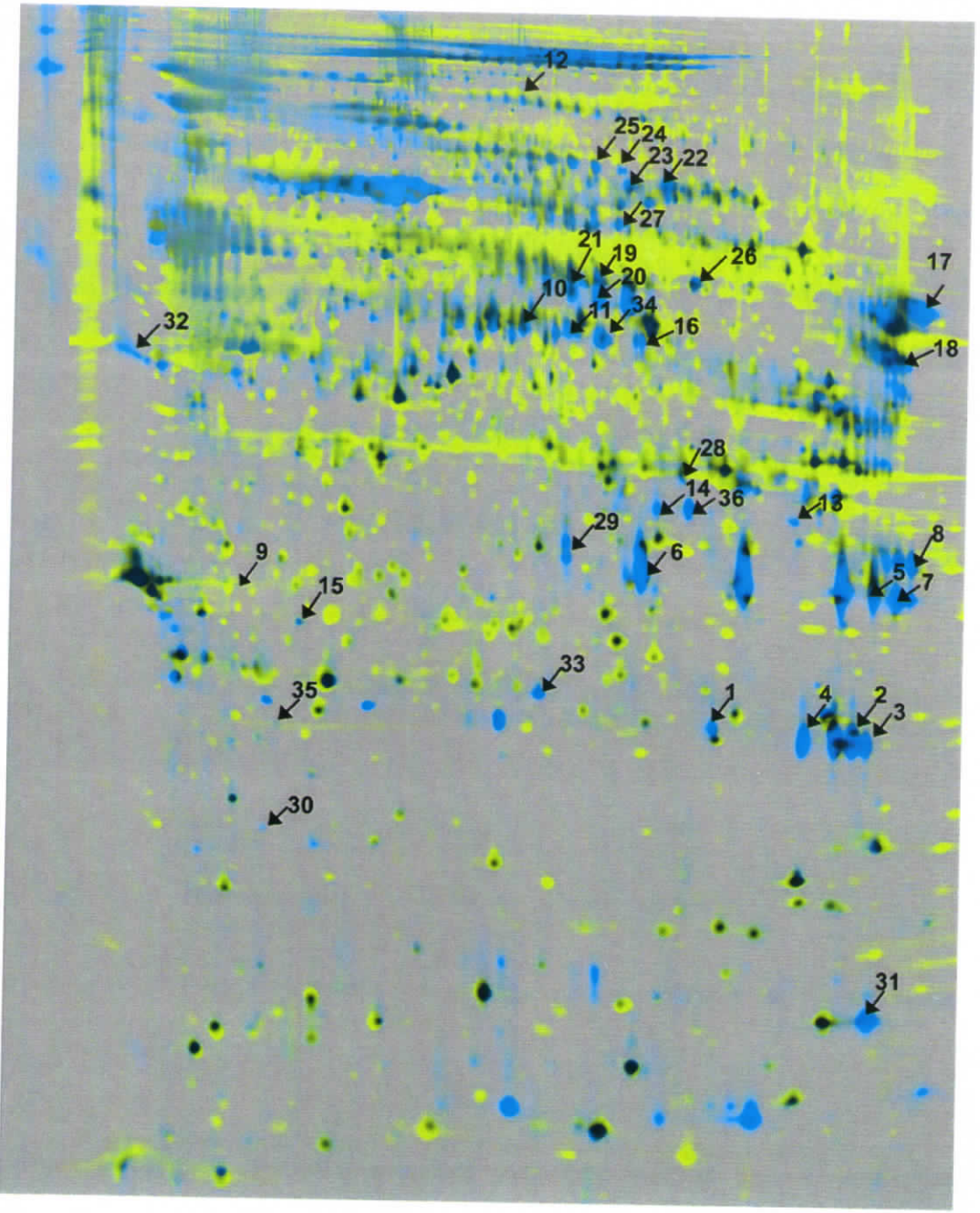

Figure 3-43: 2D gel composite image of collected medium (blue) and cellular extract (yellow) of primary cells from NIPAAm-MMA. The labelled spots were identified by mass spectrometry and prefixed by VPP in the text.

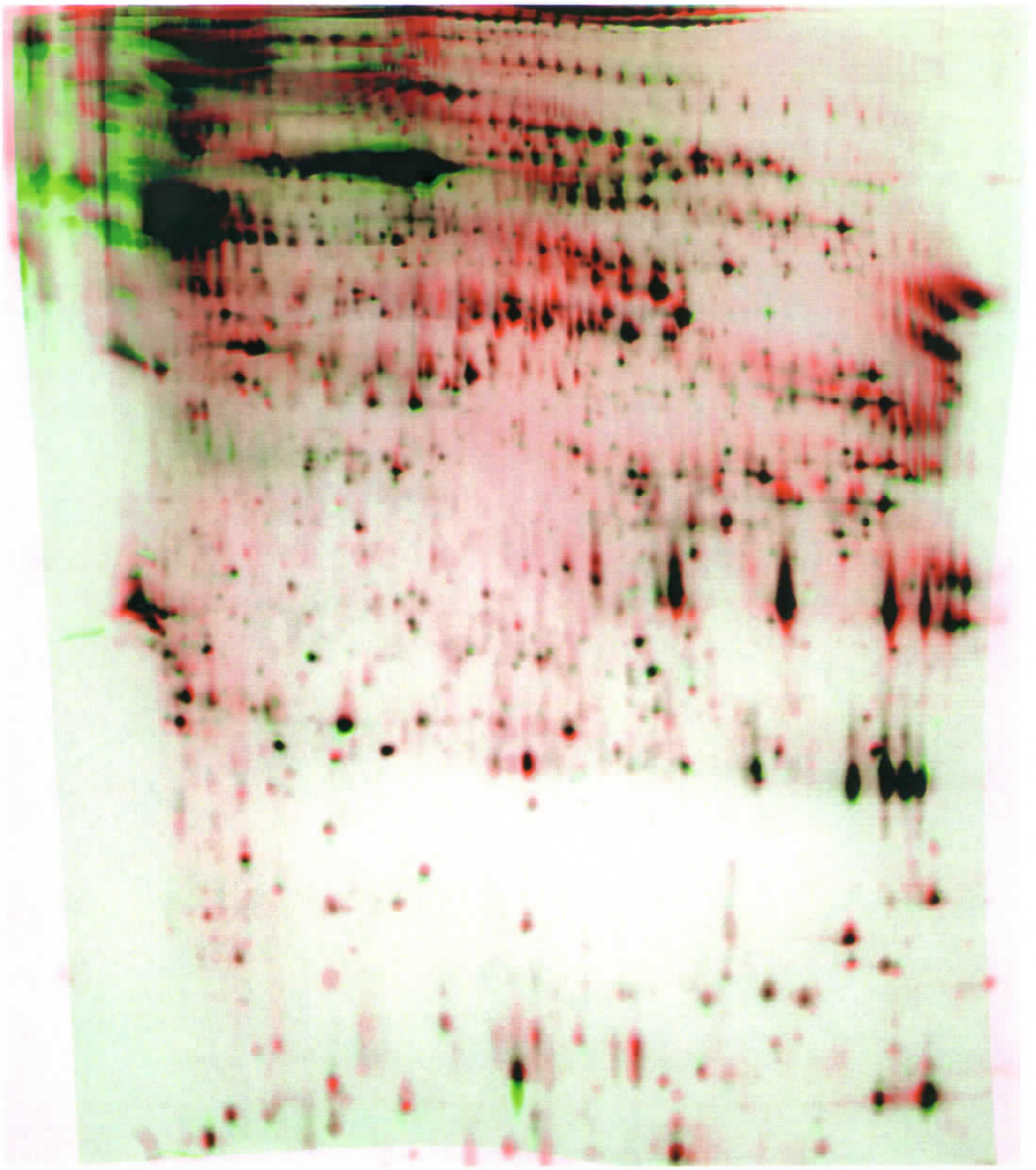

Figure 3-44: 2D gel composite image of collected medium from TCPS and NIPAAm-MMA. No unique spots were observed in either of the gels. Black represents the matched spots in both gels.

Figure 3-45: 2D gel composite image of collected medium (red) and cellular extract (green) of primary cells from AM. The common spots corresponding to VPP are labelled with simple numbers and unique spots in secretome from AM by 'VAP' numbers

3.3.5 Comparison of cell line and primary cells

There are several reports available which had utilised cell lines to study the secretome of a certain tissue and to analyse potential biomarkers for carcinomas (Gronborg et al., 2006; Wu et al., 2008). In this study, both cell line and primary cells had been used to study secretome, enabling a comparison between the two. This comparison

Figure 3-45: 2D gel composite image of collected medium (red) and cellular extract (green) of primary cells from AM. The common spots corresponding to VPP are labelled with simple numbers and unique spots in secretome from AM by 'VAP' numbers

3.3.5 Comparison of cell line and primary cells

There are several reports available which had utilised cell lines to study the secretome of a certain tissue and to analyse potential biomarkers for carcinomas (Gronborg et al., 2006; Wu et al., 2008). In this study, both cell line and primary cells had been used to study secretome, enabling a comparison between the two. This comparison

Figure 3-45: 2D gel composite image of collected medium (red) and cellular extract (green) of primary cells from AM. The common spots corresponding to VPP are labelled with simple numbers and unique spots in secretome from AM by 'VAP' numbers

3.3.5 Comparison of cell line and primary cells

There are several reports available which had utilised cell lines to study the secretome of a certain tissue and to analyse potential biomarkers for carcinomas (Gronborg et al., 2006; Wu et al., 2008). In this study, both cell line and primary cells had been used to study secretome, enabling a comparison between the two. This comparison

will give a clear picture about how well the cell line correlates with/represents the secretome of corresponding primary cells.

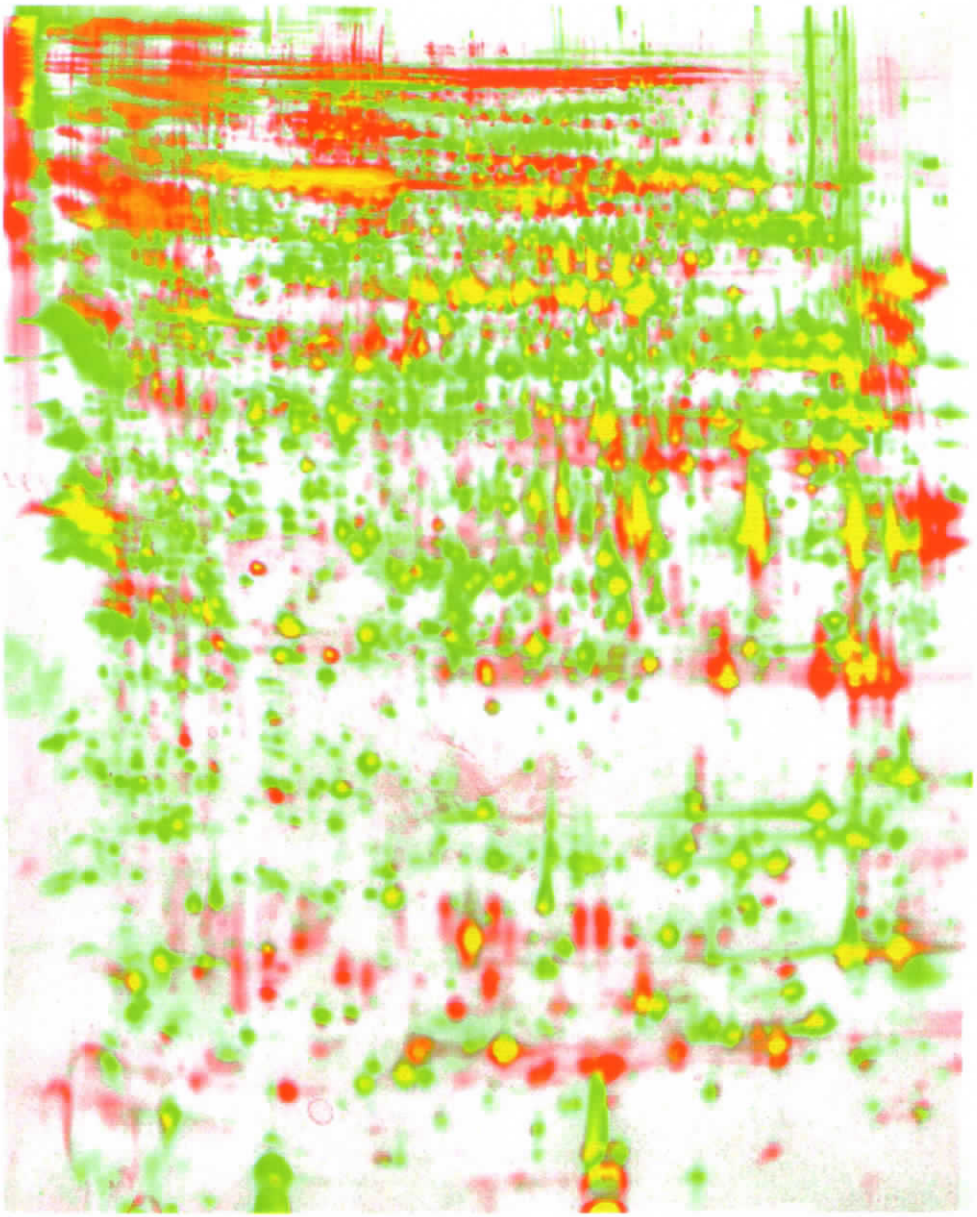

Figure 3-46: 2D gel composite image of primary (red) and cell line (green) secretome from cells cultured on TCPS. Eventhough green spots are more in number, most of them are cellular proteins.

It is evident on comparison (Figure 3-46) that the presence of intercellular proteins in the cell line secretome is much more compared to that of primary cells. This can be confirmed by analysing the composite images of both with their respective cellular extracts (Figure 3-38 & Figure 3-42). This could be due to the high cell turn over of immortalised cells compared to primary cells. The amount and number of potential secreted proteins was found to be more in primary cell secretome (Figure 3-46). The

llular protein contamination might have reduced the proportion of secreted proteins in e collected medium fraction of cell line. Another possible reason could be the mortalised and *in vitro* nature of cell line which may reduce the expression of many oteins that would have been necessary for primary cells. When amounts of equal otein was loaded (120 µg) in gels of both primary (Figure 3-47 a) and cell line cretome (Figure 3-47 b), some of the spots corresponding to secreted proteins were not ident in cell line secretome. A higher load of cell line secretome (200 µg) (Figure 3-47 revealed presence of some of these proteins, eventhough in small amounts (eg: VPP1 VLP24, labelled by blue arrows in Figure 3-47 a & c). This less amount of secreted oteins in cell line could be due to higher cellular protein contamination or lower amount secretion. Even in the comparatively high load, spots corresponding to some of the imary cell secretory proteins are completely absent in cell line (eg: VPP7 & 8, labelled green arrows in Figure 3-47 a). The presence of many primary secretory proteins could t be deduced in cell line secretome as the spots were not evident (eg: VPP12, 14, 28). contrast, it was observed that VLP20 (VPP32) was upregulated in cell line compared to imary cells (labelled by red arrows in Figure 3-47 a & b). Among the primary cell cretomes, AM appeared to have lowest amount of this protein.

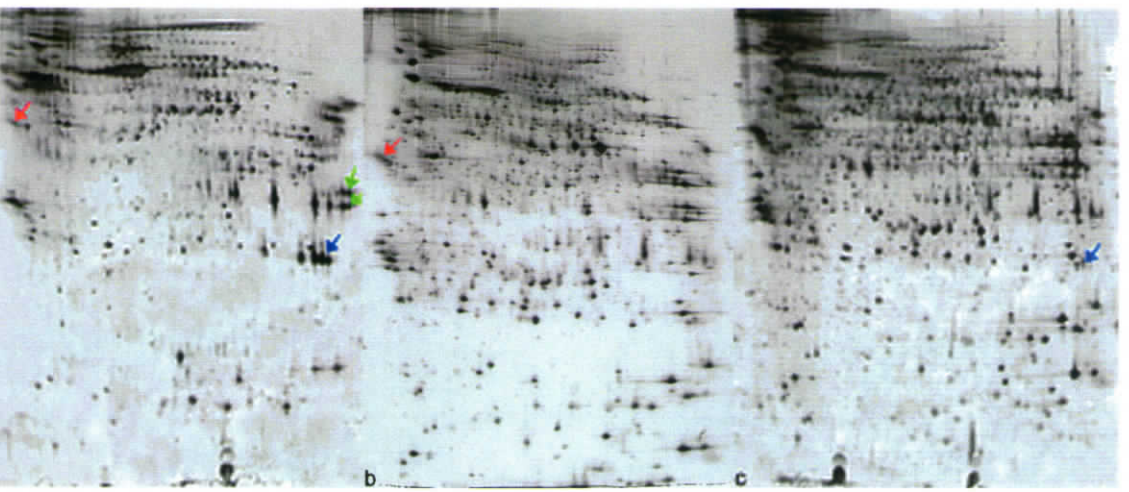

gure 3-47: Gel images a) 120 µg of proteins loaded in primary secretome, b) 120 µg of proteins ded in cell line secretome, c) 200 µg of proteins loaded in cell line secretome

3.6 Mass spectrometric characterisation of potential spots

All of the potential spots for secreted proteins from both the cell line and primary lls were subjected to mass spectrometric characterisation. The peptides were subjected PMF analysis after MALDI TOF. Summarised data of PMF searches of the spots from th cell line and primary secretome are given in Table 3-5.

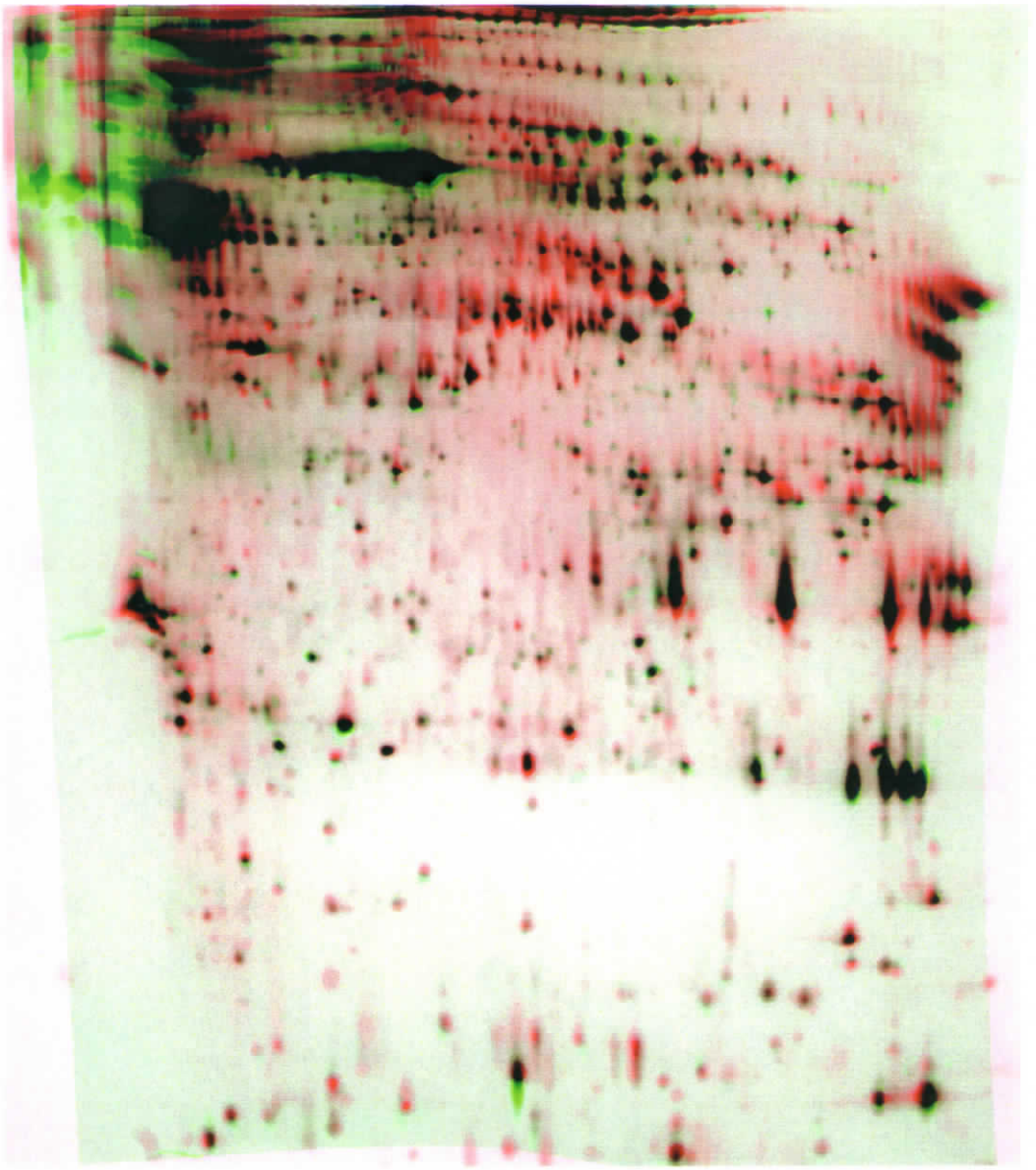

Figure 3-44: 2D gel composite image of collected medium from TCPS and NIPAAm-MMA. No unique spots were observed in either of the gels. Black represents the matched spots in both gels.

Protein Name	Spot ID	Accession No.	Mr (Da) theoretical	pI theoretical	Score	No. of matching peptides	E-Value	Sequence Coverage (%)
Cystatin C	VLP1,VPP31	P01034	16017	9	81	4	0.0031	36
Proteasome alpha type-3	VLP2	P25788	28643	5.19	76	5	0.01	23
Acidic leucine-rich nuclear phosphoprotein 32 family member B	VLP3	Q92688	28941	3.94	97	6	0.000078	27
Proprotein convertase subtilisin/kexin type 9 precursor	VLP4	Q8NBP7	75808	6.09	60	5	0.42	9
Cholera enterotoxin subunit A precursor-Vibrio Cholerae	VLP5	P01555	29431	6.1	105	6	0.000012	32
14-3-3 protein beta/alpha	VLP6	P31946	28179	4.76	63	5	0.19	26
Proteasome subunit alpha type-3	VLP7	P25788	28643	5.19	65	4	0.13	20
Metalloproteinase inhibitor 2 [Precursor]	VLP8,VPP33	P16035	25067	7.45	74	5	0.017	15
Lamin-A/C	VLP9	P02545	74380	6.57	98	9	5.9e-05	13
Renin receptor [Precursor]	VLP10	O75787	38983	5.76	78	5	0.0065	16
Thrombospondin-1 [Precursor]	VLP11	P07996	133291	4.71	60	5	0.43	4
Purine nucleoside phosphorylase	VLP12	P00491	32325	6.45	130	9	0.000000039	39
Metalloproteinase inhibitor 1 [Precursor]	VLP13,VPP6	P01033	23840	8.46	83	5	0.0021	35
Metalloproteinase inhibitor 1 [Precursor]	VLP14	P01033	23840	8.46	119	7	0.00000049	47
Annexin A2	VLP15	P07355	38808	7.57	177	11	7.80E-13	36
Annexin A2	VLP16, VPP13	P07355	38808	7.57	171	12	3.10E-12	35
Annexin A2	VLP17	P07355	38808	7.57	149	10	4.90E-10	36
Epidermal growth factor receptor kinase substrate 8-like protein 2	VLP18	Q9H6S3	81197	6.39	56	4	0.054	6

Plasminogen activator inhibitor 1	VLP19, VPP34	P05121	45088	6.68	74	5	0.016	13
SPARC [Precursor]	VLP20, VPP32	P09486	35465	4.73	83	5	0.0019	16
Complement C3 precursor	VLP21	P01024	188569	6.02	220	21	3.90E-17	17
Metalloproteinase inhibitor 1 [Precursor]	VLP22	P01033	23840	8.46	94	6	0.00014	43
Transforming growth factor-beta-induced protein ig-h3 precursor	VLP23	Q15582	75261	7.62	145	10	1.20E-09	18
Neutrophil gelatinase-associated lipocalin	VLP24, VPP3	P80188	22745	9.02	161	9	3.3e-11	58
Matrix metalloproteinase I	VLP25, VPP20	P03956	30138	8.25	124	10	1.60E-07	23
Neutrophil gelatinase-associated lipocalin	VPP1	P80188	22745	9.02	128	7	6.10E-08	43
Neutrophil gelatinase-associated lipocalin	VPP2	P80188	22745	9.02	179	10	4.90E-13	61
Neutrophil gelatinase-associated lipocalin	VPP4	P80188	22745	9.02	161	9	3.3e-11	58
Metalloproteinase inhibitor 1	VPP5	P01033	23840	8.46	83	5	0.0021	35
Kallikrein- 7	VPP7	P49862	28191	8.82	114	7	1.50E-06	35
Kallikrein-10	VPP8	O43240	30803	8.95	75	5	0.012	24
Rho GDP- dissociation inhibitor 1	VPP9	P52565	33250	5.02	81	5	0.0032	25
Carboxypeptidase A4	VPP10	Q9UI42	47550	6.23	113	8	1.90E-06	26
Plasminogen activator inhibitor-1	VPP11	P05121	45088	6.68	116	8	9.80E-07	23

Complement factor B	VPP12	P00751	86847	6.67	70	5	0.035	8
Insulin like growth factor-binding protein 2	VPP14	P18065	36198	7.48	205	12	1.20E-15	45
Renin receptor	VPP15	O75787	38983	5.76	80	5	0.0042	19
Plasminogen activator inhibitor-1	VPP16	P05121	45088	6.68	116	8	9.80E-07	23
Laminin subunit gamma-2	VPP17	Q13753	134769	5.83	126	11	9.80E-08	12
Laminin subunit alpha-3	VPP18	Q16787	191582	8.41	73	7	0.018	4
MMP-1(interstitial collagenase)	VPP19	P03956	30138	8.25	152	11	2.50E-10	27
MMP-1(interstitial collagenase)	VPP21	P03956	30138	8.25	158	12	6.20E-11	29
Complement C3	VPP22	P01024	188569	6.02	128	11	6.20E-08	10
Complement C3	VPP23	P01024	188569	6.02	114	11	1.60E-06	10
Serotransferrin	VPP24	Q29443	79870	6.75	91	8	0.0003	14
Serotransferrin	VPP25	Q29443	79870	6.75	128	18	6.20E-17	32
Serine protease HTRA1	VPP26	Q92743	52167	8.09	113	8	2.00E-06	19
Transforming growth factor-beta-induced protein ig-h3	VPP27	Q15582	75261	7.62	109	8	4.90E-06	16
Insulin-like growth factor binding protein 7	VPP28	Q16270	30138	8.25	94	5	0.00015	21

Metalloproteinase inhibitor 1	VPP29	P01033	23840	8.46	73	4	0.021	28
Lysozyme like protein 1	VPP30	Q6UWQ5	17156	8.35	63	3	0.0096	29
Interleukin-6	VPP35	Q6UWQ5	23931	6.17	66	4	0.0047	24
Insulin like growth factor-binding protein 2	VPP36	P18065	36198	7.48	158	9	6.20E-11	33
Beta-2-microglobulin	VAP1	P61769	13820	6.06	68	4	0.003	54
Mixture of Keratin type II cuticular Hb6 and Type I cuticular Ha1	VAP2	O43790	55120	5.56	110	12	3.90E-06	32
Mixture of Keratin type II cuticular Hb6 and Type I cuticular Ha1	VAP2	Q15323	48628	4.87	108	11	6.20E-06	32
Mimecan	VAP3	P20774	34243	5.46	79	5	0.0054	17
Mimecan	VAP4	P20774	34243	5.46	66	4	0.0048	11
Macrophage capping protein	VAP5	P40121	38779	5.88	70	4	0.036	16

Table 3-5: Compiled data of PMF searches of identified spots in all secretomes. Accession number is the identification number for each protein in the Swiss-Prot/TrEMBL databases. Mr (Da) theoretical and pI theoretical are the theoretical mass and pI respectively of the full length protein. These along with score, number of matching peptides, expect (E) value and sequence coverage were obtained when the peptide peak values from MALDI-TOF were searched against already available theoretical digests of all proteins in protein databases using http://www.matrixscience.com/

3.3.6.1 Cell line

Only 25 out of 50 selected spots achieved a confident score after repeated experiments (Table 3-6, Table 3-5).

From the identified spots (labelled with arrows in Figure 3-38 & Figure 3-39), 64% of the analysed spots were characterised as being secreted proteins (Figure 3-48, Table 3-6). Despite cellular proteins being eliminated during gel analysis by comparing the protein profile of media with cellular extract, 28% of identified proteins were characterised as intercellular (Figure 3-48, Table 3-6). This could be due to two possible reasons. First, the total cell proteins were extracted using TBST, which is a relatively weak detergent-based lysis buffer, which solubilises cell membranes and soluble/non-structural proteins. TBST was employed to reduce the extraction of structural proteins therefore extracting predominantly soluble-cytoplasmic proteins. With this in mind, the results suggest TBST was not efficient in extracting nuclear proteins which would remain encapsulated in insoluble structure of the cell. This may explain why 43% of identified intercellular proteins were characterised as nuclear. Second, these intercellular proteins could also be part of some non-classical secretory pathway or part of exosomes that are actively transported out of cell (Volmer et al., 2005), but not reported till now.

The remaining spots did not get a significant score probably due to low molecular weight protein, poor trypsin cleavage sites or the excised spot containing contamination from an additional protein. These result in a low number of peptide fragments which makes accurate characterisation difficult. In PMF, the obtained peptide peaks are matched against already available theoretical digests of all proteins in protein databases. Thus low amount of protein in gel, poor quality and less number of peptide fragments could result in a non significant score.

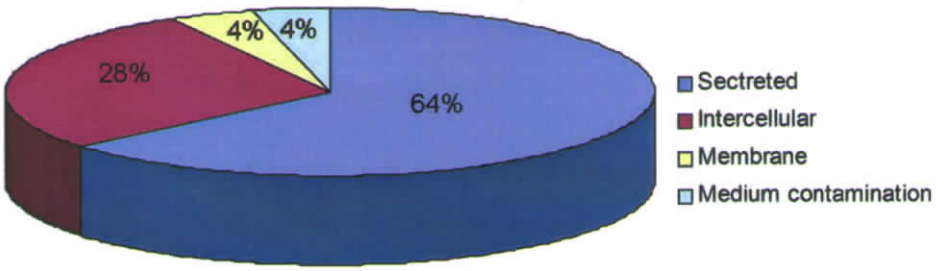

Figure 3-48: Pie chart showing the subcellular location of analysed spots from gels of cell line

Some proteins like tissue inhibitor of metalloproteinases-1 (TIMP-1) (VLP 13, 14 & 15) and Annexin A2 (VLP 16, 17 & 18) appeared as multiple spots in gel probably due to post-translational modification resulting in subtle changes in the protein charge. Modifications during the 2DE process like carbamylation also could be another reason for the multiple spots of same protein, called charge trains (Tannu and Hemby, 2006). Isocyanate, which is a degradation product of urea, causes carbamylation of proteins. However, for this study precautions were taken to minimise experimental modification of proteins, therefore the charge differences are most likely a result of biological modifications. One of the spots in the secretome was identified as cholera toxin (VLP 5) which is a medium supplement. This spot could be used as an internal control for semi-quantitative comparison of secreted proteins as the concentration of cholera toxin in the medium and the volume of the collected medium is known.

Secreted protein acidic and rich in cysteine (SPARC)/osteonectin (VLP 20) was found to be secreted more in cell line. SPARC play an important role in matrix remodelling. It had been reported to enhance production of MMP-1 and MMP-9 in monocytic cells (Shankavaram et al., 1997). Reduction in TIMP-2 levels during ECM remodelling had also been attributed to SPARC. In eye, SPARC could be playing a role in regulation of intraocular pressure (Rhee et al., 2003). SPARC had been reported to be involved in corneal epithelial wound healing process (Berryhill et al., 2003), modulation of cell adhesion of endothelial cells and in cancer cell migration. Shimmura et al reported a higher secretion of SPARC by limbal fibroblasts compared to corneal/limbal epithelial cells (Shimmura et al., 2006). They also noticed that exogenous SPARC inhibited cell adhesion of a corneal epithelial cell line.

Spot no	Protein name	Subcellular location	Accession no:	Identification method	Function
1	Cystatin-C	Secreted	P01034	PMF & MS/MS	As an inhibitor of cysteine proteinases, this protein is thought to serve an important physiological role as a local regulator of this enzyme activity.
2	Proteasome subunit alpha type-3	cytoplasm	P25788	PMF	The proteasome is a multicatalytic proteinase complex which is characterized by its ability to cleave peptides with Arg, Phe, Tyr, Leu, and Glu adjacent to the leaving group at neutral or slightly basic pH. The proteasome has an ATP-dependent proteolytic activity
3	Acidic leucine-rich nuclear phosphoprotein 32 family member B	nucleus	Q92688	PMF	Multifunctional protein working as a cell cycle progression factor as well as a cell survival factor. Required for the progression from the G1 to the S phase. Anti-apoptotic protein which functions as a caspase-3 inhibitor.
4	Proprotein convertase subtilisin/kexin type 9	secreted	Q8NBP7	PMF	May be implicated in the differentiation of cortical neurons and may play a role in cholesterol homeostasis
5	Cholera enterotoxin subunit A precursor - Vibrio cholerae	Medium contamination	P01555	PMF	--------
6	14-3-3 protein beta/alpha	cytoplasm	P31946	PMF	Adapter protein implicated in the regulation of a large spectrum of both general and specialized signalling pathway
7	Proteasome subunit alpha type-3	cytoplasm	P25788	PMF	Multicatalytic proteinase complex which is characterized by its ability to cleave peptides
8	Metalloproteinase inhibitor 2	secreted	P16035	PMF	Complexes with metalloproteinases (such as collagenases) and irreversibly inactivates them. Known to act on MMP-1, MMP-2, MMP-3, MMP-7, MMP-8, MMP-9, MMP-10, MMP-13, MMP-14, MMP-15, MMP-16 and MMP-19

9	Lamin-A/C	nucleus	P02545	PMF	Lamins are components of the nuclear lamina, a fibrous layer on the nucleoplasmic side of the inner nuclear membrane, which is thought to provide a framework for the nuclear envelope and may also interact with chromatin.
10	Renin receptor	membrane	O75787	PMF	Functions as a renin and prorenin cellular receptor
11	Thrombospondin-1	secreted	P07996	PMF	Adhesive glycoprotein that mediates cell-to-cell and cell-to-matrix interactions. Can bind to fibrinogen, fibronectin, laminin, type V collagen and integrins alpha-V/beta-1, alpha-V/beta-3 and alpha-IIb/beta-3.
12	Purine nucleoside phosphorylase	nucleus	P00491	PMF	-------
13	Metalloproteinase inhibitor 1	secreted	P01033	PMF	Complexes with metalloproteinases (such as collagenases) and irreversibly inactivates them. Also mediates erythropoiesis in vitro; but, unlike IL-3, it is species-specific, stimulating the growth and differentiation of only human and murine erythroid progenitors. Known to act on MMP-1, MMP-2, MMP-3, MMP-7, MMP-8, MMP-9, MMP-10, MMP-11, MMP-12, MMP-13 and MMP-16
14	Metalloproteinase inhibitor 1				
15	Annexin A2	Secreted, extracellular space, ECM, basement membrane	P07355	PMF	Calcium-regulated membrane-binding protein, May be involved in heat-stress response
16	Annexin A2				
17	Annexin A2				
18	Epidermal growth factor receptor kinase substrate 8-like protein 2	cytoplasm	Q9H6S3	PMF	Stimulates guanine exchange activity of SOS1. May play a role in membrane ruffling and remodelling of the actin cytoskeleton
19	Plasminogen activator inhibitor 1	Secreted	P05121	PMF	This inhibitor acts as 'bait' for tissue plasminogen activator, urokinase, and protein C. Its rapid interaction with TPA may function as a major control point in the regulation of fibrinolysis

20	SPARC	secreted	P09486	PMF & MS/MS	Appears to regulate cell growth through interactions with the extracellular matrix and cytokines
21	Complement C3	secreted	P01024	PMF	Plays a central role in the activation of the complement system
22	Metalloproteinase inhibitor 1	secreted	P01033	PMF	Given in spot no 13,14 & 15
23	Transforming growth factor-beta-induced protein ig-h3	secreted, ECM	Q15582	PMF	Binds to type I, II, and IV collagens. This adhesion protein may play an important role in cell-collagen interactions
24	Neutrophil gelatinase-associated lipocalin	secreted	P80188	PMF	Transport of small lipophilic substances
25	Matrix metalloproteinase I	secreted	P03956	PMF	Complexes with metalloproteinases (such as collagenases) and irreversibly inactivates them. Known to act on MMP-1, MMP-2, MMP-3, MMP-7, MMP-8, MMP-9, MMP-10, MMP-11, MMP-12, MMP-13 and MMP-16. Does not act on MMP-14.

Table 3-6: Identified spots from cell line secretome by mass spectrometry. Subcellular location and functions of proteins are given based on information from http://www.expasy.ch/sprot/. Spots confirmed using MS/MS analysis were 1 and 20.

3.3.6.2 Primary LiEC

From the primary secretome, 36 spots for potential secreted proteins from TCPS and NIPAAm-MMA were analysed (Table 3-7) and out of that 89.2% were secreted proteins (Figure 3-49) Out of this 68.7% were purely secreted, 12.5% were both secreted and part of ECM, 9.4% were probably secreted and part of ECM, 6.3% were probably secreted and 3.1% were categorised as secreted by similarity (Figure 3-50). As per http://www.expasy.ch/sprot/ proteins 'probably secreted' and 'secreted by similarity' are those which are not experimentally proven to be secreted. Probably secreted are the ones with some experimental evidence and yet not proven completely. In 'by similarity' the facts are proven for a protein or part of it which is then compared to other family members.

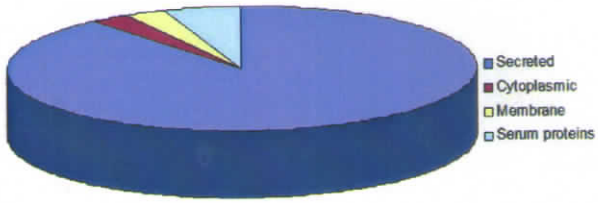

Figure 3-49: Pie chart showing subcellular location of proteins analysed from collected medium of primary cell on both TCPS and copolymer

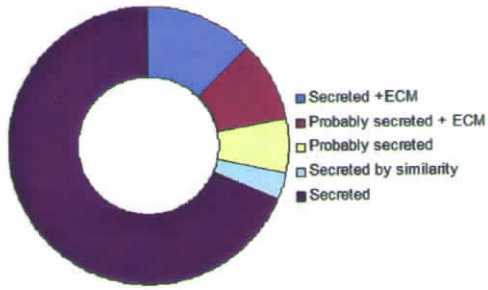

Figure 3-50: Different categories of proteins in the secreted portion

2.7% of the total characterised proteins (1 spot) belonged to membrane protein category and another 2.7% was cytoplasmic protein (Figure 3-49). Serum proteins counted for 5.4% of the total proteins. The analysed 36 spots represented only 23 different proteins because of the presence of multiple spots for same protein (Table 3-7). Presence of serotransferrin of bovine origin indicated some residual serum contamination despite extensive washing and transferring to SFCEM.

Delta 2D software analysis of composite gels of collected medium from explant cultured on AM revealed additional spots (represented by VAP in Figure 3-45). The major secreted protein found unique to AM is mimecan (Figure 3-45, VAP 3& 4). Results of analysis of additional spots from AM by Mass spectrometry are given in Table 3-8.

Spot no	Protein name	Source	Accession no	Identification method	Function
1	Neutrophil gelatinase-associated lipocalin	Secreted	P80188	PMF	Transport of small lipophilic substances
2	Neutrophil gelatinase-associated lipocalin	Secreted	P80188	PMF & MS/MS	
3	Neutrophil gelatinase-associated lipocalin	Secreted	P80188	PMF	
4	Neutrophil gelatinase-associated lipocalin	Secreted	P80188	PMF	
5	Metalloproteinase inhibitor 1	Secreted	P01033	PMF & MS/MS	Complexes with metalloproteinases (such as collagenases) and irreversibly inactivates them. Known to act on MMP-1, MMP-2, MMP-3, MMP-7, MMP-8, MMP-9, MMP-10, MMP-11, MMP-12, MMP-13 and MMP-16. Does not act on MMP-14.
6	Metalloproteinase inhibitor 1	Secreted	P01033	PMF	
7	Kallikrein- 7	Secreted	P49862	PMF	May catalyze the degradation of intercellular cohesive structures in the cornified layer of the skin in the continuous shedding of cells from the skin surface, Could play a role in the activation of precursors to inflammatory cytokines
8	Kallikrein-10	Probably secreted	O43240	PMF	Has a tumor-suppressor role for NES1 in breast and prostate cancer
9	Rho GDP- dissociation inhibitor 1	Cytoplasm	P52565	PMF	Regulates the GDP/GTP exchange reaction of the Rho proteins by inhibiting the dissociation of GDP from them, and the subsequent binding of GTP to them
10	Carboxypeptidase A4	Secreted by similarity	Q9UI42	PMF	Metalloprotease that could be involved in the histone hyperacetylation pathway
11	Plasminogen activator inhibitor-1	Secreted	P05121	PMF	This inhibitor acts as 'bait' for tissue plasminogen activator, urokinase, and protein C. Its rapid interaction with TPA may function as a major control point in the regulation of fibrinolysis

12	Complement factor B	Secreted	P00751	PMF	Factor B is part of the alternate pathway of the complement system. It has also been implicated in proliferation and differentiation of preactivated B-lymphocytes, rapid spreading of peripheral blood monocytes, stimulation of lymphocyte blastogenesis and lysis of erythrocytes.
13	Annexin A2	Secreted, ECM, basement membrane	P07355	PMF	Calcium-regulated membrane-binding protein whose affinity for calcium is greatly enhanced by anionic phospholipids. It binds two calcium ions with high affinity. May be involved in heat-stress response
14	Insulin like growth factor-binding protein 2	Secreted	P18065	PMF	IGF-binding proteins prolong the half-life of the IGFs and have been shown to either inhibit or stimulate the growth promoting effects of the IGFs on cell culture. They alter the interaction of IGFs with their cell surface receptors
15	Renin receptor	Membrane, single pass type I membrane protein	O75787	PMF	Functions as a renin and prorenin cellular receptor. It may also play a role in the renin-angiotensin system (RAS)
16	Plasminogen activator inhibitor-1	Secreted	P05121	PMF	Given in Spot no:11
17	Laminin subunit gamma-2	Secreted, ECM, basement membrane	Q13753	PMF	Binding to cells via a high affinity receptor, laminin is thought to mediate the attachment, migration and organization of cells into tissues during embryonic development by interacting with other extracellular matrix components
18	Laminin subunit alpha-3	Secreted, ECM, basement membrane	Q16787	PMF	
19	MMP-1(interstitial collagenase)	Secreted, extra cellular space, ECM (probable)	P03956	PMF	Cleaves collagens of types I, II, and III at one site in the helical domain. Also cleaves collagens of types VII and X
20	MMP-1(interstitial collagenase)				
21	MMP-1(interstitial collagenase)				
22	Complement C3	Secreted	P01024	PMF	Plays a central role in the activation of the complement system
23	Complement C3				

24	Serotransferrin	Medium contamination	Q29443	PMF	Transferrins are iron binding transport proteins which can bind two Fe(3+) ions in association with the binding of an anion, usually bicarbonate. It is responsible for the transport of iron from sites of absorption and heme degradation to those of storage and utilization. Serum transferrin may also have a further role in stimulating cell proliferation.
25	Serotransferrin				
26	Serine protease HTRA1	Secreted	Q92743	PMF	Protease that regulate the availability of IGFs by cleaving IGF-binding proteins
27	Transforming growth factor-beta-induced protein ig-h3	Secreted, ECM	Q15582	PMF & MS/MS	Binds to type I, II, and IV collagens. This adhesion protein may play an important role in cell-collagen interactions
28	Insulin-like growth factor binding protein 7	Secreted	Q16270	PMF	Binds IGF-I and IGF-II with a relatively low affinity. Stimulates prostacyclin (PGI2) production
29	Metalloproteinase inhibitor 1	Secreted	P01033	PMF	Given in spot no. 5& 6
30	Lysozyme like protein 1	Probably secreted	Q6UWQ5	PMF	Hydrolysis of 1,4-beta-linkages between N-acetylmuramic acid and N-acetyl-D-glucosamine residues in a peptidoglycan and between N-acetyl-D-glucosamine residues in chitodextrins
31	Cystatin-C	Secreted	P01034	PMF	As an inhibitor of cysteine proteinases, this protein is thought to serve an important physiological role as a local regulator of this enzyme activity.
32	SPARC	Secreted	P09486	PMF	Appears to regulate cell growth through interactions with the extracellular matrix and cytokines
33	Metalloproteinase inhibitor 2	Secreted	P16035	PMF	Complexes with metalloproteinases (such as collagenases) and irreversibly inactivates them. Known to act on MMP-1, MMP-2, MMP-3, MMP-7, MMP-8, MMP-9, MMP-10, MMP-13, MMP-14, MMP-15, MMP-16 and MMP-19
34	Plasminogen activator inhibitor 1	Secreted	P05121	PMF	Given in spot no.11

35	Interleukin-6	Secreted	P05231	PMF	IL-6 is a cytokine with a wide variety of biological functions: it plays an essential role in the final differentiation of B-cells into Ig-secreting cells, it induces myeloma and plasmacytoma growth, it induces nerve cells differentiation, in hepatocytes it induces acute phase reactants
36	Insulin-like growth factor binding protein 2	Secreted	P18065	PMF	Given in spot no.14

Table 3-7: Results of mass spectrometry analysis of secretome of primary epithelial cells cultured on TCPS & NIPAAm-MMA. Subcellular location and functions of proteins are given based on information from http://www.expasy.ch/sprot/. Spots confirmed using MS/MS analysis were 2, 5 and 27.

Spot no	Protein name	Source	Accession no	Identification method	Function
1	Beta-2-microglobulin	Secreted	P61769	PMF	Beta-2-microglobulin is the beta-chain of major histocompatibility complex class I molecules.
2	Mixture of Keratin type II cuticular Hb6 and Type I cuticular Ha1	Intermediate filament, contamination (probable)	O43790 Q15323	PMF	
3	Mimecan	Secreted, extracellular space, ECM (probable)	P20774	PMF	Induces bone formation in conjunction with TGF-beta-1 or TGF-beta-2
4	Mimecan	Secreted, extracellular space, ECM (probable)	P20774	PMF	
5	Macrophage capping protein	Cytoplasm	P40121	PMF	Calcium-sensitive protein which reversibly blocks the barbed ends of actin filaments but does not sever preformed actin filaments. May play an important role in macrophage function

Table 3-8: Identified additional spots of primary secretome from AM. Subcellular location and functions of proteins are given based on information from http://www.expasy.ch/sprot/

Mimecan/Osteoglycin (Figure 3-45, VAP 3 & 4), a keratan sulfate proteoglycan, was reported both in corneal stroma and AM (Hopkinson et al., 2006a). In cornea, it may help maintenance of corneal transparency and cellular growth. Presence of mimecan mRNA had been reported in corneal keratocytes. It is found glycosylated in corneal tissue which is required for corneal transparency (Martins et al., 2007). Mimecan was also reported to have a role in UV response (Tasheva and Conrad, 2003). Mimecan in the secretome of cells cultured on AM could be, as mentioned above, a result of matrix remodelling ie; released from AM by matrix metalloproteinases. Further confirmation became necessary to see whether there was any contribution from the cultured LiEC. Beta-microglobulin could not be labelled in the gel images of primary secretome from NIPAAm-MMA and TCPS because the lower weight proteins had run out of the gel during some experiments. In one of the gels in which lower weight proteins were present, the spot corresponding to this protein could be marked (Figure 3-51), which indicated that it is not a unique spot present in primary secretome from AM.

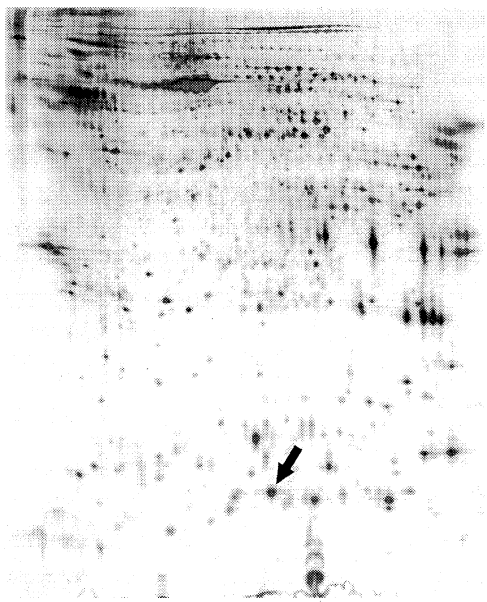

Figure 3-51: Beta microglobulin is marked by arrow in gel image of primary secretome from TCPS

The other unique analysed spots turned out to be cytoplasmic proteins and hence they are of little interest for this study. Further analysis is necessary to unravel the whole secretome of LiEC cultured on all the substrates.

Several of the proteins common to all primary secretomes and known to play some role in cornea are detailed below.

All the primary cell secretome had **MMP-1** (VPP19, 20 & 21), a collagenase, which cleaves interstitial collagens type I, II and III. Spot corresponding to MMP-1 was found in cell line secretome also (VLP25). Matrix metalloproteinases are zinc dependent extracellular endoproteinases that are capable of degrading and remodelling whole ECM during various physiological and pathological conditions. They are classified into collagenases, stromelysins, gelatinases, membrane type MMPs and others based on their substrate specificity (Li et al., 2003). MMP-1 plays a role in the migration and re-epithelialisation during corneal wound healing (Daniels et al., 2003). TIMP regulate the function of MMPs by interfering with active MMP and MMP proenzyme activation (Ye and Azar, 1998). Two of them, **TIMP-1** (VLP13 &14, VPP5, 6 & 29) and **2** (VLP8, VPP33) were also characterised in all secretomes. Both MMP-1 and TIMP-1 were found as multiple spots in the secretome.

Kallikreins (KLK) are peptidases, reported to be found in skin and other tissues. There are 15 known kallikreins and two of them, KLK-7 (VPP7) and 10 (VPP8) were found in the primary secretomes. KLK-7 was reported to be involved in degradation of intercellular adhesion molecules during cell desquamation (Lundstrom and Egelrud, 1991). In another way it could be considered as a marker of terminal epithelial differentiation (Ekholm and Egelrud, 2000) and might be responsible for cell shedding from corneal surface. Its presence in primary secretome could be expected as some portion of the epithelial population on different substrates might be terminally differentiated cells. KLK-10, normal epithelial cell specific-1 protein, was reported to be highly expressed in many tissues. Its expression is dramatically decreased in cancer cell lines (Sidiropoulos et al., 2005). Few reports revealed their expression in cornea. Confirmation studies should be done to understand their presence and role in corneal epithelium. Comparison of gel images suggested that the expression of these proteins was relatively less in cells cultured on AM. Repeated experiments and further studies are required to confirm this factor.

Plasminogen activator inhibitor (PAI-1) (VPP11, 16 & 34, VLP19) inhibits activity of urokinase plasminogen activator. This enzyme activates plasminogen into plasmin which cleaves fibronectin, laminin and other ECM molecules. It has also been reported that PAI-1 plays a role in epithelial adhesion and migration. Increased expression was reported in normal migrating cells and metastasizing tumor cells (Sumiyoshi et al., 1991). Wang et al suggested a dual role for PAI in corneal wound

healing (Wang et al., 2005). According to them, PAI-1 may support migration and re-epithelialisation as a chemotactic agent initially and proper cell adhesion to the matrix afterwards.

Insulin growth factor binding proteins (IGFBP) modulate actions of Insulin growth factors (IGF) by either stimulating or inhibiting them, thereby influencing effects of IGF on cell culture and growth. There are seven genes transcribing for IGFBP. IGFBP-2 (VPP14 & 36) and 7 (VPP28) were found in the secretome of primary cells grown in all substrates. IGFBP-2 expression is increased during fasting and various pathological conditions. In the review by Wolf et al, they suggested inhibitory effects for IGFBP-2 on IGF actions (Wolf et al., 2000). Schoen et al had reported expression of IGFBP-2 in different ocular tissues including corneal epithelium in developing chick embryo (Schoen et al., 1995). IGFBP-7 was reported to induce apoptosis, inhibit growth rate and reduce colony formation efficiency *in vitro* (Ruan et al., 2007). It was also suggested as a tumor suppressor protein in many carcinomas. Another protein that was characterised in primary secretome was **serine protease HTRA1 (VPP26)**. This protein was reported to regulate the availability of IGF by cleaving IGFBP. The intensity of spot corresponding to this protein was less in secretome of cells cultured on AM. It is indeed intriguing and will be interesting to carry out further studies to learn the causes for this differential expression. This protein has various expression levels in different tissues, with the highest in placenta (De Luca et al., 2004), suggesting different roles in different cell types (De Luca et al., 2003). Eventhough the highest expression is in placenta, AM did not seem to enhance its expression/secretion in limbal epithelial cells.

Cystatin C (VPP31, VLP1) is an inhibitor of cysteine proteinases especially cathepsin B, H, L, F and S. Cathepsins may degrade extracellular substrata like laminin. It has been reported that cystatin C inhibited cathepsin F and thereby restored laminin-10 and integrin $\alpha 3\beta 1$ staining patterns (Saghizadeh et al., 2005). Its presence has been reported in various ocular tissues like ciliary epithelium and retinal pigmented epithelium along with corneal epithelium.

Annexin A2 (VPP13, VLP15, 16 & 17) is a calcium regulated membrane binding protein which is present in BM and ECM. It is a pleiotropic protein ie; its function is dependent on place and time in the body. It was reported to be present in basal cells of central cornea and basal/suprabasal layers of limbus in rat cornea (Matsuda et al., 1999).

They also observed that Annexin A2 is translocated from cytoplasm to extracellular space during wound healing, indicating its role in epithelial cell migration.

NGAL/lipocalin 2 (VPP1, 2, 3 & 4, VLP24) were found as multiple spots in all primary cell secretomes. This protein was first isolated from human neutrophils. Expression of this protein is upregulated in epithelial cells during inflammatory conditions and cancers (Nielsen et al., 1996). It was also reported as a bacteriostatic agent which sequesters iron (Goetz et al., 2002). NGAL protects MMP-9 from degradation by binding with it (Yan et al., 2001). Tong et al showed that a reduction in NGAL availability resulted in increased susceptibility of cells towards toxic agents (Tong et al., 2005). Thus, this protein may be having an extracellular cell defense role. From the gel images, it seems expression/secretion of this protein is downregulated in primary cell secretome from AM. Further confirmatory work is needed to prove this observation.

IL-6 (VPP35) is both an anti inflammatory and pro inflammatory cytokine found in the primary secretomes. After corneal injury, levels of IL-6 along with IL-1α increases according to the severity of injury (Agrawal and Tsai, 2003). This increase initiates the process of wound healing. IL-6 promotes epithelial migration by upregulating expression of fibronectin receptors on corneal epithelial cells (Nishida et al., 1992).

βig-h3 or transforming growth factor β induced protein (VPP27 & VLP23) was first detected in a lung adenocarcinoma cell line after inducing with TGFβ. It had been reported that mutations in the gene for this protein resulted in autosomal dominant corneal dystrophies (Hilton et al., 2007). This protein was also reported to be present in amniotic membrane (Hopkinson et al., 2006a). βig-h3 acts as adhesion substratum for skeletal muscle cells *in vitro* (Ferguson et al., 2003).

3.3.7 Western blotting of selected proteins

Proteins extracted from the secretome and whole cell extract of CECL and primary cells expanded on different substrates were subjected to western blot analysis and immuno-probed for NGAL, IL-6, Mimecan and βig-h3. NGAL and IL-6 were selected based on their differential expression in cell line and primary cells.

Mimecan was identified only in cultures on AM by Mass spectrometry. The expression of these proteins in different conditions as analysed by western blotting is given in Figure 3-52.

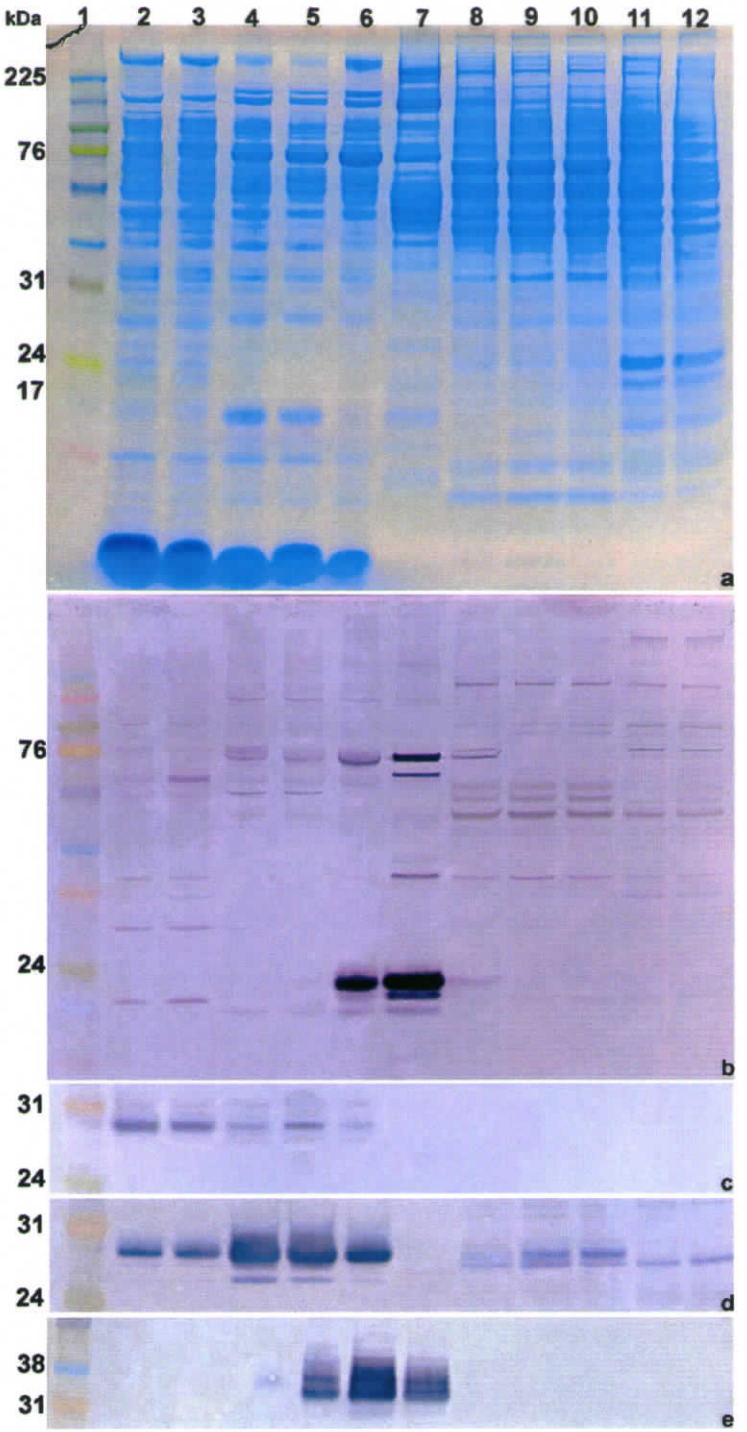

Figure 3-52: a) Nupage 12% Bis-Tris gel stained with Coomassie blue. Western blot analysis of b) βig-h3, c) IL-6, d) NGAL, e) Mimecan. Lanes are 1- Marker, 2- Cell line secretome from TCPS, 3- Cell line secretome from NIPAAm-MMA, 4- Primary cell secretome (TCPS), 5- Primary cell secretome (NIPAAm-MMA), 6- Primary cell secretome (AM), 7- LDS extract of thermolysin treated AM, 8- LDS extract of primary cells (AM), 9- LDS extract of primary cells (NIPAAm-MMA), 10- LDS extract of primary cells (TCPS), 11- LDS extract of cell line (TCPS), 12- LDS extract of cell line (NIPAAm-MMA).

βig-h3 (75 kDa) was identified in cell line and primary cell secretome from all substrates by mass spectrometry and confirmed in primary cell secretome by QTOF.

However only weak staining for βig-h3 was observed in primary secretome samples except in AM primary cell secretome and thermolysin treated AM (Figure 3-52 b). The abundance in AM primary secretome could be due to the release of the protein from AM stroma during culture. One possible reason for the different sized bands in the two AM lanes (Figure 3-52 b, lanes 6 & 7) may be the cleavage products due to thermolysin action during denudation.

Interleukin-6 (24 kDa) was initially identified from AM primary cell secretome by mass spectrometry. Although the protein spot was not identified by mass spectrometry in cell line protein profile, western blot results showed increased expression in cell line compared to primary cells (Figure 3-52 c). However, there was no detectable change in IL-6 expression in the cell line secretome on either substrate. Changes in the gene and protein expression due to immortalization might have led to an increased production of IL-6 from cell line.

Staining for NGAL (23 kDa) showed strong bands in all the secretome. Presence of NGAL was considerably higher in primary cell secretomes compared to that of cell line. Strong staining for NGAL was obtained from a low protein load of 5 µg in secretome samples (Figure 3-52 d, lane 2-6) suggesting its abundance in the secretome. Staining in primary cell secretome from AM was less compared to that from other two substrates. This may be due to the incorporation of NGAL-MMP 9 complex (Yan et al., 2001) in AM reducing its presence in the collected medium portion. The results confirmed observation from 2D gel analysis.

Intense staining for mimecan (34 kDa) appeared within 5 minutes of addition of NBT/BCIP substrate in primary secretome cultures from AM (Figure 3-52 e), whereas incubation for over an hour was required for the bands to develop in primary secretome from NIPAAm-MMA and TCPS (Figure 3-53). This confirms the identification of corresponding spots only in 2DE gel of primary secretome from AM.

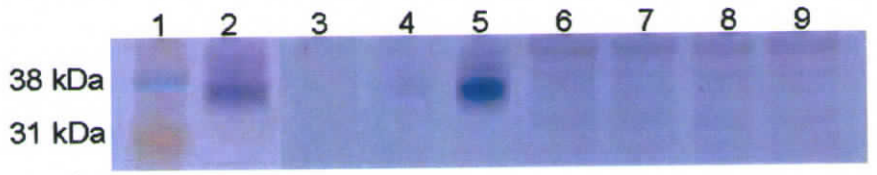

Figure 3-53: Western blot for Mimecan. Bands were seen in Primary TCPS and NIPAAm-MMA secretome, after developing for more than one hour. Lanes 1- marker, 2- Primary cell secretome (TCPS), 3- Cell line secretome from TCPS, 4- Cell line secretome from NIPAAm-MMA, 5- Primary cell secretome (NIPAAm-MMA), 6- 9- LDS extract of the cells corresponding to 2-5 respectively

The presence of mimecan in the primary secretome from NIPAAm-MMA and TCPS must be solely due to the secretion from epithelial cells. Presence of strong staining in LDS extract of thermolysin treated AM and cellular extract from AM indicated that mimecan is a major protein in AM stroma and therefore the additional staining in secretome from AM could also be due to the release of mimecan from AM. Further analysis is necessary to confirm this fact.

3.4 Generation and characterisation of limbal epithelial cell sheet

3.4.1 Goat limbal cell sheet

Goat limbal cell sheet was retrieved in order to standardise retrieval technique of primary contiguous cell sheets. Incubation below LCST of copolymer resulted in easy peeling of goat cell sheet.

3.4.2 Analysis of cell sheet

When viewed under stereo microscope, phase contrast microscope and ESEM, the cell sheet was found to be intact (Figure 3-54). Melanin pigmentation in limbal cells was visible in the cell sheet (arrow in Figure 3-54 a).

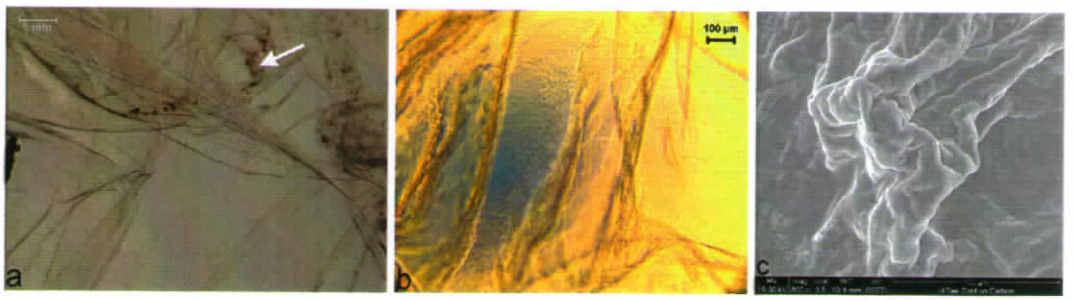

Figure 3-54: Goat limbal cell sheet a) transmittance mode of stereo dissection microscope, b) phase contrast microscope, c) ESEM

Cytoskeletal organisation showed a cortical pattern (Figure 3-55 a) indicating continuous nature of cell sheet. Positive staining for CK3 (Figure 3-55 b) and p63 (Figure 3-55 c) indicated presence of both differentiated and progenitor population in the cell sheet. Depth code analysis revealed presence of p63 throughout the different planes of cell sheet (Figure 3-55 d).

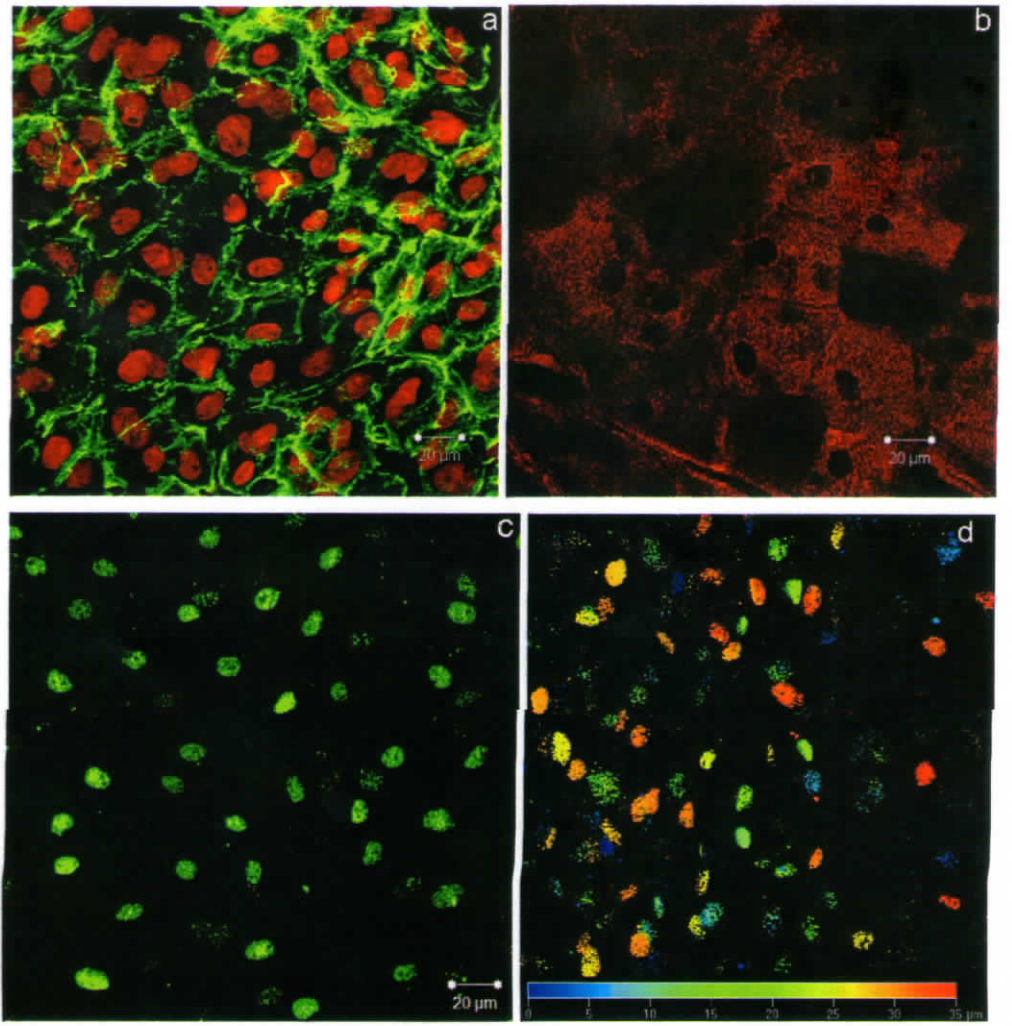

Figure 3-55: a) Actin cytoskeletal organisation, b) CK3 expression, c) p63 expression, d) depth code analysis of p63 in cell sheet.

3.4.3 Rabbit limbal cell sheet

Incubating the confluent cell layer under LCST of the copolymer resulted in an easy detachment of the cells as a continuous sheet with intact cell-cell interactions (Figure 3-56 a). Cellular remnant was not found on the culture dishes, indicating complete detachment of the cell layer. The results of this study correlated with the observation that the cell sheet shrinks in size after retrieval due to the lack of forces of adhesion to support cytoskeletal organization (da Silva et al., 2007). Avoidance of folding of retrieved cell sheet by transferring to an inert support would greatly help in handling cell sheets for transplantation. The peeled off sheet was successfully mounted onto inert doughnut shaped PVDF membrane in order to facilitate transplantation studies (Figure 3-56 b).

The medium in which the cells were grown also had an important role in formation and retrieval of cell sheet. As discussed in the first section of this chapter,

eventhough continuous cell layer was formed in all culture systems except culture system 1, multilayer formation was found only in culture system 4. When cell sheet from cells grown in culture system 2 was retrieved, it was found to be very delicate, easy to tear and difficult to handle. Meanwhile, the cell sheet from culture system 4 was quite strong and thick during harvesting.

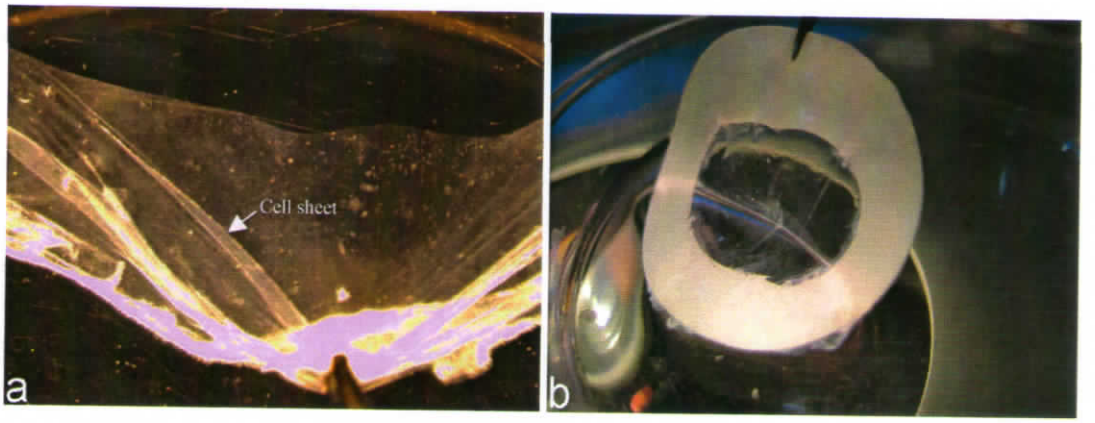

***Figure 3-56: Cell sheet retrieval after incubation under LCST* of copolymer. a) Peeling off using a forceps, b) Mounted on a doughnut shaped PVDF membrane**

The shift of the copolymer into a hydrophilic state due to hydration in the low temperatures enabled the retrieval of the cell sheet. Under the LCST, a hydration layer forms in between the copolymer surface and attached cells which results in the detachment (Yang et al., 2007). It was also reported that active cellular metabolic processes are also required for proper cell detachment (Okano et al., 1995). In order to ensure a proper cell metabolism, it was made customary to feed the cells with fresh medium the day before retrieval. The optimum temperature and time taken for detaching cells depend upon the cell type (Okano et al., 1995). For limbal cells, it was observed that 0 minute incubation at 20°C was sufficient.

When observed under digital camera (macroscopic view, Figure 3-57 a), phase contrast microscope (Figure 3-57 b) and stereo microscope (Figure 3-57 c&d) the cell sheet was found to be intact except the regions where explants were kept. As the explants were removed only before retrieval, gaps corresponding to these were obvious in the sheet.

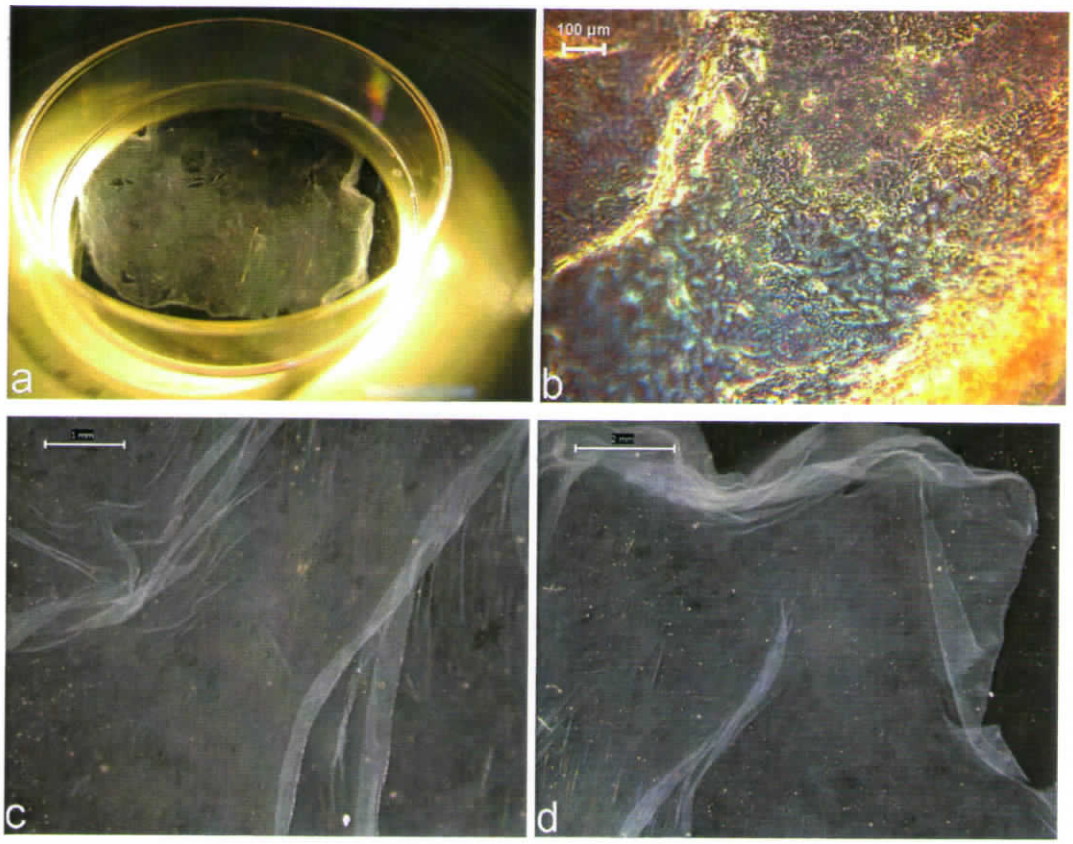

Figure 3-57: Cell sheet images revealing intactness a) macroscopic view, b) phase contrast microscope, c & d) stereo microscope

As the cell sheet retrieval is a non invasive technique in which no enzyme was used to dissociate cells from the culture substrate, deposited ECM could also be harvested along with cell sheet (Kushida et al., 1999). This deposited ECM would help rapid and stable integration of the cell sheet with host tissues during transplantation.

3.4.4 Analysis of cell sheet

3.4.4.1 ESEM

Environmental scanning electron microscope allows observation of biological materials without any complex and time consuming preparation techniques as unprocessed samples can be viewed. Intactness of cell sheet at a high resolution and magnification was observed under ESEM (Figure 3-58). An intact continuous cell sheet was seen in higher magnification also (Figure 3-58 b).

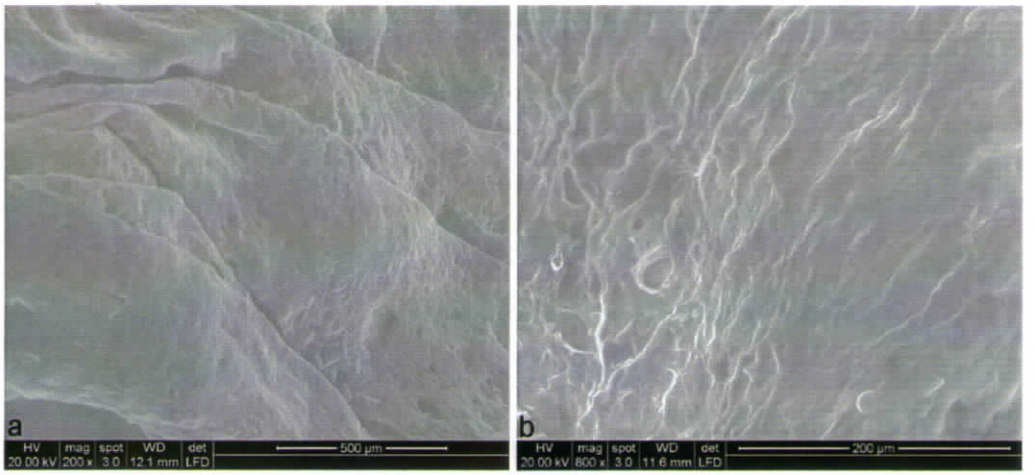

Figure 3-58: ESEM pictures of rabbit limbal cell sheet at different magnifications

3.4.4.2 Cell viability

The cells were stained with FDA immediately after retrieval. This was mainly to assess whether the cells stay viable after low temperature incubation and retrieval technique. All the cells in the retrieved sheet remained viable (Figure 3-59). FDA is a non fluorescent compound which will be converted to green fluorescein by non specific esterases in live cells. As enzymatic conversion is involved, it could be concluded that the cells are not 'just' live, but active and healthy. FDA is also used to estimate various enzyme activities like lipase, esterase and protease, especially in microbiology field (Schnurer and Rosswall, 1982).

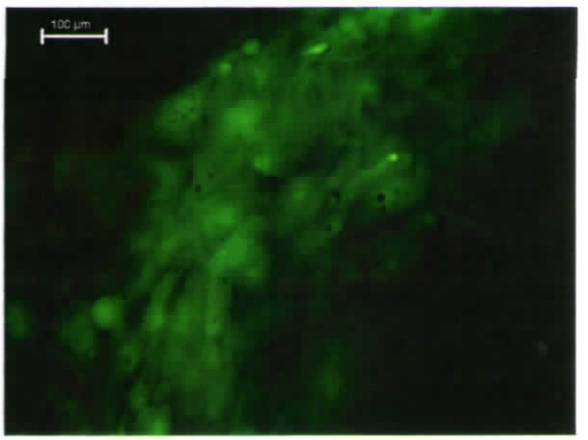

Figure 3-59: Viable cells in the cell sheet after FDA staining

The optimum temperature for mammalian cell culture is 37°C as it mimics body temperature. Primary cells *in vitro* are more sensitive to temperature changes in the environment. Lower temperature incubation for longer periods may compromise cell

and functions. Viability of the sheet after retrieval indicated that incubation at 30 minutes did not damage the cells.

Assessment of transparency

As the major function of cornea is to refract light into the eye, corneal ency can not be compromised. Hence, one of the major requisite for an *in vitro* d epithelial cell sheet is transparency. In this study, transparency of the cell sheet essed by keeping the cell sheet over alphabets printed on a PET sheet. The s were completely visible through the cell sheet (Figure 3-60). This suggested the y of the cell sheet for corneal surface reconstruction.

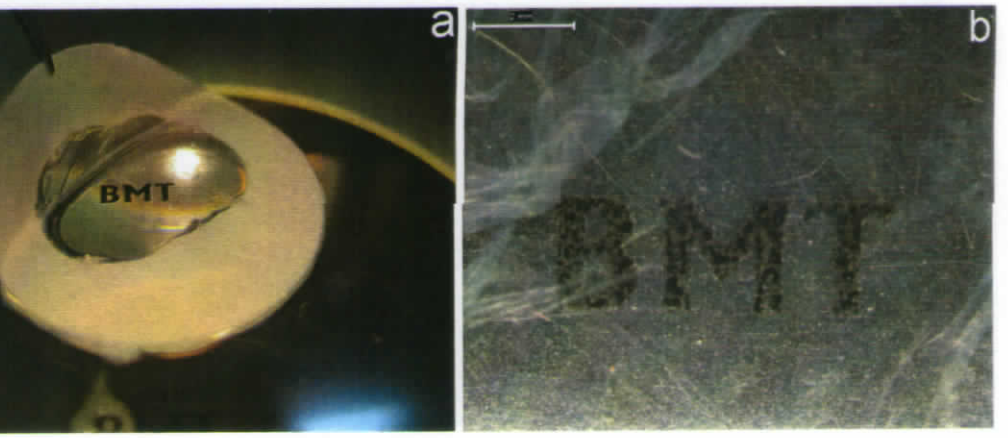

60: Transparency of cell sheet a)macroscopic view and b) stereo dissection microscope

Cytoskeletal organization

Actin cytoskeletal organisation a cortical pattern (Figure dicating the contiguous nature heet and maintenance of good contacts.

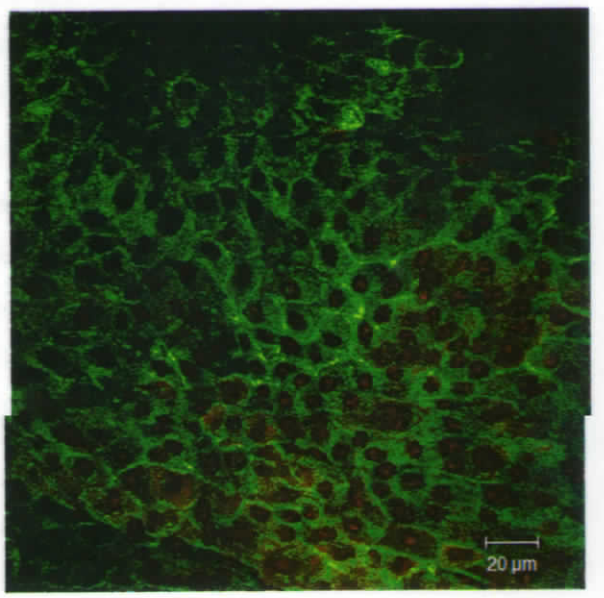

Figure 3-61: Actin cytoskeletal organisation in retrieved cell sheet after 2 weeks of culture

Assessment of barrier function

he cell sheet retrieved after ks of culture was fixed and for occludin and ZO-1, tight proteins. Tight junctions the barrier function in corneal m by which it regulates the movement of fluid, electrolytes and other molecules

to the eye from outside environment. Transmembrane proteins like occludins and claudins and membrane associated proteins like ZO-1 form this cell-cell junction. Positive staining for occludin and ZO-1 was observed in the cell sheet (Figure 3-62 a&b). ZO-1 was reported to be found in superficial layer as well as between wing cells and basal epithelial cells in rabbit cornea (Sugrue and Zieske, 1997). Presence of these proteins indicated formation of functional tight junctions in the cell sheet, which could be a success criterion for transplantation. In addition to that, these proteins provided evidence for preservation of cell-cell interactions during the retrieval technique.

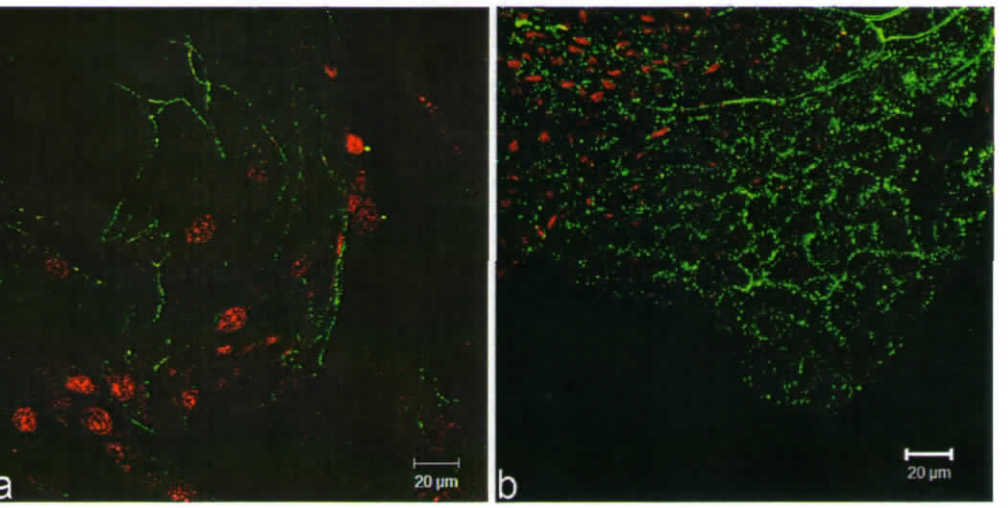

Figure 3-62: Presence of tight junction proteins in cell sheet. a) Occludin, b) ZO-1

3.4.4.6 Characterisation using different markers

The cell sheet was stained for connexin 43, a gap junctional protein. A punctate staining pattern was reported for connexin 43 (Matic et al., 1997) which correlated with our results. (Figure 3-63 a). In the corneal epithelium of different species, two of the gap junctional proteins, connexin 43 and connexin 50, are reported to be present (Dong et al., 1994). In rabbit cornea, it is present in basal layer and suprabasal layers, with very rare staining in squamous, terminally differentiated cells (Matic et al., 1997). It was reported by the same group that compared to human, chick and mouse limbus, the punctate staining pattern was more obvious in rabbit limbus eventhough a huge difference existed between cornea and limbus. Therefore, positively stained cells could be TAC also.

The cell sheet was also stained for p63 to analyse progenitor population. Strong positive staining was observed, as given in Figure 3-63 b. Presence of p63 in the cell sheet ensured progenitor population. Maintenance of a progenitor population is essential for the long term success of cell sheet transplantation towards the treatment of LSCD.

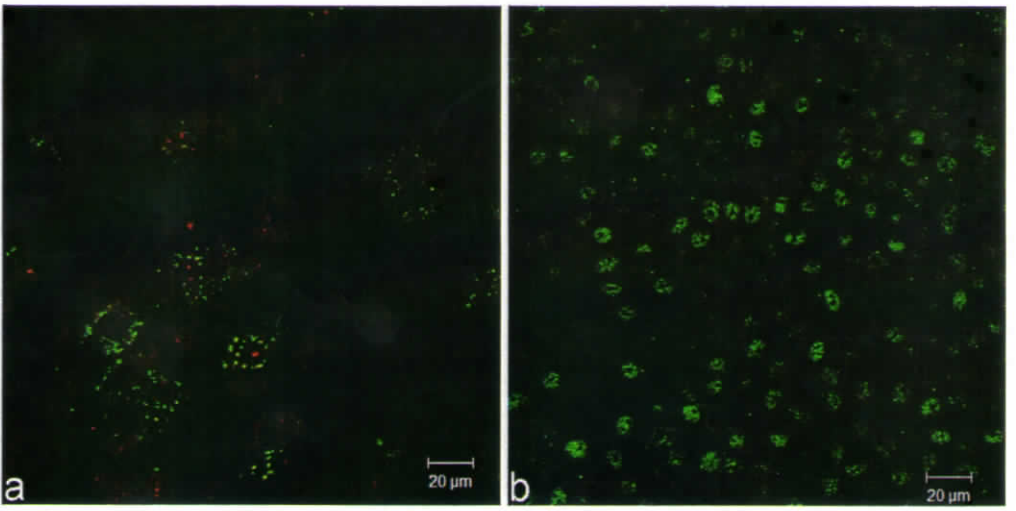

Figure 3-63: Immunofluorescent staining of different markers in rabbit limbal cell sheet retrieved after 14 days of culture. a) Connexin 43, b) p63

CHAPTER 4

SUMMARY AND CONCLUSIONS

4.1 Summary & conclusion

Limbal stem cell deficiency can not be treated with conventional penetrating keratoplasty as the grafted donor cornea does not have the limbal region, thus lacking the stem cell source. *Ex vivo* expansion of limbal cells followed by transplantation is the golden choice of treatment for LSCD. The commonly used scaffolds for this *ex vivo* expansion are biological like amniotic membrane and fibrin gel, which certainly carry risk of disease transmission. Scaffolds based on biomaterials are not suitable for transplantation as it would hinder vision. Therefore scaffold free constructs would be ideal for transplantation. This could be achieved by utilising a thermoresponsive substrate which is capable to undergo phase transition around LCST. The hydrophobic-hydrophilic property shift of the substrate results in detachment of cultured cells as an intact contiguous sheet upon incubation below LCST.

Use of 3T3 feeder layers for *ex vivo* expansion of limbal cells is a widely accepted methodology. Presence of feeder layer helps in the clonal expansion, proliferation and maintenance of progenitor characteristics of limbal cells. As there is a high risk of disease transmission and uptake of xeno molecules from feeder layer in to human system, there is an ever increasing demand for a xeno-feeder free culture system.

In this context, the present study was aimed in the generation of a scaffold free limbal epithelial sheet using a cytocompatible thermoresponsive copolymer in a xeno-feeder free microenvironment. The study was carried out in four phases. In the **first phase**, limbal cells from different sources were cultured and characterised. Cell population freshly isolated from goat limbus were found positive for p63 (69%) and ABCG2 (3.2%), when analysed by flow cytometry. The migrated cells *in vitro* had melanin pigmentation similar to the limbal basal cells and stained positive for p63, CK3

and ABCG2, indicating a mixed cell population in the culture. In rabbit limbal cell culture, it was observed that as duration of dispase incubation increased, deterioration of cells also increased. When cell migratory distance was evaluated using phase contrast microscopy and image analysis, it was found that dispase treatment did not imply any significant change in the migratory distance of cells from limbal explants by 4^{th} day. Therefore, initial enzyme treatment could be avoided for long term limbal explant cultures, which would be ideal for transplantation studies. Out of the different culture systems used, culture system 4 (culture system 2 was substituted by culture system 3 in the later days) supported formation of a top epithelial layer on a layer of already migrated cells, mimicking natural tissue architecture. All culture systems except 2 were found to be supporting maintenance of stem cell characteristics. Culture system 4 was selected for all further studies as it supported formation of an autofeeder layer, thereby enabling avoidance of xeno-feeders and maintained progenitor population.

In the **second phase**, a thermoresponsive copolymer was prepared, characterised and analysed for cytocompatibility. NIPAAm and MMA were copolymerised by free radical polymerisation. FTIR spectrum showed characteristic peaks of both monomers and DSC scan revealed LCST of the copolymer to be around $30^{o}C$. Coating of the copolymer solution on TCPS provided a cost effective and simple technique for preparation of thermoresponsive surfaces. Coating of the copolymer was confirmed using profilometry, ATR spectra and contact angle measurement. Surface roughness of NIPAAm-MMA plates were considerably less when compared to TCPS. Change in wettability between both surfaces gave evidence for copolymer coating. ATR spectrum showed characteristic peak of NIPAAm (amide carbonyl group) on NIPAAm-MMA coated surface. The copolymer was non cytotoxic and the L929 & SIRC cells cultured on the NIPAAm-MMA were viable and healthy. Attachment rate and doubling time of L929 cells on copolymer was similar to that on TCPS. No significant difference was found in the metabolic activity of L929 cells when cultured on TCPS and NIPAAm-MMA. Staining of actin cytoskeleton showed good cell spreading on copolymer. The cell cycle of L929 cells was not affected when grown on copolymer. Reverse transcriptase PCR revealed expression of dNp63, ABCG2, Connexin 43 and CK3 in human limbal cells cultured till confluency on copolymer. Transfer of cells from NIPAAm-MMA surface to PVDF membrane after incubation below LCST confirmed thermoresponsive nature of substrate.

In the **third phase**, molecular level cytocompatibility of the copolymer was studied by analysing secretome of cell line and primary cells. Protein profiles of the collected medium from a SV40 immortalised human corneal cell line cultured on TCPS and NIPAAm-MMA were similar. There was no unique potential secretory protein in either of secretome upon analysis with delta2D software. Similar results were observed when secretome of primary human limbal cells cultured on TCPS and copolymer were compared. Secretome of primary cells cultured on AM had some unique spots probably due to the matrix remodelling in AM. Selected spots from all secretomes were identified using mass spectrometry. Proteins of interest based on the difference in expression in different secretomes were confirmed using MS/MS analysis and western blotting. Comparison of cell line and primary secretome against each other clearly depicted significance of use of primary cells in studying specific cell functions. Specific cytocompatibility studies using human limbal cells proved the suitability of NIPAAm-MMA as substrate towards ocular surface regeneration.

In the **fourth phase**, primary limbal cell sheet was generated by incubating confluent cells on copolymer under its LCST and the cell sheet was functionally characterised. Incubation under LCST of copolymer resulted in easy retrieval of cells as a continuous sheet. The goat cell sheet was checked for intactness and expression of different markers. Results showed that it was intact and contained progenitor population. Rabbit cell sheet was found to be viable, intact and transparent. Presence of cell junctional proteins like ZO-1, occludin and connexin 43 indicated functionally active cell sheet and provided evidence for maintenance of cell-cell interactions after retrieval. Actin cytoskeletal organisation showed a cortical pattern in both cell sheets and gave evidence for the contiguous nature of cell sheet. Presence of both functionally differentiated and progenitor cells in cell sheet increased the chance for successful ocular surface regeneration.

4.2 Significance of the study

- ✓ Optimised culture conditions resulted in formation of autofeeder layer in rabbit explant culture, thereby avoiding use of xeno-feeder layers. Thus a xeno-feeder free culture system was developed for *ex vivo* expansion of limbal cells.
- ✓ A cost effective and simple technique for preparation of thermoresponsive surfaces was employed which would enable increased use of thermoresponsive

surfaces for tissue reconstruction and other various tissue engineering applications as it could be done in any laboratory.

- ✓ Only scanty reports are available about the use of NIPAAm-MMA for cell culture purposes.
- ✓ This study proposed use of secretome analysis as a tool in delineating molecular level cytocompatibility of substrates.
- ✓ This study was the first known initiative towards analysing cytocompatibility of thermoresponsive substrate at molecular level.
- ✓ A contiguous scaffold free cell sheet with intact cell-cell interactions was generated utilising the thermoresponsive copolymer.
- ✓ Cell sheet retrieval proved the concept of thermoresponsive efficacy of in-house synthesised copolymer.
- ✓ Feasibility of cell sheet to integrate with host tissue can avoid the use of sutures, making it suture less.

CHAPTER 5

FUTURE DIRECTIONS

In this study, xeno-feeder free culture system was achieved for generation of limbal epithelial construct. For clinical transplantation purposes, use of xenobiotic free epithelial equivalents is ideal, which would be free of all animal products. Serum free conditions with addition of defined constituents may help to achieve this aim. But as serum contains a lot of unidentified factors, a complete substitution is very difficult. Instead **use of autologous serum** along with autofeeder culture system will result in development of a xenobiotic free limbal epithelial construct.

Preclinical studies are important in determining suitability of any medical application/ product before going to clinical level. Animal experiments with long term follow up will be necessary to find out the efficiency of the cell sheet in restoring and maintaining vision. Only a successful preclinical study will enable the clinical application of cell sheet.

Safety of various newly developed chemicals in compounds like cosmetics and insecticides is assessed, mainly in rabbit models using different *in vivo* tests including eye irritancy test. Different *in vitro* and *ex vivo* tests are being suggested as alternatives to reduce and refine the use of animals used in testing. The cell sheet generated can be used as a **model to study toxicity** as an *in vitro* alternative for animal experiments.

Corneal diseases can affect stromal as well as endothelial layer. Due to increasing donor shortages, attempts are being made all over the world to generate artificial cornea. Endothelial cell sheet construction using PIPAAm was already reported (Sumide et al., 2006). It would be interesting to check suitability of the thermoresponsive substrate in **developing stromal and endothelial layers** separately or in generation of a corneal equivalent by layering different cell sheets one after the other.

Western blotting confirmed an increased presence of mimecan and βig-h3 in secretome collected from primary limbal cells cultured on AM. These proteins along with many others like lumican and decorin are present in abundance in AM stroma and have definite role in many corneal functions. To mimic the AM niche/microenvironment, **incorporation of these protein molecules into the thermoresponsive substrate** will be a good future perspective.

REFERENCES

ISO 10993-1 Biological evaluation of Medical devices-Part 1: Evaluation and testing. 2003. Third ed.

Agrawal VB, Tsai RJ. Corneal epithelial wound healing. 2003. Indian J Ophthalmol 51(1):5-15.

Ahmad S, Stewart R, Yung S, Kolli S, Armstrong L, Stojkovic M, Figueiredo F, Lako M. Differentiation of human embryonic stem cells into corneal epithelial-like cells by in vitro replication of the corneal epithelial stem cell niche. 2007. Stem Cells 25(5):1145-1155.

Allen LT, Fox EJ, Blute I, Kelly ZD, Rochev Y, Keenan AK, Dawson KA, Gallagher WM. Interaction of soft condensed materials with living cells: phenotype/transcriptome correlations for the hydrophobic effect. 2003. Proc Natl Acad Sci U S A 100(11):6331-6336.

Anderson DF, Ellies P, Pires RT, Tseng SC. Amniotic membrane transplantation for partial limbal stem cell deficiency. 2001a. Br J Ophthalmol 85(5):567-575.

Anderson DF, Prabhasawat P, Alfonso E, Tseng SC. Amniotic membrane transplantation after the primary surgical management of band keratopathy. 2001b. Cornea 20(4):354-361.

Ang LP, Tan DT. Ocular surface stem cells and disease: current concepts and clinical applications. 2004. Ann Acad Med Singapore 33(5):576-580.

Anil Kumar PR, Sreenivasan K, Kumary TV. Alternate method for grafting thermoresponsive polymer for transferring *in vitro* cell sheet structures. 2007a. Journal of Applied Polymer Science 105:2245-2251.

Anil Kumar PR, Varma HK, Kumary TV. Cell patch seeding and functional analysis of cellularized scaffolds for tissue engineering. 2007b. Biomed Mater 2(1):48-54.

Arpitha P, Prajna NV, Srinivasan M, Muthukkaruppan V. High expression of p63 combined with a large N/C ratio defines a subset of human limbal epithelial cells: implications on epithelial stem cells. 2005. Invest Ophthalmol Vis Sci 46(10):3631-3636.

Aucoin L, Griffith CM, Pleizier G, Deslandes Y, Sheardown H. Interactions of corneal epithelial cells and surfaces modified with cell adhesion peptide combinations. 2002. J Biomater Sci Polym Ed 13(4):447-462.

Bachle M, Hubner U, Kohal RJ, Han JS, Wiedmann-Al-Ahmad M. Structure and in vitro cytocompatibility of the gastropod shell of Helix pomatia. 2006. Tissue Cell 38(5):337-344.

Barker SL, Ross D, Tarlov MJ, Gaitan M, Locascio LE. Control of flow direction in microfluidic devices with polyelectrolyte multilayers. 2000. Anal Chem 72(24):5925-5929.

Barrandon Y, Green H. Three clonal types of keratinocyte with different capacities for multiplication. 1987. Proc Natl Acad Sci U S A 84(8):2302-2306.

Bentz K, Molcanyi M, Riess P, Elbers A, Pohl E, Sachinidis A, Hescheler J, Neugebauer E, Schafer U. Embryonic stem cells produce neurotrophins in response to cerebral tissue extract: Cell line-dependent differences. 2007. J Neurosci Res 85(5):1057-1064.

Berryhill BL, Kane B, Stramer BM, Fini ME, Hassell JR. Increased SPARC accumulation during corneal repair. 2003. Exp Eye Res 77(1):85-92.

Bhang SH, Jeon O, Choi CY, Kwon YH, Kim BS. Controlled release of nerve growth factor from fibrin gel. 2007. J Biomed Mater Res A 80(4):998-1002.

Bordenave L, Bareille R, Lefebvre F, Caix J, Baquey C. Cytocompatibility study of NHLBI primary reference materials using human endothelial cells. 1992. J Biomater Sci Polym Ed 3(6):509-516.

Boulton M, Albon J. Stem cells in the eye. 2004. Int J Biochem Cell Biol 36(4):643-657.

Buck RC. Cell migration in repair of mouse corneal epithelium. 1979. Invest Ophthalmol Vis Sci 18(8):767-784.

Buck RC. Measurement of centripetal migration of normal corneal epithelial cells in the mouse. 1985. Invest Ophthalmol Vis Sci 26(9):1296-1299.

Burgalassi S, Chetoni P, Monti D, Saettone MF. Cytotoxicity of potential ocular permeation enhancers evaluated on rabbit and human corneal epithelial cell lines. 2001. Toxicol Lett 122(1):1-8.

Canavan HE, Cheng X, Graham DJ, Ratner BD, Castner DG. Cell sheet detachment affects the extracellular matrix: a surface science study comparing thermal liftoff, enzymatic, and mechanical methods. 2005. J Biomed Mater Res A 75(1):1-13.

Cao Y, Zhang C, Shen W, Cheng Z, Yu LL, Ping Q. Poly(N-isopropylacrylamide)-chitosan as thermosensitive in situ gel-forming system for ocular drug delivery. 2007. J Control Release 120(3):186-194.

Cardoen L, Foets B. Limbal transplantation after chemical injuries of the eye. 1999. Bull Soc Belge Ophtalmol 272:105-110.

Casolaro M. 1998. Stimuli responsive polymers(thermodynamics in drug delivery technology) Salamone JC, editor: CRC press. 1513 p.

Chee KY, Kicic A, Wiffen SJ. Limbal stem cells: the search for a marker. 2006. Clin Experiment Ophthalmol 34(1):64-73.

Chen G, Imanishi Y, Ito Y. Effect of protein and cell behavior on pattern-grafted thermoresponsive polymer. 1998. J Biomed Mater Res 42(1):38-44.

Chen JJ, Tseng SC. Corneal epithelial wound healing in partial limbal deficiency. 1990. Invest Ophthalmol Vis Sci 31(7):1301-1314.

Chen JJ, Tseng SC. Abnormal corneal epithelial wound healing in partial-thickness removal of limbal epithelium. 1991. Invest Ophthalmol Vis Sci 32(8):2219-2233.

Chen YT, Li W, Hayashida Y, He H, Chen SY, Tseng DY, Kheirkhah A, Tseng SC. Human amniotic epithelial cells as novel feeder layers for promoting ex vivo expansion of limbal epithelial progenitor cells. 2007. Stem Cells 25(8):1995-2005.

Chen Z, de Paiva CS, Luo L, Kretzer FL, Pflugfelder SC, Li DQ. Characterization of putative stem cell phenotype in human limbal epithelia. 2004. Stem Cells 22(3):355-366.

Chung JE, Yokoyama M, Yamato M, Aoyagi T, Sakurai Y, Okano T. Thermo-responsive drug delivery from polymeric micelles constructed using block copolymers of poly(N-isopropylacrylamide) and poly(butylmethacrylate). 1999. J Control Release 62(1-2):115-127.

Cotsarelis G, Cheng SZ, Dong G, Sun TT, Lavker RM. Existence of slow-cycling limbal epithelial basal cells that can be preferentially stimulated to proliferate: implications on epithelial stem cells. 1989. Cell 57(2):201-209.

da Silva RM, Mano JF, Reis RL. Smart thermoresponsive coatings and surfaces for tissue engineering: switching cell-material boundaries. 2007. Trends Biotechnol 25(12):577-583.

Daniels JT, Dart JK, Tuft SJ, Khaw PT. Corneal stem cells in review. 2001. Wound Repair Regen 9(6):483-494.

Daniels JT, Limb GA, Saarialho-Kere U, Murphy G, Khaw PT. Human corneal epithelial cells require MMP-1 for HGF-mediated migration on collagen I. 2003. Invest Ophthalmol Vis Sci 44(3):1048-1055.

Daya SM, Ilari FA. Living related conjunctival limbal allograft for the treatment of stem cell deficiency. 2001. Ophthalmology 108(1):126-133; discussion 133-124.

de Las Heras Alarcon C, Pennadam S, Alexander C. Stimuli responsive polymers for biomedical applications. 2005. Chem Soc Rev 34(3):276-285.

De Luca A, De Falco M, Fedele V, Cobellis L, Mastrogiacomo A, Laforgia V, Tuduce IL, Campioni M, Giraldi D, Paggi MG, Baldi A. The serine protease HtrA1 is upregulated in the human placenta during pregnancy. 2004. J Histochem Cytochem 52(7):885-892.

De Luca A, De Falco M, Severino A, Campioni M, Santini D, Baldi F, Paggi MG, Baldi A. Distribution of the serine protease HtrA1 in normal human tissues. 2003. J Histochem Cytochem 51(10):1279-1284.

de Paiva CS, Chen Z, Corrales RM, Pflugfelder SC, Li DQ. ABCG2 transporter identifies a population of clonogenic human limbal epithelial cells. 2005. Stem Cells 23(1):63-73.

De Paiva CS, Pflugfelder SC, Li DQ. Cell size correlates with phenotype and proliferative capacity in human corneal epithelial cells. 2006. Stem Cells 24(2):368-375.

Deolinda de Oliveira Pena J, Melo GB, Gomes JA, Haapalainen EF, Komagome CM, Santos NC, Souza Lima Filho AA, Rizzo LV. [Ultrastructural and growth factor analysis of amniotic membrane preserved by different methods for ocular surgery]. 2007. Arq Bras Oftalmol 70(5):756-762.

Diaz-Valle D, Santos-Bueso E, Benitez-Del-Castillo JM, Mendez-Fernandez R, Lopez-Abad C, Martinez-de-la-Casa JM, Garcia-Sanchez J. [Sectorial conjunctival epitheliectomy and amniotic membrane transplantation for partial limbal stem cells deficiency]. 2007. Arch Soc Esp Oftalmol 82(12):769-772.

Dong Y, Roos M, Gruijters T, Donaldson P, Bullivant S, Beyer E, Kistler J. Differential expression of two gap junction proteins in corneal epithelium. 1994. Eur J Cell Biol 64(1):95-100.

Du Y, Chen J, Funderburgh JL, Zhu X, Li L. Functional reconstruction of rabbit corneal epithelium by human limbal cells cultured on amniotic membrane. 2003. Mol Vis 9:635-643.

Dua HS. Stem cells of the ocular surface: scientific principles and clinical applications. 1995. Br J Ophthalmol 79(11):968-969.

Dua HS, Azuara-Blanco A. Allo-limbal transplantation in patients with limbal stem cell deficiency. 1999a. Br J Ophthalmol 83(4):414-419.

Dua HS, Azuara-Blanco A. Amniotic membrane transplantation. 1999b. Br J Ophthalmol 83(6):748-752.

Dua HS, Azuara-Blanco A. Autologous limbal transplantation in patients with unilateral corneal stem cell deficiency. 2000a. Br J Ophthalmol 84(3):273-278.

Dua HS, Azuara-Blanco A. Limbal stem cells of the corneal epithelium. 2000b. Surv Ophthalmol 44(5):415-425.

Dua HS, Gomes JA, Singh A. Corneal epithelial wound healing. 1994. Br J Ophthalmol 78(5):401-408.

Dua HS, Joseph A, Shanmuganathan VA, Jones RE. Stem cell differentiation and the effects of deficiency. 2003. Eye 17(8):877-885.

Dua HS, Saini JS, Azuara-Blanco A, Gupta P. Limbal stem cell deficiency: concept, aetiology, clinical presentation, diagnosis and management. 2000. Indian J Ophthalmol 48(2):83-92.

Dua HS, Shanmuganathan VA, Powell-Richards AO, Tighe PJ, Joseph A. Limbal epithelial crypts: a novel anatomical structure and a putative limbal stem cell niche. 2005. Br J Ophthalmol 89(5):529-532.

Earl LK, Jones PA, Dixit MB, O'Brien KAF. Comparison of five potential methods for assessing ocular irritation *in vitro*. 1995. Toxicology in vitro 9(3):245-250.

Ebara M, Yamato M, Hirose M, Aoyagi T, Kikuchi A, Sakai K, Okano T. Copolymerization of 2-carboxyisopropylacrylamide with N-isopropylacrylamide accelerates cell detachment from grafted surfaces by reducing temperature. 2003. Biomacromolecules 4(2):344-349.

Ebato B, Friend J, Thoft RA. Comparison of central and peripheral human corneal epithelium in tissue culture. 1987. Invest Ophthalmol Vis Sci 28(9):1450-1456.

Ebato B, Friend J, Thoft RA. Comparison of limbal and peripheral human corneal epithelium in tissue culture. 1988. Invest Ophthalmol Vis Sci 29(10):1533-1537.

Ekholm E, Egelrud T. Expression of stratum corneum chymotryptic enzyme in relation to other markers of epidermal differentiation in a skin explant model. 2000. Exp Dermatol 9(1):65-70.

Endo K, Nakamura T, Kawasaki S, Kinoshita S. Human amniotic membrane, like corneal epithelial basement membrane, manifests the alpha5 chain of type IV collagen. 2004. Invest Ophthalmol Vis Sci 45(6):1771-1774.

Epstein SP, Wolosin JM, Asbell PA. P63 expression levels in side population and low light scattering ocular surface epithelial cells. 2005. Trans Am Ophthalmol Soc 103:187-199.

Espana EM, Grueterich M, Romano AC, Touhami A, Tseng SC. Idiopathic limbal stem cell deficiency. 2002. Ophthalmology 109(11):2004-2010.

Espana EM, Kawakita T, Romano A, Di Pascuale M, Smiddy R, Liu CY, Tseng SC. Stromal niche controls the plasticity of limbal and corneal epithelial differentiation in a rabbit model of recombined tissue. 2003. Invest Ophthalmol Vis Sci 44(12):5130-5135.

Ferguson JW, Thoma BS, Mikesh MF, Kramer RH, Bennett KL, Purchio A, Bellard BJ, LeBaron RG. The extracellular matrix protein betaIG-H3 is expressed at myotendinous junctions and supports muscle cell adhesion. 2003. Cell Tissue Res 313(1):93-105.

Frucht-Pery J, Siganos CS, Solomon A, Scheman L, Brautbar C, Zauberman H. Limbal cell autograft transplantation for severe ocular surface disorders. 1998. Graefes Arch Clin Exp Ophthalmol 236(8):582-587.

Gao J, Frisken BJ. Influence of secondary components on the synthesis of self-cross-linked N-isopropylacrylamide microgels. 2005. Langmuir 21(2):545-551.

German MJ, Pollock HM, Zhao B, Tobin MJ, Hammiche A, Bentley A, Cooper LJ, Martin FL, Fullwood NJ. Characterization of putative stem cell populations in the cornea using synchrotron infrared microspectroscopy. 2006. Invest Ophthalmol Vis Sci 47(6):2417-2421.

Gipson IK. The epithelial basement membrane zone of the limbus. 1989. Eye 3 (Pt 2):132-140.

Goetz DH, Holmes MA, Borregaard N, Bluhm ME, Raymond KN, Strong RK. The neutrophil lipocalin NGAL is a bacteriostatic agent that interferes with siderophore-mediated iron acquisition. 2002. Mol Cell 10(5):1033-1043.

Goldberg MF, Bron AJ. Limbal palisades of Vogt. 1982. Trans Am Ophthalmol Soc 80:155-171.

Gomes JA, Santos MS, Ventura AS, Donato WB, Cunha MC, Hofling-Lima AL. Amniotic membrane with living related corneal limbal/conjunctival allograft for ocular surface reconstruction in Stevens-Johnson syndrome. 2003. Arch Ophthalmol 121(10):1369-1374.

Gragnani A, Sobral CS, Ferreira LM. Thermolysin in human cultured keratinocyte isolation. 2007. Braz J Biol 67(1):105-109.

Green LM, Reade JL, Ware CF. Rapid colorimetric assay for cell viability: application to the quantitation of cytotoxic and growth inhibitory lymphokines. 1984. J Immunol Methods 70(2):257-268.

Gronborg M, Kristiansen TZ, Iwahori A, Chang R, Reddy R, Sato N, Molina H, Jensen ON, Hruban RH, Goggins MG, Maitra A, Pandey A. Biomarker discovery from pancreatic cancer secretome using a differential proteomic approach. 2006. Mol Cell Proteomics 5(1):157-171.

Grueterich M, Espana E, Tseng SC. Connexin 43 expression and proliferation of human limbal epithelium on intact and denuded amniotic membrane. 2002. Invest Ophthalmol Vis Sci 43(1):63-71.

Grueterich M, Espana EM, Tseng SC. Ex vivo expansion of limbal epithelial stem cells: amniotic membrane serving as a stem cell niche. 2003. Surv Ophthalmol 48(6):631-646.

Han B, Schwab IR, Madsen TK, Isseroff RR. A fibrin-based bioengineered ocular surface with human corneal epithelial stem cells. 2002. Cornea 21(5):505-510.

Harkin DG, Barnard Z, Gillies P, Ainscough SL, Apel AJ. Analysis of p63 and cytokeratin expression in a cultivated limbal autograft used in the treatment of limbal stem cell deficiency. 2004. Br J Ophthalmol 88(9):1154-1158.

Hernandez Galindo EE, Theiss C, Steuhl KP, Meller D. Gap junctional communication in microinjected human limbal and peripheral corneal epithelial cells cultured on intact amniotic membrane. 2003. Exp Eye Res 76(3):303-314.

Higa K, Shimmura S, Miyashita H, Shimazaki J, Tsubota K. Melanocytes in the corneal limbus interact with K19-positive basal epithelial cells. 2005. Exp Eye Res 81(2):218-223.

Hilton EN, Black GC, Manson FD, Schorderet DF, Munier FL. De novo mutation in the BIGH3/TGFB1 gene causing granular corneal dystrophy. 2007. Br J Ophthalmol 91(8):1083-1084.

Holland EJ, Schwartz GS. Iatrogenic limbal stem cell deficiency. 1997. Trans Am Ophthalmol Soc 95:95-107.

Homma R, Yoshikawa H, Takeno M, Kurokawa MS, Masuda C, Takada E, Tsubota K, Ueno S, Suzuki N. Induction of epithelial progenitors in vitro from mouse embryonic stem cells and application for reconstruction of damaged cornea in mice. 2004. Invest Ophthalmol Vis Sci 45(12):4320-4326.

Hopkinson A, McIntosh RS, Shanmuganathan V, Tighe PJ, Dua HS. Proteomic analysis of amniotic membrane prepared for human transplantation: characterization of proteins and clinical implications. 2006a. J Proteome Res 5(9):2226-2235.

Hopkinson A, McIntosh RS, Tighe PJ, James DK, Dua HS. Amniotic membrane for ocular surface reconstruction: donor variations and the effect of handling on TGF-beta content. 2006b. Invest Ophthalmol Vis Sci 47(10):4316-4322.

Hopkinson A, Shanmuganathan VA, Gray T, Yeung AM, Lowe J, James DK, Dua HS. Optimization of Amniotic Membrane (AM) Denuding for Tissue Engineering. 2008. Tissue Eng Part C Methods 14(4):371-381.

Huang HH, Ho CT, Lee TH, Lee TL, Liao KK, Chen FL. Effect of surface roughness of ground titanium on initial cell adhesion. 2004. Biomol Eng 21(3-5):93-97.

Huhtala A, Pohjonen T, Salminen L, Salminen A, Kaarniranta K, Uusitalo H. In vitro biocompatibility of degradable biopolymers in cell line cultures from various ocular tissues: extraction studies. 2008. J Mater Sci Mater Med 19(2):645-649.

Hyeong Kwon O, Kikuchi A, Yamato M, Okano T. Accelerated cell sheet recovery by co-grafting of PEG with PIPAAm onto porous cell culture membranes. 2003. Biomaterials 24(7):1223-1232.

Ilari L, Daya SM. Long-term outcomes of keratolimbal allograft for the treatment of severe ocular surface disorders. 2002. Ophthalmology 109(7):1278-1284.

Imanishi J, Kamiyama K, Iguchi I, Kita M, Sotozono C, Kinoshita S. Growth factors: importance in wound healing and maintenance of transparency of the cornea. 2000. Prog Retin Eye Res 19(1):113-129.

Inatomi T, Nakamura T, Koizumi N, Sotozono C, Yokoi N, Kinoshita S. Midterm results on ocular surface reconstruction using cultivated autologous oral mucosal epithelial transplantation. 2006. Am J Ophthalmol 141(2):267-275.

Ito Y. Surface micropatterning to regulate cell functions. 1999. Biomaterials 20(23-24):2333-2342.

Joseph A, Dua HS, King AJ. Failure of amniotic membrane transplantation in the treatment of acute ocular burns. 2001. Br J Ophthalmol 85(9):1065-1069.

Kanazawa H, Kashiwase Y, Yamamoto K, Matsushima Y, Kikuchi A, Sakurai Y, Okano T. Temperature-responsive liquid chromatography. 2. Effects of hydrophobic groups in N-isopropylacrylamide copolymer-modified silica. 1997. Anal Chem 69(5):823-830.

Kaye DB. Epithelial response in penetrating keratoplasty. 1980. Am J Ophthalmol 89(3):381-387.

Kenyon KR. Limbal autograft transplantation for chemical and thermal burns. 1989. Dev Ophthalmol 18:53-58.

Kenyon KR, Tseng SC. Limbal autograft transplantation for ocular surface disorders. 1989. Ophthalmology 96(5):709-722.

Kheirkhah A, Casas V, Raju VK, Tseng SC. Sutureless amniotic membrane transplantation for partial limbal stem cell deficiency. 2008. Am J Ophthalmol 145(5):787-794.

Khokhar S, Natung T, Sony P, Sharma N, Agarwal N, Vajpayee RB. Amniotic membrane transplantation in refractory neurotrophic corneal ulcers: a randomized, controlled clinical trial. 2005. Cornea 24(6):654-660.

Kikuchi A, Okano T. Pulsatile drug release control using hydrogels. 2002. Adv Drug Deliv Rev 54(1):53-77.

Kim HS, Jun Song X, de Paiva CS, Chen Z, Pflugfelder SC, Li DQ. Phenotypic characterization of human corneal epithelial cells expanded ex vivo from limbal explant and single cell cultures. 2004a. Exp Eye Res 79(1):41-49.

Kim HW, Koh YH, Kong YM, Kang JG, Kim HE. Strontium substituted calcium phosphate biphasic ceramics obtained by a powder precipitation method. 2004b. J Mater Sci Mater Med 15(10):1129-1134.

Kim IS, Jeong YI, Cho CS, Kim SH. Thermo-responsive self-assembled polymeric micelles for drug delivery in vitro. 2000. Int J Pharm 205(1-2):165-172.

Kinoshita S. The corneal epithelial stem cell puzzle: what future discoveries lie on the horizon? 2008. Arch Ophthalmol 126(5):725-726.

Kinoshita S, Adachi W, Sotozono C, Nishida K, Yokoi N, Quantock AJ, Okubo K. Characteristics of the human ocular surface epithelium. 2001. Prog Retin Eye Res 20(5):639-673.

Kinoshita S, Friend J, Thoft RA. Sex chromatin of donor corneal epithelium in rabbits. 1981. Invest Ophthalmol Vis Sci 21(3):434-441.

Kinoshita S, Koizumi N, Nakamura T. Transplantable cultivated mucosal epithelial sheet for ocular surface reconstruction. 2004. Exp Eye Res 78(3):483-491.

Kinoshita S, Nakamura T. Development of cultivated mucosal epithelial sheet transplantation for ocular surface reconstruction. 2004. Artif Organs 28(1):22-27.

Kneser U, Voogd A, Ohnolz J, Buettner O, Stangenberg L, Zhang YH, Stark GB, Schaefer DJ. Fibrin gel-immobilized primary osteoblasts in calcium phosphate bone cement: in vivo evaluation with regard to application as injectable biological bone substitute. 2005. Cells Tissues Organs 179(4):158-169.

Koizumi N, Fullwood NJ, Bairaktaris G, Inatomi T, Kinoshita S, Quantock AJ. Cultivation of corneal epithelial cells on intact and denuded human amniotic membrane. 2000a. Invest Ophthalmol Vis Sci 41(9):2506-2513.

Koizumi N, Inatomi T, Suzuki T, Sotozono C, Kinoshita S. Cultivated corneal epithelial stem cell transplantation in ocular surface disorders. 2001. Ophthalmology 108(9):1569-1574.

Koizumi NJ, Inatomi TJ, Sotozono CJ, Fullwood NJ, Quantock AJ, Kinoshita S. Growth factor mRNA and protein in preserved human amniotic membrane. 2000b. Curr Eye Res 20(3):173-177.

Kolli S, Lako M, Figueiredo F, Mudhar H, Ahmad S. Loss of corneal epithelial stem cell properties in outgrowths from human limbal explants cultured on intact amniotic membrane. 2008. Regen Med 3(3):329-342.

Kruse FE, Tseng SC. Serum differentially modulates the clonal growth and differentiation of cultured limbal and corneal epithelium. 1993. Invest Ophthalmol Vis Sci 34(10):2976-2989.

Kumari TV, Vasudev U, Kumar A, Menon B. Cell surface interactions in the study of biocompatibility. 2002. Trends in biomaterials and artificial organs 15(2):37-41.

Kushida A, Yamato M, Kikuchi A, Okano T. Two-dimensional manipulation of differentiated Madin-Darby canine kidney (MDCK) cell sheets: the noninvasive harvest from temperature-responsive culture dishes and transfer to other surfaces. 2001. J Biomed Mater Res 54(1):37-46.

Kushida A, Yamato M, Konno C, Kikuchi A, Sakurai Y, Okano T. Decrease in culture temperature releases monolayer endothelial cell sheets together with deposited fibronectin matrix from temperature-responsive culture surfaces. 1999. J Biomed Mater Res 45(4):355-362.

Lakhiari H, Okano T, Nurdin N, Luthi C, Descouts P, Muller D, Jozefonvicz J. Temperature-responsive size-exclusion chromatography using poly(N-isopropylacrylamide) grafted silica. 1998. Biochim Biophys Acta 1379(3):303-313.

Langer R, Vacanti JP. Tissue engineering. 1993. Science 260(5110):920-926.

Lavker RM, Tseng SC, Sun TT. Corneal epithelial stem cells at the limbus: looking at some old problems from a new angle. 2004. Exp Eye Res 78(3):433-446.

Lehrer MS, Sun TT, Lavker RM. Strategies of epithelial repair: modulation of stem cell and transit amplifying cell proliferation. 1998. J Cell Sci 111 (Pt 19):2867-2875.

Li DQ, Shang TY, Kim HS, Solomon A, Lokeshwar BL, Pflugfelder SC. Regulated expression of collagenases MMP-1, -8, and -13 and stromelysins MMP-3, -10, and -11 by human corneal epithelial cells. 2003. Invest Ophthalmol Vis Sci 44(7):2928-2936.

Li DQ, Tseng SC. Three patterns of cytokine expression potentially involved in epithelial-fibroblast interactions of human ocular surface. 1995. J Cell Physiol 163(1):61-79.

Li W, Hayashida Y, Chen YT, Tseng SC. Niche regulation of corneal epithelial stem cells at the limbus. 2007. Cell Res 17(1):26-36.

Li W, He H, Kuo CL, Gao Y, Kawakita T, Tseng SC. Basement membrane dissolution and reassembly by limbal corneal epithelial cells expanded on amniotic membrane. 2006. Invest Ophthalmol Vis Sci 47(6):2381-2389.

Lindberg K, Brown ME, Chaves HV, Kenyon KR, Rheinwald JG. In vitro propagation of human ocular surface epithelial cells for transplantation. 1993. Invest Ophthalmol Vis Sci 34(9):2672-2679.

Liu S, Li J, Wang C, Tan D, Beuerman R. Human limbal progenitor cell characteristics are maintained in tissue culture. 2006. Ann Acad Med Singapore 35(2):80-86.

Lonnroth EC, Dahl JE. Cytotoxicity of dental glass ionomers evaluated using dimethylthiazol diphenyltetrazolium and neutral red tests. 2001. Acta Odontol Scand 59(1):34-39.

Lundstrom A, Egelrud T. Stratum corneum chymotryptic enzyme: a proteinase which may be generally present in the stratum corneum and with a possible involvement in desquamation. 1991. Acta Derm Venereol 71(6):471-474.

Ma Y, Xu Y, Xiao Z, Yang W, Zhang C, Song E, Du Y, Li L. Reconstruction of chemically burned rat corneal surface by bone marrow-derived human mesenchymal stem cells. 2006. Stem Cells 24(2):315-321.

Madhira SL, Vemuganti G, Bhaduri A, Gaddipati S, Sangwan VS, Ghanekar Y. Culture and characterization of oral mucosal epithelial cells on human amniotic membrane for ocular surface reconstruction. 2008. Mol Vis 14:189-196.

Maharajan VS, Shanmuganathan V, Currie A, Hopkinson A, Powell-Richards A, Dua HS. Amniotic membrane transplantation for ocular surface reconstruction: indications and outcomes. 2007. Clin Experiment Ophthalmol 35(2):140-147.

Mann I. A Study of Epithelial Regeneration in the Living Eye. 1944. Br J Ophthalmol 28(1):26-40.

Marinucci L, Balloni S, Becchetti E, Belcastro S, Guerra M, Calvitti M, Lilli C, Calvi EM, Locci P. Effect of titanium surface roughness on human osteoblast proliferation and gene expression in vitro. 2006. Int J Oral Maxillofac Implants 21(5):719-725.

Martin MJ, Muotri A, Gage F, Varki A. Human embryonic stem cells express an immunogenic nonhuman sialic acid. 2005. Nat Med 11(2):228-232.

Martins SA, Campos MQ, Vidal BC, Berto AG, Aguiar JA, Michelacci YM. Proteoglycan synthesis by human corneal explants submitted to laser in situ keratomileusis (LASIK). 2007. Mol Vis 13:142-150.

Masui T, Wakefield LM, Lechner JF, LaVeck MA, Sporn MB, Harris CC. Type beta transforming growth factor is the primary differentiation-inducing serum factor for normal human bronchial epithelial cells. 1986. Proc Natl Acad Sci U S A 83(8):2438-2442.

Matic M, Petrov IN, Chen S, Wang C, Dimitrijevich SD, Wolosin JM. Stem cells of the corneal epithelium lack connexins and metabolite transfer capacity. 1997. Differentiation 61(4):251-260.

Matsuda A, Tagawa Y, Yamamoto K, Matsuda H, Kusakabe M. Identification and immunohistochemical localization of annexin II in rat cornea. 1999. Curr Eye Res 19(4):368-375.

Meallet MA, Espana EM, Grueterich M, Ti SE, Goto E, Tseng SC. Amniotic membrane transplantation with conjunctival limbal autograft for total limbal stem cell deficiency. 2003. Ophthalmology 110(8):1585-1592.

Meller D, Pires RT, Tseng SC. Ex vivo preservation and expansion of human limbal epithelial stem cells on amniotic membrane cultures. 2002. Br J Ophthalmol 86(4):463-471.

Merrett K, Griffith CM, Deslandes Y, Pleizier G, Sheardown H. Adhesion of corneal epithelial cells to cell adhesion peptide modified pHEMA surfaces. 2001. J Biomater Sci Polym Ed 12(6):647-671.

Mosmann T. Rapid colorimetric assay for cellular growth and survival: application to proliferation and cytotoxicity assays. 1983. J Immunol Methods 65(1-2):55-63.

Murakami D, Yamato M, Nishida K, Ohki T, Takagi R, Yang J, Namiki H, Okano T. The effect of micropores in the surface of temperature-responsive culture inserts on the fabrication of transplantable canine oral mucosal epithelial cell sheets. 2006. Biomaterials 27(32):5518-5523.

Nair MB, Suresh Babu S, Varma HK, John A. A triphasic ceramic-coated porous hydroxyapatite for tissue engineering application. 2008. Acta Biomater 4(1):173-181.

Nakamura T, Ang LP, Rigby H, Sekiyama E, Inatomi T, Sotozono C, Fullwood NJ, Kinoshita S. The use of autologous serum in the development of corneal and oral epithelial equivalents in patients with Stevens-Johnson syndrome. 2006. Invest Ophthalmol Vis Sci 47(3):909-916.

Nakamura T, Kinoshita S. Ocular surface reconstruction using cultivated mucosal epithelial stem cells. 2003. Cornea 22(7 Suppl):S75-80.

Nakamura T, Koizumi N, Tsuzuki M, Inoki K, Sano Y, Sotozono C, Kinoshita S. Successful regrafting of cultivated corneal epithelium using amniotic membrane as a carrier in severe ocular surface disease. 2003. Cornea 22(1):70-71.

Nandkumar MA, Yamato M, Kushida A, Konno C, Hirose M, Kikuchi A, Okano T. Two-dimensional cell sheet manipulation of heterotypically co-cultured lung cells utilizing temperature-responsive culture dishes results in long-term maintenance of differentiated epithelial cell functions. 2002. Biomaterials 23(4):1121-1130.

Nielsen BS, Borregaard N, Bundgaard JR, Timshel S, Sehested M, Kjeldsen L. Induction of NGAL synthesis in epithelial cells of human colorectal neoplasia and inflammatory bowel diseases. 1996. Gut 38(3):414-420.

Nishida K, Yamato M, Hayashida Y, Watanabe K, Maeda N, Watanabe H, Yamamoto K, Nagai S, Kikuchi A, Tano Y, Okano T. Functional bioengineered corneal epithelial sheet grafts from corneal stem cells expanded ex vivo on a temperature-responsive cell culture surface. 2004a. Transplantation 77(3):379-385.

Nishida K, Yamato M, Hayashida Y, Watanabe K, Yamamoto K, Adachi E, Nagai S, Kikuchi A, Maeda N, Watanabe H, Okano T, Tano Y. Corneal reconstruction with tissue-engineered cell sheets composed of autologous oral mucosal epithelium. 2004b. N Engl J Med 351(12):1187-1196.

Nishida T, Nakamura M, Mishima H, Otori T. Interleukin 6 promotes epithelial migration by a fibronectin-dependent mechanism. 1992. J Cell Physiol 153(1):1-5.

Nishiwaki-Dantas MC, Dantas PE, Reggi JR. Ipsilateral limbal translocation for treatment of partial limbal deficiency secondary to ocular alkali burn. 2001. Br J Ophthalmol 85(9):1031-1033.

Notara M, Haddow DB, MacNeil S, Daniels JT. A xenobiotic-free culture system for human limbal epithelial stem cells. 2007. Regen Med 2(6):919-927.

Okano T, Yamada N, Okuhara M, Sakai H, Sakurai Y. Mechanism of cell detachment from temperature-modulated, hydrophilic-hydrophobic polymer surfaces. 1995. Biomaterials 16(4):297-303.

Okano T, Yamada N, Sakai H, Sakurai Y. A novel recovery system for cultured cells using plasma-treated polystyrene dishes grafted with poly(N-isopropylacrylamide). 1993. J Biomed Mater Res 27(10):1243-1251.

Ozdemir O, Tekeli O, Ornek K, Arslanpence A, Yalcindag NF. Limbal autograft and allograft transplantations in patients with corneal burns. 2004. Eye 18(3):241-248.

Pajoohesh-Ganji A, Stepp MA. In search of markers for the stem cells of the corneal epithelium. 2005. Biol Cell 97(4):265-276.

Paridaens D, Beekhuis H, van Den Bosch W, Remeyer L, Melles G. Amniotic membrane transplantation in the management of conjunctival malignant melanoma and primary acquired melanosis with atypia. 2001. Br J Ophthalmol 85(6):658-661.

Pellegrini G, Dellambra E, Golisano O, Martinelli E, Fantozzi I, Bondanza S, Ponzin D, McKeon F, De Luca M. p63 identifies keratinocyte stem cells. 2001. Proc Natl Acad Sci U S A 98(6):3156-3161.

Pellegrini G, Golisano O, Paterna P, Lambiase A, Bonini S, Rama P, De Luca M. Location and clonal analysis of stem cells and their differentiated progeny in the human ocular surface. 1999. J Cell Biol 145(4):769-782.

Polisetty N, Fatima A, Madhira SL, Sangwan VS, Vemuganti GK. Mesenchymal cells from limbal stroma of human eye. 2008. Mol Vis 14:431-442.

Prasad CK, Muraleedharan CV, Krishnan LK. Bio-mimetic composite matrix that promotes endothelial cell growth for modification of biomaterial surface. 2007. J Biomed Mater Res A 80(3):644-654.

Puangsricharern V, Tseng SC. Cytologic evidence of corneal diseases with limbal stem cell deficiency. 1995. Ophthalmology 102(10):1476-1485.

Quan CY, Wei H, Sun YX, Cheng SX, Shen K, Gu ZW, Zhang XZ, Zhuo RX. Polyethyleneimine modified biocompatible poly(N-isopropylacrylamide)-based nanogels for drug delivery. 2008. J Nanosci Nanotechnol 8(5):2377-2384.

Radu E, Simionescu O, Regalia T, Dumitrescu D, Popescu LM. Stem cells (p63(+)) in keratinocyte cultures from human adult skin. 2002. J Cell Mol Med 6(4):593-598.

Rama P, Bonini S, Lambiase A, Golisano O, Paterna P, De Luca M, Pellegrini G. Autologous fibrin-cultured limbal stem cells permanently restore the corneal surface of patients with total limbal stem cell deficiency. 2001. Transplantation 72(9):1478-1485.

Reddy TT, Kano A, Maruyama A, Hadano M, Takahara A. Thermosensitive transparent semi-interpenetrating polymer networks for wound dressing and cell adhesion control. 2008. Biomacromolecules 9(4):1313-1321.

Repetto G, del Peso A, Zurita JL. Neutral red uptake assay for the estimation of cell viability/cytotoxicity. 2008. Nat Protoc 3(7):1125-1131.

Rhee DJ, Fariss RN, Brekken R, Sage EH, Russell P. The matricellular protein SPARC is expressed in human trabecular meshwork. 2003. Exp Eye Res 77(5):601-607.

Rollason G, Davies JE, Sefton MV. Preliminary report on cell culture on a thermally reversible copolymer. 1993. Biomaterials 14(2):153-155.

Romano AC, Espana EM, Yoo SH, Budak MT, Wolosin JM, Tseng SC. Different cell sizes in human limbal and central corneal basal epithelia measured by confocal microscopy and flow cytometry. 2003. Invest Ophthalmol Vis Sci 44(12):5125-5129.

Ruan W, Xu E, Xu F, Ma Y, Deng H, Huang Q, Lv B, Hu H, Lin J, Cui J, Di M, Dong J, Lai M. IGFBP7 plays a potential tumor suppressor role in colorectal carcinogenesis. 2007. Cancer Biol Ther 6(3):354-359.

Saghizadeh M, Kramerov AA, Tajbakhsh J, Aoki AM, Wang C, Chai NN, Ljubimova JY, Sasaki T, Sosne G, Carlson MR, Nelson SF, Ljubimov AV. Proteinase and growth factor alterations revealed by gene microarray analysis of human diabetic corneas. 2005. Invest Ophthalmol Vis Sci 46(10):3604-3615.

Sandvig KU, Haaskjold E, Bjerknes R, Refsum SB, Kravik K. Cell kinetics of conjunctival and corneal epithelium during regeneration of different-sized corneal epithelial defects. 1994. Acta Ophthalmol (Copenh) 72(1):43-48.

Sangwan VS, Matalia HP, Vemuganti GK, Rao GN. Amniotic membrane transplantation for reconstruction of corneal epithelial surface in cases of partial limbal stem cell deficiency. 2004. Indian J Ophthalmol 52(4):281-285.

Satake Y, Dogru M, Yamane GY, Kinoshita S, Tsubota K, Shimazaki J. Barrier function and cytologic features of the ocular surface epithelium after autologous cultivated oral mucosal epithelial transplantation. 2008. Arch Ophthalmol 126(1):23-28.

Schermer A, Galvin S, Sun TT. Differentiation-related expression of a major 64K corneal keratin in vivo and in culture suggests limbal location of corneal epithelial stem cells. 1986. J Cell Biol 103(1):49-62.

Schlotzer-Schrehardt U, Dietrich T, Saito K, Sorokin L, Sasaki T, Paulsson M, Kruse FE. Characterization of extracellular matrix components in the limbal epithelial stem cell compartment. 2007. Exp Eye Res 85(6):845-860.

Schlotzer-Schrehardt U, Kruse FE. Identification and characterization of limbal stem cells. 2005. Exp Eye Res 81(3):247-264.

Schneider A, Spitkovsky D, Riess P, Molcanyi M, Kamisetti N, Maegele M, Hescheler J, Schaefer U. "The good into the pot, the bad into the crop!"--a new technology to free stem cells from feeder cells. 2008. PLoS ONE 3(11):e3788.

Schnurer J, Rosswall T. Fluorescein Diacetate Hydrolysis as a Measure of Total Microbial Activity in Soil and Litter. 1982. Appl Environ Microbiol 43(6):1256-1261.

Schoen TJ, Bondy CA, Zhou J, Dhawan R, Mazuruk K, Arnold DR, Rodriguez IR, Waldbillig RJ, Beebe DC, Chader GJ. Differential temporal and spatial expression of insulin-like growth factor binding protein-2 in developing chick ocular tissues. 1995. Invest Ophthalmol Vis Sci 36(13):2652-2662.

Schwartz GS, Holland EJ. Iatrogenic limbal stem cell deficiency. 1998. Cornea 17(1):31-37.

Shankavaram UT, DeWitt DL, Funk SE, Sage EH, Wahl LM. Regulation of human monocyte matrix metalloproteinases by SPARC. 1997. J Cell Physiol 173(3):327-334.

Sharma A, Coles WH. Kinetics of corneal epithelial maintenance and graft loss. A population balance model. 1989. Invest Ophthalmol Vis Sci 30(9):1962-1971.

Shimazaki J, Kaido M, Shinozaki N, Shimmura S, Munkhbat B, Hagihara M, Tsuji K, Tsubota K. Evidence of long-term survival of donor-derived cells after limbal allograft transplantation. 1999. Invest Ophthalmol Vis Sci 40(8):1664-1668.

Shimazaki J, Yang HY, Tsubota K. Limbal autograft transplantation for recurrent and advanced pterygia. 1996. Ophthalmic Surg Lasers 27(11):917-923.

Shimizu T, Yamato M, Isoi Y, Akutsu T, Setomaru T, Abe K, Kikuchi A, Umezu M, Okano T. Fabrication of pulsatile cardiac tissue grafts using a novel 3-dimensional cell sheet manipulation technique and temperature-responsive cell culture surfaces. 2002. Circ Res 90(3):e40.

Shimmura S, Miyashita H, Higa K, Yoshida S, Shimazaki J, Tsubota K. Proteomic analysis of soluble factors secreted by limbal fibroblasts. 2006. Mol Vis 12:478-484.

Shivakumar K, Nair RR, Valiathan MS. Paradoxical effect of cerium on collagen synthesis in cardiac fibroblasts. 1992. J Mol Cell Cardiol 24(7):775-780.

Sidiropoulos M, Pampalakis G, Sotiropoulou G, Katsaros D, Diamandis EP. Downregulation of human kallikrein 10 (KLK10/NES1) by CpG island hypermethylation in breast, ovarian and prostate cancers. 2005. Tumour Biol 26(6):324-336.

Siegwart DJ, Bencherif SA, Srinivasan A, Hollinger JO, Matyjaszewski K. Synthesis, characterization, and in vitro cell culture viability of degradable poly(N-isopropylacrylamide-co-5,6-benzo-2-methylene-1,3-dioxepane)-based polymers and crosslinked gels. 2008. J Biomed Mater Res A 87(2):345-358.

Singh R, Joseph A, Umapathy T, Tint NL, Dua HS. Impression cytology of the ocular surface. 2005. Br J Ophthalmol 89(12):1655-1659.

Sinha R, Sharma N, Vajpayee RB. Corneal blindness-Present status. 2005. Cataract & Refractive Surgery today(Oct):59-61.

Sitalakshmi G, Sudha B, Madhavan HN, Vinay S, Krishnakumar S, Mori Y, Yoshioka H, Abraham S. Ex Vivo Cultivation of Corneal Limbal Epithelial Cells in a Thermoreversible Polymer (Mebiol Gel) and Their Transplantation in Rabbits: An Animal Model. 2008. Tissue Eng Part A.

Smith A. A glossary for stem-cell biology. 2006. Nature 441:1060.

Solomon A, Ellies P, Anderson DF, Touhami A, Grueterich M, Espana EM, Ti SE, Goto E, Feuer WJ, Tseng SC. Long-term outcome of keratolimbal allograft with or without penetrating keratoplasty for total limbal stem cell deficiency. 2002. Ophthalmology 109(6):1159-1166.

Solomon A, Wajngarten M, Alviano F, Anteby I, Elchalal U, Pe'er J, Levi-Schaffer F. Suppression of inflammatory and fibrotic responses in allergic inflammation by the amniotic membrane stromal matrix. 2005. Clin Exp Allergy 35(7):941-948.

Spurr SJ, Gipson IK. Isolation of corneal epithelium with Dispase II or EDTA. Effects on the basement membrane zone. 1985. Invest Ophthalmol Vis Sci 26(6):818-827.

Sridhar MS, Sangwan VS, Bansal AK, Rao GN. Amniotic membrane transplantation in the management of shield ulcers of vernal keratoconjunctivitis. 2001. Ophthalmology 108(7):1218-1222.

Sudha B, Madhavan HN, Sitalakshmi G, Malathi J, Krishnakumar S, Mori Y, Yoshioka H, Abraham S. Cultivation of human corneal limbal stem cells in Mebiol gel--A thermo-reversible gelation polymer. 2006. Indian J Med Res 124(6):655-664.

Sudha B, Sitalakshmi G, Iyer GK, Krishnakumar S. Putative stem cell markers in limbal epithelial cells cultured on intact & denuded human amniotic membrane. 2008. Indian J Med Res 128(2):149-156.

Sugiyama H, Maeda K, Yamato M, Hayashi R, Soma T, Hayashida Y, Yang J, Shirakabe M, Matsuyama A, Kikuchi A, Sawa Y, Okano T, Tano Y, Nishida K. Human adipose tissue-derived mesenchymal stem cells as a novel feeder layer for epithelial cells. 2008. J Tissue Eng Regen Med 2(7):445-449.

Sugrue SP, Zieske JD. ZO1 in corneal epithelium: association to the zonula occludens and adherens junctions. 1997. Exp Eye Res 64(1):11-20.

Sumide T, Nishida K, Yamato M, Ide T, Hayashida Y, Watanabe K, Yang J, Kohno C, Kikuchi A, Maeda N, Watanabe H, Okano T, Tano Y. Functional human corneal endothelial cell sheets harvested from temperature-responsive culture surfaces. 2006. Faseb J 20(2):392-394.

Sumiyoshi K, Baba S, Sakaguchi S, Urano T, Takada Y, Takada A. Increase in levels of plasminogen activator and type-1 plasminogen activator inhibitor in human breast cancer: possible roles in tumor progression and metastasis. 1991. Thromb Res 63(1):59-71.

Sun CC, Cheng CY, Chien CS, Pang JH, Ku WC, Chen PY, Yang CM. Role of matrix metalloproteinase-9 in ex vivo expansion of human limbal epithelial cells cultured on human amniotic membrane. 2005. Invest Ophthalmol Vis Sci 46(3):808-815.

Sun CC, Su Pang JH, Cheng CY, Cheng HF, Lee YS, Ku WC, Hsiao CH, Chen JK, Yang CM. Interleukin-1 receptor antagonist (IL-1RA) prevents apoptosis in ex vivo expansion of human limbal epithelial cells cultivated on human amniotic membrane. 2006. Stem Cells 24(9):2130-2139.

Takezawa T, Mori Y, Yoshizato K. Cell culture on a thermo-responsive polymer surface. 1990. Biotechnology (N Y) 8(9):854-856.

Talbot M, Carrier P, Giasson CJ, Deschambeault A, Guerin SL, Auger FA, Bazin R, Germain L. Autologous transplantation of rabbit limbal epithelia cultured on fibrin gels for ocular surface reconstruction. 2006. Mol Vis 12:65-75.

Tani N, Kinoshita S, Okamoto Y, Kotani M, Itagaki H, Murakami N, Sugiura S, Usami M, Kato K, Kojima H, Ohno T, Saijo K, Kato M, Hayashi M, Ohno Y. Interlaboratory validation of the *in vitro* eye irritation tests for cosmetic ingredients.(8)Evaluation of cytotoxicity tests on SIRC cells. 1999. Toxicology in vitro 13:175-187.

Tanioka H, Kawasaki S, Yamasaki K, Ang LP, Koizumi N, Nakamura T, Yokoi N, Komuro A, Inatomi T, Kinoshita S. Establishment of a cultivated human conjunctival epithelium as an alternative tissue source for autologous corneal epithelial transplantation. 2006. Invest Ophthalmol Vis Sci 47(9):3820-3827.

Tannu NS, Hemby SE. Two-dimensional fluorescence difference gel electrophoresis for comparative proteomics profiling. 2006. Nat Protoc 1(4):1732-1742.

Tasheva ES, Conrad GW. The UV responsive elements in the human mimecan promoter: a functional characterization. 2003. Mol Vis 9:1-9.

Thoft RA, Friend J. The X, Y, Z hypothesis of corneal epithelial maintenance. 1983. Invest Ophthalmol Vis Sci 24(10):1442-1443.

Thomas R, Paul P, Rao GN, Muliyil JP, Mathai A. Present status of eye care in India. 2005. Surv Ophthalmol 50(1):85-101.

Tong Z, Wu X, Ovcharenko D, Zhu J, Chen CS, Kehrer JP. Neutrophil gelatinase-associated lipocalin as a survival factor. 2005. Biochem J 391(Pt 2):441-448.

Torricelli P, Verne E, Brovarone CV, Appendino P, Rustichelli F, Krajewski A, Ravaglioli A, Pierini G, Fini M, Giavaresi G, Giardino R. Biological glass coating on ceramic materials: in vitro evaluation using primary osteoblast cultures from healthy and osteopenic rat bone. 2001. Biomaterials 22(18):2535-2543.

Touhami A, Grueterich M, Tseng SC. The role of NGF signaling in human limbal epithelium expanded by amniotic membrane culture. 2002. Invest Ophthalmol Vis Sci 43(4):987-994.

Tsai RJ, Tseng SC. Human allograft limbal transplantation for corneal surface reconstruction. 1994. Cornea 13(5):389-400.

Tseng SC, Prabhasawat P, Barton K, Gray T, Meller D. Amniotic membrane transplantation with or without limbal allografts for corneal surface reconstruction

in patients with limbal stem cell deficiency. 1998. Arch Ophthalmol 116(4):431-441.

Tsuda Y, Kikuchi A, Yamato M, Nakao A, Sakurai Y, Umezu M, Okano T. The use of patterned dual thermoresponsive surfaces for the collective recovery as co-cultured cell sheets. 2005. Biomaterials 26(14):1885-1893.

Tsuda Y, Kikuchi A, Yamato M, Sakurai Y, Umezu M, Okano T. Control of cell adhesion and detachment using temperature and thermoresponsive copolymer grafted culture surfaces. 2004. J Biomed Mater Res A 69(1):70-78.

Tuori A, Uusitalo H, Burgeson RE, Terttunen J, Virtanen I. The immunohistochemical composition of the human corneal basement membrane. 1996. Cornea 15(3):286-294.

Uludag H, Sefton MV. Colorimetric assay for cellular activity in microcapsules. 1990. Biomaterials 11(9):708-712.

Varani J, Mitra RS, Gibbs D, Phan SH, Dixit VM, Mitra R, Jr., Wang T, Siebert KJ, Nickoloff BJ, Voorhees JJ. All-trans retinoic acid stimulates growth and extracellular matrix production in growth-inhibited cultured human skin fibroblasts. 1990. J Invest Dermatol 94(5):717-723.

Vij N, Roberts L, Joyce S, Chakravarti S. Lumican suppresses cell proliferation and aids Fas-Fas ligand mediated apoptosis: implications in the cornea. 2004. Exp Eye Res 78(5):957-971.

Volmer MW, Stuhler K, Zapatka M, Schoneck A, Klein-Scory S, Schmiegel W, Meyer HE, Schwarte-Waldhoff I. Differential proteome analysis of conditioned media to detect Smad4 regulated secreted biomarkers in colon cancer. 2005. Proteomics 5(10):2587-2601.

von Recum H, Okano T, Wan Kim S. Growth factor release from thermally reversible tissue culture substrates. 1998. J Control Release 55(2-3):121-130.

Wang DY, Hsueh YJ, Yang VC, Chen JK. Propagation and phenotypic preservation of rabbit limbal epithelial cells on amniotic membrane. 2003. Invest Ophthalmol Vis Sci 44(11):4698-4704.

Wang MX, Gray TB, Park WC, Prabhasawat P, Culbertson W, Forster R, Hanna K, Tseng SC. Reduction in corneal haze and apoptosis by amniotic membrane matrix in excimer laser photoablation in rabbits. 2001. J Cataract Refract Surg 27(2):310-319.

Wang Z, Sosne G, Kurpakus-Wheater M. Plasminogen activator inhibitor-1 (PAI-1) stimulates human corneal epithelial cell adhesion and migration in vitro. 2005. Exp Eye Res 80(1):1-8.

Waring GO, 3rd, Roth AM, Ekins MB. Clinical and pathologic description of 17 cases of corneal intraepithelial neoplasia. 1984. Am J Ophthalmol 97(5):547-559.

Watanabe K, Nishida K, Yamato M, Umemoto T, Sumide T, Yamamoto K, Maeda N, Watanabe H, Okano T, Tano Y. Human limbal epithelium contains side population cells expressing the ATP-binding cassette transporter ABCG2. 2004. FEBS Lett 565(1-3):6-10.

Werner L, Legeais JM, Nagel MD, Renard G. Neutral red assay of the cytotoxicity of fluorocarbon-coated polymethylmethacrylate intraocular lenses in vitro. 1999. J Biomed Mater Res 48(6):814-819.

Wolf E, Lahm H, Wu M, Wanke R, Hoeflich A. Effects of IGFBP-2 overexpression in vitro and in vivo. 2000. Pediatr Nephrol 14(7):572-578.

Wolosin JM, Xiong X, Schutte M, Stegman Z, Tieng A. Stem cells and differentiation stages in the limbo-corneal epithelium. 2000. Prog Retin Eye Res 19(2):223-255.

Wu CC, Chen HC, Chen SJ, Liu HP, Hsieh YY, Yu CJ, Tang R, Hsieh LL, Yu JS, Chang YS. Identification of collapsin response mediator protein-2 as a potential marker of colorectal carcinoma by comparative analysis of cancer cell secretomes. 2008. Proteomics 8(2):316-332.

Yamada N, Okano T, Sakai H, Karikusa F, Sawasaki Y, Sakurai Y. Thermo-responsive polymeric surfaces; control of attachment and detachment of cultured cells. 1990. Makromol. Chem.,Rapid. Commun. 11(11):571-576.

Yamanaka H, Yoshizako K, Akiyama Y, Sota H, Hasegawa Y, Shinohara Y, Kikuchi A, Okano T. Affinity chromatography with collapsibly tethered ligands. 2003. Anal Chem 75(7):1658-1663.

Yamato M, Konno C, Kushida A, Hirose M, Utsumi M, Kikuchi A, Okano T. Release of adsorbed fibronectin from temperature-responsive culture surfaces requires cellular activity. 2000. Biomaterials 21(10):981-986.

Yamato M, Okuhara M, Karikusa F, Kikuchi A, Sakurai Y, Okano T. Signal transduction and cytoskeletal reorganization are required for cell detachment from cell culture surfaces grafted with a temperature-responsive polymer. 1999. J Biomed Mater Res 44(1):44-52.

Yamato M, Utsumi M, Kushida A, Konno C, Kikuchi A, Okano T. Thermo-responsive culture dishes allow the intact harvest of multilayered keratinocyte sheets without dispase by reducing temperature. 2001. Tissue Eng 7(4):473-480.

Yan L, Borregaard N, Kjeldsen L, Moses MA. The high molecular weight urinary matrix metalloproteinase (MMP) activity is a complex of gelatinase B/MMP-9 and neutrophil gelatinase-associated lipocalin (NGAL). Modulation of MMP-9 activity by NGAL. 2001. J Biol Chem 276(40):37258-37265.

Yang J, Yamato M, Shimizu T, Sekine H, Ohashi K, Kanzaki M, Ohki T, Nishida K, Okano T. Reconstruction of functional tissues with cell sheet engineering. 2007. Biomaterials 28(34):5033-5043.

Ye HQ, Azar DT. Expression of gelatinases A and B, and TIMPs 1 and 2 during corneal wound healing. 1998. Invest Ophthalmol Vis Sci 39(6):913-921.

Ye J, Yao K, Kim JC. Mesenchymal stem cell transplantation in a rabbit corneal alkali burn model: engraftment and involvement in wound healing. 2006. Eye 20(4):482-490.

Yeung AM, Schlotzer-Schrehardt U, Kulkarni B, Tint NL, Hopkinson A, Dua HS. Limbal epithelial crypt: a model for corneal epithelial maintenance and novel limbal regional variations. 2008. Arch Ophthalmol 126(5):665-669.

Yokoyama M, Miwa H, Maeda S, Wakitani S, Takagi M. Influence of fetal calf serum on differentiation of mesenchymal stem cells to chondrocytes during expansion. 2008. J Biosci Bioeng 106(1):46-50.

Zhang X, Sun H, Tang X, Ji J, Li X, Sun J, Ma Z, Yuan J, Han ZC. Comparison of cell-suspension and explant culture of rabbit limbal epithelial cells. 2005. Exp Eye Res 80(2):227-233.

Zhang XZ, Wu DQ, Chu CC. Synthesis, characterization and controlled drug release of thermosensitive IPN-PNIPAAm hydrogels. 2004. Biomaterials 25(17):3793-3805.

Zhang XZ, Zhuo RX, Cui JZ, Zhang JT. A novel thermo-responsive drug delivery system with positive controlled release. 2002. Int J Pharm 235(1-2):43-50.

APPENDIX I - LIST OF REAGENTS

Minimal essential medium

For stock medium, MEM powder was dissolved in 960 ml sterile water and autoclaved. For completion of medium (100 ml):

MEM stock medium	96 ml
7.5% sodium bicarbonate	2.93 ml
3% glutamine	1 ml
Penicillin streptomycin solution	100 µl (final concentration – 100 IU/ml penicillin and 100 µg/ml streptomycin)

Corneal epithelial medium (CEM) 500ml

The medium consisted of Dulbecco's modified Eagles medium and HAMS F12 (1:1), foetal calf serum (5%,), cholera toxin (0.1 µg /ml), insulin (5 µg/ml,), epidermal growth factor (10 ng/ml,), amphotericin (5 µg/ml) and dimethyl sulphoxide-DMSO (0.5%).

Iscove's Modified Dulbecco's Medium with glutamine

IMDM powder was dissolved in 950 ml sterile water. 3.024 g of sodium bicarbonate was added into the solution and the final volume was made upto 1 litre. The medium was filter sterilised and stored in 4°C.

Phosphate buffered saline (0.1 M) (50 ml) pH 7.2-7.4

Sodium chloride	400 mg
Potassium chloride	10 mg
Disodium hydrogen phosphate	57.5 mg
Potassium dihydrogen phosphate	10 mg

Dissolved in deionised water. If required, pH can be adjusted with 0.1 N HCl or 0.1 N NaOH.

TPVG (50 ml) pH 7.2-7.4

PBS	44 ml
Trypsin (1:250)	125 mg
EDTA (0.2%)	5 ml
Glucose (10%)	250 µl

If required, pH can be adjusted with 0.1 N HCl or 0.1 N NaOH

Hanks' balanced salt solution without Ca & Mg (1 L)

Potassium chloride	400 mg
Potassium phosphate monobasic anhydrous	60 mg
Sodium bicarbonate	350 mg
Sodium Chloride	8 g
Sodium phosphate dibasic anhydrous	47.68 mg
D-glucose	1 g

Dissolved in deionised water. If required, pH can be adjusted with 0.1 N HCl or 0.1 N NaOH

4% Paraformaldehyde (100 ml)

4 g of PFA was dissolved in 100 ml of 0.1 M PBS with slight heating on a magnetic stirrer.

Neutral buffered formalin (1 L)

Disodium hydrogen phosphate anhydrous	6.5 g
Sodium dihydrogen phosphate monohydrate	4.0 g
Formalin	100 ml
Distilled water	900 ml

Dissolved the salts in the distilled water and formalin was added to it. pH should be 7.

1.1 x Rehydration buffer (50 ml)

7.7 M Urea	23.123 g
2.2M Thiourea	8.373 g
2.2% CHAPS	1.1 g
Amberlite resin	Two specks

Urea and thiourea was weighed into a 50 ml tube, 30-40 ml ultra pure water was added and left for stirring on a rocker till it dissolved. Two specks of amberlite resin was added to the solution and again put on the rocker for another half an hour. Afterwards, it was left to settle down and the supernatant was decanted through a strainer. CHAPS was added to the supernatant and kept on the rocker till it dissolved. The solution was aliquoted into 2 ml tubes and stored at -20 °C.

1.1 x IEF buffer (50 ml)

7.7 M Urea	23.123 g
2.2M Thiourea	8.373 g
4.4% CHAPS	2.2 g

The procedure for preparing 1.1 x IEF buffer was same as given for 1.1x rehydration buffer.

1 x Rehydration buffer (1 ml)

1.1 x rehydration buffer	900 µl
Destreak	15 µl
IPG buffer	5 µl
Bromophenol blue	2 µl
Ultrapure water	78 µl

1x IEF buffer (1 ml)

1.1 x IEF buffer	900 µl
DTT (1M)	50 µl
IPG buffer	5 µl
Bromophenol blue	4 µl

Ultrapure water	41 µl

SDS equilibration buffer (500 ml)

6 M Urea	180 g
1.5 M Tris-Cl	16.6 ml
Glycerol	150 ml
SDS	10 g
Bromophenol blue	Trace

Urea was weighed into a conical flask and Tris-Cl was added. The volume was made up to 300 ml with deionised water. It was left on magnetic stirrer for some time and glycerol was added. After the urea got dissolved, SDS was added and the volume was made up to 500 ml. To this, bromophenol blue was added. The solution was aliquoted into 50 ml tubes and stored at -20 °C.

Buffers for PAGE

- **Gel casting solution**

Reagent	**Stock Concentration**	**Final Concentration**	**Volume needed to make 450 ml of solution**
Protogel	30% w/v	12.5% w/v	188 ml
Tris-Cl	1.5 M	37 mM	113 ml
SDS	10%	0.2% w/v	9 ml
De-ionised H2O			135 ml
Ammonium persulphate	10% w/v	0.1% w/v	4.5 ml
TEMED	100% w/v	0.05% w/v	225 µl

- **Fixation solution (1 L)**

Methanol	400 ml
Acetic acid	100 ml
Deionised water	500 ml

- **Sensitizer (1 L)**

Methanol	300 ml

Sodium thiosulphate	2 g
Sodium acetate	68 g
Deionised water	up to 1 L

- **Developer (1 L)**

Sodium carbonate	25 g
Methanal	400 µl
Sodium thiosulphate	28 µl
Deionised water	up to 1 L

1 x LDS (10 ml)

4 x LDS	2.5 ml
DTT (0.5 M)	1 ml
Water	6.5 ml

1 x Transfer buffer for western blot (1 L)

Constituents	One blot	Two blots
20 x transfer buffer	50 ml	50 ml
Methanol	100 ml	200 ml
Deionised water	850 ml	750 ml

LIST OF PAPERS PRESENTED AT CONFERENCES/PUBLISHED

1. Viji Mary Varghese, Sreenivasan K, Kumary TV. Generation of limbal cell sheet using a cytocompatible thermoresponsive surface for ocular surface reconstruction. 21st Kerala Science Congress, Kollam, Jan 28-31,2009
2. A Hopkinson, Viji Mary Varghese, Sreenivasan K, Kumary TV and HS Dua. A novel cytocompatible thermoresponsive co-polymer for corneal tissue engineering. EVER 2008, Slovenia, October 1-4.
3. Viji Mary Varghese, Vidya N, A Hopkinson, K Sreenivasan, TV kumary and HS Dua. A novel thermoresponsive copolymer as a suitable substrate for tissue reconstruction. TERMIS-EU 2008, Porto, Portugal, June 22-26.
4. Viji Mary Varghese, Thomas N Abraham, Sreenivasan K and Kumari TV. Reconstruction and evaluation of three dimensional corneal epithelial construct for ocular surface regeneration using a novel stimuli responsive copolymer. 1st International conference of SCRFI, 2007, Bangalore, January 29-31.
5. Viji Mary Varghese and Kumary TV. Ex vivo expansion of stem cells from limbal explant cultures towards ocular surface regeneration. International Conference on Design of biomaterials (BIND – 06) & XVII Annual meeting of SBAOI, Indian Institute of Technology, Kanpur, Dec 8 -11, 2006.
6. Viji Mary Varghese, PV Mohanan, Usha Vasudev and TV Kumary. Evaluation of a potential corneal culture system for assessing ocular irritation of biomaterials as an *in vitro* alternative. Annual conference of STOX, 2004. SCTIMST, October 28-30.
7. A novel thermoresponsive copolymer as a suitable substrate for tissue reconstruction. Viji Mary Varghese, Vidya N, A Hopkinson, K Sreenivasan, TV kumary and HS Dua. Abstract published in Tissue engineering Part A, 14,2008
8. A novel cytocompatible thermoresponsive co-polymer for corneal tissue engineering. A Hopkinson, Viji Mary Varghese, Sreenivasan K, Kumary TV and HS Dua. Abstract published in Acta Ophthalmologica, 86 (s 243), 2008
9. Evaluation Of A Potential Corneal Culture System For Assessing Ocular Irritation Of Biomaterials As An In Vitro Alternative, Viji Mary Varghese, PV Mohanan, Usha Vasudev and TV Kumary, Abstract published in Toxicology International Journal Vol.21 (1), 2005
10. Optimisation of culture conditions for and efficient xeno-feeder free limbal culture system towards ocular surface regeneration. Viji Mary Varghese, Kumary TV. Microscopy research and technique (Under Revision)
11. *In vitro* interaction of fibroblast cells with a smart copolymeric surface intended for tissue reconstruction. Viji Mary Varghese, Vidya Raj, Sreenivasan K, Kumary TV. Journal of Materials Science: Materials in Medicine (Communicated)